frontiers

RESEARCH TOPICS

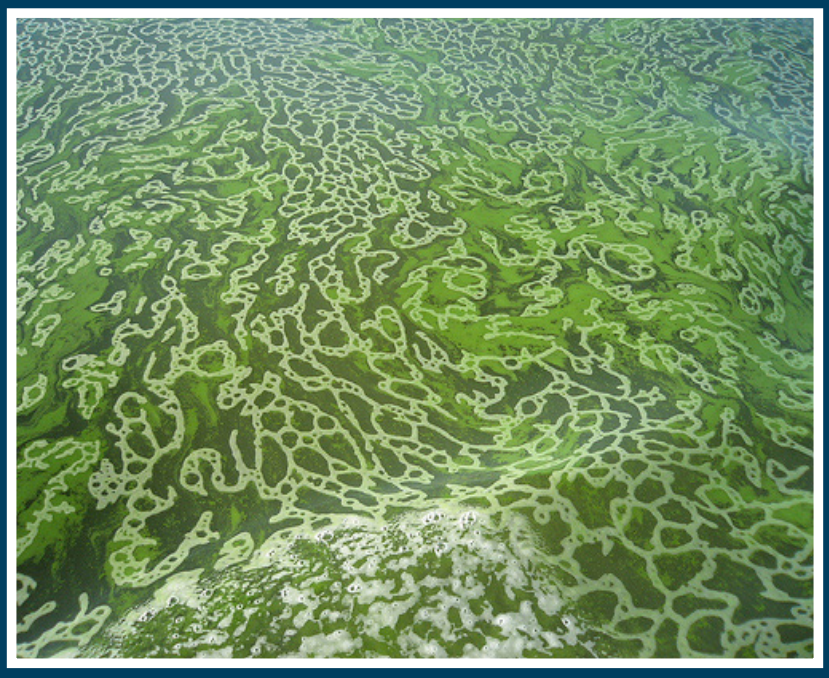

PHYSIOLOGICAL AND MOLECULAR ECOLOGY OF AQUATIC CYANOBACTERIA

Topic Editors
George S. Bullerjahn and Anton F. Post

frontiers in MICROBIOLOGY

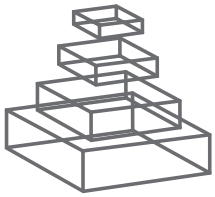

frontiers

ISSN 1664-8714
ISBN 978-2-88919-318-9
DOI 10.3389/978-2-88919-318-9

ABOUT FRONTIERS

Frontiers is more than just an open-access publisher of scholarly articles: it is a pioneering approach to the world of academia, radically improving the way scholarly research is managed. The grand vision of Frontiers is a world where all people have an equal opportunity to seek, share and generate knowledge. Frontiers provides immediate and permanent online open access to all its publications, but this alone is not enough to realize our grand goals.

FRONTIERS JOURNAL SERIES

The Frontiers Journal Series is a multi-tier and interdisciplinary set of open-access, online journals, promising a paradigm shift from the current review, selection and dissemination processes in academic publishing.
All Frontiers journals are driven by researchers for researchers; therefore, they constitute a service to the scholarly community. At the same time, the Frontiers Journal Series operates on a revolutionary invention, the tiered publishing system, initially addressing specific communities of scholars, and gradually climbing up to broader public understanding, thus serving the interests of the lay society, too.

DEDICATION TO QUALITY

Each Frontiers article is a landmark of the highest quality, thanks to genuinely collaborative interactions between authors and review editors, who include some of the world's best academicians. Research must be certified by peers before entering a stream of knowledge that may eventually reach the public - and shape society; therefore, Frontiers only applies the most rigorous and unbiased reviews.
Frontiers revolutionizes research publishing by freely delivering the most outstanding research, evaluated with no bias from both the academic and social point of view.
By applying the most advanced information technologies, Frontiers is catapulting scholarly publishing into a new generation.

WHAT ARE FRONTIERS RESEARCH TOPICS?

Frontiers Research Topics are very popular trademarks of the Frontiers Journals Series: they are collections of at least ten articles, all centered on a particular subject. With their unique mix of varied contributions from Original Research to Review Articles, Frontiers Research Topics unify the most influential researchers, the latest key findings and historical advances in a hot research area!
Find out more on how to host your own Frontiers Research Topic or contribute to one as an author by contacting the Frontiers Editorial Office: researchtopics@frontiersin.org

PHYSIOLOGICAL AND MOLECULAR ECOLOGY OF AQUATIC CYANOBACTERIA

Topic Editors:
George S. Bullerjahn, Bowling Green State University, USA
Anton F. Post, Marine Biological Laboratory, USA

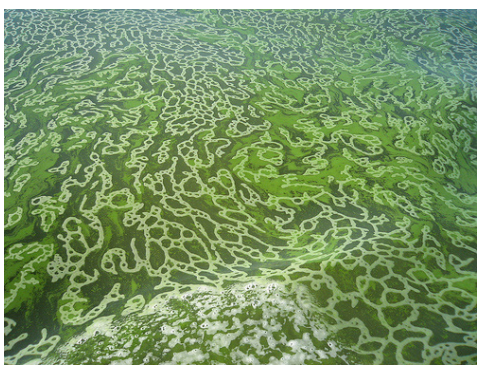

Surface water, western Lake Erie (Laurentian Great Lakes, USA) during the 2010 Microcystis bloom event.
Photo credit: Jerry Wicks, Bowling Green State University

The cyanobacteria inhabit every illuminated environment on Earth, from polar lakes to desert crusts and through their phototrophic metabolism play essential roles in global geochemical cycles. With the discovery of marine Synechococcus and Prochlorococcus almost 30 years ago, cyanobacteria have now earned their place as dominant primary producers contributing over 25 percent of global photosynthesis. Their global abundance is now explained from the coexistence of ecotypes that occupy different niches along spatial and temporal gradients. New ecotypes of Synechococcus have been identified as abundant components of microbial communities in freshwater environments and marginal seas. Extensive comparative genomics of marine and freshwater picocyanobacteria have begun to unmask adaptations to light and nutrient (N, P, Fe) limitation that these diverse environments present. Novel types of cyanobacterial diazotrophy input new N and structure microbial communities in the open sea. Current challenges include the understanding of the interactions between marine cyanobacteria and other microbes in their immediate community.

In contrast, mesotrophic and eutrophic environments such as the Laurentian Great Lakes have been increasingly affected by nuisance and toxic cyanobacterial blooms that have yielded severe declines in water quality. Factors promoting bloom formation and the functional roles of toxins are important issues being addressed today.

This collection of papers is designed to highlight the ecological roles played by cyanobacteria, focusing primarily on their adaptations that allow their dominance and niche differentiation in diverse aquatic environments. These issues are particularly important as we face global environmental alterations that influence aquatic habitats through climate change, ocean acidification and nutrient inputs leading to toxic bloom events.

Table of Contents

frontiers in
MICROBIOLOGY

EDITORIAL
published: 16 July 2014
doi: 10.3389/fmicb.2014.00359

Physiology and molecular biology of aquatic cyanobacteria

George S. Bullerjahn[1]* and Anton F. Post[2]

[1] *Department of Biological Sciences, Bowling Green State University, Bowling Green, OH, USA*
[2] *Marine Biological Laboratory Woods Hole, Woods Hole, MA, USA*
**Correspondence: bullerj@bgsu.edu*

Edited and reviewed by:
Jonathan P. Zehr, University of California, Santa Cruz, USA

Keywords: cyanobacteria, HABs, Prochlorococcus, Synechococcus, nitrogen fixation

Cyanobacteria thrive in every illuminated aquatic environment known, contributing at least 25% of primary productivity worldwide. Given their importance in carbon and nutrient cycles, cyanobacteria are essential geochemical agents that have shaped the composition of the Earth's crust, oceans and atmosphere for billions of years. The high diversity of cyanobacteria is reflected in the panoply of unique physiological adaptations across the phylum, including different strategies to optimize light harvesting or sustain nitrogen fixation, but also different lifestyles like psychrotrophy, and oligotrophy. Some cyanobacteria produce secondary metabolites of cryptic function, many of which are toxic to eukaryotes. Consequently, bloom-forming toxic cyanobacteria are global hazards that are of increasing concern in surface waters affected by anthropogenic nutrient loads and climate change. While focusing on cyanobacteria in aquatic environments, the collection of papers herein touches on this broad range of topics.

Regarding the role of cyanobacteria in the ocean, the importance of the unicellular picocyanobacteria is paramount. Indeed, *Synechococcus* and *Prochlorococcus* are the abundant genera in the oligotrophic open sea. Given that cyanobacteria are under regular assault imposed by photooxidative stresses, and that such stresses constrain photosynthetic performance, the paper by Mella-Flores et al. (2012) describes different strategies employed by model strains of *Synechococcus* and *Prochlorococcus* to high light and UV. Nonetheless, in the ocean, *Synechococcus* is composed of several clades that likely define particular ecotypes. Detection and enumeration of distinct *Synechococcus* clades is essential in understanding how these organisms co-exist with one another. To this end, Ahlgren and Rocap (2012) developed a suite of qPCR tools enabling a thorough analysis of *Synechococcus* community structure and dynamics.

Nitrogen fixation by the unicellular *Crocosphaera watsonii* is now recognized to be a significant source of new N to marine environments. Two papers describe physiological properties of *Crocosphaera* relevant to their ecological importance. Sohm et al. (2011) demonstrate that a strain of *C. watsonii* produces high amounts of extracellular polysaccharides. The high level of organic carbon production suggests that this strain may directly support significant heterotrophy in the marine C cycle. Given that arsenate is a toxic anion that can interfere with the transport and metabolism of phosphate, Dyhrman and Haley (2011) report mechanisms of arsenate resistance in *Crocosphaera*, whose habitat includes P-limited ocean gyres. Such regions often have high arsenate:phosphate ratios, thus detoxification mechanisms are an important strategy for N fixation in these oligotrophic regions.

The structure and physiological performance of arctic cyanobacterial mats is of particular interest, given their dominant contribution to biomass at high latitudes, and the stresses imposed by global warming on such fragile environments. Lionard et al. (2012) examine the composition of an artic microbial mat, and demonstrate the robust adaptation of the cyanobacteria to osmotic stress, a likely outcome of climate change.

The characterization of chlorophyll-*b* containing *Prochlorothrix* spp. by Pinevich et al. (2012) indicate that despite the scarcity of this genus in aquatic environments, molecular methods suggest it is more widely distributed. The authors compare the physiological characteristics of the two known species and discuss the evolution of their light harvesting apparatus.

Four papers explore the physiology of bloom-forming and toxic cyanobacteria. Kaplan et al. (2012) address the enigmatic function of the microcystins and cylindrospermopsins, describing experimental evidence for their role in cell-cell communication among bloom-formers. Sukenik et al. (2012) explore the spread of *Aphanizomenon* and *Cylindrospermopsis* to temperate freshwater environments. The appearance of such blooms is a likely consequence of global warming along with anthropogenic nutrient load, leading to a sustained invasion of into the middle latitudes. Given that management of phosphorus inputs is a strategy for limiting algal blooms in freshwaters, Saxton et al. (2012) describe the phosphorus quotas (intracellular and total) of the toxic colonial cyanobacterium, *Microcystis aeruginosa*. In response to increased phosphorus, *Microcystis* exhibited a higher cell P quota, yet a stable growth rate compared to lower phosphorus treatments. Such work has implications in modeling *Microcystis* blooms from P loadings into freshwaters. Gagnon and Pick (2012) contribute a study showing that the potent neurotoxin anatoxin-a is associated with nitrogen availability in *Aphanizomenon*. Understanding environmental cues for toxin production is essential in ultimately mitigating bloom toxigenicity.

Together, these important contributions cover many of the issues tackled in the field today: the role of cyanobacteria in the global carbon and nutrient cycles, cyanobacterial evolution, the adaptation of cyanobacteria to climate change and the consequences of toxigenicity. The studies described in this collection provide an excellent introduction to these topics, while providing

important clues regarding the future directions that studies of cyanobacteria will take.

REFERENCES

Ahlgren, N. A., and Rocap, G. (2012). Diversity and distribution of marine Synechococcus: multiple gene phylogenies for consensus classification and development of qPCR assays for sensitive measurement of clades in the ocean. *Front. Microbiol.* 3:213. doi: 10.3389/fmicb.2012.00213

Dyhrman, S. T., and Haley, S. T. (2011). Arsenate resistance in the unicellular marine Diazotroph *Crocosphaera watsonii*. *Front. Microbiol.* 2:214. doi: 10.3389/fmicb.2011.00214

Gagnon, A., and Pick, F. R. (2012). Effect of nitrogen on cellular production and release of the neurotoxin anatoxin-a in a nitrogen-fixing cyanobacterium. *Front. Microbiol.* 3:211. doi: 10.3389/fmicb.2012.00211

Kaplan, A., Harel, M., Kaplan-Levy, R. N., Hadas, O., Sukenik, A., and Dittmann, E. (2012). The languages spoken in the water body (or the biological role of cyanobacterial toxins). *Front. Microbiol.* 3:138. doi: 10.3389/fmicb.2012.00138

Lionard, M., Péquin, B., Lovejoy, C., and Vincent, W. F. (2012). Benthic cyanobacterial mats in the high Arctic: multi-layer structure and fluorescence responses to osmotic stress. *Front. Microbiol.* 3:140. doi: 10.3389/fmicb.2012.00140

Mella-Flores, D., Six, C., Ratin, M., Partensky, F., Boutte, C., Le Corguillé, G., et al. (2012). Prochlorococcus and Synechococcus have evolved different adaptive mechanisms to cope with light and UV stress. *Front. Microbiol.* 3:285. doi: 10.3389/fmicb.2012.00285

Pinevich, A., Velichko, N., and Ivanikova, N. (2012). Cyanobacteria of the genus Prochlorothrix. *Front. Microbiol.* 3:173. doi: 10.3389/fmicb.2012.00173

Saxton, M. A., Arnold, R. J., Bourbonniere, R. A., McKay, R. M. L., and Wilhelm, S. W. (2012). Plasticity of total and intracellular phosphorus quotas in *Microcystis aeruginosa* cultures and Lake Erie algal assemblages. *Front. Microbiol.* 3:3. doi: 10.3389/fmicb.2012.00003

Sohm, J. A., Edwards, B. R., Wilson, B. G., and Webb, E. A. (2011). Constitutive extracellular polysaccharide (EPS) production by specific isolates of *Crocosphaera watsonii*. *Front. Microbiol.* 2:229. doi: 10.3389/fmicb.2011.00229

Sukenik, A., Hadas, O., Kaplan, A., and Quesada, A. (2012). Invasion of Nostocales (cyanobacteria) to subtropical and temperate freshwater lakes – physiological, regional, and global driving forces. *Front. Microbiol.* 3:86. doi: 10.3389/fmicb.2012.00086

Conflict of Interest Statement: The authors declare that the research was conducted in the absence of any commercial or financial relationships that could be construed as a potential conflict of interest.

Received: 17 June 2014; accepted: 26 June 2014; published online: 16 July 2014.
*Citation: Bullerjahn GS and Post AF (2014) Physiology and molecular biology of aquatic cyanobacteria. Front. Microbiol. **5**:359. doi: 10.3389/fmicb.2014.00359*
This article was submitted to Aquatic Microbiology, a section of the journal Frontiers in Microbiology.

frontiers in
MICROBIOLOGY

ORIGINAL RESEARCH ARTICLE
published: 08 August 2012
doi: 10.3389/fmicb.2012.00285

Prochlorococcus and *Synechococcus* have evolved different adaptive mechanisms to cope with light and UV stress

Daniella Mella-Flores[1,2,3], Christophe Six[1,2], Morgane Ratin[1,2], Frédéric Partensky[1,2], Christophe Boutte[1,2], Gildas Le Corguillé[1,4], Dominique Marie[1,2], Nicolas Blot[1,2,5,6], Priscillia Gourvil[1,2], Christian Kolowrat[1,2,7] and Laurence Garczarek[1,2]*

[1] Station Biologique, UPMC-Université Paris VI, Roscoff, France
[2] Groupe Plancton Océanique, CNRS, UMR 7144, Roscoff, France
[3] Departamento de Ecología, Facultad de Ciencias Biologicas, Pontificia Universidad Catolica de Chile, Santiago, Chile
[4] CNRS, FR 2424, Service Informatique et Génomique, Roscoff, France
[5] Laboratoire Microorganismes: Génome et Environnement, Clermont Université, Université Blaise Pascal, Clermont-Ferrand, France
[6] Laboratoire Microorganismes: Génome et Environnement, CNRS, UMR 6023, Aubière, France
[7] Center for Doctoral Studies, University of Vienna, Vienna, Austria

Edited by:
George S. Bullerjahn, Bowling Green State University, USA

Reviewed by:
Eric A. Webb, University of Southern California, USA
Tom Bibby, University of Southampton, UK

***Correspondence:**
Laurence Garczarek, Station Biologique, UPMC-Université Paris VI, Places Georges Teissier, 29680 Roscoff, France.
e-mail: laurence.garczarek@sb-roscoff.fr

Prochlorococcus and *Synechococcus*, which numerically dominate vast oceanic areas, are the two most abundant oxygenic phototrophs on Earth. Although they require solar energy for photosynthesis, excess light and associated high UV radiations can induce high levels of oxidative stress that may have deleterious effects on their growth and productivity. Here, we compared the photophysiologies of the model strains *Prochlorococcus marinus* PCC 9511 and *Synechococcus* sp. WH7803 grown under a bell-shaped light/dark cycle of high visible light supplemented or not with UV. *Prochlorococcus* exhibited a higher sensitivity to photoinactivation than *Synechococcus* under both conditions, as shown by a larger drop of photosystem II (PSII) quantum yield at noon and different diel patterns of the D1 protein pool. In the presence of UV, the PSII repair rate was significantly depressed at noon in *Prochlorococcus* compared to *Synechococcus*. Additionally, *Prochlorococcus* was more sensitive than *Synechococcus* to oxidative stress, as shown by the different degrees of PSII photoinactivation after addition of hydrogen peroxide. A transcriptional analysis also revealed dramatic discrepancies between the two organisms in the diel expression patterns of several genes involved notably in the biosynthesis and/or repair of photosystems, light-harvesting complexes, CO_2 fixation as well as protection mechanisms against light, UV, and oxidative stress, which likely translate profound differences in their light-controlled regulation. Altogether our results suggest that while *Synechococcus* has developed efficient ways to cope with light and UV stress, *Prochlorococcus* cells seemingly survive stressful hours of the day by launching a minimal set of protection mechanisms and by temporarily bringing down several key metabolic processes. This study provides unprecedented insights into understanding the distinct depth distributions and dynamics of these two picocyanobacteria in the field.

Keywords: marine cyanobacteria, *Synechococcus*, *Prochlorococcus*, light/dark cycle, light stress, UV radiations, oxidative stress, photophysiology

INTRODUCTION

Phytoplanktonic cells, and in particular cyanobacteria, experience dramatic daily fluctuations of solar radiations, which can become suboptimal for photosynthetic processes around midday. Photosystem II (PSII) is particularly sensitive to these changes in photon fluxes and under unfavorable or stressful conditions its activity can decline more rapidly than most other physiological processes (Berry and Björkman, 1980; Demmig-Adams and Adams, 1992; Aro et al., 1993; Andersson and Aro, 2001). Photodamages to PSII are thought to start by the inactivation of the oxygen-evolving complex, which is caused by the dissociation of the Mn_4Ca^{2+} cluster. This process leads to the production of long-lived P_{680}^{+}, the oxidized form of the reaction center chlorophyll (Chl) pair, a particularly strong oxidant which in turn provokes the destruction of the PSII core protein D1 (Hakala et al., 2006; Nishiyama, 2006). At low irradiances, the rate of photosynthetic electron transport is proportional to the photon flux density and damaged D1 polypeptides can be removed from the PSII reaction center and rapidly replaced by newly synthesized D1 proteins (Park et al., 1995; Tyystjarvi and Aro, 1996; Nixon et al., 2005; Ohnishi et al., 2005). However, at higher irradiances, the rate at which the PSII reaction center is damaged can exceed its repair rate, which results in an

increase of inactivated PSII centers and a subsequent decline of the quantum yield of photosynthesis, resulting from photoinhibitory fluorescence quenching (Powles, 1984; Prásil et al., 1992; Aro et al., 1993; Andersson and Aro, 2001).

Although the visible part of the solar spectrum (400–700 nm), also called photosynthetically active radiations (PAR), is responsible for most photoinhibitory effects, the contribution of UV-B (280–315 nm) and, to a least extent, UV-A (315–400 nm) is also notable in the uppermost layer of the ocean (Dring et al., 2001; van de Poll et al., 2001; He and Häder, 2002b). UV-B can indeed damage the photosynthetic apparatus about 100-fold more efficiently than visible light and these radiations might directly affect PSII proteins and the Mn_4Ca^{2+} cluster (Sarvikas et al., 2006; Caldwell et al., 2007). UV and high visible radiations can also cause indirect photoinhibitory effects via the production of reactive oxygen species (ROS; He and Häder, 2002a,b; Rastogi et al., 2010), mainly formed within reaction centers (Asada, 1999) and light-harvesting complexes (Knox and Dodge, 1985; Zolla and Rinalducci, 2002). ROS are powerful oxidizing agents which can react with DNA, lipids, and proteins. Although these compounds are inevitably produced by cell metabolism, even under optimal growth conditions, their production is drastically enhanced when cells are exposed to a variety of stresses, including excess visible light and UV radiations (UVR; Latifi et al., 2005; Ross et al., 2006; Houot et al., 2007; Allakhverdiev and Murata, 2008). The effect of ROS on PSII photoinhibition is thought to act primarily by inhibiting the *de novo* synthesis of proteins, including those required for the repair of PSII (Nishiyama et al., 2004; Nishiyama, 2006; Takahashi and Murata, 2008). A direct effect of ROS on the inactivation of PSII reaction center has also been suggested through triggering D1 degradation (Vass et al., 1992; Aro et al., 1993; Miyao et al., 1995; Keren et al., 1997; Lupinkova and Komenda, 2004). In any case, ROS clearly have a major role in light-mediated photoinhibition as well as in other environmental stresses (Nishiyama, 2006; Allakhverdiev and Murata, 2008; Latifi et al., 2009). Thus, survival of phototrophic organisms depends upon the amount of ROS produced and their efficiency in scavenging these oxygen species.

In this context, marine picocyanobacteria belonging to the genera *Synechococcus* and *Prochlorococcus* constitute two relevant and complementary models to study acclimation processes to high light and UVR and their interrelationships with oxidative stress. In oceanic ecosystems, these two organisms numerically dominate the phytoplanktonic community (Partensky et al., 1999a; Scanlan, 2003) and are considered to be the two most abundant photosynthetic organisms on Earth, with a substantial contribution to Chl biomass and primary production (Liu et al., 1997; Partensky et al., 1999a; Agawin et al., 2000; Garcia-Pichel et al., 2003). Members of the marine *Synechococcus* genus are ubiquitously distributed and are most abundant in coastal regions and mesotrophic open ocean surface waters (Partensky et al., 1999a; Zwirglmaier et al., 2008), whereas *Prochlorococcus* preferentially thrives in warm, stratified, oligotrophic tropical, and subtropical marine areas (Partensky et al., 1999b; Zubkov et al., 2000; Johnson et al., 2006). In the field, these organisms experience large variations in irradiance, linked to the combination of the light/dark (L/D) cycle, water mixing, and a variable cloudiness (MacIntyre et al., 2000). Moreover, their tiny size (0.5–0.8 and 0.8–1.2 μm diameter for *Prochlorococcus* and *Synechococcus*, respectively) confers them a high surface to volume ratio, optimizing their photon capture, and making them particularly sensitive to UVR (Llabres and Agusti, 2006, 2010).

Like other photosynthetic organisms, marine cyanobacteria have evolved a variety of protection mechanisms to ensure their growth and survival in highly illuminated habitats. These mechanisms include thermal dissipation of excess light excitation, structural changes of the photosynthetic machinery as well as enzymatic and non-enzymatic scavenging systems to eliminate ROS, in particular those produced in photosynthetic membranes (for reviews, see Bailey and Grossman, 2008; Latifi et al., 2009). However, several pieces of evidence suggest that *Prochlorococcus* and *Synechococcus* lineages could deal differently with light stress. Indeed, two *P. marinus* strains (PCC 9511 and SS120, a high light- and a low-light-adapted ecotype, respectively) were found to be more sensitive to a transient exposure to high irradiances than three *Synechococcus* spp. strains representative of various trophic environments and exhibiting different pigmentation (RS9917, RCC307, and WH8102; Six et al., 2007b). Similarly, measurements of cell abundances and/or mortality rates of field populations of picocyanobacteria exposed to different levels of natural solar radiations showed that *Prochlorococcus* exhibited a lower resistance to UVR than *Synechococcus* in surface waters of the central Atlantic Ocean (Llabres and Agusti, 2006; Agusti and Llabres, 2007) and the Mediterranean Sea (Sommaruga et al., 2005; Llabres and Agusti, 2010).

In order to reveal potential differences in circadian metabolic rhythms between these two genera, the photophysiology of the model strains *P. marinus* PCC 9511 and *Synechococcus* sp. WH7803 was examined at different times of a modulated L/D cycle of visible light (hereafter VL) with or without UV. Additionally, the diel variability of the sensitivity of *Prochlorococcus* and *Synechococcus* to oxidative stress, as triggered by different H_2O_2 concentrations was investigated. Expression of key genes involved in photosynthesis, light, and oxidative stress response and a number of other processes were also monitored in order to get insights about the molecular bases of the observed physiological differences.

MATERIALS AND METHODS

STRAINS AND CULTURE CONDITIONS

The two model strains *P. marinus* PCC 9511 [a strain genetically very close, if not identical, to MED4 (Rippka et al., 2000; Rocap et al., 2003)] and *Synechococcus* sp. WH7803 (Scanlan et al., 2009) used in this study were grown at 22°C in PCR-S11 medium (Rippka et al., 2000), supplemented with 1 mM $NaNO_3$. All experiments were performed under modulated L/D conditions using a computer-controlled illumination device (cyclostat), as detailed elsewhere (Holtzendorff et al., 2001; Kolowrat et al., 2010). This system allows the simulation of a bell-shaped 12/12 h L/D cycle, which induces a good synchronization of cell division, as observed for field populations (Vaulot et al., 1995; Jacquet et al., 1998). The maximal VL irradiance (at virtual noon) was set at 870 μmol photons m^{-2} s^{-1}, corresponding to the reference light condition. In order to test the specific effects of UVR, the same experiments were repeated but with supplementing the VL

condition with modulated UV-A and UV-B radiations (hereafter VL + UV), provided by UV-A-340 fluorescent lamps (Q-Panel Lab products, Cleveland, OH, USA). UVR reached 7.59 W m^{-2} UV-A (320–340 nm) and 0.57 W m^{-2} UV-B (280–320 nm) at virtual noon, corresponding to levels representative of natural doses measured in the upper layer of nutrient-poor, oceanic areas (Helbling et al., 1992). Two replicate cultures were acclimated to L/D cycles for at least 2 weeks prior to start monitoring the different parameters. During the experiment, two replicate cultures were grown with a continuous input of fresh medium, in order to maintain cells in exponential growth throughout the whole sampling period. One microliter aliquots were taken every hour, fixed for 10 min with grade I glutaraldehyde (0.25% final concentration; Sigma Aldrich, Saint-Louis, MO, USA), then frozen at −80°C for delayed analyses of cell abundance and cell cycle using a FACS Canto flow cytometer (Becton Dickinson Biosciences, San Jose, CA, USA), as previously described (Marie et al., 1997, 1999). Because of the continuous dilution, growth rate of these cultures was indirectly assessed from cell cycle data (μ_{cc}) using the method described by Carpenter and Chang (1988), as detailed earlier (Kolowrat et al., 2010). To study the kinetics of response to light fluctuations, cultures were sampled at 6, 9, 12, 15, 18, 20, 22, and 2 h over 3 days for measuring a variety of parameters described below.

PIGMENT AND FLUORESCENCE MEASUREMENTS

Photosynthetic pigments were extracted in 95% methanol and analyzed by HPLC, as previously described (Everroad et al., 2006). Whole cell fluorescence emission spectra with excitation at 530 nm were recorded for *Synechococcus* using a LS-50B spectrofluorometer (Perkin Elmer, Waltham, MA, USA). The PSII quantum yield (F_V/F_M) was measured using a Pulse Amplitude Modulated fluorimeter (PhytoPAM, Walz, Effeltrich, Germany) connected to a LabPro chart recorder allowing the direct visualization of fluorescence traces (Vernier, Beaverton, OR, USA). A 2 mL aliquot was dark acclimated for 5 min in a quartz cuvette with a mirrored facet facing the photomultiplier to enhance the signal. The modulated light was then turned on to measure the basal fluorescence level F_0 with modulated excitation at 440 nm for *Prochlorococcus* cells and 520 nm for *Synechococcus*. The maximal fluorescence F_M was determined by applying a light saturating pulse in the presence of 50 μM of the PSII inhibitor 3-(30,4-dichlorophenyl)-1,1-dimethylurea (DCMU) under ca. 2,000 μmol photons m^{-2} s^{-1}. The PSII quantum yield was calculated as:

$$F_V/F_M = (F_M - F_0)/F_M \quad (1)$$

where F_V is the variable fluorescence.

PHOTOSYSTEM II REPAIR

At each sampling time point, a 20 mL volume of each replicate culture was sampled and split into two 100 mL quartz Erlenmeyer flasks, and one of them was supplemented with 500 μg mL^{-1} lincomycin, an inhibitor of protein translation (Six et al., 2007a). The two flasks were immediately brought back into the culture system and 2 mL aliquots were collected at 0, 15, 30, and 60 min after the sampling to measure the PSII quantum yield, as described above. The PSII quantum yield was then plotted over time for both the control and lincomycin-treated sub-cultures and plots were fitted with an exponential decay function. The PSII repair rate was estimated as the difference between the exponential decay rates in the absence and presence of lincomycin (Six et al., 2007a, 2009; Campbell and Tyystjarvi, 2012).

IMMUNOBLOTTING

Cell pellets were resuspended in extraction buffer (140 mM Tris base, 105 mM Tris-HCl, 0.5 mM ethylenediaminetetraacetic acid, 2% lithium dodecyl sulfate, 10% glycerol, and 0.1 mg mL^{-1} Pefa-Bloc protease inhibitor (Roche, Basel, Switzerland) and total protein concentration was determined using a Lowry protein assay kit (Bio-Rad, Hercules, CA, USA) and bovine serum albumin as protein standards. Samples were then denatured with 50 mM dithiothreitol and heated for 2 min at 80°C and 2 μg total protein was loaded on a 4–12% gradient acrylamide precast NuPAGE Bis-Tris mini-gel (Invitrogen, Carlsbad, CA, USA) along with recombinant standards of D1 or D2 proteins (Agrisera, Vännäs, Sweden) to establish a standard curve. Gels were electrophoresed and the proteins were transferred onto a polyvinylidene fluoride (PVDF) membrane, then immediately immersed into Tris Buffer Saline-Tween (TBS-T) buffer, pH 7.6 (0.1% Tween 20, 350 mM sodium chloride, 20 mM Trizma base) containing 2% (w:v) ECL Advance blocking agent (Amersham Biosciences, Piscataway, NJ, USA). Aliquots of primary antibodies against D1 or D2 proteins (Agrisera) were diluted at 1:50 000 in TBS-T in the presence of 2% blocking agent and membranes were soaked into this solution for 1 h with agitation. After extensive washing of the membrane with TBS-T buffer, anti-rabbit secondary antibodies were applied with the same procedure as for primary antibodies. Membranes were developed by chemoluminescence using the ECL Advance reagent kit (Amersham Biosciences) and visualized with a LAS4000 imager equipped with a CCD camera (GE Healthcare, Waukesha, WI, USA). Signals were quantified using the ImageQuant software and the recombinant protein standard curve. To ease comparisons of the diel trends between strains and conditions, data were normalized at 6:00 am.

OXIDATIVE STRESS ASSAYS

Samples collected from dawn to dusk (6, 9, 12, 15, and 18 h time points) were split into aliquots of 2.5 mL and subjected to a series of H_2O_2 concentrations ranging from 0.1 to 1,800 μM. These culture aliquots were then incubated in the culturing system for 50 min and the PSII quantum yield was measured as described above. To quantitatively estimate the PSII resistance to such oxidative stress at each time point, the decay of F_V/F_M as a function of increasing H_2O_2 concentration was plotted as a percentage of F_V/F_M of the control cultures. The decay curves were then fitted with a two-parameter hyperbolic decay function:

$$y = ab/(b + x) \quad (2)$$

The b-value proved to be informative because it integrates both the minimal H_2O_2 concentration needed to cause a decrease of F_V/F_M and the decrease rate of the PSII quantum yield. Thus, this parameter can be used as a proxy to assess the global resistance of PSII to oxidative stress induced by H_2O_2.

RNA EXTRACTION AND REAL TIME QUANTITATIVE PCR

Samples for RNA extraction were harvested and extracted as previously described in Kolowrat et al. (2010) for eight data points per L/D cycle and for two different days, corresponding to biological replicates. Briefly, cell pellets, resuspended in Trizol (Invitrogen, Carlsbad, CA, USA), were extracted using the miRNeasy kit as recommended by the manufacturers (Qiagen, Valencia, CA, USA), followed by two successive DNase treatments performed on the miRNeasy columns using the Qiagen RNase-free DNase Set (Qiagen).

Real time quantitative PCR (hereafter qPCR) was performed on a set of *P. marinus* PCC 9511 and *Synechococcus* sp. WH7803 genes, representative of key metabolic processes (Table S1 in Supplementary Material). Design and optimization of gene specific primers were performed as previously described (Six et al., 2007b) using PrimerExpress™ software v2.0 (Applied Biosystems) and by checking for every set of primers, the linearity of the CT (cycle at threshold) vs. cDNA content within a dilution range of cDNA. Reverse transcription was carried out on 100 ng RNA using SuperScriptII reverse transcriptase (Gibco-BRL, Gaithersburg, MD, USA). qPCR was performed in triplicate on the cDNA obtained after dilution, using the DNA Engine/Chromo4 Real Time PCR-Detector (Bio-Rad, Hercules, CA, USA) and the absolute SYBR Green ROX Mix (Abgene, Epsom, UK), as previously described (Garczarek et al., 2008). Gene expression profiles monitored during L/D cycles were expressed as the ratio of gene expression vs. expression of the aperiodic gene *rnpB* (Mary and Vaulot, 2003; Zinser et al., 2009; Kolowrat et al., 2010) and normalized to the 6:00 time point sampled under VL conditions, using the $2^{-\Delta\Delta CT}$ method (Schmittgen and Livak, 2008).

RESULTS

CELL CYCLE

The cell cycle of *Synechococcus* sp. WH7803 was strongly synchronized by the alternation of light and darkness, with a peak of DNA replicating cells (S cells) occurring at ca. 16–17:00, i.e., 1–2 h before the light-to-dark transition (LDT; 18:00), in modulated VL only and about 3 h later for cells acclimated to modulated VL + UV (**Figure 1**). A comparable delay of the S phase was previously reported for *P. marinus* PCC 9511 in the presence of UVR, but the peak of S cells occurred at the LDT in VL and about at the same time as for *Synechococcus* in VL + UV (Kolowrat et al., 2010). Another notable difference with *Prochlorococcus* is the occurrence of a second minor S peak in the early morning followed by a small bump of G_2 cell abundance around noon-time (mainly visible during the first and third cycle), suggesting some ultradian growth (Shalapyonok et al., 1998). Mean growth rates of *Synechococcus* cultures were assessed from the percentages of cells in S and G_2 (μ_{cc}) using the method described by Carpenter and Chang (1988). They were not statistically distinct between the two conditions (average over 3 days and two replicates: $\mu_{cc} = 1.00 \pm 0.21\ day^{-1}$ in VL; $\mu_{cc} = 1.23 \pm 0.11\ day^{-1}$ in VL + UV) but were higher than in *Prochlorococcus* ($\mu_{cc} = 0.67 \pm 0.05\ day^{-1}$ in VL; $\mu_{cc} = 0.68 \pm 0.03\ day^{-1}$ in VL + UV; Kolowrat et al., 2010). This difference is attributable in part to the shorter delay observed between the maxima of S and G_2 cells in *Synechococcus* ($t_{G2} - t_S \sim 2.5$ h) than in *Prochlorococcus* ($t_{G2} - t_S \sim 4$ h), as this parameter is used for the calculation of growth rates in the μ_{cc} method (Carpenter and Chang, 1988).

PIGMENT RATIOS

Comparative diel variations of molar ratios of the main pigments in the two marine picocyanobacteria under both light conditions are reported in **Figure 2**. For *Synechococcus* grown under VL, the zeaxanthin (Zea) to Chl *a* ratio (**Figure 2A**) was maximal between noon and the early afternoon, and then decreased sharply till the LDT and at a lower rate during the night. In VL + UV, the pattern was globally similar, except that (i) the values were higher in VL + UV than in VL, (ii) the midday peak had a lower average amplitude (15.4 vs. 25.4% increase under VL + UV and VL, respectively), and (iii) the ratio remained stable during the night. By comparison, the β-carotene (β-Car) to Chl *a* ratio of *Synechococcus* grown in VL systematically peaked at 9:00, decreased till 15:00 then increased again for the rest of the diel cycle (**Figure 2C**). The pattern was very similar under UV, except that night values were slightly lower during the first two L/D cycles. The pattern of pigment ratios observed in *Prochlorococcus* exhibited a number of differences compared to *Synechococcus*. In VL, the Zea to divinyl-(DV-) Chl *a* ratio started to increase at mid-morning and was maximal around 20:00, then decreased during the rest of the night (**Figure 2B**), corresponding to the cell division phase. The same diel pattern was observed under VL + UV. Although the variation range was moderate for the α-Car to DV-Chl *a* ratio in VL, its diel pattern was comparable to that of the Zea to DV-Chl *a*, except that it increased immediately after dawn (**Figure 2D**). There were almost no diel oscillations of this ratio under VL + UV. The DV-Chl *b* to *a* ratio exhibited no clear diel pattern in either light condition (data not shown).

PHOTOSYSTEM II FUNCTION AND REPAIR

In order to investigate how the daily variations of VL and UVR could affect the PSII activity of cells, we followed the PSII quantum yield in *Synechococcus* sp. WH7803 and *P. marinus* PCC 9511 cultures during three consecutive L/D cycles (**Figure 3**). For both strains and under both light conditions, the F_V/F_M ratio showed a cyclic evolution, reaching a maximum at night and a minimum at virtual noon. This midday drop, originating either from PSII photoinactivation or from dissipative non-photochemical quenching (NPQ) of fluorescence (or both), was larger for *Prochlorococcus* than for *Synechococcus* under both light conditions. Indeed, there was a relative decrease of the PSII quantum yield of about 40% for *Prochlorococcus*, while in *Synechococcus* it never exceeded 20% (**Figure 3**). The diel patterns of PSII activities showed also some differences between VL and VL + UV, with slightly higher late night and morning yields for *Synechococcus* and lower yields at 6:00, 12:00, and 15:00 for *Prochlorococcus* cells in the latter condition.

Variations in the PSII repair activity of the cells, as assessed by comparing the PSII quantum yield of sub-cultures incubated with or without lincomycin, an inhibitor of protein synthesis, also showed a cyclic pattern, with no measurable PSII repair occurring during the night (**Figure 4**). Moreover, cells acclimated to VL and VL + UV conditions exhibited a very different repair rate,

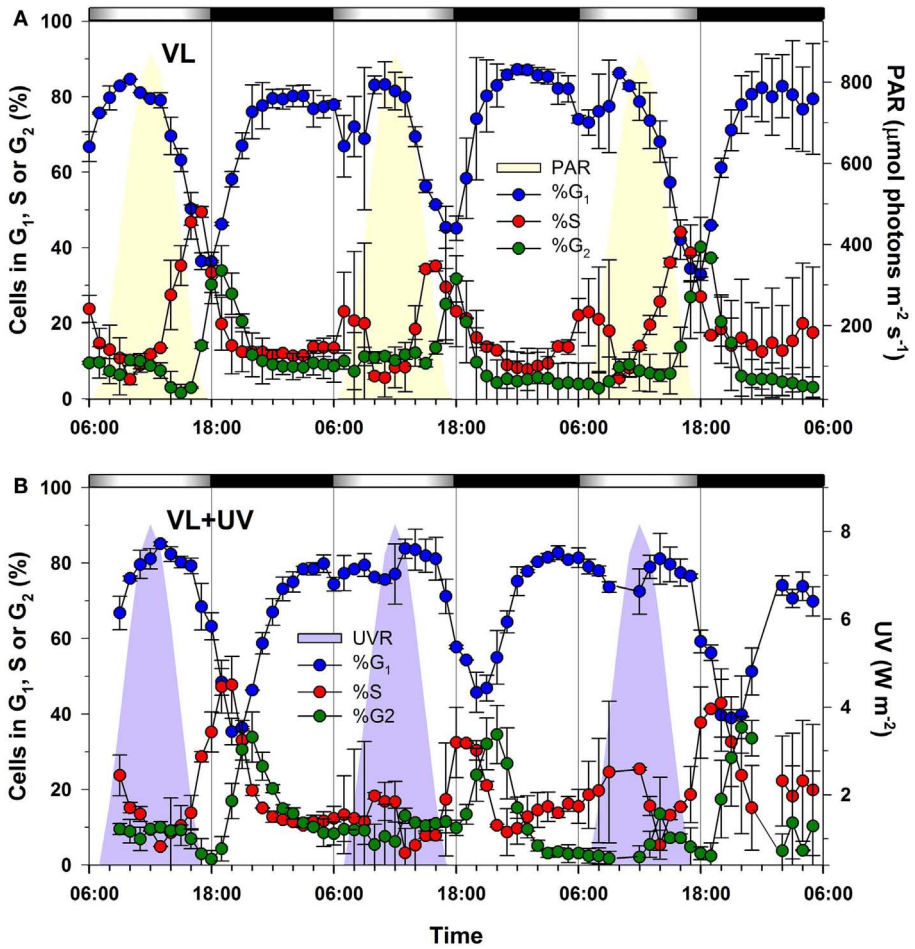

FIGURE 1 | Effect of UV exposure on the timing of the cell cycle phases of *Synechococcus* sp. WH7803 cells grown over a modulated 12/12 h L/D cycle with or without UV radiations. (A) Distribution of G_1 (blue), S (red), and G_2 (green) phases for cells acclimated to VL. **(B)** Same for VL + UV conditions. Error bars indicate mean deviation for two biological replicates. Note that only the total UVR (UV-A + UV-B) plot is shown in graph **(B)** since PAR was the same as in graph **(A)**. White and black bars above graphs indicate light and dark periods, also delineated by gray vertical bars and areas filled in yellow (PAR) or purple (UV). Abbreviations: L/D, light/dark; PAR, photosynthetically available radiations; VL, visible light; UV, ultraviolet.

especially in *Synechococcus*. While VL exposure only led to a moderate induction of the PSII repair rate with regard to night levels in *Synechococcus*, a sharp increase of this rate (from three- to six-fold) was observed for cells acclimated to UV-supplemented light (**Figure 4A**). Such an UV-induced increase of the daily PSII repair rate was also observed in *Prochlorococcus* cells, although much more limited (less than twofold), and the maximal rate were already reached at 9:00 (**Figure 4B**).

PHOTOSYSTEM II CORE PROTEIN POOLS

In *Synechococcus* cells grown under VL, both the D1 and D2 protein pools showed no significant diel oscillations during the L/D cycle (**Figure 5**). Under VL + UV, while D2 also remained stable, cells progressively accumulated D1 proteins during daytime and the pool reached a maximum at the LDT (40% increase compared to the value at 6:00). *Prochlorococcus* cells showed a quite different diel pattern of D1 and D2 protein pools. Under VL, both proteins showed minimal contents during the day (30–40% decrease), when irradiance was maximal, with a subsequent full recovery during the night. A similar pattern was observed under VL + UV, but with an extended period of low PSII core protein content.

RESISTANCE OF PSII TO OXIDATIVE STRESS

Synechococcus and *Prochlorococcus* grown under VL and VL + UV conditions exhibited quite different PSII responses to oxidative stress (**Figure 6**). *Synechococcus* sub-cultures sampled at 6:00 (i.e., at the dark-to-light transition) showed no significant change in their PSII quantum yield until H_2O_2 concentrations as high as 300 and 1,800 µM in VL + UV and VL, respectively. Sub-cultures sampled at 12:00 were affected by concentrations as low as 10 and 50 µM H_2O_2, the photoinhibitory effect increasing with the concentration of oxidizing agent until a total shutdown of PSII activity at 300 and 900 µM H_2O_2 for VL + UV and VL, respectively (**Figure 6A**). PSII inactivation occurred at lower doses in *Prochlorococcus* at both time points, starting at about 100 µM H_2O_2 for cultures collected at 6:00 and reaching 60 and 50% of photoinhibition at 1,800 µM H_2O_2 in VL and VL + UV, respectively (**Figure 6B**), compared to less than 20% for *Synechococcus*

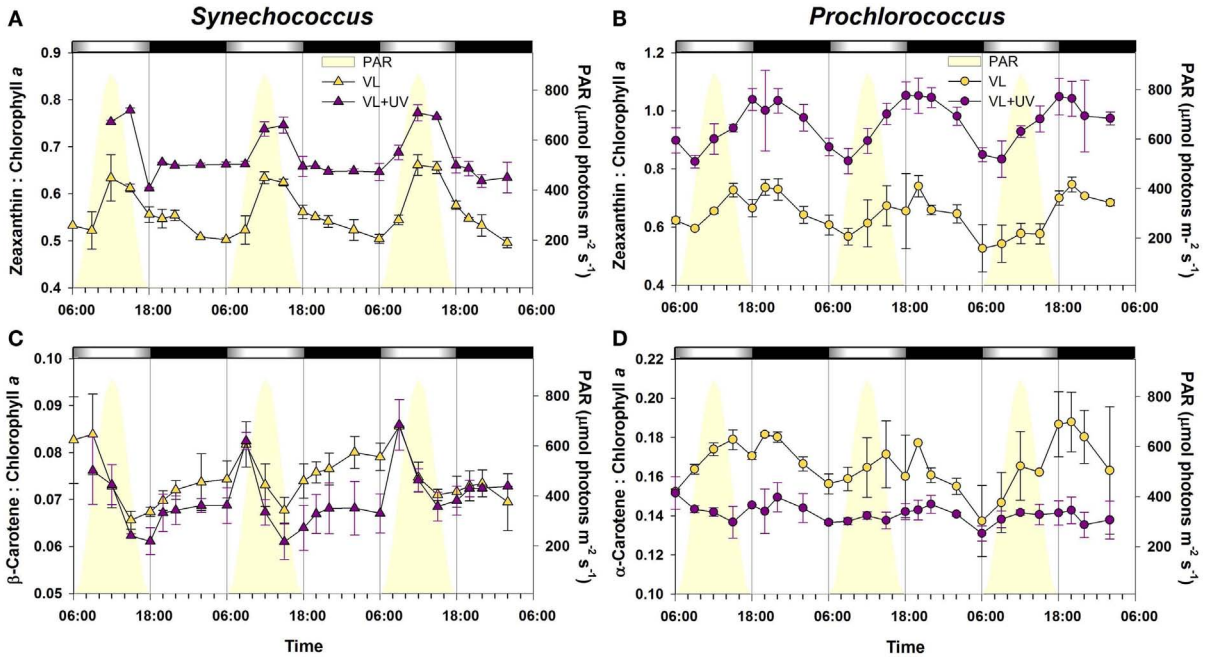

FIGURE 2 | Daily variations of the ratios of the two major carotenoids (zeaxanthin and carotene) to chlorophyll *a* for picocyanobacterial cells acclimated to a modulated 12/12 h L/D cycle of VL with or without UV radiations. (A,C) *Synechococcus* sp. WH7803. **(B,D)** *Prochlorococcus marinus* PCC 9511. White and black bars above graphs indicate light and dark periods, also delineated by vertical bars and areas filled in yellow. Error bars indicate mean deviation for two biological replicates. Abbreviations as in **Figure 1**.

cells at the same time point. Furthermore, as for *Synechococcus*, *Prochlorococcus* sub-cultures sampled at noon were sensitive to lower H_2O_2 concentrations than cultures sampled at 6:00.

In order to compare the rates of decay of the PSII quantum yield obtained at various times of the day, F_V/F_M vs. H_2O_2 concentration curves for all time points (only those obtained for 6:00 and 12:00 are shown in **Figures 6A,B**) were fitted with a two-parameter hyperbolic decay function. The daily variations of the *b*-value, characterizing the global resistance of PSII to oxidative stress induced by H_2O_2 (see Materials and Methods), are shown in **Figures 6C,D**. As expected from results at 6:00 and 12:00 (**Figures 6A,B**), PSII proved to be much more sensitive to an artificially induced oxidative stress during the day than during the night in both picocyanobacteria. Still, *Synechococcus* PSII was seemingly much more resistant than *Prochlorococcus* to this stress, when applied in the dark. It is also worth noting that the sensitivity to oxidative stress was enhanced for UV-acclimated cells, especially in *Prochlorococcus*, which displayed a dramatic drop of the *b*-value at 09:00 compared to those grown in VL only. However, after this sharp mid-morning drop, the *b*-value rose again during the day in both strains.

TRANSCRIPTOMIC RESPONSE

Photosynthesis

The diel expression pattern of a selection of genes involved in photosynthesis and a number of other processes related to (or affected by) light or UV stress were analyzed by qPCR in *P. marinus* PCC 9511 and *Synechococcus* sp. WH7803 strains, grown under both VL and VL + UV conditions (**Figure 7**). As expected, photosynthetic genes were among those showing the strongest diel oscillations. In both strains, the daily variations of the total pools of *psbA* and *psbD* transcripts, encoding the two major subunits of the reaction center II (D1 and D2, respectively), closely matched the modulated fluctuations of growth irradiance, with a slight increase in the relative amplitude of the peak of *psbA* transcripts under UVR. It is worth noting that in the case of *Synechococcus*, which possesses four *psbA* genes (compared to only one in *P. marinus* MED4/PCC9511; Garczarek et al., 2008), this global expression pattern translates the temporal succession of the single copy gene encoding the D1.1 isoform (*SynWH7803_0784*) and the three copies encoding the D1.2 isoforms (*SynWH7803_0790*, *0366*, and *2084*), the former being repressed at noon and maximum at the LDT, while the three latter exhibited an opposite behavior (note that the expression levels of *SynWH7803_0366* and *2084* cannot be measured separately). Accordingly, the expression pattern of *PMM0743* and *SynWH7803_1216*, encoding the FtsH2 protease that is involved in the clearance of damaged D1 proteins from inactivated PSII (Komenda et al., 2006, 2010), showed a broad maximum during the period of highest photon fluxes (9:00–15:00) in both species. However, in *Prochlorococcus*, this gene showed a minimum at dusk, then a continuous increase during the dark period and the early morning, while in *Synechococcus* its relative expression levels were minimal all over the dark period from 18:00 to 6:00.

In contrast to reaction center II genes, the diel expression pattern of *psaB*, encoding one of the two major subunits of the PSI core, was very different between the two cyanobacteria. While in *Synechococcus* its expression level peaked between 15:00 and 18:00 and remained low for the rest of the L/D cycle, *Prochlorococcus*

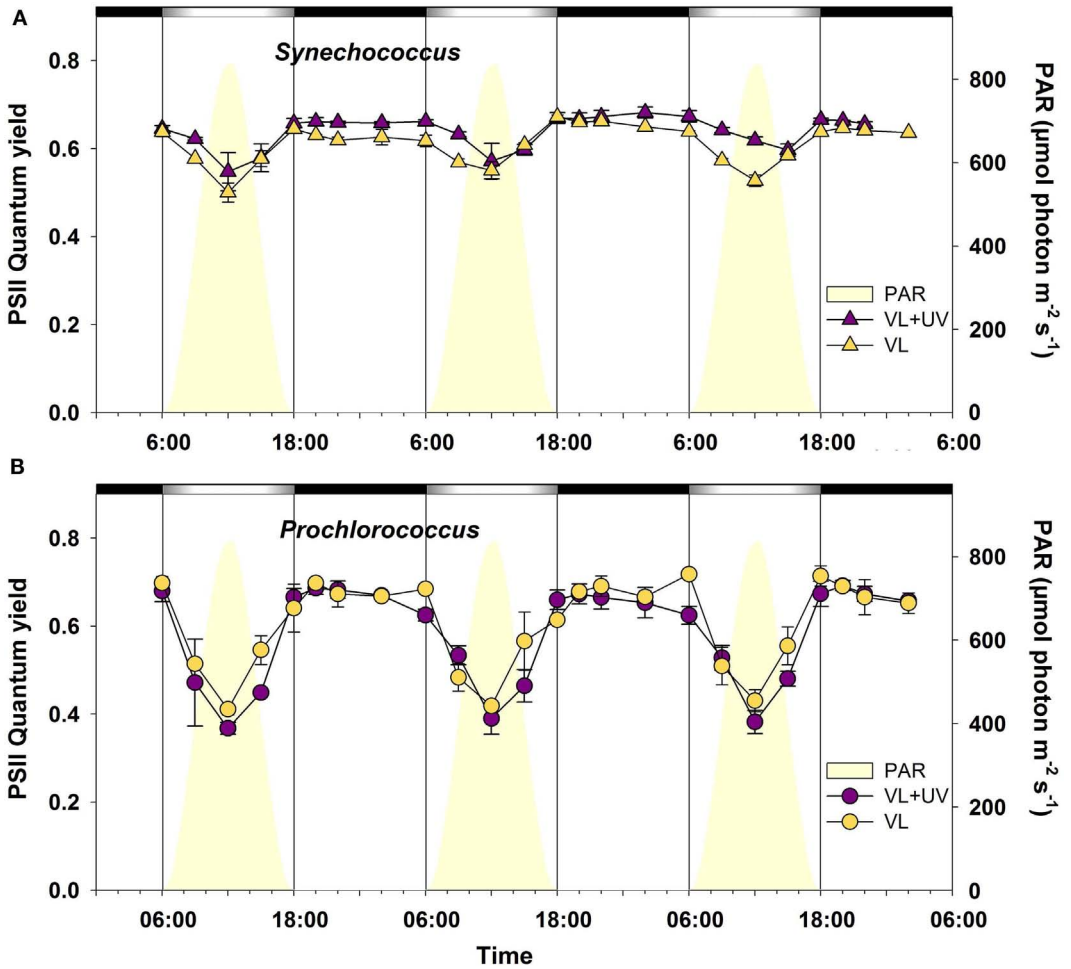

FIGURE 3 | Daily variations of the photosystem II maximal quantum yield (F_V/F_M) for picocyanobacterial cells acclimated to a modulated 12/12 h L/D cycle of VL with or without UV radiations. **(A)** *Synechococcus* sp. WH7803, **(B)** *Prochlorococcus marinus* PCC 9511. White and black bars above graphs indicate light and dark periods, also delineated by vertical bars and areas filled in yellow. Error bars indicate mean deviation for two biological replicates. Abbreviations as in **Figure 1**.

psaB transcript level was at its lowest around noontime and was maximal during the night period. Genes encoding light-harvesting systems also behaved quite differently between *Prochlorococcus* and *Synechococcus*. In the former organism, *pcbA* transcripts displayed a comparable pattern during the day to that of *psaB* transcripts with a significant downregulation in both light conditions, though the relative level of expression was even lower at noon for UV-irradiated cells. In contrast, for *Synechococcus* in VL, all genes encoding the different phycobiliprotein α-subunits (*apcA*, *rpcA*, *cpeA*, and *mpeA*) and phycoerythrin (PE) linkers (*cpeE*, *mpeD*, *mpeE*) were highly upregulated during the light period, with maximal expression at 15:00. While the expression patterns of genes coding for allophycocyanin, phycocyanin, and PEI subunits and their linkers were little affected by UVR, the expression of PEII genes showed a drop at noon. Interestingly, the *mpeE* gene, encoding the linker binding the distal PEII disk in this strain (Six et al., 2007c), even exhibited a 3-h delay of its maximal expression level in VL + UV compared to VL only.

Pigment biosynthesis genes also showed large variations of relative expression over the day under both light conditions. The *chlG* gene, encoding the chlorophyll *a* synthase, also behaved in an opposite way between *Prochlorococcus* and *Synechococcus*, with minimal and maximal expression levels at noon, respectively, in both cases more marked for UV-acclimated cells. Accordingly, the diel expression pattern of *PcCao*, a *Prochlorococcus*-specific gene encoding the chlorophyll *b* synthase (Satoh and Tanaka, 2006), also somewhat mirrored diel variations of growth irradiances. In contrast, the *ctrR* gene, encoding the β-Car hydroxylase that catalyzes the last biosynthesis step of zeaxanthin, usually considered as a photoprotective pigment, was maximally expressed during daytime in both organisms, but with a different global pattern, since in *Prochlorococcus* there was a strong surge in expression levels at 9:00 am followed by a progressive decline for the rest of the day, whereas in *Synechococcus* the diel pattern again closely matched the growth irradiance oscillations.

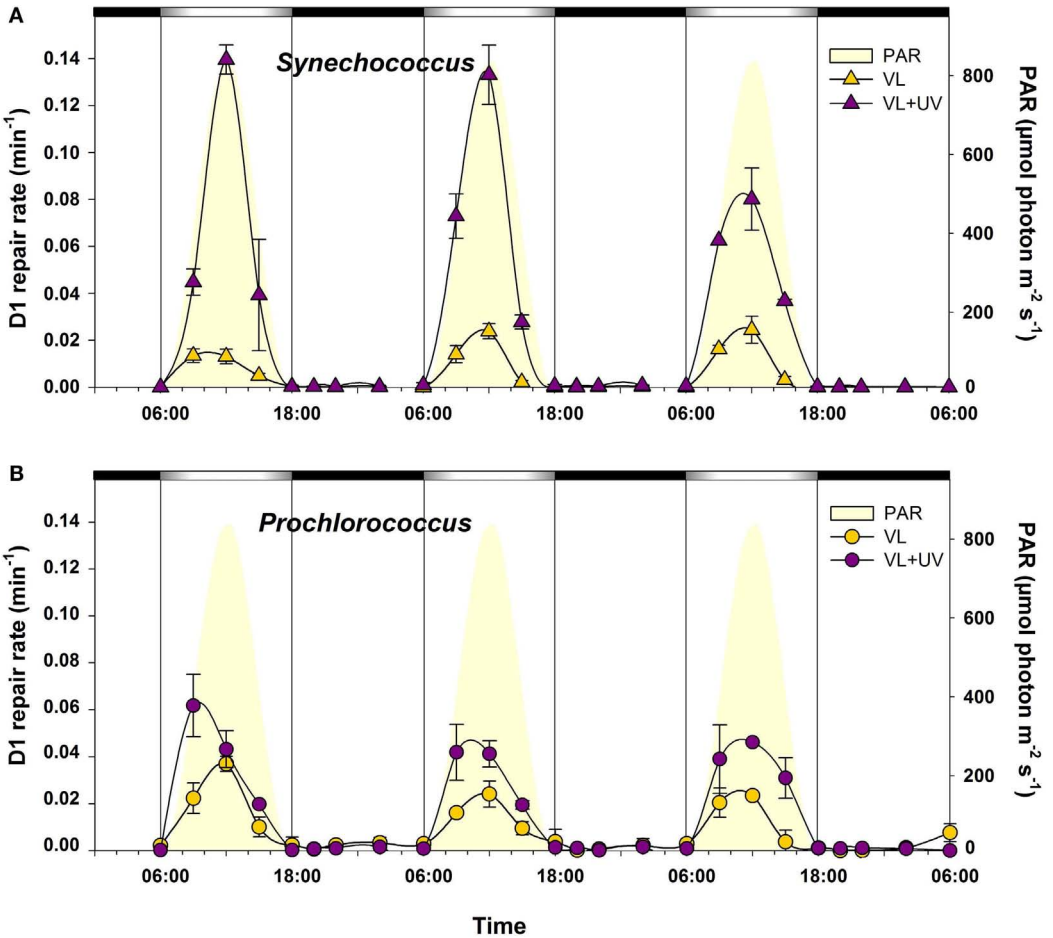

FIGURE 4 | Daily variations of the photosystem II repair activity for picocyanobacterial cells acclimated to a modulated 12/12 h L/D cycle of VL with or without UV radiations. (A) *Synechococcus* sp. WH7803, **(B)** *Prochlorococcus marinus* PCC 9511. White and black bars above graphs indicate light and dark periods, also delineated by vertical bars and areas filled in yellow. Error bars indicate mean deviation for two biological replicates. Abbreviations as in **Figure 1**.

Most marine *Synechococcus* strains, including WH7803, contain the *ocp* gene, which encodes the orange carotenoid protein (OCP), a pigment-protein complex likely located between the phycobilisomes (PBS) and the PSII reaction center and involved in the dissipation of excess energy as heat (Boulay et al., 2008; Kirilovsky and Kerfeld, 2012). In VL, WH7803 *ocp* was maximally expressed during the day with a peak at 9:00, whereas the expression maximum was considerably higher and broadened toward noontime in UV-acclimated cells, suggesting a key role of this gene in the protection against UVR. Although all *Prochlorococcus* strains lack *ocp*, due to the absence of functional PBS, high light-adapted *Prochlorococcus* strains (including MED4/PCC9511), low-light-adapted ecotype LLI (Scanlan et al., 2009) as well as a few marine *Synechococcus* strains (though not WH7803) possess another potentially important gene for photoprotection, *ptox*, which encodes a plastid terminal oxidase. This enzyme was suggested to extract electrons from the electron transport chain between PSII and PSI and to re-oxide the plastoquinone pool reduced by PSII (Bailey et al., 2008; Berg et al., 2011). Interestingly, *ptox* exhibited very large variations in relative expression with a maximum at 15:00 (**Figure 7**), though contrary to *ocp*, its diel expression pattern was virtually identical between VL and VL + UV.

The ATPase genes *atpD* et *atpH* showed similar expression patterns in *Synechococcus* with high values from 9:00 to 15:00 in VL and even higher under VL + UV, whereas expression of these genes decreased all over the day in *Prochlorococcus* followed by a night recovery (**Figure 7**; see also Figure S3 in Kolowrat et al., 2010). An opposite behavior between the two strains was also observed for the *rbcL* gene, coding for the large subunit of RuBisCO (ribulose-1,5-bisphosphate carboxylase/oxygenase), the major enzyme of the carbon fixation process, except that in *Prochlorococcus*, there was a much sharper drop of expression levels than for *atp* genes at 15:00 in VL, and at 18:00 under VL + UV (**Figure 7**).

The strikingly different diel expression patterns observed between *Prochlorococcus* and *Synechococcus* for genes involved in light-harvesting, ATP formation, as well as the light-independent reactions of photosynthesis (Calvin–Benson cycle) suggest that

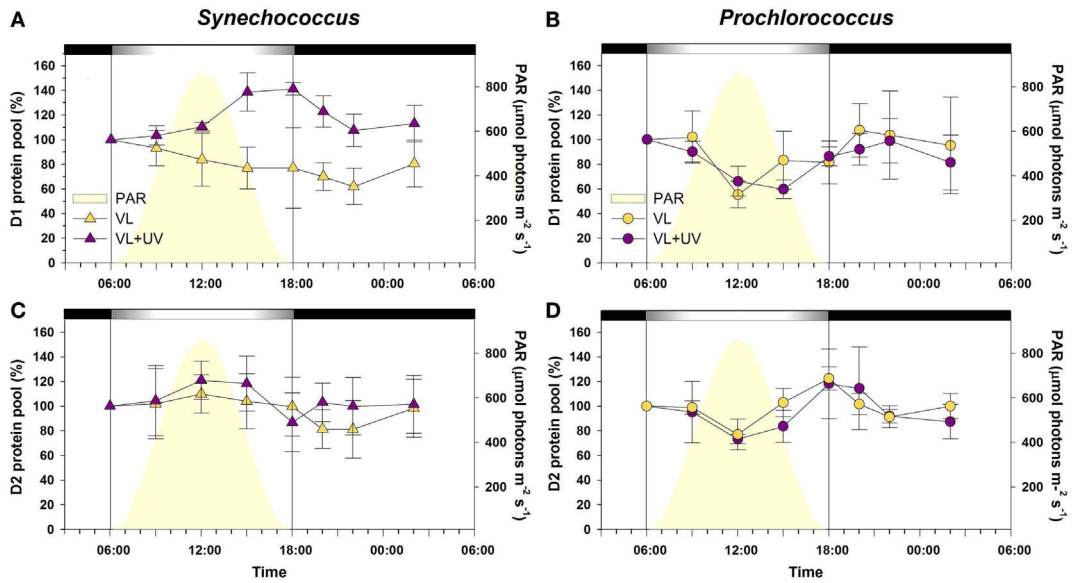

FIGURE 5 | Daily variations of the total pools of photosystem II core proteins D1 and D2 for picocyanobacterial cells acclimated to a modulated 12/12 h L/D cycle of high visible light with or without UV radiations. (A,C) *Synechococcus* sp. WH7803, **(B,D)** *Prochlorococcus marinus* PCC 9511. White and black bars above graphs indicate light and dark periods, also delineated by vertical bars and areas filled in yellow. Data represent the mean ± standard deviation ($n = 3$–4) of two biological replicates and two consecutive days. Abbreviations as in **Figure 1**.

most photosynthetic processes are probably controlled by distinct regulation networks in these two cyanobacteria, despite their close phylogenetic relatedness.

Redox and ROS detoxification

Most genes involved in the regulation of redox state and ROS detoxification pathways that are shared by *Synechococcus* sp. WH7803 and *P. marinus* PCC 9511 were differentially regulated during the L/D cycle in both picocyanobacteria and their diel expression patterns were comparable in VL and VL + UV conditions. However, the daily amplitudes of variations of ROS genes were often much larger in *Synechococcus* than in *Prochlorococcus*. Three of the most differentially expressed genes in the former organism, i.e., those coding for rubredoxin (*rub*), glutathione peroxidase (*SynWH7803_0151*), and a 2-cys peroxiredoxin (*2-Cys prx*), had their maximal daily expression around noontime, again suggesting a tight regulation by light, and their relative expression level significantly increased under UV. In contrast, in *Prochlorococcus*, orthologs of these three genes (*PMM0295*, *PMM1006*, and *PMM0856*, respectively) showed no clear diel pattern. Interestingly, for each cyanobacterium, the different peroxiredoxin gene copies exhibited diel patterns very distinct from one another.

Synechococcus sp. WH7803 and *P. marinus* PCC 9511 also possess specific sets of genes involved in ROS-scavenging systems. Among these strain-specific genes, it is worth noting that the catalase-peroxidase gene *katG* of *Synechococcus* was notably upregulated during the day, with a peak at 15:00, while *Prochlorococcus PMM0211*, a NADPH-dependent thioredoxin-disulfide reductase (NTR system) was by far the most differentially expressed ROS-scavenging gene of this organism, with a maximal expression at 18:00 in VL. At last, while the only *sod* gene present in *Prochlorococcus*, *sodN*, encoding a Ni-binding superoxide dismutase (SOD), was slightly downregulated at noon relative to nighttime in VL and VL + UV, *Synechococcus sodB*, encoding a Fe-binding SOD, was in contrast strongly upregulated during the light period under both conditions. The second *sod* gene of *Synechococcus*, *sodC* that encodes a Cu/Zn-binding SOD, showed only faint diel variations of its expression in VL, but was slightly downregulated at 20:00 in VL + UV.

Cell cycle, DNA repair, and circadian clock

In *Synechococcus* sp. WH7803, the DNA replication initiation factor gene *dnaA* was upregulated during the day with a broad peak of expression during the 9:00–15:00 time period in both light conditions. Subtle differences can however be noted between the two conditions, since the expression maximum seemingly occurred at 9:00 in VL and at noon in VL + UV (**Figure 7**). The *ftsZ* gene, which controls the biosynthesis of the Z-ring formed in the middle of the cell prior to cell division, showed very similar diel expression patterns to *dnaA*, except for systematically lower amplitudes of variations over the L/D cycle. The last cell cycle gene that was examined, *sepF*, which codes for a protein interacting with FtsZ during septum formation, showed a bell-shaped diel expression pattern peaking at 15:00 in both light conditions, though relative mRNA levels were again slightly higher in UV-acclimated cells.

In *P. marinus* PCC 9511 grown in VL, the *ftsZ* gene expression level peaked at 15:00, whereas *dnaA* and *sepF* both reached a maximum 3 h later. The relative expression levels of all three genes were considerably lower during the day when cells were grown under VL + UV, as previously reported (Kolowrat et al., 2010).

Since UVR are known to have deleterious effects on DNA structure, we also examined the diel expression patterns of a few

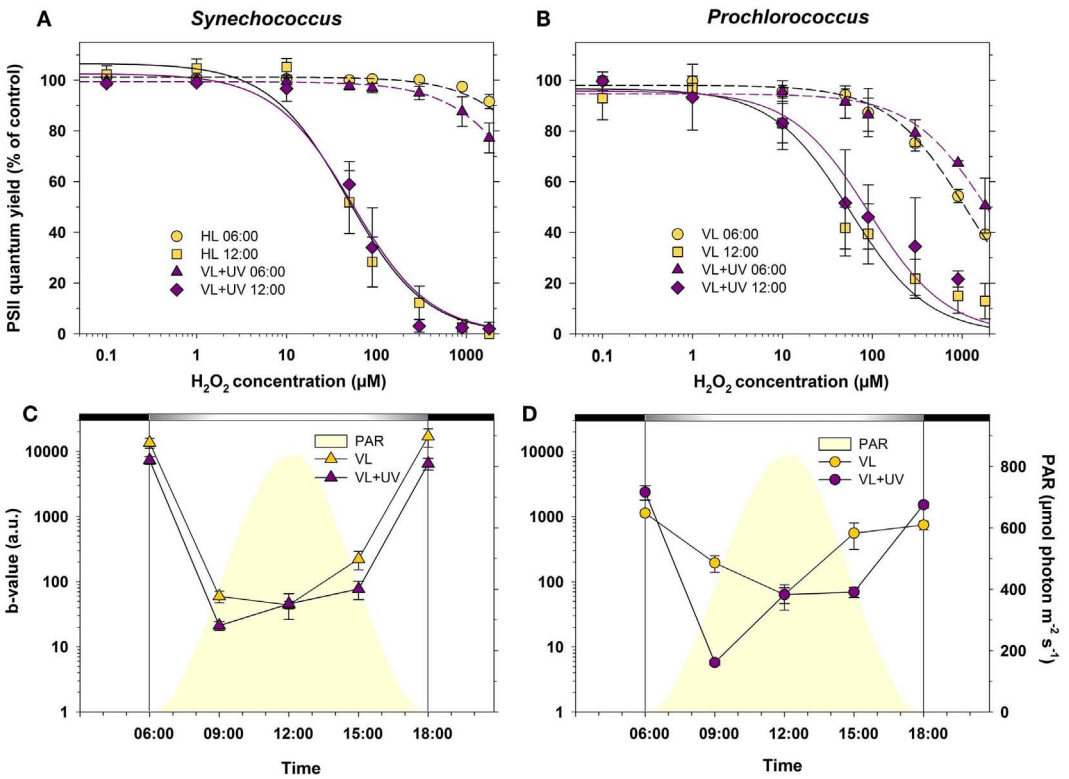

FIGURE 6 | Daily variations of photosystem II (PSII) resistance to oxidative stress for picocyanobacterial cells acclimated to a modulated 12/12 h L/D cycle of high visible light with or without UV radiations. (A,B) Maximal PSII quantum yield (F_V/F_M) measured at 06:00 and at noon, after 50 min exposure to a range of H_2O_2 concentrations of *Synechococcus* sp. WH7803 **(A)** or *Prochlorococcus marinus* PCC 9511 cells **(B)**. Data were fitted with a two-parameter hyperbolic decay function. **(C,D)** PSII resistance to oxidative stress in *Synechococcus* **(C)** and *Prochlorococcus* **(D)** cells, as estimated by the *b*-value (see Materials and Methods). White and black bars above graphs **(C,D)** indicate light and dark periods, also delineated by vertical bars and areas filled in yellow. Data represent the mean ± standard deviation ($n = 4$) of two biological replicates and two consecutive days. Abbreviations as in **Figure 1**.

genes involved in DNA repair pathways. The *recA* gene, which encodes an ATPase involved in the repair of double-strand breaks (DSBs) by homologous recombination (Chen et al., 2008), showed a broad maxima during daytime in *Synechococcus* cells grown in VL, while the relative expression of this gene was enhanced under VL + UV and remain high until 20:00 (**Figure 7**). In contrast, in *Prochlorococcus*, the *recA* expression peak occurred at the LDT in VL and was delayed by 2 h in the presence of UVR. The *uvrA* gene, encoding one subunit of the excinuclease UvrABC, an enzyme of the nucleotide excision DNA repair (NER) pathway, exhibited a sharp increase of its expression level during the lit period in both picocyanobacteria, with a peak at noon under both VL and VL + UV conditions. However, the maximal *uvrA* expression level was higher in UV-acclimated *Synechococcus* cells than in VL, whereas in *Prochlorococcus*, patterns were comparable between the two conditions (except at 9:00; **Figure 7**; Kolowrat et al., 2010).

Both picocyanobacteria also possess a family of genes related to DNA photolyases. In *Synechococcus*, the pattern of the photolyase gene *phrA* (Ng et al., 2000) closely matched the L/D cycle, with a peak at noon, which was threefold higher in VL + UV with regard to VL only (**Figure 7**). On the contrary, in *Prochlorococcus*, the *phrA* expression peak heights were similar in the two light conditions, even though the relative *phrA* mRNA level was higher at mid-morning in VL than VL + UV (Kolowrat et al., 2010). Like other marine *Synechococcus* but unlike *Prochlorococcus*, WH7803 possesses a second member of the DNA photolyase family (PhrB), which was recently suggested to be a cryptochrome (Goosen and Moolenaar, 2008). Interestingly, its diel expression pattern was quite similar to *phrA*, but with a reduced amplitude of variation of the relative mRNA amounts during daytime, even if there was again a very strong relative increase of the expression maximum under UV. The same was observed for a gene encoding an uncharacterized photolyase relative in *Synechococcus* (*SynWH7803_1271*), while its ortholog in *Prochlorococcus* (*PMM0425*) showed no clear diel pattern. Other, shorter members of the Phr family were also analyzed. Indeed, *Synechococcus* possesses a cluster of two genes (*SynWH7803_0266* and *0267*), each of which corresponds to one of the two domains of photolyases (photolyase and FAD-binding domains, respectively). So, once translated, they might potentially form an additional heterodimeric photolyase complex, as suggested by their diel pattern similar to *phrA* and high relative expression level (**Figure 7**). Interestingly, *Prochlorococcus* also possesses a gene (*PMM1360*) encoding a FAD-binding domain-containing protein, but surprisingly

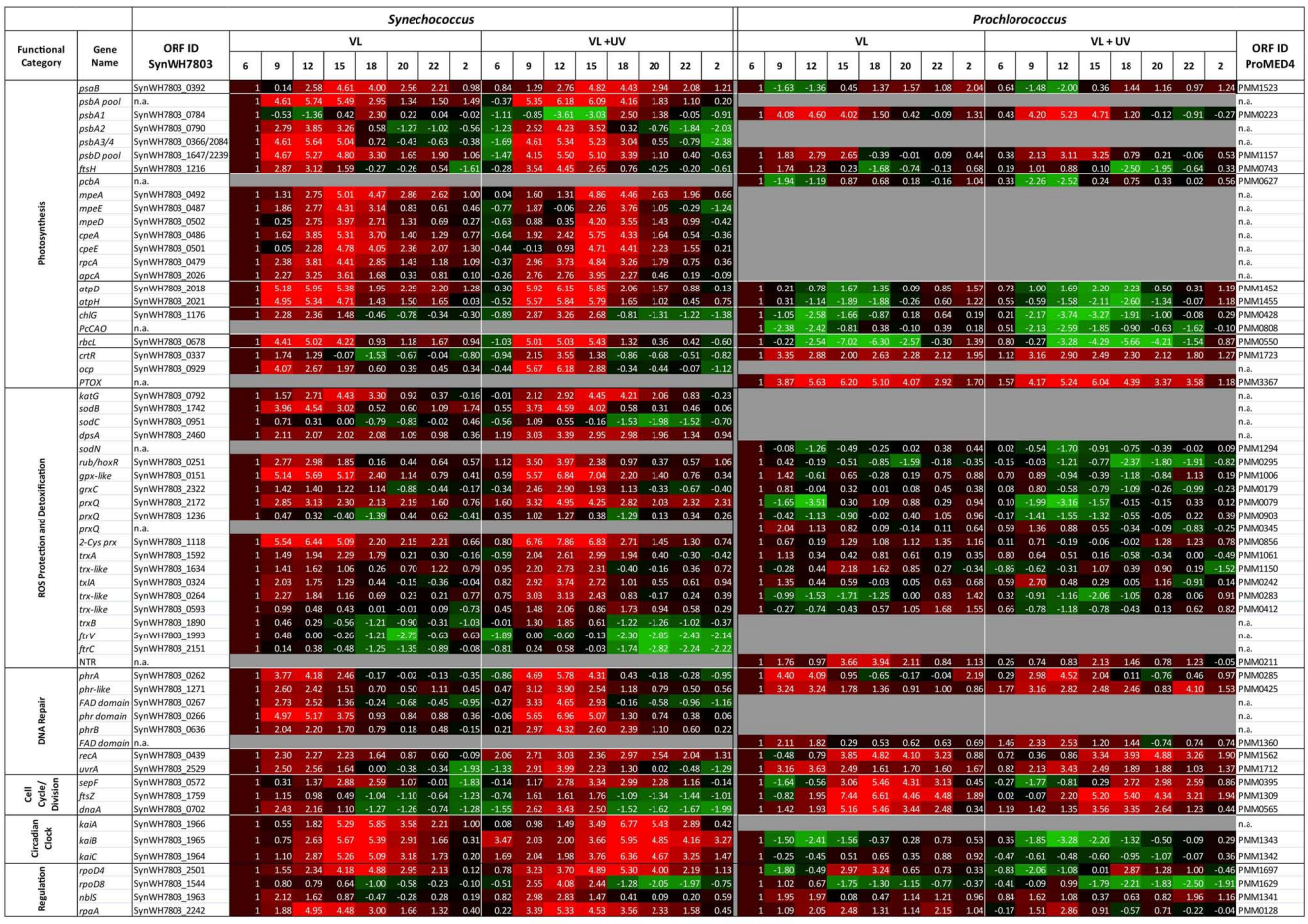

FIGURE 7 | Daily variations of the relative expression of selected genes, as measured by quantitative real time PCR, for picocyanobacterial cells acclimated to a modulated 12/12 h L/D cycle of high visible light with or without UV radiations. All data, expressed as $\log_2$ (Fold Change), were normalized to the value observed at 06:00 in the VL condition for each strain and are shown as a range of red (relative upregulation) or green (relative downregulation) colors, with intensity depending on gene expression levels, as indicated in the scale bar below the data. Genes are classified by functional categories, as indicated in the first column. A more detailed listing of these data showing mean deviation for two biological replicates as well as gene products is provided as Table S2 in Supplementary Material.

no gene coding for the other half of a photolyase (Scanlan et al., 2009; Partensky and Garczarek, 2010). Again, this gene had a very similar diel pattern as *phrA* from the same organism but with a much lower expression level.

The diel expression of genes involved into the circadian clock machinery was also studied given their central role in controlling global rhythmic transcriptional activity of the cells. While all marine *Synechococcus* possess the three *kai* genes coding for the core circadian oscillator, *Prochlorococcus* lacks *kaiA* and its circadian clock rather behaves like an "hourglass" that is reset every morning (Holtzendorff et al., 2008; Axmann et al., 2009). Interestingly, *kai* genes had a completely different behavior between the two cyanobacteria. In VL, all three *kai* genes of *Synechococcus* sp. WH7803 exhibited large diel variations with a broad maximum relative expression level at the end of the light period (15:00–18:00), while in *Prochlorococcus*, the expression of *kaiB* was minimal at noon, then increased continuously until dawn and there was no significant diel oscillation of *kaiC* mRNA. Presence of UVR caused a strong decrease of the level of expression of *kaiABC* genes at 15:00 in *Synechococcus* leading to a sharpening of their expression peaks, whereas in *Prochlorococcus*, the *kaiB* gene was further downregulated at noon without time shift. We also looked at the expression of *rpaA*, which codes for a DNA-binding protein acting as the response regulator of the KaiC-interacting kinase *SasA*, a two-component system that mediates the diel oscillations generated by KaiC phosphorylation to global transcription rhythms (Takai et al., 2006). RpaA is also known to be involved in the regulation of energy transfer from PBS to PSI and to interact with ferredoxin (Ashby and Mullineaux, 1999; Hanke et al., 2011). In both organisms, *rpaA* was maximally expressed around noon-time and UVR had no significant effect on its diel transcription pattern.

Two genes encoding type II σ factors (*rpoD4* and *rpoD8*), that have been shown to modulate gene expression under different

conditions and to respond to L/D stimuli (Imamura et al., 2003; Summerfield and Sherman, 2007), were also analyzed to assess their potential role in controlling global gene expression during L/D transitions. In *Synechococcus*, *rpoD4* exhibited a comparable diel expression pattern in VL and VL + UV, with a continuous increase during the day, a peak at the LDT then a progressive night decrease. In contrast, *rpoD8* showed only mild variations in VL while its diel pattern was prominent in UV-acclimated cells, with a strong upregulation during the day and a downregulation during the night. In *Prochlorococcus*, the pattern of these genes has been previously described (Kolowrat et al., 2010). Briefly, *rpoD8* has a low maximal expression in the mid-morning to noon period, whereas *rpoD4* peaked at the end of the light period (see also **Figure 7**).

At last, we looked at the expression of *nblS*, encoding a membrane-bound, sensor histidine kinase involved in the control by light of the expression of several photosynthesis-related genes, including all three *psbA* genes, the *cpcBA* operon, and some *hli* genes (van Waasbergen et al., 2002; Kappell et al., 2006). In VL, this gene was upregulated during the day with a peak in the morning and its maximum expression level increased almost twofold in the presence of UVR (**Figure 7**).

DISCUSSION

DIFFERENCES IN PHOTOSYSTEM ACTIVITY AND REGULATION BETWEEN *PROCHLOROCOCCUS* AND *SYNECHOCOCCUS*

The alternation of light and darkness is one of the most predictive events that cyanobacteria have to deal with in the field. Strong variations of PAR occur over a daily timescale and are associated, in near surface waters, with concomitant changes of UVR fluxes. Here, we compare PCC9511, a strain representative of the *Prochlorococcus* HLI clade found in near surface oligotrophic waters, to WH7803, a *Synechococcus* strain characteristic of mesotrophic areas. Although these model strains do not represent the whole physiological diversity existing within these two genera, our data clearly show that both *Prochlorococcus* and *Synechococcus* cells are able to tune their photosynthetic apparatus to diurnal irradiance fluctuations. However, *Prochlorococcus* proved to be more sensitive than *Synechococcus* to photoinhibition by high photon fluxes, as suggested by a marked drop of the cellular pool of PSII core proteins (**Figure 5**) and a larger decrease of the PSII quantum yield (**Figure 3**) around noontime. It is noteworthy however that the latter phenomenon might also partly be due to NPQ of PSII fluorescence associated with photoprotective dissipation of light energy as heat (Bailey et al., 2005; Boulay et al., 2008). The diel changes of the photosynthetic activity observed here for *P. marinus* PCC 9511 (**Figure 3**) are quite comparable with those previously described for this strain grown in similar light conditions (Bruyant et al., 2005), except that our cultures exhibited a higher F_V/F_M during the night (∼0.7 vs. ∼0.55), likely translating a slightly better physiological status. However, they contrast with those obtained on the closely related MED4 strain by Zinser et al. (2009), who did not observed any significant diel variation of the F_V/F_M, likely because it was grown at lower irradiance (∼230 vs. 870 μmol photon m^{-2} s^{-1} here) and over a different L/D cycle (14/10 vs. 12/12 h). Another noticeable observation from our study was that UVR did not cause any appreciably stronger photoinhibitory effect than VL in both genera, likely due to an increased repair rate under VL + UV compared to VL. However, this UV-induced repair was much more important for *Synechococcus* than *Prochlorococcus* (∼twofold vs. ∼fivefold at noon, respectively). Accordingly, in the former organism, the relative D1 content was enhanced in the presence of UVR, while in *Prochlorococcus* the noontime drop of D1 was somewhat extended for UV-acclimated cells (see also transcriptomic analyses of the *psbA* genes below). These results are consistent with those obtained by Six et al. (2007a), who observed that in response to a transient high light exposure, *P. marinus* PCC 9511 exhibited a lower PSII repair rate (0.9 PSII gained per second) than a range of marine *Synechococcus* strains (1.1–1.6 PSII s^{-1}). In both strains in VL, this rate was more or less proportional to the instantaneous irradiance. However for cells grown under VL + UV, while the repair rate was comparable between the two strains at 9:00 and 15:00, it was significantly depressed at noon in *Prochlorococcus* compared to *Synechococcus*. This suggests that the PSII repair capacity of *Prochlorococcus* was already maximum around 400 μmol photons m^{-2} s^{-1} (**Figure 4B**).

The occurrence of different D1 encoding gene copies in *Prochlorococcus* and *Synechococcus* could, at least partially, explain such a distinct behavior. Indeed, while *Prochlorococcus* strains have one to three identical *psbA* gene copies (one in PCC 9511), coding for a single D1:1-like isoform (Hess et al., 1995; Partensky and Garczarek, 2003), *Synechococcus* strains possess three to six *psbA* genes, with only one copy coding for a D1:1 isoform and two to five copies (three in WH7803), coding for D1:2 isoforms (Garczarek et al., 2008). The respective role of these isoforms has been widely studied in the literature, both in freshwater cyanobacteria (Bustos et al., 1990; Clarke et al., 1993; Campbell et al., 1995, 1998a; Sass et al., 1997; Kos et al., 2008) and in marine picocyanobacteria (Garcia-Fernandez et al., 1998; Garczarek et al., 2008). Although some variations among cyanobacteria have been observed, it is generally accepted that the D1:1 isoform would confer a higher PSII activity (Campbell et al., 1996), while D1:2 would provide a lower quantum yield but a higher PSII resistance to photoinhibition (Krupa et al., 1991;Campbell et al., 1995, 1998a; Tichy et al., 2003). A variety of environmental cues, including UV exposure, can induce the exchange of these isoforms (Sicora et al., 2006, 2008; Garczarek et al., 2008; for a review, see Bouchard et al., 2006). Here, we indeed noticed in *Synechococcus* sp. WH7803 an opposite expression pattern of D1:1 (*SynWH7803*_0784) and D1:2 isoforms encoding genes (*SynWH7803_0790*, *0366*, and *2084*) during daytime (**Figure 7**). It is worth noting that while there were only slight discrepancies in the expression levels of the different D1:2 encoding genes between VL and VL + UV, the D1:1 encoding gene was about fivefold more repressed at noon under the latter condition, suggesting a complete replacement of the D1:1 isoform by D1:2 isoform(s) that may contribute to the slight midday decrease in PSII quantum yield (**Figure 3**). Interestingly, although the single isoform in *Prochlorococcus* is phylogenetically a D1:1 isoform, as confirmed by the occurrence of a Gln residue at position 130 of the amino acid sequence (instead of Glu in D1:2; Clarke et al., 1993; Giorgi et al., 1996), its transcriptomic pattern was clearly closer from that of D1:2 isoforms, at least in our culture conditions. It is likely however that it presents a lower resistance to PSII

photoinactivation compared to a true D1:2, as suggested by the larger drop of F_V/F_M at noon (**Figure 3**) and the concomitant lower PSII repair rate (**Figure 4**), compared to *Synechococcus*.

Interestingly, the D2 subunit of the PSII core is also encoded by a single *psbD* gene in all *Prochlorococcus* genomes, whereas all *Synechococcus* sequenced so far possess two nearly identical *psbD* genes, as in most other cyanobacteria (such as e.g., *Synechococcus* sp. PCC 7942; Golden et al., 1989), with one co-transcribed with *psbC* that encodes the internal PSII antenna protein CP43 (Garczarek et al., 2001) and the other isolated in the genome. It is likely that as for *psbA*, the two copies are differently regulated in response to light and/or UV stress as previously reported in freshwater model cyanobacteria (Bustos and Golden, 1992; Kos et al., 2008), although this was not checked in the present study. Alternatively, this may simply contribute to a higher expression level of this key photosynthetic gene, possibly enabling a higher turnover of the corresponding protein.

Another strategy used by cyanobacteria to cope with excess light energy is to decrease the relative amount of PSI reaction center complexes, an adjustment that was shown to decelerate the rate of photosynthetic electron transport (Murakami and Fujita, 1991; Hihara et al., 1998; Muramatsu and Hihara, 2003). Indeed, experiments on *Synechocystis* sp. PCC 6803 mutants impaired in their ability to modulate photosystem stoichiometry showed that this capacity is indispensable for growth under continuous high irradiance (Hihara et al., 1998; Fujimori et al., 2005). Accordingly, in *Synechococcus* sp. WH7803 the relative *psaB* levels were low before dawn (**Figure 7**), likely reflecting a lower PSI cell content at this time of the day, as previously observed in *Crocosphaera watsonii* (Saito et al., 2011). In contrast, this was not the case in *Prochlorococcus*, in which PSI core transcripts were maximal over most of the dark period.

DIFFERENTIAL REGULATION OF LIGHT-HARVESTING SYSTEMS IN RESPONSE TO HIGH LIGHT AND UV RADIATIONS

The striking structural differences between the major PSII antenna complexes of *Prochlorococcus* and *Synechococcus* may also be partially responsible for the different sensitivity of these picocyanobacteria to UV stress. Indeed, whilst *Synechococcus*, as most cyanobacteria, possess a large membrane-extrinsic antenna, the PBS (Sidler, 1994; Six et al., 2007c), *Prochlorococcus*, like the other two green oxyphotobacteria, *Prochloron* and *Prochlorothrix*, use a transmembrane Chl *a/b*-binding Pcb antenna (LaRoche et al., 1996; Garczarek et al., 2003; Partensky and Garczarek, 2003). These dissimilar antenna structures may have important consequences on the way excitation energy is funneled downhill toward the reaction centers, on the regulation of this process as well as on the amount and nature of damages caused by UVR on *Prochlorococcus* and *Synechococcus* cells, since both organisms show some absorption capacities in the 300- to 400-nm band, which are likely related to their antenna (see e.g., Ong and Glazer, 1991; Claustre et al., 2002). Comparing and monitoring UV cross-sections for both picocyanobacteria would help answering this question.

Here, we indeed observed an opposite expression pattern between the genes encoding antenna systems from these two organisms, with a strong downregulation of the *pcb* gene in *Prochlorococcus* during day time under VL (see also Garczarek et al., 2001) that was even more dramatic under VL + UV, while all examined PBS genes were upregulated in the afternoon in both light conditions (**Figure 8**). A similar result was previously obtained in L/D-entrained *Cyanothece* sp. ATCC 51142 cultures, though in the latter case maximum expression was centered at midday (Toepel et al., 2008). These observations suggest that the biosynthesis of antenna complexes occurs at different times of the day in the two picocyanobacteria and is under different light regulation controls. The fact that PBS genes remained upregulated under VL + UV suggests that the buildup of PBS complexes was only moderately affected by these radiations. This contrasts with a previous study where cultures of *Synechococcus* sp. WH8102 grown in continuous low-light were subjected to a sudden shift to UV (Six et al., 2007b). This stress provoked a strong decrease in the relative expression of all PBS genes, associated with a disconnection of the PBS complexes from the thylakoid membrane as well as a dissociation of the distal PEII disks of PBS rods. In the present study, where cells were acclimated to either VL or VL + UV for several weeks, the PE to PC fluorescence emission ratio did not exhibit a peak at noon in either light condition, as would be expected if terminal PE subunits (i.e., PEII) were disrupted (**Figure A1** in Appendix). The higher values of this ratio in UV-acclimated *Synechococcus* cells are likely not related to a higher PE content of the PBS, but rather to permanently decoupled PEII subunits, which would dissipate incident light as fluorescence. Consistently, UV also induced a slight drop of the expression of most PEII genes at noon and a 3-h delay in the timing of the expression peak of *mpeE*, which encodes the linker binding the terminal PEII disk in *Synechococcus* sp. WH7803 (Six et al., 2007c).

DIFFERENTIAL PHOTOPROTECTION MECHANISMS

Prochlorococcus and *Synechococcus* have also developed specific mechanisms to dissipate excess light energy. Most *Synechococcus* strains possess one gene encoding the orange carotenoid protein (OCP; for a recent review, see Kirilovsky and Kerfeld, 2012), which is thought to mediate energy dissipation as heat through interaction with the PBS core, thus inducing a NPQ of PSII fluorescence. Here, we observed that the *ocp* gene was upregulated during daytime in VL and that UVR dramatically enhanced its expression in the early light period that may trigger a temporary increase of the OCP cellular pool and/or activity. To our knowledge, this is a first time that UV is shown to control the expression of this gene since it is usually believed that OCP is only blue light sensitive (Wilson et al., 2008; Kirilovsky and Kerfeld, 2012).

While all *Prochlorococcus* strains lack OCP, all high light-adapted strains (including PCC 9511) and some low-light-adapted strains possess an homolog of *PTOX*, which is thought to extract electrons between PSII and PSI and to combine them with protons and oxygen to generate water (Bailey et al., 2005, 2008). The *ptox* gene was (with *ftsZ*) one of the two most differentially expressed genes among those analyzed here in PCC 9511, with a maximal relative fold change over the day of ∼73-fold [or log2(FC) = 6.2] at 15:00. These high values are consistent with previous results on the closely related strain *P. marinus* MED4 (Zinser et al., 2009; Berg et al., 2011). So the alternative electron flow to oxygen triggered by PTOX might be an important mechanism used by *Prochlorococcus* to struggle against excess light energy arising to PSII (Bailey

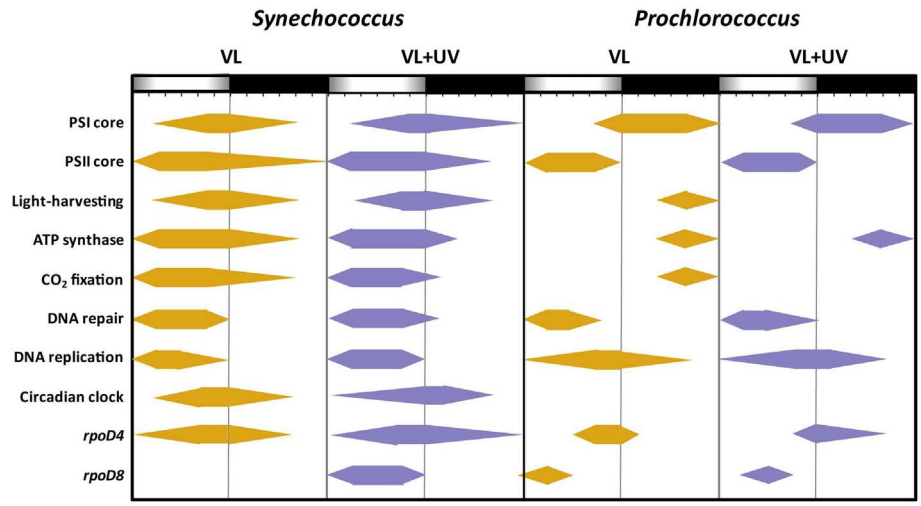

FIGURE 8 | Scheme of the daily patterns of gene upregulation for several important functional for picocyanobacterial cells acclimated to a modulated 12/12 h L/D cycle of high visible light with or without UV radiations. This figure, derived from **Figure 7**, shows for each individual the time intervals during which they were significantly upregulated [$|\log_2$ (Fold Change)$| > 1.0$], with regard to the expression level measured at 6:00 in VL.

et al., 2008; Berg et al., 2011), although high light induced proteins (HLIPs), which were not analyzed in the present study, are also likely important contributors in this process (He et al., 2001).

Other key actors in photoprotection mechanisms are carotenoids. While the cellular localization and precise action mechanism of Zea is unclear yet, Car are known to be mostly bound to PS reaction centers, two of them in close vicinity of Chls, and help mitigate oxidative damages, mainly by quenching the $^1O_2$ species resulting from the de-excitation of Chl triplets (Telfer, 2005). Both Zea:Chl *a* and Car:Chl *a* ratios appeared to be tightly coupled to the L/D cycle in *Synechococcus*, but less so in *Prochlorococcus*, for which we observed a continuous increase of both ratios during most of the day and a symmetrical drop during the night concomitant with cell division, as previously noticed by Claustre et al. (2002). In *Synechococcus*, the sharp drop of the β-Car:Chl *a* ratio from noon to dusk, which was more pronounced in UV-exposed cells (**Figure 2C**), likely reflects the progressive destruction of β-Car molecules by oxidative stress (Telfer, 2005). β-Car was then seemingly regenerated at low rate during the night, then much more rapidly during the first hours of the day, suggesting a light-dependency of the β-Car biosynthesis process, as previously reported in other cyanobacteria (Steiger et al., 2005; Ryu et al., 2010). Similarly, the light-modulated variations of the Zea:Chl *a* ratio during the day in *Synechococcus* in both light conditions could be due either to a higher degradation rate of Chl *a* relative to Zea or to a higher synthesis rate of the latter pigment, a likely photoprotective mechanism against high mid-day photon fluxes. The observed strong upregulation of *crtR* at high irradiances tend to favor the second hypothesis (**Figure 7**). A further increase of the relative *crtR* transcript levels at noon in VL + UV, which was not translated into a significantly higher mid-day increase in the Zea:Chl *a* ratio than in VL (**Figure 3A**), suggests that Zea msolecules might have a particularly high turnover under UV. In both genera, the systematically higher values of Zea:Chl *a* ratio under VL + UV than VL only suggest that UV exposure induces a comparable response as a long-term acclimation to high irradiance, as previously reported in other marine cyanobacterial strains (Kana and Glibert, 1987; Moore et al., 1995; Six et al., 2004). Altogether, our results suggest the occurrence of a light-controlled anabolism/catabolism cycle of both photoprotectants (Car and Zea) in *Synechococcus*, while diel changes in the pigment content of *Prochlorococcus* cells were rather related to the cell division cycle or other factors not analyzed here such as PS stoichiometry and/or antenna size.

DIFFERENTIAL PROTECTION MECHANISMS AGAINST REACTIVE OXYGEN SPECIES-INDUCED DAMAGES

Light-harvesting complexes are not only sources but also major targets of ROS (Sies and Menck, 1992; Krieger-Liszkay, 2005). Because of their localization within the thylakoid membrane around PSII complexes (Bibby et al., 2003), the divinyl-Chl *a*/*b*-binding Pcb antennae of *P. marinus* PCC 9511 likely produce ROS, particularly noxious for this photosystem. Indeed, it has been shown in other Chl *b*-containing organisms that excited singlet Chls lead to the synthesis of Chl triplet states that can react with $^3O_2$ to produce the very reactive species $^1O_2$ (Sies and Menck, 1992; Krieger-Liszkay, 2005). Assays performed here by directly adding H_2O_2 to sub-cultures at different time points of the modulated L/D cycle strongly suggest that the effect of ROS increased in a light-dependent manner for both organisms. Consistently, a synergistic effect of light and oxidative stress on PSII photoinactivation was previously demonstrated by Blot et al. (2011) who showed in *Synechococcus* sp. WH7803 that ROS may induce PSII inactivation through both direct damages to the reaction center II and inhibition of the PSII repair cycle. The latter phenomenon resulted in faster PSII inactivation in high light- than in low-light-acclimated cultures, due to their higher D1 turnover. Furthermore, *Prochlorococcus* was also more sensitive to H_2O_2-triggered stress than *Synechococcus* during the night, which might be related to a lower intrinsic resistance of its PSII.

The difference in ROS sensitivity between *Prochlorococcus* and *Synechococcus* strains might be explained, at least partially, by a more complete set of genes involved in ROS protection and detoxification in *Synechococcus*. Indeed, most *Prochlorococcus* lineages have experienced an extensive genome streamlining during evolution, resulting in the loss of a large number of non-essential but potentially useful genes in this context (**Figure 7**; Dufresne et al., 2005; Scanlan et al., 2009; Partensky and Garczarek, 2010). For instance, while *Synechococcus* sp. WH7803 synthesizes one catalase/peroxidase (KatG), *Prochlorococcus* has neither catalases nor peroxidases. *Prochlorococcus* also lack the *ftrC* and *ftrV* genes, encoding the two subunits of ferredoxin-thioredoxin reductase (FTR), as well as one ferredoxin and one thioredoxin, potentially associated to this complex (Dufresne et al., 2008). Furthermore, while *Synechococcus* possesses two superoxide dismutase (SOD), one Fe-type and one Cu-Zn-type, *Prochlorococcus* has only one, Ni-type SOD (SodN; Scanlan et al., 2009). In the present study, the expression levels of most ROS genes showed strikingly higher amplitudes of variation over the day in *Synechococcus* than in *Prochlorococcus*. Even though transcriptomic data are not necessarily synchronized with the activity of the corresponding enzymes, the lower resistance of *Prochlorococcus* to high VL and UVR could at least partially be due to a higher sensitivity to light-driven oxidative stress.

CONCLUSION

The comparison of *Synechococcus* and *Prochlorococcus* cultures acclimated to VL supplemented or not with UVR revealed relatively few physiological responses specific to UV. This notably includes a shift of the DNA synthesis phase (**Figure 1**; see also Kolowrat et al., 2010), an increase of the Zea:Chl *a* ratio (**Figure 2**) and an enhanced PSII repair rate (**Figure 4**). Accordingly, UVR seemingly also had limited effects at the transcriptomic level, as shown by the globally similar diel expression patterns between VL and VL + UV in both strains (**Figures 7** and **8**). It is worth noting however that the relative expression of a few genes was either enhanced (e.g., *psbD* in both strains, D1:2 encoding genes and *crtR* in *Synechococcus* only) or reduced (e.g., *Synechococcus* D1:1 encoding gene or *Prochlorococcus pcbA*) in UV-acclimated cultures. A handful of genes, including *rpoD4*/8 in *Prochlorococcus* and *kaiABC* in *Synechococcus*, also exhibited a delayed expression peak by about 3 h. However, this surprisingly did not translate into any conspicuous changes in the diel patterns of most of the other genes examined here, as could have been expected from the known regulatory role of the circadian clock and sigma factors on gene transcription (see e.g., Summerfield and Sherman, 2007; Ito et al., 2009).

The most striking result of the present study is likely the markedly distinct response to diurnal light variations between *Prochlorococcus* and *Synechococcus*, despite their close phylogenetic relatedness (Scanlan et al., 2009). These two picocyanobacteria indeed exhibited very different degrees of PSII photoinactivation at noon that can be partly explained by their distinct (i) PSII repair capacity (**Figure 4**; see also Six et al., 2007a), (ii) ability to modulate photoprotective pigments (Zea and Car, **Figure 2**), and (iii) resistance capacity against oxidative stress (**Figure 6**). Comparative transcriptomic analyses also revealed that, in *Synechococcus*, genes coding for a number of protective systems were maximally expressed during hours of highest irradiance, i.e., when these mechanisms are most critical to cope with transitory stressful conditions. This includes several genes involved in ROS detoxification enzymes, DNA repair genes as well as genes involved in photoprotection and/or dissipation of excess energy, such as *crtR* and *ocp* (**Figure 7**). In contrast, in *Prochlorococcus*, very few genes of these pathways, including *ptox* and *psbA*, were maximally expressed around midday, while others, such as *phrA* and *crtR*, had already reached their maximal (saturating) expression at mid-morning. Furthermore, many photosynthetic genes that were upregulated during the day in *Synechococcus* were in contrast downregulated in *Prochlorococcus*, including the PSI core gene *psaB* as well as genes involved in light-harvesting, ATP synthase and CO_2 fixation (**Figure 8**). Similarly, *glgA* (encoding glycogen synthase) mRNA abundance was recently shown to exhibit a maximum diel expression at midday in *Synechococcus* sp. WH8103 grown under a 16/8-h L/D cycle, while it peaked in concert with *rbcLS* in *Prochlorococcus marinus* MED4 during the LDT (Wyman and Thom, 2012). Thus altogether, it seems that while *Synechococcus*, as many other cyanobacteria (Kucho et al., 2004, 2005; Stockel et al., 2008; Toepel et al., 2008, 2009; Shi et al., 2010), efficiently copes with the diurnal changes in photon fluxes, *Prochlorococcus* rather displays a stress-like response at midday. The latter response is most likely related to the high irradiance level used in the present study (reaching 870 μmol photons m^{-2} s^{-1} at noon), which are typically found in the upper mixed layer of tropical oligotrophic oceans (Holtzendorff et al., 2001). Indeed, several genes that were found here to be downregulated during the light period (e.g., *pcb*, *rbcL*, *chlG*) were in contrast upregulated in *Prochlorococcus* cultures grown at lower irradiances, provided as continuous (Berg et al., 2011) or cyclic light (Zinser et al., 2009). Despite the very atypical transcriptomic response observed here, *Prochlorococcus* was able to recover high PSII quantum yield at night and to maintain an optimal growth rate under these conditions. Thus, we hypothesize that, in contrast to *Synechococcus* sp. WH7803, *P. marinus* PCC 9511 cells manage to cope with harmful light conditions by bringing down temporarily some of the main metabolic processes and by launching a minimal set of protection mechanisms during stressful hours. Whether the absence of a true circadian clock in *Prochlorococcus* (Holtzendorff et al., 2008; Axmann et al., 2009) is involved in this differential management of excess light compared to *Synechococcus* still remains to be investigated.

Altogether, our study reinforces previous studies depicting *Prochlorococcus* as a very specialized organism restricted to a narrow environmental niche, while *Synechococcus* has adopted a generalist strategy enabling it to cope with more variable environmental conditions, a difference consistent with the distinct habitats in which these two organisms predominate (Scanlan, 2003; Kettler et al., 2007; Dufresne et al., 2008; Scanlan et al., 2009).

ACKNOWLEDGMENTS

This work was supported by the French programs ANR PELICAN (PCS-09-GENM-200) and EMBRC France (INFRA-2010-2.2.5), the European Union programs MicroB3 (UE-contract-287589) MaCuMBA (FP7-KBBE-2012-6-311975). Daniella Mella-Flores was supported by the National Commission of Scientific and

Technological Investigation of Chile (CONICYT). We thank Roseline Edern, Fabienne Jalabert, and the Roscoff Culture Collection for maintaining the *Synechococcus* and *Prochlorococcus* strains used in this study.

SUPPLEMENTARY MATERIAL

The Supplementary Material for this article can be found online at http://www.frontiersin.org/Aquatic_Microbiology/10.3389/fmicb.2012.00285/abstract

Table S1 | List of primers used for real time PCR reactions. Most primers are targeting a specific gene. Exceptions include the *psbD pool* and *psbA pool* primers, which were designed to amplify the two *psbD* gene copies and all four *psbA* copies present in *Synechococcus* sp. WH7803, respectively. Furthermore, one primer set targets two *psbA* genes (*SynWH7803_0366* and *2084*), which have nearly identical coding sequence and 5′-UTR. Genes are classified by functional categories, as indicated in the first column. The Cyanorak database of picocyanobacteria protein families is publicly accessible at http://www.sb-roscoff.fr/Phyto/cyanorak/

Table S2 | Daily variations of the expression of selected genes, as measured by real time quantitative PCR, for picocyanobacterial cells acclimated to a modulated 12/12 h L/D cycle of VL with or without UV radiations. All data are expressed as $\log_2$ (Fold Change) ± mean deviation for two biological replicates. For each gene, transcript levels are normalized to the reference time point 6:00 in VL. Genes are classified by functional categories, as indicated in the first column. This table is a detailed version of **Figure 7** of the main manuscript.

REFERENCES

Agawin, N. S. R., Duarte, C. M., and Agusti, S. (2000). Nutrient and temperature control of the contribution of picoplankton to phytoplankton biomass and production. *Limnol. Oceanogr.* 45, 591–600.

Agusti, S., and Llabres, M. (2007). Solar radiation-induced mortality of marine pico-phytoplankton in the oligotrophic ocean. *Photochem. Photobiol.* 83, 793–801.

Allakhverdiev, S. I., and Murata, N. (2008). Salt stress inhibits photosystems II and I in cyanobacteria. *Photosyn. Res.* 98, 529–539.

Andersson, B., and Aro, E. M. (2001). "Photodamage and D1 protein turnover in photosystem II," in *Regulation of Photosynthesis*, eds E. M. Aro and B. Andersson (Dordrecht: Springer), 377–393.

Aro, E. M., Virgin, I., and Andersson, B. (1993). Photoinhibition of photosystem 2 – inactivation, protein damage and turnover. *Biochim. Biophys. Acta* 1143, 113–134.

Asada, K. (1999). The water-water cycle in chloroplasts: Scavenging of active oxygens and dissipation of excess photons. *Annu. Rev. Plant Physiol. Plant Mol. Biol.* 50, 601–639.

Ashby, M. K., and Mullineaux, C. W. (1999). Cyanobacterial ycf27 gene products regulate energy transfer from phycobilisomes to photosystems I and II. *FEMS Microbiol. Lett.* 181, 253–260.

Axmann, I. M., Duhring, U., Seeliger, L., Arnold, A., Vanselow, J. T., Kramer, A., and Wilde, A. (2009). Biochemical evidence for a timing mechanism in Prochlorococcus. *J. Bacteriol.* 191, 5342–5347.

Bailey, S., and Grossman, A. (2008). Photoprotection in cyanobacteria: regulation of light harvesting. *Photochem. Photobiol.* 84, 1410–1420.

Bailey, S., Mann, N. H., Robinson, C., and Scanlan, D. J. (2005). The occurrence of rapidly reversible non-photochemical quenching of chlorophyll a fluorescence in cyanobacteria. *FEBS Lett.* 579, 275–280.

Bailey, S., Melis, A., MacKey, K. R., Cardol, P., Finazzi, G., Van Dijken, G., Berg, G. M., Arrigo, K., Shrager, J., and Grossman, A. (2008). Alternative photosynthetic electron flow to oxygen in marine *Synechococcus*. *Biochim. Biophys. Acta* 1777, 269–276.

Berg, G. M., Shrager, J., Van Dijken, G., Mills, M. M., Arrigo, K. R., and Grossman, A. R. (2011). Responses of *psbA*, *hli* and *ptox* genes to changes in irradiance in marine *Synechococcus* and *Prochlorococcus*. *Aquat. Microb. Ecol.* 65, 1–14.

Berry, J., and Björkman, O. (1980). Photosynthetic response and adaptation to temperature in higher plants. *Annu. Rev. Plant Physiol. Plant Mol. Biol.* 31, 491–543.

Bibby, T. S., Mary, I., Nield, J., Partensky, F., and Barber, J. (2003). Low-light-adapted *Prochlorococcus* species possess specific antennae for each photosystem. *Nature* 424, 1051–1054.

Blot, N., Mella-Flores, D., Six, C., Le Corguille, G., Boutte, C., Peyrat, A., Monnier, A., Ratin, M., Gourvil, P., Campbell, D. A., and Garczarek, L. (2011). Light history influences the response of the marine cyanobacterium *Synechococcus* sp. WH7803 to oxidative stress. *Plant Physiol.* 156, 1934–1954.

Bouchard, J. N., Roy, S., and Campbell, D. A. (2006). UVB effects on the photosystem II D1 protein of phytoplankton and natural phytoplankton communities. *Photochem. Photobiol. Sci.* 82, 936–951.

Boulay, C., Abasova, L., Six, C., Vass, I., and Kirilovsky, D. (2008). Occurrence and function of the orange carotenoid protein in photoprotective mechanisms in various cyanobacteria. *Biochim. Biophys. Acta* 1777, 1344–1354.

Bruyant, F., Babin, M., Genty, B., Prasil, O., Behrenfeld, M. J., Claustre, H., Bricaud, A., Garczarek, L., Holtzendorff, J., Koblizek, M., Dousova, H., and Partensky, F. (2005). Diel variations in the photosynthetic parameters of *Prochlorococcus* strain PCC 9511: combined effects of light and cell cycle. *Limnol. Oceanogr.* 50, 850–863.

Bustos, S. A., and Golden, S. S. (1992). Light-regulated expression of the *psbD* gene family in *Synechococcus* sp. strain PCC 7942: evidence for the role of duplicated *psbD* genes in cyanobacteria. *Mol. Gen. Genet.* 232, 221–230.

Bustos, S. A., Schaefer, M. R., and Golden, S. S. (1990). Different and rapid responses of four cyanobacterial *psbA* transcripts to changes in light intensity. *J. Bacteriol.* 172, 1998–2004.

Caldwell, M. M., Bornman, J. F., Ballaré, C. L., Flint, S. D., and Kulandaivelu, G. (2007). Terrestrial ecosystems, increased solar ultraviolet radiation, and interactions with other climate change factors. *Photochem. Photobiol. Sci.* 6, 252–266.

Campbell, D., Bruce, D., Carpenter, C., Gustafsson, P., and Oquist, G. (1996). Two forms of the photosystem II D1 protein alter energy dissipation and state transitions in the cyanobacterium *Synechococcus* sp. PCC 7942. *Photosyn. Res.* 47, 131–144.

Campbell, D., Eriksson, M. J., Oquist, G., Gustafsson, P., and Clarke, A. K. (1998a). The cyanobacterium *Synechococcus* resists UV-B by exchanging photosystem II reaction-center D1 proteins. *Proc. Natl. Acad. Sci. U.S.A.* 95, 364–369.

Campbell, D., Hurry, V., Clarke, A. K., Gustafsson, P., and Öquist, G. (1998b). Chlorophyll fluorescence analysis of cyanobacterial photosynthesis and acclimation. *Microbiol. Mol. Biol. Rev.* 667–683, 62.

Campbell, D., Zhou, G. Q., Gustafsson, P., Oquist, G., and Clarke, A. K. (1995). Electron transport regulates exchange of two forms of photosystem II D1 protein in the cyanobacterium *Synechococcus*. *EMBO J.* 14, 5457–5466.

Campbell, D. A., and Tyystjarvi, E. (2012). Parameterization of photosystem II photoinactivation and repair. *Biochim. Biophys. Acta* 1817, 258–265.

Carpenter, E. J., and Chang, J. (1988). Species-specific phytoplankton growth rates via diel DNA synthesis cycles. I. Concept of the method. *Mar. Ecol. Prog. Ser.* 43, 105–111.

Chen, Z., Yang, H., and Pavletich, N. P. (2008). Mechanism of homologous recombination from the RecA-ssDNA/dsDNA structures. *Nature* 453, 489–484.

Clarke, A. K., Hurry, V. M., Gustafsson, P., and Öquist, G. (1993). Two functionally distinct forms of the photosystem II reaction center D1 protein in the cyanobacterium *Synechococcus* sp. PCC7942. *Proc. Natl. Acad. Sci. U.S.A.* 90, 11985–11989.

Claustre, H., Bricaud, A., Babin, M., Bruyant, F., Guillou, L., Le Gall, F., Marie, D., and Partensky, F. (2002). Diel variations in *Prochlorococcus* optical properties. *Limnol. Oceanogr.* 47, 1637–1647.

Demmig-Adams, B., and Adams, W. W. (1992). Photoprotection and other responses of plants to high light stress. *Annu. Rev. Plant Physiol. Plant Mol. Biol.* 7, 1–116.

Dring, M. J., Wagner, A., and Luning, K. (2001). Contribution of the UV component of natural sunlight to photoinhibition of photosynthesis in six species of subtidal brown and red seaweeds. *Plant Cell Environ.* 24, 1153–1164.

Dufresne, A., Garczarek, L., and Partensky, F. (2005). Accelerated evolution associated with genome reduction in a free-living prokaryote. *Genome Biol.* 6, R14.

Dufresne, A., Ostrowski, M., Scanlan, D. J., Garczarek, L., Mazard, S., Palenik, B. P., Paulsen, I. T., Tandeau De Marsac, N., Wincker, P., Dossat, C., Ferriera, S., Johnson, J., Post, A. F., Hess, W. R., and Partensky, F. (2008). Unraveling the genomic mosaic of a ubiquitous genus of marine cyanobacteria. *Genome Biol.* 9, R90.

Everroad, C., Six, C., Partensky, F., Thomas, J. C., Holtzendorff, J., and Wood, A. M. (2006). Biochemical bases of type IV chromatic adaptation in marine *Synechococcus* spp. *J. Bacteriol.* 188, 3345–3356.

Fujimori, T., Higuchi, M., Sato, H., Aiba, H., Muramatsu, M., Hihara, Y., and Sonoike, K. (2005). The mutant of *sll1961*, which encodes a putative transcriptional regulator, has a defect in regulation of photosystem stoichiometry in the cyanobacterium *Synechocystis* sp. PCC 6803. *Plant Physiol.* 139, 408–416.

Garcia-Fernandez, J. M., Hess, W. R., Houmard, J., and Partensky, F. (1998). Expression of the *psbA* gene in the marine oxyphotobacteria *Prochlorococcus* spp. *Arch. Biochem. Biophys.* 359, 17–23.

Garcia-Pichel, F., Johnson, S. L., Youngkin, D., and Belnap, J. (2003). Small-scale vertical distribution of bacterial biomass and diversity in biological soil crusts from arid lands in the Colorado Plateau. *Microb. Ecol.* 46, 312–321.

Garczarek, L., Dufresne, A., Blot, N., Cockshutt, A. M., Peyrat, A., Campbell, D. A., Joubin, L., and Six, C. (2008). Function and evolution of the *psbA* gene family in marine *Synechococcus*: *Synechococcus* sp. WH7803 as a case study. *ISME J.* 2, 937–953.

Garczarek, L., Partensky, F., Irlbacher, H., Holtzendorff, J., Babin, M., Mary, I., Thomas, J. C., and Hess, W. R. (2001). Differential expression of antenna and core genes in *Prochlorococcus* PCC 9511 (Oxyphotobacteria) grown under a modulated light-dark cycle. *Environ. Microbiol.* 3, 168–175.

Garczarek, L., Poupon, A., and Partensky, F. (2003). Origin and evolution of transmembrane Chl-binding proteins: hydrophobic cluster analysis suggests a common one-helix ancestor for prokaryotic (Pcb) and eukaryotic (LHC) antenna protein superfamilies. *FEMS Microbiol. Lett.* 222, 59–68.

Giorgi, L. B., Nixon, P. J., Merry, S. A., Joseph, D. M., Durrant, J. R., De Las Rivas, J., Barber, J., Porter, G., and Klug, D. R. (1996). Comparison of primary charge separation in the photosystem II reaction center complex isolated from wild-type and D1-130 mutants of the cyanobacterium *Synechocystis* PCC 6803. *J. Biol. Chem.* 271, 2093–2101.

Golden, S. S., Cho, D. S., and Nalty, M. S. (1989). Two functional *psbD* genes in the cyanobacterium *Synechococcus* sp. strain PCC 7942. *J. Bacteriol.* 171, 4707–4713.

Goosen, N., and Moolenaar, G. F. (2008). Repair of UV damage in bacteria. *DNA Repair (Amst.)* 7, 353–379.

Hakala, M., Rantamaki, S., Puputti, E. M., Tyystjarvi, T., and Tyystjarvi, E. (2006). Photoinhibition of manganese enzymes: insights into the mechanism of photosystem II photoinhibition. *J. Exp. Bot.* 57, 1809–1816.

Hanke, G. T., Satomi, Y., Shinmura, K., Takao, T., and Hase, T. (2011). A screen for potential ferredoxin electron transfer partners uncovers new, redox dependent interactions. *Biochim. Biophys. Acta* 1814, 366–374.

He, Q. F., Dolganov, N., Bjorkman, O., and Grossman, A. R. (2001). The high light-inducible polypeptides in *Synechocystis* PCC6803 – expression and function in high light. *J. Biol. Chem.* 276, 306–314.

He, Y.-Y., and Häder, D.-P. (2002a). Involvement of reactive oxygen species in the UV-B damage to the cyanobacterium *Anabaena* sp. *J. Photochem. Photobiol. B* 66, 73–80.

He, Y. Y., and Häder, D. P. (2002b). Reactive oxygen species and UV-B: effect on cyanobacteria. *Photochem. Photobiol. Sci.* 1, 729–736.

Helbling, E. W., Villafane, V. E., Ferrario, M., and Holm-Hansen, O. (1992). Impact of natural ultraviolet radiation on rates of photosynthesis and on specific marine phytoplankton species. *Mar. Ecol. Prog. Ser.* 80, 80–89.

Hess, W. R., Weihe, A., Loiseaux-De Goër, S., Partensky, F., and Vaulot, D. (1995). Characterization of the single *psbA* gene of *Prochlorococcus marinus* CCMP 1375 (Prochlorophyta). *Plant Mol. Biol.* 27, 1189–1196.

Hihara, Y., Sonoike, K., and Ikeuchi, M. (1998). A novel gene, *pmgA*, specifically regulates photosystem stoichiometry in the cyanobacterium *Synechocystis* species PCC 6803 in response to high light. *Plant Physiol.* 117, 1205–1216.

Holtzendorff, J., Partensky, F., Jacquet, S., Bruyant, F., Marie, D., Garczarek, L., Mary, I., Vaulot, D., and Hess, W. R. (2001). Diel expression of cell cycle-related genes in synchronized cultures of *Prochlorococcus* sp strain PCC 9511. *J. Bacteriol.* 183, 915–920.

Holtzendorff, J., Partensky, F., Mella, D., Lennon, J. F., Hess, W. R., and Garczarek, L. (2008). Genome streamlining results in loss of robustness of the circadian clock in the marine cyanobacterium *Prochlorococcus marinus* PCC 9511. *J. Biol. Rhythms* 23, 187–199.

Houot, L., Floutier, M., Marteyn, B., Michaut, M., Picciocchi, A., Legrain, P., Aude, J.-C., Cassier-Chauvat, C., and Chauvat, F. (2007). Cadmium triggers an integrated reprogramming of the metabolism of *Synechocystis* PCC6803, under the control of the Slr1738 regulator. *BMC Genomics* 8, 350. doi:10.1186/1471-2164-8-350

Imamura, S., Yoshihara, S., Nakano, S., Shiozaki, N., Yamada, A., Tanaka, K., Takahashi, H., Asayama, M., and Shirai, M. (2003). Purification, characterization, and gene expression of all sigma factors of RNA polymerase in a cyanobacterium. *J. Mol. Biol.* 325, 857–872.

Ito, H., Mutsuda, M., Murayama, Y., Tomita, J., Hosokawa, N., Terauchi, K., Sugita, C., Sugita, M., Kondo, T., and Iwasaki, H. (2009). Cyanobacterial daily life with Kai-based circadian and diurnal genome-wide transcriptional control in *Synechococcus elongatus*. *Proc. Natl. Acad. Sci. U.S.A.* 106, 14168–14173.

Jacquet, S., Lennon, J. F., Marie, D., and Vaulot, D. (1998). Picoplankton population dynamics in coastal waters of the northwestern Mediterranean Sea. *Limnol. Oceanogr.* 43, 1916–1931.

Johnson, Z. I., Zinser, E. R., Coe, A., Mcnulty, N. P., Woodward, E. M., and Chisholm, S. W. (2006). Niche partitioning among *Prochlorococcus* ecotypes along ocean-scale environmental gradients. *Science* 311, 1737–1740.

Kana, T. M., and Glibert, P. M. (1987). Effect of irradiances up to 2000 μE m^{-2} s^{-1} on marine *Synechococcus* WH7803 – I. Growth, pigmentation, and cell composition. *Deep Sea Res.* 34, 479–485.

Kappell, A. D., Bhaya, D., and Van Waasbergen, L. G. (2006). Negative control of the high light-inducible *hliA* gene and implications for the activities of the NblS sensor kinase in the cyanobacterium *Synechococcus elongatus* strain PCC 7942. *Arch. Microbiol.* 186, 403–413.

Keren, N., Berg, A., Vankan, P. J. M., Levanon, H., and Ohad, I. (1997). Mechanism of photosystem II photoinactivation and D1 protein degradation at low light: the role of back electron flow. *Proc. Natl. Acad. Sci. U.S.A.* 94, 1579–1584.

Kettler, G., Martiny, A. C., Huang, K., Zucker, J., Coleman, M. L., Rodrigue, S., Chen, F., Lapidus, A., Ferriera, S., Johnson, J., Steglich, C., Church, G., Richardson, P., and Chisholm, S. W. (2007). Patterns and implications of gene gain and loss in the evolution of *Prochlorococcus*. *PLoS Genet.* 3, e231. doi:10.1371/journal.pgen.0030231

Kirilovsky, D., and Kerfeld, C. A. (2012). The orange carotenoid protein in photoprotection of photosystem II in cyanobacteria. *Biochim. Biophys. Acta* 1817, 158–166.

Knox, J. P., and Dodge, A. D. (1985). Singlet oxygen and plants. *Phytochemistry* 24, 889–896.

Kolowrat, C., Partensky, F., Mella-Flores, D., Le Corguillé, G., Boutte, C., Blot, N., Ratin, M., Ferréol, M., Lecomte, X., Gourvil, P., Lennon, J. F., Kehoe, D. M., and Garczarek, L. (2010). Ultraviolet stress delays chromosome replication in light/dark synchronized cells of the marine cyanobacterium *Prochlorococcus marinus* PCC9511. *BMC Microbiol.* 10, 204. doi:10.1186/1471-2180-10-204

Komenda, J., Barker, M., Kuvikova, S., De Vries, R., Mullineaux, C. W., Tichy, M., and Nixon, P. J. (2006). The FtsH protease Slr0228 is important for quality control of photosystem II in the thylakoid membrane of *Synechocys*tis sp. PCC 6803. *J. Biol. Chem.* 281, 1145–1151.

Komenda, J., Knoppova, J., Krynicka, V., Nixon, P. J., and Tichy, M. (2010). Role of FtsH2 in the repair of Photosystem II in mutants of the cyanobacterium *Synechocystis* PCC 6803 with impaired assembly or stability of the CaMn(4) cluster. *Biochim. Biophys. Acta* 1797, 566–575.

Kos, P. B., Deak, Z., Cheregi, O., and Vass, I. (2008). Differential regulation of *psbA* and *psbD* gene expression, and the role of the different D1 protein copies in the cyanobacterium *Thermosynechococcus elongatus* BP-1. *Biochim. Biophys. Acta* 1777, 74–83.

Krieger-Liszkay, A. (2005). Singlet oxygen production in photosynthesis. *J. Exp. Bot.* 56, 337–346.

Krupa, Z., Oquist, G., and Gustafsson, P. (1991). Photoinhibition of photosynthesis and growth responses at different light levels in *psbA* gene mutants of the cyanobacterium

Synechococcus. *Physiol. Plant.* 82, 1–8.

Kucho, K., Okamoto, K., Tsuchiya, Y., Nomura, S., Nango, M., Kanehisa, M., and Ishiura, M. (2005). Global analysis of circadian expression in the cyanobacterium *Synechocystis* sp. strain PCC 6803. *J. Bacteriol.* 187, 2190–2199.

Kucho, K., Tsuchiya, Y., Okumoto, Y., Harada, M., Yamada, M., and Ishiura, M. (2004). Construction of unmodified oligonucleotide-based microarrays in the thermophilic cyanobacterium *Thermosynechococcus elongatus* BP-1: screening of the candidates for circadianly expressed genes. *Genes Genet. Syst.* 79, 319–329.

LaRoche, J., Van Der Staay, G. W., Partensky, F., Ducret, A., Aebersold, R., Li, R., Golden, S. S., Hiller, R. G., Wrench, P. M., Larkum, A. W., and Green, B. R. (1996). Independent evolution of the prochlorophyte and green plant chlorophyll *a/b* light-harvesting proteins. *Proc. Natl. Acad. Sci. U.S.A.* 93, 15244–15248.

Latifi, A., Jeanjean, R., Lemeille, S., Havaux, M., and Zhang, C. C. (2005). Iron starvation leads to oxidative stress in *Anabaena* sp. strain PCC 7120. *J. Bacteriol.* 187, 6596–6598.

Latifi, A., Ruiz, M., and Zhang, C. (2009). Oxidative stress in cyanobacteria. *FEMS Microbiol. Rev.* 33, 258–278.

Liu, H. B., Nolla, H. A., and Campbell, L. (1997). *Prochlorococcus* growth rate and contribution to primary production in the equatorial and subtropical North Pacific Ocean. *Aquat. Microb. Ecol.* 12, 39–47.

Llabres, M., and Agusti, S. (2006). Picophytoplankton cell death induced by UV radiation: evidence for oceanic Atlantic communities. *Limnol. Oceanogr.* 51, 21–29.

Llabres, M., and Agusti, S. (2010). Effects of ultraviolet radiation on growth, cell death and the standing stock of Antarctic phytoplankton. *Aquat. Microb. Ecol.* 59, 151–160.

Lupinkova, L., and Komenda, J. (2004). Oxidative modifications of the photosystem II D1 protein by reactive oxygen species: from isolated protein to cyanobacterial cells. *Photochem. Photobiol.* 79, 152–162.

MacIntyre, H. L., Kana, T. M., and Geider, R. J. (2000). The effect of water motion on short-term rates of photosynthesis by marine phytoplankton. *Trends Plant Sci.* 5, 12–17.

Marie, D., Partensky, F., Jacquet, S., and Vaulot, D. (1997). Enumeration and cell cycle analysis of natural populations of marine picoplankton by flow cytometry using the nucleic acid stain SYBR Green I. *Appl. Environ. Microbiol.* 63, 186–193.

Marie, D., Partensky, F., Vaulot, D., and Brussaard, C. (1999). Enumeration of phytoplankton, bacteria, and viruses in marine samples. *Curr. Protoc. Cytom.* 10, 11.11.11–11.11.15.

Mary, I., and Vaulot, D. (2003). Two-component systems in *Prochlorococcus* MED4: Genomic analysis and differential expression under stress. *FEMS Microbiol. Lett.* 226, 135–144.

Miyao, M., Ikeuchi, M., Yamamoto, N., and Ono, T. (1995). Specific degradation of the D1 protein of photosystem-II by treatment with hydrogen-peroxide in darkness – implications for the mechanism of degradation of the D1 protein under illumination. *Biochemistry* 34, 10019–10026.

Moore, L. R., Goericke, R., and Chisholm, S. W. (1995). Comparative physiology of *Synechococcus* and *Prochlorococcus*: influence of light and temperature on growth, pigments, fluorescence and absorptive properties. *Mar. Ecol. Prog. Ser.* 116, 259–275.

Mullineaux, C. W., and Emlyn-Jones, D. (2005). State transitions: an example of acclimation to low-light stress. *J. Exp. Bot.* 56, 389–393.

Murakami, A., and Fujita, Y. (1991). Regulation of photosystem stoichiometry in the photosynthetic system of the cyanophyte *Synechocystis* PCC 6714 in response to light intensity. *Plant Cell Physiol.* 32, 223–230.

Muramatsu, M., and Hihara, Y. (2003). Transcriptional regulation of genes encoding subunits of photosystem I during acclimation to high-light conditions in *Synechocystis* sp. PCC 6803. *Planta* 216, 446–453.

Ng, W. O., Zentella, R., Wang, Y. S., Taylor, J. S. A., and Pakrasi, H. B. (2000). PhrA, the major photoreactivating factor in the cyanobacterium *Synechocystis* sp strain PCC 6803 codes for a cyclobutane-pyrimidine-dimer-specific DNA photolyase. *Arch. Microbiol.* 173, 412–417.

Nishiyama, Y. (2006). A new paradigm for the action of reactive oxygen species in the photoinhibition of photosystem II. *Biochim. Biophys. Acta* 1757, 742–749.

Nishiyama, Y., Allakhverdiev, S. I., Yamamoto, H., Hayashi, H., and Murata, N. (2004). Singlet oxygen inhibits the repair of photosystem II by suppressing the translation elongation of the D1 protein in *Synechocystis* sp. PCC 6803. *Biochemistry* 43, 11321–11330.

Nixon, P. J., Sarcina, M., and Diner, B. A. (2005). The D1 and D2 core proteins. *Photosystem II* 22, 71–93.

Ohnishi, N., Allakhverdiev, S. I., Takahashi, S., Higashi, S., Watanabe, M., Nishiyama, Y., and Murata, N. (2005). Two-step mechanism of photodamage to photosystem II: step 1 occurs at the oxygen-evolving complex and step 2 occurs at the photochemical reaction center. *Biochemistry* 44, 8494–8499.

Ong, L. J., and Glazer, A. N. (1991). Phycoerythrins of the marine unicellular cyanobacteria. *J. Biol. Chem.* 266, 9519–9527.

Park, Y. I., Chow, W. S., and Anderson, J. M. (1995). The quantum yield of photoinactivation of photosystem II in pea leaves is greater at low than high photon exposure. *Plant Cell Physiol.* 36, 1163–1167.

Partensky, F., Blanchot, J., and Vaulot, D. (1999a). "Differential distribution and ecology of *Prochlorococcus* and *Synechococcus* in oceanic waters: a review," in *Marine Cyanobacteria*, eds L. Charpy and A. Larkum (Monaco: Musée Océanographique), 457–475.

Partensky, F., Hess, W. R., and Vaulot, D. (1999b). Prochlorococcus, a marine photosynthetic prokaryote of global significance. *Microbiol. Mol. Biol. Rev.* 63, 106–127.

Partensky, F., and Garczarek, L. (2003). "The photosynthetic apparatus of chlorophyll *b*- and *d*-containing oxychlorobacteria," in *Photosynthesis in Algae*, eds A. W. D. Larkum, S. E. Douglas, and J. A. Raven (Dordrecht: Kluwer Academic Publishers), 29–62.

Partensky, F., and Garczarek, L. (2010). *Prochlorococcus*: advantages and limits of minimalism. *Annu. Rev. Mar. Sci.* 2, 305–331.

Powles, S. B. (1984). Photoinhibition of photosynthesis induced by visible light. *Annu. Rev. Plant Physiol. Plant Mol. Biol.* 35, 15–44.

Prásil, O., Adir, A., and Ohad, I. (1992). "Dynamics of photosystem II: mechanism of photoinhibition and recovery processes," in *Topics in photosynthesis – the photosystems: structure, function and molecular biology*, ed. J. Barber (Amsterdam: Elsevier Science Publishers), 295–348.

Rastogi, R. P., Singh, S. P., Hader, D. P., and Sinha, R. P. (2010). Detection of reactive oxygen species (ROS) by the oxidant-sensing probe 2′,7′-dichlorodihydrofluorescein diacetate in the cyanobacterium *Anabaena variabilis* PCC 7937. *Biochem. Biophys. Res. Commun.* 397, 603–607.

Rippka, R., Coursin, T., Hess, W., Lichtlé, C., Scanlan, D. J., Palinska, K. A., Iteman, I., Partensky, F., Houmard, J., and Herdman, M. (2000). *Prochlorococcus marinus* Chisholm et al. 1992 *subsp. pastoris subsp. nov.* strain PCC 9511, the first axenic chlorophyll a_2/b_2-containing cyanobacterium (Oxyphotobacteria). *Int. J. Syst. Evol. Microbiol.* 50, 1833–1847.

Rocap, G., Larimer, F. W., Lamerdin, J., Malfatti, S., Chain, P., Ahlgren, N. A., Arellano, A., Coleman, M., Hauser, L., Hess, W. R., Johnson, Z. I., Land, M., Lindell, D., Post, A. F., Regala, W., Shah, M., Shaw, S. L., Steglich, C., Sullivan, M. B., Ting, C. S., Tolonen, A., Webb, E. A., Zinser, E. R., and Chisholm, S. W. (2003). Genome divergence in two *Prochlorococcus* ecotypes reflects oceanic niche differentiation. *Nature* 424, 1042–1047.

Ross, C., Santiago-Vazquez, L., and Paul, V. (2006). Toxin release in response to oxidative stress and programmed cell death in the cyanobacterium *Microcystis aeruginosa*. *Aquat. Toxicol.* 78, 66–73.

Ryu, J. Y., Song, J. Y., Chung, Y., Park, Y. M., Chow, W. S., and Park, Y. I. (2010). Transcript accumulation of carotenoid biosynthesis genes in the cyanobacterium *Synechocystis* sp. PCC 6803 during the dark-to-light transition is mediated by photosynthetic electron transport. *Plant Biotechnol. Rep.* 4, 149–155.

Saito, M. A., Bertrand, E. M., Dutkiewicz, S., Bulygin, V. V., Moran, D. M., Monteiro, F. M., Follows, M. J., Valois, F. W., and Waterbury, J. B. (2011). Iron conservation by reduction of metalloenzyme inventories in the marine diazotroph *Crocosphaera watsonii*. *Proc. Natl. Acad. Sci. U.S.A.* 108, 2184–2189.

Sarvikas, P., Hakala, M., Patsikka, E., Tyystjarvi, T., and Tyystjarvi, E. (2006). Action spectrum of photoinhibition in leaves of wild type and npq1-2 and npq4-1 mutants of *Arabidopsis thaliana*. *Plant Cell Physiol.* 47, 391–400.

Sass, L., Spetea, C., Mate, Z., Nagy, F., and Vass, I. (1997). Repair of UV-B induced damage of photosystem II via de novo synthesis of the D1 and D2 reaction centre subunits in *Synechocystis* sp. PCC 6803. *Photosyn. Res.* 54, 55–62.

Satoh, S., and Tanaka, A. (2006). Identification of chlorophyllide a oxygenase in the *Prochlorococcus* genome by a comparative genomic approach. *Plant Cell Physiol.* 47, 1622–1629.

Scanlan, D. J. (2003). Physiological diversity and niche adaptation in marine *Synechococcus*. *Adv. Microb. Physiol.* 47, 1–64.

Scanlan, D. J., Ostrowski, M., Mazard, S., Dufresne, A., Garczarek, L., Hess, W. R., Post, A. F., Hagemann, M., Paulsen, I., and Partensky, F. (2009). Ecological genomics of marine picocyanobacteria. *Microbiol. Mol. Biol. Rev.* 73, 249–299.

Schmittgen, T. D., and Livak, K. J. (2008). Analyzing real-time PCR data by the comparative C(T) method. *Nat. Protoc.* 3, 1101–1108.

Shalapyonok, A., Olson, R. J., and Shalapyonok, L. S. (1998). Ultradian growth in *Prochlorococcus* spp. *Appl. Environ. Microbiol.* 64, 1066–1069.

Shi, T., Ilikchyan, I., Rabouille, S., and Zehr, J. P. (2010). Genome-wide analysis of diel gene expression in the unicellular N_2-fixing cyanobacterium *Crocosphaera watsonii* WH 8501. *ISME J.* 4, 621–632.

Sicora, C. I., Appleton, S. E., Brown, C. M., Chung, J., Chandler, J., Cockshutt, A. M., Vass, I., and Campbell, D. A. (2006). Cyanobacterial *psbA* families in *Anabaena* and *Synechocystis* encode trace, constitutive and UVB-induced D1 isoforms. *Biochim. Biophys. Acta* 1757, 47–56.

Sicora, C. I., Brown, C. M., Vass, I., Cheregi, O., and Campbell, D. A. (2008). The *psbA* gene family responds differentially to light and UVB stress in *Gloeobacter violaceus* PCC 7421, a deeply divergent cyanobacterium. *Biochim. Biophys. Acta* 777, 130–139.

Sidler, W. A. (1994). "Phycobilisome and phycobiliprotein structure," in *The Molecular Biology of Cyanobacteria*, ed. D. A. Bryant (Dordrecht: Kluwer Academic Publishers), 139–216.

Sies, H., and Menck, C. F. M. (1992). Singlet oxygen induced DNA damage. *Mutat. Res.* 275, 367–375.

Six, C., Finkel, Z. V., Irwin, A. J., and Campbell, D. A. (2007a). Light variability illuminates niche-partitioning among marine picocyanobacteria. *PLoS ONE* 2, e1341. doi:10.1371/journal.pone.0001341

Six, C., Joubin, L., Partensky, F., Holtzendorff, J., and Garczarek, L. (2007b). UV-induced phycobilisome dismantling in the marine picocyanobacterium *Synechococcus* sp. WH8102. *Photosyn. Res.* 92, 75–86.

Six, C., Thomas, J. C., Garczarek, L., Ostrowski, M., Dufresne, A., Blot, N., Scanlan, D. J., and Partensky, F. (2007c). Diversity and evolution of phycobilisomes in marine *Synechococcus* spp.: a comparative genomics study. *Genome Biol.* 8, R259.

Six, C., Sherrard, R., Lionard, M., Roy, S., and Campbell, D. A. (2009). Photosystem II and pigment dynamics among ecotypes of the green alga *Ostreococcus*. *Plant Physiol.* 151, 379–390.

Six, C., Thomas, J. C., Brahamsha, B., Lemoine, Y., and Partensky, F. (2004). Photophysiology of the marine cyanobacterium *Synechococcus* sp. WH8102, a new model organism. *Aquat. Microb. Ecol.* 35, 17–29.

Sommaruga, R., Hofer, J. S., Alonso-Saez, L., and Gasol, J. A. (2005). Differential sunlight sensitivity of picophytoplankton from surface Mediterranean coastal waters. *Appl. Environ. Microbiol.* 71, 2154–2157.

Steiger, S., Jackisch, Y., and Sandmann, G. (2005). Carotenoid biosynthesis in *Gloeobacter violaceus* PCC4721 involves a single crtI-type phytoene desaturase instead of typical cyanobacterial enzymes. *Arch. Microbiol.* 184, 207–214.

Stockel, J., Welsh, E. A., Liberton, M., Kunnvakkam, R., Aurora, R., and Pakrasi, H. B. (2008). Global transcriptomic analysis of *Cyanothece* 51142 reveals robust diurnal oscillation of central metabolic processes. *Proc. Natl. Acad. Sci. U.S.A.* 105, 6156–6161.

Summerfield, T. C., and Sherman, L. A. (2007). Role of sigma factors in controlling global gene expression in light/dark transitions in the cyanobacterium *Synech*ocystis sp. strain PCC 6803. *J. Bacteriol.* 189, 7829–7840.

Takahashi, S., and Murata, N. (2008). How do environmental stresses accelerate photoinhibition? *Trends Plant Sci.* 13, 178–182.

Takai, N., Nakajima, M., Oyama, T., Kito, R., Sugita, C., Sugita, M., Kondo, T., and Iwasaki, H. (2006). A KaiC-associating SasA-RpaA two-component regulatory system as a major circadian timing mediator in cyanobacteria. *Proc. Natl. Acad. Sci. U.S.A.* 103, 12109–12114.

Telfer, A. (2005). Too much light? How beta-carotene protects the photosystem II reaction centre. *Photochem. Photobiol. Sci.* 4, 950–956.

Tichy, M., Lupinkova, L., Sicora, C., Vass, I., Kuvikova, S., Prasil, O., and Komenda, J. (2003). *Synechocystis* 6803 mutants expressing distinct forms of the Photosystem II D1 protein from *Synechococcus* 7942: relationship between the *psbA* coding region and sensitivity to visible and UV-B radiation. *Biochim. Biophys. Acta* 1605, 55–66.

Toepel, J., Mcdermott, J. E., Summerfield, T. C., and Sherman, L. A. (2009). Transcriptional analysis of the unicellular, diazotrophic cyanobacterium *Cyanothece sp.* ATCC 51142 grown under short day / night cycles. *J. Phycol.* 45, 610–620.

Toepel, J., Welsh, E., Summerfield, T. C., Pakrasi, H. B., and Sherman, L. A. (2008). Differential transcriptional analysis of the cyanobacterium *Cyanothece* sp. strain ATCC 51142 during light-dark and continuous-light growth. *J. Bacteriol.* 190, 3904–3913.

Tyystjarvi, E., and Aro, E. M. (1996). The rate constant of photoinhibition, measured in lincomycin-treated leaves, is directly proportional to light intensity. *Proc. Natl. Acad. Sci. U.S.A.* 93, 2213–2218.

van de Poll, W. H., Eggert, A., Buma, A. G. J., and Breeman, A. M. (2001). Effects of UV-B-induced DNA damage and photoinhibition on growth of temperate marine red macrophytes: habitat-related differences in UV-B tolerance. *J. Phycol.* 37, 30–37.

van Waasbergen, L. G., Dolganov, N., and Grossman, A. R. (2002). *nblS*, a gene involved in controlling photosynthesis-related gene expression during high light and nutrient stress in *Synechococcus elongatus* PCC 7942. *J. Bacteriol.* 184, 2481–2490.

Vass, I., Styring, S., Hundal, T., Koivuniemi, A., Aro, E. M., and Andersson, B. (1992). Reversible and irreversible intermediates during photoinhibition of photosystem II: stable reduced QA species promote chlorophyll triplet formation. *Proc. Natl. Acad. Sci. U.S.A.* 89, 1408–1412.

Vaulot, D., Marie, D., Olson, R. J., and Chisholm, S. W. (1995). Growth of *Prochlorococcus*, a photosynthetic prokaryote, in the equatorial Pacific Ocean. *Science* 268, 1480–1482.

Wilson, A., Punginelli, C., Gall, A., Bonetti, C., Alexandre, M., Routaboul, J. M., Kerfeld, C. A., Van Grondelle, R., Robert, B., Kennis, J. T., and Kirilovsky, D. (2008). A photoactive carotenoid protein acting as light intensity sensor. *Proc. Natl. Acad. Sci. U.S.A.* 105, 12075–12080.

Wyman, M., and Thom, C. (2012). Temporal orchestration of glgA (encoding glycogen synthase) expression and glycogen accumulation in the oceanic picoplanktonic cyanobacterium, *Synechococcus* sp. strain WH8103. *Appl. Environ. Microbiol.* 78, 4744–4747.

Zinser, E. R., Lindell, D., Johnson, Z. I., Futschik, M. E., Steglich, C., Coleman, M. L., Wright, M. A., Rector, T., Steen, R., Mcnulty, N., Thompson, L. R., and Chisholm, S. W. (2009). Choreography of the transcriptome, photophysiology, and cell cycle of a minimal photoautotroph, *Prochlorococcus*. *PLoS ONE* 4, e5135. doi:10.1371/journal.pone.0005135

Zolla, L., and Rinalducci, S. (2002). Involvement of active oxygen species in degradation of light-harve sting proteins under light stresses. *Biochemistry* 41, 14391–14402.

Zubkov, M. V., Sleigh, M. A., and Burkill, P. H. (2000). Assaying picoplankton distribution by flow cytometry of underway samples collected along a meridional transect across the Atlantic Ocean. *Aquat. Microb. Ecol.* 21, 13–20.

Zwirglmaier, K., Jardillier, L., Ostrowski, M., Mazard, S., Garczarek, L., Vaulot, D., Not, F., Massana, R., Ulloa, O., and Scanlan, D. J. (2008). Global phylogeography of marine *Synechococcus* and *Prochlorococcus* reveals a distinct partitioning of lineages among oceanic biomes. *Environ. Microbiol.* 10, 147–161.

Conflict of Interest Statement: The authors declare that the research was conducted in the absence of any commercial or financial relationships that could be construed as a potential conflict of interest.

Received: 10 April 2012; paper pending published: 12 May 2012; accepted: 19 July 2012; published online: 08 August 2012.
Citation: Mella-Flores D, Six C, Ratin M, Partensky F, Boutte C, Le Corguillé G, Marie D, Blot N, Gourvil P, Kolowrat C and Garczarek L (2012) Prochlorococcus and Synechococcus have evolved different adaptive mechanisms to cope with light and UV stress. Front. Microbio. ***3****:285. doi: 10.3389/fmicb.2012.00285*
This article was submitted to Frontiers in Aquatic Microbiology, a specialty of Frontiers in Microbiology.

APPENDIX

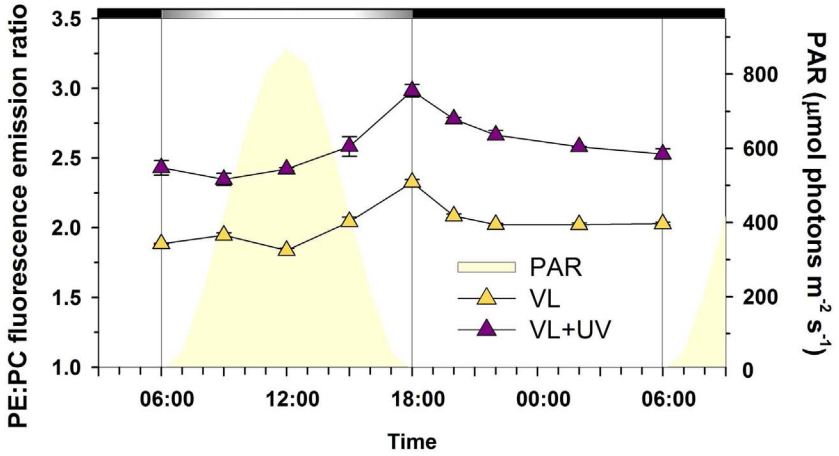

FIGURE A1 | Phycoerythrin to phycocyanin (PE:PC) fluorescence emission ratio as measured by spectrofluorimetry (at 572 and 651 nm, respectively) in *Synechococcus* sp. WH7803 cells grown under a L/D cycle with and without UV. This ratio showed significantly higher values in VL + UV than in VL-acclimated cells. In both light conditions, it increased during the day by ∼25% compared to the value at dawn then decreased during the night. The amplitude of these oscillations (ca 0.4 unit) was very low compared to those reported for *Synechococcus* sp. WH8102 acclimated to a large range of irradiance (2.5 units; Six et al., 2004). Further investigation is required to determine whether the diel pattern of PE:PC fluorescence emission ratio rather results from a decrease in the efficiency of energy transfer in the PBS rod and/or a progressive accumulation of free phycoerythrins during the day. These light-induced oscillations might be indirectly related with state transitions (Campbell et al., 1998b; Mullineaux and Emlyn-Jones, 2005), a light-dependent process which usually exhibits large amplitudes in marine *Synechococcus* (Six et al., personal communication).

frontiers in
MICROBIOLOGY

ORIGINAL RESEARCH ARTICLE
published: 19 June 2012
doi: 10.3389/fmicb.2012.00213

Diversity and distribution of marine *Synechococcus*: multiple gene phylogenies for consensus classification and development of qPCR assays for sensitive measurement of clades in the ocean

Nathan A. Ahlgren and Gabrielle Rocap*

School of Oceanography, Center for Environmental Genomics, University of Washington, Seattle, WA, USA

Edited by:
Anton F. Post, Marine Biological Laboratory, USA

Reviewed by:
David J. Scanlan, University of Warwick, UK
Kathleen Scott, University of South Florida, USA

****Correspondence:***
Gabrielle Rocap, School of Oceanography, University of Washington, Box 357940, Seattle, WA 98195, USA.
e-mail: rocap@ocean.washington.edu

Marine *Synechococcus* is a globally significant genus of cyanobacteria that is comprised of multiple genetic lineages or clades. These clades are thought to represent ecologically distinct units, or ecotypes. Because multiple clades often co-occur together in the oceans, *Synechococcus* are ideal microbes to explore how closely related bacterial taxa within the same functional guild of organisms co-exist and partition marine habitats. Here we sequenced multiple gene loci from cultured strains to confirm the congruency of clade classifications between the 16S–23S rDNA internally transcribed spacer (ITS), 16S rDNA, *narB*, *ntcA*, and *rpoC1* loci commonly used in *Synechococcus* diversity studies. We designed quantitative PCR (qPCR) assays that target the ITS for 10 *Synechococcus* clades, including four clades, XV, XVI, CRD1, and CRD2, not covered by previous assays employing other loci. Our new qPCR assays are very sensitive and specific, detecting down to tens of cells per ml. Application of these qPCR assays to field samples from the northwest Atlantic showed clear shifts in *Synechococcus* community composition across a coastal to open-ocean transect. Consistent with previous studies, clades I and IV dominated cold, coastal *Synechococcus* communities. Clades II and X were abundant at the two warmer, off-shore stations, and at all stations multiple *Synechococcus* clades co-occurred. qPCR assays developed here provide valuable tools to further explore the dynamics of microbial community structure and the mechanisms of co-existence.

Keywords: microbial ecology, cyanobacteria, *Synechococcus*, microbial diversity, quantitative PCR, multiple gene locus phylogeny, biogeography, ecotype

INTRODUCTION

Marine *Synechococcus* is an abundant and environmentally significant group of unicellular cyanobacteria that provides an ideal system to explore the ecology and evolution of closely related bacterial taxa and their niche partitioning of the global oceans (Scanlan and West, 2002). These small cyanobacteria (0.6–1.7 μm) belong to the functional class of picophytoplankton, the smallest (<2 μm) guild of photoautotrophs and contribute significantly to primary production (Waterbury et al., 1986; Li, 1994; Liu et al., 1997; Partensky et al., 1999; Jardillier et al., 2010). Molecular phylogeny has revealed a large genetic diversity amongst *Synechococcus* found in marine and estuarine waters. Based on 16S rDNA phylogeny, these strains have been classified into three major groups, labeled subclusters 5.1, 5.2, and 5.3 (Herdman et al., 2001; Dufresne et al., 2008; Scanlan et al., 2009). Phylogenies based on several additional loci reveal that these subclusters contain more than 20 distinct genetic clades. Genes used to study the diversity of marine *Synechococcus* include the 16S–23S internally transcribed spacer (ITS; Rocap et al., 2002; Ahlgren and Rocap, 2006; Chen et al., 2006; Choi and Noh, 2009; Cai et al., 2010; Huang et al., 2012), *narB* (nitrate reductase; Jenkins et al., 2006; Paerl et al., 2008, 2011), *ntcA* (a nitrogen regulatory gene; Penno et al., 2006; Post et al., 2011), *rpoC1* (subunit of RNA polymerase; Palenik, 1994; Toledo and Palenik, 1997; Ferris and Palenik, 1998; Muhling et al., 2005), *rbcL* (Rubisco large subunit; Chen et al., 2006; Paerl et al., 2012), *psbA* (photosystem I gene; Zeidner et al., 2003), *cpeB* (phycoerythrin gene; Steglich et al., 2003), and *petB* (encoding the cytochrome b_6 subunit of the cytochrome b_{6f} complex; Mazard et al., 2012).

These distinct clades are thought to represent physiologically and ecologically distinct lineages, or ecotypes, as has been seen in *Prochlorococcus*, the sister genus to marine *Synechococcus*. Genetically distinct clades of *Prochlorococcus* contain strains with ecologically relevant differences in light adaptation and nutrient utilization (Moore et al., 1998, 2002; Moore and Chisholm, 1999; Rocap et al., 2002), and these clades occupy distinct oceanic habitats that reflect their specific adaptations (West and Scanlan, 1999; Ahlgren et al., 2006; Johnson et al., 2006). Several *Synechococcus* clades similarly possess distinguishing physiologies that potentially impact their ecology (**Figure 1**). For example clade III strains possess a unique form of motility that is absent in most other clades and may allow them to find and scavenge nutrients in oligotrophic waters (Waterbury et al., 1985; Toledo et al., 1999; Chen et al., 2004). Other clades differ in their accessory light harvesting pigments

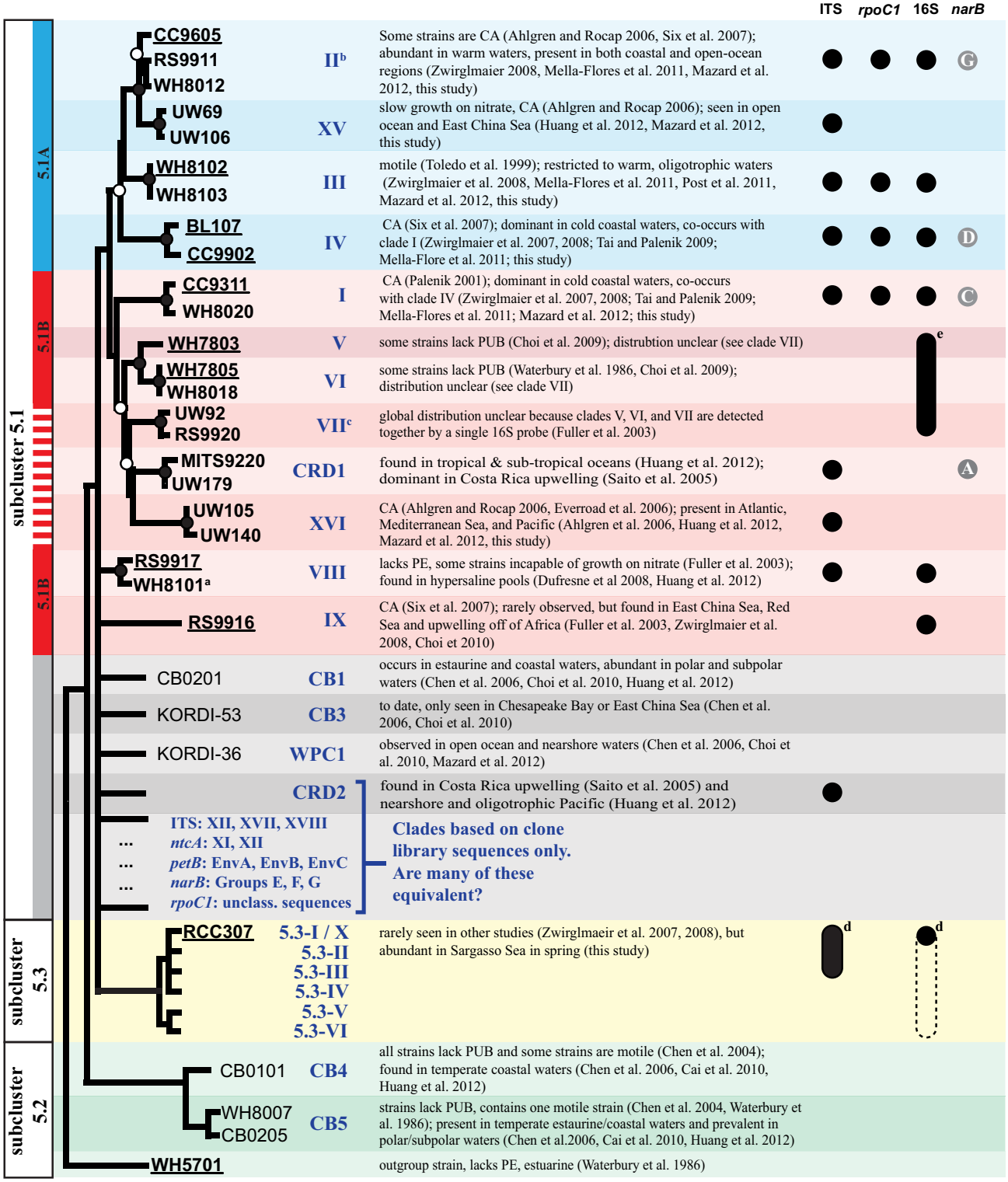

FIGURE 1 | Schematic phylogenetic tree summarizing the genetic and ecological diversity of marine *Synechococcus* and molecular assays that have been developed to measure particular clades in the oceans. The depicted tree is approximately based on a four loci concatenated tree (**Figure A6** in Appendix). Examples of commonly studied strains ("type" strains) in each clade are shown. Strains in bold were selected for multiple gene loci analysis, and strains with sequenced genomes are underlined. Branch tips without taxa names indicate clades that are only represented by environmental sequences (e.g., clade CRD2). Nodes with bootstrap support

(Continued)

FIGURE 1 | Continued
of ≥55% are denoted with circles (closed circles indicate >75% support and open circles indicate 55–75% support). Polytomies indicate cases where the placement of clades is uncertain because of low bootstrap support or the absence of sequences available for multiple loci. Marine *Synechococcus* are classified into three subclusters 5.1, 5.2, and 5.3 (black vertical boxes on left), and phylogeny based on 1,129 core genes from 11 strains with sequenced genomes supports the division of strains in subcluster 5.1 into two groups 5.1A (blue bar) and 5.1B (solid red bar) (Dufresne et al., 2008). The four loci concatenated phylogeny in **Figure A6** in Appendix also supports the grouping of 5.1A strains, including clade XV. Strains in clades VII, CRD1, and XVI cluster with 5.1B strains in clades V and VI with high bootstrap support, however it is still unknown if these additional new strains without sequenced genomes form a single monophyletic cluster with all 5.1B strains (dashed red line). Information about specific physiologies, ecology, or biogeography of clades is summarized with relevant references. Chromatic adaptation (CA) is the ability to shift the ratio of accessory pigments phycourobilin (PUB) and phycoerythrobilin (PEB) according to the spectral quality of light (Palenik, 2001; Six et al., 2007). Circles (or ovals, see footnotes) indicate clades for which quantitative molecular assays have been designed to measure their abundance in the environment. [ITS, this study; *rpoC1* (Tai and Palenik, 2009; Tai et al., 2011); 16S rDNA (Fuller et al., 2003); *narB* (Paerl et al., 2011)]. *narB* sequences have been classified to groups "A" to "G" rather than the convention of clades used by other loci (Paerl et al., 2011; see **Figure A3** in Appendix). Circles with letters indicate the clade(s) for which *narB* qPCR primers designed for that *narB* group have perfect matches to at least one of the sequences in the clade (see **Figure A3** in Appendix for more info on primer coverage). [a]WH8101 was formerly classified as belonging to cluster 5.2 (Herdman et al., 2001), but this and other phylogenies suggest it belongs in cluster 5.1. [b]Clade II includes clade WPC2 following the convention of Huang et al. (2012). [c]Clade XIII is congruent with and has been subsumed into clade VII (see **Figure A4** in Appendix). [d]ITS qPCR primers were designed to perfectly match clade X strains, now classified as clade 5.3-I. These primers have perfect matches to sequences from 5.3-I through 5.3-III (but not 5.3-IV through 5.3-VI; see **Figure A2** in Appendix). Similarly, the clade X 16S rDNA probe was designed before the discovery of clades 5.3-II–5.3-VI. Because there are no corresponding 16S rDNA sequences for clades 5.3-II–5.3-VI, it is unknown if the clade X probe detects these other subcluster 5.3 clades as indicated by the dashed oval. [e]This 16S rDNA probe detects clades V, VI, VII together.

(Waterbury et al., 1986; Rocap et al., 2002; Six et al., 2007; Choi and Noh, 2009) or the ability to change their light harvesting apparatus in response to the spectral quality of light they experience (chromatic adaptation; Palenik, 2001; Ahlgren and Rocap, 2006; Six et al., 2007). While *Synechococcus* clades are hypothesized to represent ecotypes, physiological characterization of isolates from many clades unfortunately still remains sparse, making it difficult to predict what distinct niches they may occupy (**Figure 1**).

Quantitative molecular assays measuring the abundance of specific *Synechococcus* clades have been used to characterize their biogeography and confirm that these clades occupy different niches and thus represent ecotypes. Assays include a suite of eight oligonucleotide probes that target 10 16S rDNA clades (clades I–X), three of which are detected together by a single probe (V, VI, and VII; Fuller et al., 2003); quantitative PCR (qPCR) assays that target four clades (I–IV) using the *rpoC1* gene (Tai and Palenik, 2009); and qPCR assays that target seven groups of *narB* sequences that each contain one or more clades (Paerl et al., 2011; **Figure 1**). The use of coding genes for quantitative assays can be problematic because the third codon position often necessitates the use of degenerate primers, as is the case for the *rpoC1* and *narB* assays. Furthermore, strains in some clades lack the *narB* gene and cannot utilize nitrate, such as RR9917 in clade IX (Scanlan et al., 2009) and MITS9220 in clade CRD1 (Moore et al., 2002). More recently, deep pyrosequencing of the 16S rDNA has been used to track clade abundances over time in the Red Sea (Post et al., 2011), non-degenerate *petB* primers have been developed for construction of *Synechococcus* specific clone libraries (Mazard et al., 2012), and DNA probes attached to fluorescent beads have been used to follow the abundances of subpopulations within clades I–IV (Tai et al., 2011). While each of the above methods targets a different locus, they reveal some cohesive patterns in the distribution of some of the major clades in the oceans. Clades I and IV are most abundant in colder, nutrient rich coastal waters while clade II and the combined group of clades V/VI/VII are widely distributed in tropical and sub-tropical waters (Zwirglmaier et al., 2007, 2008; **Figure 1**). Clade III is most prevalent in warm, oligotrophic waters, and appears to be specialized to these habitats (Fuller et al., 2003; Zwirglmaier et al., 2007, 2008; Mella-Flores et al., 2011; Post et al., 2011). Clade VIII may be specifically adapted to hypersaline waters (Dufresne et al., 2008; Huang et al., 2012) while other clades such as IX and X have been rarely seen and only at low abundance (Zwirglmaier et al., 2007, 2008).

The growing number of *Synechococcus* diversity studies and molecular assays to study their biogeography are valuable in describing the ecology of putative *Synechococcus* ecotypes, but the use of several different loci has made classification confusing and comparison of results from the different assays difficult. The various loci differ in their relative level of divergence, thus some clades may be defined too broadly or too narrowly. For example, the highly conserved 16S rDNA is less divergent than other loci and does not allow the development of specific oligonucleotides that can resolve clades V, VI, and VII unlike the ITS and other coding genes (Fuller et al., 2003; Ahlgren and Rocap, 2006; Huang et al., 2012). The use of different loci also makes it difficult to determine if clades defined by independent loci correspond to one another. This is especially the case for clades that contain only sequences obtained from environmental clone libraries (e.g., see Saito et al., 2005; Penno et al., 2006). Sequencing multiple loci in cultured isolates is necessary to verify potential overlap of clades identified by different loci. Recently, Mazard et al. (2012) conducted a classical multiple-locus sequence analysis (MLSA) study that established congruence among clades by using core genes including the *rpoC1* and *petB* genes. They also examined the 16S rDNA and ITS, although these genes could not be included in MLSA as most *Synechococcus* genomes contain two identical copies of the 16S rDNA and ITS. Their analysis however did not include the commonly used *ntcA* or *narB* sequences (Ahlgren and Rocap, 2006; Jenkins et al., 2006; Penno et al., 2006; Paerl et al., 2008; Post et al., 2011), and the portion of the *rpoC1* gene they sequenced did not overlap with the portion used in the large dataset of available *rpoC1* sequences (Toledo and Palenik, 1997; Ferris and Palenik, 1998).

In order to further the consensus in the classification of *Synechococcus* clades, we sequenced five loci commonly used in field studies, 16S rDNA, ITS, *narB*, *ntcA*, and *rpoC1*, in cultured isolates distributed across 14 clades and compared the phylogenies of

the different loci. After confirming that strains formed congruent clades across the loci examined, we developed an expanded set of qPCR assays that target ITS sequences for 10 genetic clades of marine *Synechococcus*, including newly described clades not detected by previous assays. The ITS was chosen because it is divergent enough to allow clear resolution of clades but still contains conserved regions for design of non-degenerate primers. Furthermore, because the ITS has been widely used it is the locus with the largest number of sequences available for primer design. These qPCR assays represent the most comprehensive set of quantitative assays for this genus and provide a valuable tool to further characterize the ecology of *Synechococcus* clades. Application of qPCR assays to a transect in the North Atlantic off of the eastern United States shows co-existence of multiple clades and large shifts in *Synechococcus* community composition between open-ocean and coastal environments.

MATERIALS AND METHODS

ISOLATION OF *SYNECHOCOCCUS* STRAINS AND ENVIRONMENTAL SEQUENCES

Three new *Synechococcus* isolates were obtained following the procedures outlined in (Ahlgren and Rocap, 2006). UW1 was isolated from surface waters of Hood Canal (47° 36.4′ N 122° 56.4′ W) within Puget Sound (Washington state) on March 27, 2002. Strains UW179 and UW180 were isolated from the Equatorial Pacific south of Hawaii (12° 42.7′ N 157° 59.8′ W) from 125 m on February 2, 2004. A single colony was picked for each strain from pour plates made from cells grown in enrichment cultures. The ITS sequence CHA22 was obtained from a clone library constructed from surface water sampled off of San Juan Channel (48° 32.5′ N, 122° 59.4′ W) off of San Juan Island, Washington on April 30, 2004. The clone library was constructed following the methods outlined in Ahlgren and Rocap (2006).

SEQUENCING OF ISOLATES

Between 1 and 5 ml of exponential phase culture was centrifuged at 18,000 × *g* for 10 min and the DNA was extracted from the cell pellet using either a DNeasy extraction kit (Qiagen, Valencia, CA, USA) or by quick heat lysis extraction: 95°C for 10 min in 50–100 μl of 10 mM Tris, 1 mM EDTA pH 8.0. PCR primers and reaction conditions used to amplify genes are listed in **Table A1** in Appendix. PCR reaction volumes were 20 or 25 μl and contained 0.2 mM each dNTPs and 1–2 μl of template DNA. All PCR reactions started with an initial step of 95°C for 5–10 to denature the template DNA or activate the polymerase, and all reactions ended with a 6- to 10-min extension step at 72°C. 16S rDNA and 16S–23S rDNA ITS sequences were obtained by sequencing purified PCR products obtained with Taq polymerase (Promega, Madison, WI, USA). Quadruplicate 20 μl reactions were pooled and purified using a Qiaquick PCR Purification Kit (Qiagen) before sequencing reactions with DYEnamic ET dye terminator kit (Amersham Biosciences Corp., Piscataway, NJ, USA) and sequencing on a MegaBACE 1000 automated sequencer (Amersham Biosciences). For *narB*, *ntcA*, and *rpoC1*, PCR products were generated using Accuzyme (high fidelity polymerase PCR mix (Bioline USA Inc., Taunton, MA, USA). Products were gel purified (Qiagen gel extraction kit), cloned into sequencing vectors (TOPO TA Kit, Invitrogen Corp., Carlsbad, CA, USA), and sequenced with M13 vector primers. Raw sequences were aligned and visually inspected using Sequencher (Gene Codes Inc., Ann Arbor, MI, USA). Sequences have been deposited in GenBank under the following accession numbers: 16S rDNA, JQ421027–JQ421036; ITS, JQ421037–JQ421042, *narB*, JQ421043–JQ421045, *ntcA*, JQ421046–JQ421052; *rpoC1*, JQ421053–JQ421055. Additional details are listed in **Table A2** in Appendix.

PHYLOGENETIC ANALYSES

Phylogenetic trees were constructed using sequences obtained in this study, from previous studies and complete genome sequences (Dufresne et al., 2008). ITS sequences from previous studies (Beja et al., 2000; Suzuki et al., 2001; Ahlgren and Rocap, 2006; Chen et al., 2006; Choi and Noh, 2009; Cai et al., 2010; Choi et al., 2011; Mella-Flores et al., 2011; Huang et al., 2012; Mazard et al., 2012) were aligned to our existing database of sequences using automatic alignment (PT_server alignment tool) in ARB (Ludwig et al., 2004) and manual adjustment. For phylogenetic analyses, the two tRNAs in the ITS and the loop portions of stem-loop structures (predicted by MFOLD; Zuker, 2003) were excluded from alignments. Other 16S rDNA, *narB*, *ntcA*, and *rpoC1* sequences were taken from previous studies (Giovannoni et al., 1990; Beja et al., 2000; Suzuki et al., 2001; Fuller et al., 2003; Muhling et al., 2005; Everroad et al., 2006; Jenkins et al., 2006; Penno et al., 2006; Dufresne et al., 2008; Kan et al., 2008; Choi and Noh, 2009; Mella-Flores et al., 2011; Mazard et al., 2012) These sequences were aligned either in ARB (16S rDNA) or using clustal (*narB*, *ntcA*, and *rpoC1*) with amino acid sequences.

Trees were constructed in PAUP* (Swofford, 1999) or RAxML (Stamatakis, 2006). The concatenated gene tree employed four loci, the 16S rDNA gene, the ITS, *ntcA*, and *rpoC1*. For the 16S rDNA, *narB*, *ntcA*, *rpoC1* genes and the four concatenated loci, trees were constructed using minimum evolution as the criterion and the HKY85 model in PAUP* with gamma distributed rates of substitution and a proportion of invariable sites (HKY + i + g) estimated by maximum likelihood. Trees found with the HKY + i + g model were very similar to trees constructed using substitutions models suggested by MODELTEST (Posada and Crandall, 1998; data not shown). Bootstrap analysis was performed using neighbor joining. For the ITS, best tree analysis was done in PAUP* using neighbor joining and the HKY + i + g substitution model and bootstrap analyses were performed in PAUP* (neighbor joining trees) and RAxML with the GTRGAMMA model. Additional bootstrap analysis was done for the concatenated loci using minimum evolution and the Jukes–Cantor model in PAUP* and maximum likelihood in RAxML with the GTRGAMMA model.

qPCR ASSAY DESIGN

Primers specific for 10 clades of marine *Synechococcus* were designed for use with qPCR assays (**Table 1**). Design of primers was guided by use of the probe design option in ARB (Ludwig et al., 2004), which searches for regions that are identical within a specified group of sequences and have several mismatches to other sequences. Primers targeted the 16S–23S rDNA ITS region and were designed to be identical to all sequences within each specified clade when possible but with significant mismatches to all other

Table 1 | Primers, plasmid standards, and optimized reaction and cycling conditions used for qPCR assays.

Clade	Primers, 5′ to 3′ (forward, reverse)	Strain/clone used for plasmid standards	Anneal temp. (°C)	Mg^{2+} (mM)	Lower limit of detection (cells/ml)[c]
I	SynIF2, CTTTGTCTAGTTCACAACCCATTA SynIR2, AAATCACAATCCATACGAGTTCAT	WH 8020	61	3.5	9.4
II	Syn2F2, CAGCTTCCTGTCATTCCAAGTTT Syn2R2, AAGGTTCTGCTAGAACTTCAAATCAA	UW86	60	1.5	120
III	Syn3F1, CTCAGCGTTGAAGCAACAGA Syn3R1, GATCATCTCCACAACACGCATC	WH 8102	60	1.5	137
IV	Syn4F1, GCAAGAGCCGAGACTCTTAGAT Syn4R1b, CTCTTAAACGCTTACTGCGGT	CHA22[b]	61	1.5	166
V[a]	n/a	WH 7803		n/a	n/a
VI[a]	n/a	WH 7805		n/a	n/a
VII[a]	n/a	UW92		n/a	n/a
VIII	Syn8F1, CCTCCACTGACCGAACGTGA Syn8R1, CTCCCACTTGCTCGACACAAG	WH 8101	60	2.5	57
X	Syn10F1, GATCCATTTGACTGTTCATTCCTA Syn10R1, CTAAGGGGTGGTGACCTAGACA	oc5m66[b]	60	2.5	678
XV	Syn15F1, TTTGAAATCAAGATGATGCA Syn15R1, AAGGTTCTGCTAGAACTTCAAACTGA	UW69	60	3.5	359
XVI	Syn16F1, CGAGCACTAAAGAGTTTGATTCCT Syn16R1, TAATCTCCATCACGCTTACCG	oc175m12[b]	60	3	86
CRD1	CRD1F, CTGATCGAACTCAATCTCCATC CRD1R, CATGAGAGATGCTTTATTCTTACAGACT	CRD1[b]	64	2.5	1830
CRD2	CRD2F, GGAGGATGAACTCGAGTGTGGT CRD2R, TCGATTCATAAAATAAAATCAAACTCA	CRD8[b]	60	3	235

[a] *qPCR assays were not developed to quantify these clades, but plasmid standards were generated for representative strains to check the specificity of the other qPCR assays.*

[b] *These plasmids are cloned environmental sequences from Ahlgren and Rocap, 2006 (oc5m66 and oc175m12), Saito et al., 2005 (CRD1 and CRD8) or this study (CHA22).*

[c] *For clade X, lower limits of detection were adjusted to two times above the level at which this assay cross-amplified with clade IV, and similarly the clade CRD1 limit was adjusted to two times the level of cross-amplification with WH 7803 (see **Table A3** in Appendix).*

Synechococcus ITS sequences. Primers were designed so that mismatches to non-specific sequences were concentrated at the 3′ end. Because at the time of primer design only a few sequences were available for clades V, VI, VII, and IX, reliable primer sets could not be designed for these clades.

Quantitative PCR assays were optimized on an ICycler thermocycler (BioRad Inc., Hercules, CA, USA). For all reactions, 5 μl of template DNA was added to a reaction cocktail of 20 μl. Reactions contained Immomix PCR mix (Bioline USA Inc., Taunton, MA, USA), 10 nM fluorescein (for normalization of well-to-well variability), 0.4× Sybr Green I (Molecular Probes, Eugene, OR, USA), and 0.1% dimethyl sulfoxide. Primers were used at a final concentration of 500 nM. Magnesium chloride concentrations and thermocycling conditions (**Table 1**) were optimized to maximize amplification efficiency, reduce amplification of no template negative controls, and reduce cross-amplification with non-specific ITS sequences (see below). Cycling programs consisted of an initial 10 min step at 95°C to activate the polymerase followed by 45 cycles of 30 s at 95°C, 30 s at an optimized annealing temperature (given in **Table 1**), and 30 s at 72°C. A melting curve was done at the end of each assay to verify the specificity of amplicons.

Plasmid standards were created by cloning ITS PCR products into *Escherichia coli* using a TOPO TA cloning kit (Invitrogen Corp., Carlsbad, CA, USA). ITS PCR products were generated using the cyanobacterial specific PCR primers 16S-1247f and 23S-241r using reaction conditions in Rocap et al. (2002). Purified plasmids were linearized with restriction enzyme *Pst*I or *Sph*I using conditions recommended by the manufacturer (New England Biolabs, Ipswich, MA, USA). Linear plasmids were run on a 1.5% agarose electrophoresis gel and bands of correct length were excised and purified from the gel using a Qiagen Gel Extraction Kit. Plasmids were diluted serially in 10 mM Tris, 0.1 mM EDTA, pH 8.0, and quantified with Picogreen DNA stain (Molecular Bioprobes, Eugene, OR, USA). Strains used for generating standards for each primer set are listed in **Table 1**. For some clades we used plasmids from previously generated ITS environmental clone libraries. Plasmid standards were also constructed for strains from clades V, VI, VII for use in testing the specificity of qPCR assays (**Table 1**). Plasmid standards generated from cultured strains were sequenced to verify that the regions to which the qPCR primers anneal were identical to the sequence originally determined for the strain.

CALIBRATION OF qPCR PLASMID STANDARDS

To report results from qPCR assays in terms of cells/ml for quantification of field samples, plasmid standards were calibrated to cell concentrations by making DNA filters with known amounts of cultured cells. Cultures were grown in artificial sea water with 800 μM ammonium, 50 μM phosphate, and trace metal mix (Moore et al., 2002) under a 12-h dark: 12 h light cycle at a light level of approximately 50 μmol Q m^{-2} s^{-1}. Cells were harvested in exponential phase. For DNA extraction 20 or 25 ml of culture was collected on filters with gentle filtration (<15 mm Hg of vacuum). DNA was extracted from the filters with a simple heat lysis protocol (Zinser et al., 2006). Six-hundred fifty microliters of 10 mM Tris 0.1 mM EDTA pH 8.0 was added to filters, and filters were vigorously vortexed using a bead beater (BioSpec Products, Bartlesville, OK, USA) for 2 min at maximum speed to shred the filter and resuspend cells. Five-hundred microliters of the cell mixture was removed from the shredded filter, added to 1.5 ml centrifuge tubes, and incubated at 95°C for 15 min. To determine cell concentrations diluted cell cultures were preserved with 0.125% glutaraldehyde and frozen and stored in liquid N_2 for later analysis using a Cytopeia InFlux flow cytometer (Cytopeia Inc., Seattle, WA, USA) following standard procedures (Marie et al., 2004). Calibration was done for clades for which we had cultured strains: clades I, II, III, VIII, XV, and XVI.

FIELD SAMPLING

Water samples were collected aboard the R/V Oceanus (cruise OC375) along a transect between Massachusetts and the northwest Atlantic in March 2002. Latitudes and longitudes for sample stations were as follows: Station 8 (Sargasso Sea), 34° 59.88′ N, 70° 13.92′ W; station 16 (Gulf Stream), 37° 36.36′ N, 70° 44.09′ W; station 17 (coastal), 38° 35.79′ N, 70° 45.69′ W; and station 19 (coastal), 40° 38.06′ N, 70° 50.59′ W. Water was sampled at discrete depths with 20 l Niskin bottles attached to a Sea-Bird conductivity, temperature, depth (CTD) package (Sea-Bird Electronics Inc., Bellevue, WA, USA). One-hundred ml of 20 μm pre-filtered sea water was filtered onto 25 mm 0.2 μm polycarbonate filters to collect DNA for analysis with qPCR. Cells were collected on filters with gentle filtration (<15 mm Hg of vacuum) and chased with Preservation Solution [0.5 M NaCl, 10 mM Tris (pH 8.0), 100 mM EDTA (pH 8.0)] following the protocols described in Ahlgren et al. (2006). Filters were flash frozen in liquid N_2 and stored at −80°C until extraction and processing.

For flow cytometric analyses whole seawater samples were preserved with 0.125% glutaraldehyde, flash frozen in liquid N_2, and stored at −80°C for later analysis. For stations 16, 17, and 19 cyanobacterial concentrations were determined using a Cytopeia InFlux flow cytometer (Cytopeia Inc., Seattle, WA, USA) following standard procedures (Marie et al., 2004). *Synechococcus* and *Prochlorococcus* concentrations were previously reported for station 8 on this cruise using a different flow cytometer (Ahlgren and Rocap, 2006). A partial depth profile from station 8 was rerun on the InFlux cytometer with slightly different results, likely due to inaccuracy in the flow rate assumed by the facility where samples were initially run. Thus the *Prochlorococcus* and *Synechococcus* abundances we report for station 8 were adjusted by a correction factor to account for discrepancies between the two measurements.

For measurement of clade abundances DNA filters were extracted with the heat lysis protocol described above. Triplicate PCR reactions were performed for each clade-specific primer set using 5 μl of template DNA in a reaction cocktail of 20 μl and other conditions described above and in **Table 1**. *Synechococcus* clades were quantified on an ICycler thermocycler (BioRad Inc., Hercules, CA, USA) using a five place plasmid standard curve (also amplified in triplicate) and cell concentrations were calculated using the calibration curves of cells versus plasmids standards.

RESULTS

PHYLOGENIES OF MULTIPLE GENE LOCI

Because multiple loci (ITS, 16S rDNA, *narB*, *ntcA*, and *rpoC1*) have been used to describe the diversity of marine *Synechococcus*, we compared phylogenies of 24 strains inferred using these five loci to establish congruency in clades defined with individual loci. Where possible at least two strains from each clade were sequenced at all loci (**Table A2** in Appendix). Comparison of the different trees reveals that the same monophyletic clades supported by high bootstrap values were seen across all loci (**Figures A1–A5** in Appendix). We therefore created a phylogenetic tree using concatenated sequences of four of these loci (**Figure A6** in Appendix; **Figure 1**) to create consensus assignments of strains to clades (**Table A2** in Appendix). The *narB* gene was excluded from the concatenated analysis because it is absent in some strains (MITS9220 and RS9917).

Sequencing of multiple loci in key strains allowed us to resolve several issues in *Synechococcus* classification. Our phylogenies confirm that strains previously classified to clade VII based on 16S rDNA (Fuller et al., 2003) actually comprise two distinct clades, VII and CRD1 (Ahlgren and Rocap, 2006; Mazard et al., 2012; **Figures A2–A5** in Appendix). Strains UW92 and RS9920 accordingly retain their classification to clade VII while strains CC9305, CC9317, CC9318, Eum14, MITS9220 are assigned to clade CRD1 (**Table A2** in Appendix). Second, the framework established here allows placement of newly isolated or previously unclassified strains into clades. We isolated two new strains, UW179 and UW180, from the Equatorial Pacific which fall into clade CRD1. Strain CC9803 (obtained from B. Palenik) is a member of clade XV. Strain M16.17 (Everroad et al., 2006) clearly belongs to clade XVI along with strains UW140 and UW105 (**Figure A1** in Appendix). On the other hand, strain M11.1 (Everroad et al., 2006) is more divergent from other strains than the typical divergence between established clades (**Figure A1** in Appendix), and may represent a novel clade.

Finally, our phylogenies also resolve the identity of a few groups of sequences previously represented only by environmental clones. For example, by sequencing multiple loci in strains UW140 and UW105, we found that a previously obtained environmental sequence from the Red Sea was closely related to clade XVI (**Figure A5** in Appendix) suggesting that this clade may be found in waters other than the Atlantic (Muhling et al., 2006). Similarly, clade XIII, previously defined only by environmental *ntcA* sequences, forms a well supported monophyletic group with clade VII strain UW92 (**Figure A4** in Appendix). We conclude that clades VII and XIII are one and the same and we propose that the label XIII no longer be used. Despite this consolidation of sequences

into previously defined clades, several clades represented only by environmental sequences still remain (e.g., clades CRD2, XVII, and XVIII for the ITS; XI and XII for *ntcA*; see **Figure 1**; **Figures A2**, **A4**, and **A5** in Appendix).

Although single gene trees provide strong bootstrap support for individual clades, they did not always give strong support for the branching order of clades relative to one another (**Figures A1–A5** in Appendix). However, a few clades do consistently branch together, often with high bootstrap support. For example clades V and VI appear as sister clades in all trees, and clades II and XV also frequently branch together. Our concatenated phylogeny of 24 strains using four loci also supports the existence of two larger subclusters of clades (5.1A and 5.1B) inferred using 11 strains and a phylogeny of >1,000 concatenated core genes (Dufresne et al., 2008). That study assigns clades II, III, IV to subcluster 5.1A and clades I, V, VI, VIII, and IX to subcluster 5.1B. Our four loci concatenated phylogeny supports the 5.1A clustering of clades II, III, and IV and adds clade XV (**Figure 1**; **Figure A6** in Appendix). This phylogeny also suggests that clades I, V, VI, VII, XVI, and CRD1 form a second cluster, but without high bootstrap support (**Figure A6** in Appendix). One difference between these phylogenies is that the core gene phylogeny places clade VIII strain RS9917 within subcluster 5.1B, but in our tree clade VIII strains appear to form a separate lineage, although there is not strong bootstrap support for this placement (**Figure A6** in Appendix).

DESIGN, SPECIFICITY AND CALIBRATION OF qPCR ASSAYS

Quantitative PCR primer sets targeting the 16S–23S rDNA ITS region were designed to quantify 10 clades of *Synechococcus* (**Figure A2** in Appendix; **Table 1**). Primers were designed to be identical to all sequences within each specified clade when possible and have significant mismatches to all other *Synechococcus* ITS sequences.

After the design of these primers, additional *Synechococcus* ITS sequences have been published, and we reevaluated specificity of our primers to all publically available sequences. The degree to which primers match sequences (with 0, 1–2, or >2 mismatches) in each clade are shown in **Figure A2** in Appendix. In most cases, our primers perfectly match the majority of sequences within each clade, and of the 758 total ITS sequences publically available for the 10 clades that our qPCR primers target, 598 or 79% of ITS sequences perfectly match our primers across the respective clades.

It is also important to note that Huang et al. (2012) identified several new sequences similar to clade X and reclassified this group of sequences into clades 5.3-I through 5.3-VI within subcluster 5.3 (see **Figure 1**), such that clade X sequences (e.g., strain RCC307) fall within clade 5.3-I. Our clade X qPCR primers are identical to most sequences within clades 5.3-I through 5.3-III but have two or three mismatches to sequences belonging to subclades 5.3-IV, 5.3-V, and 5.3-VI (**Figure A2** in Appendix; Huang et al., 2012).

After optimizing qPCR reactions for maximal PCR efficiency by adjusting $MgCl_2$ concentration and annealing temperature (**Table 1**), initial lower limits of detection for each assay were set by determining the lowest concentration of plasmid standard at which the C_T values of triplicate reactions still had an error of ≤3%. The specificity of each assay was tested by challenging clade-specific qPCR assays with plasmid standards of other clades and the lower limits of detection were adjusted as necessary. Non-specific plasmids were tested at concentrations of 1.5×10^5 copies/μl, equivalent to cell densities of approximately 3×10^5 cells/ml. Except for primer sets for clade X, XVI, and CRD1, there was no non-specific amplification above the lowest set of plasmid standards. For clade X, the clade IV standard plasmid amplified nominally and the lower limit of detection was adjusted to two times that value (678 cells/ml, **Table 1**; **Table A3** in Appendix). The CRD1 primer set amplified plasmids for strains UW92 (clade VII), WH 7803 (clade V), and clone CRD8 (clade CRD2) to starting concentrations <239 copies/μl and the lower limit of detection was adjusted to two times 239 μl/copies or the equivalent of 1830 cells/ml (**Table 1**; **Table A3** in Appendix). Cross-amplification of the CRD1 set with plasmid oc175m12 (clade XVI) was significant, so a range of oc175m12 plasmid concentrations were quantified (from 1.54×10^5 to 3.42×10^2 copies/μl). The clade XVI plasmid cross-amplified at a ratio of 1:25 (concentration of non-specific plasmid to concentration quantified, **Table A3** in Appendix). Melt curves of clade XVI plasmids were very similar to those of the clade CRD1 standards (data not shown). The detection limit reported for clade CRD1 is two times the amplification of the WH 7803 plasmid standard (**Table 1**; **Table A3** in Appendix), but because of the high cross-amplification of clade XVI plasmid, clade CRD1 qPCR concentrations must be evaluated judiciously if clade XVI sequences are present at high levels in the same sample.

Plasmid standards used for real-time PCR were calibrated to DNA extractions of known quantities of cell cultures in order to calculate and report concentrations of *Synechococcus* clades in environmental samples in terms of cells per ml. DNA was extracted from filters that were generated with cultures over a range of concentrations from strains presenting six different clades (I, II, III, VIII, and XV, and XVI). ITS concentrations determined by qPCR were plotted against the number of cells in extractions (**Figure 2**). Log–log regressions all had strong correlation coefficients, and the slopes of regressions were all very close to one (**Table 2**). There was some variability between the y-intercepts of the regressions for the different strains tested. Excluding clade XV strains, the calibration curves for the different *Synechococcus* strains had similar y-intercepts (**Table 2**), and calibration points grouped closely together (**Figure 2**). This degree of variability in y-intercepts was similar to the variability seen in previous calibrations of *Prochlorococcus* assays (range of 0.38 versus 0.46 in Zinser et al., 2006). The variability in y-intercepts translates to roughly twofold differences ($10^{0.38} = 2.4$) between calibration curves and likely represents the limitations of qPCR to reliably detect at least twofold changes in copy number (Bar et al., 2003). Clade XV strains had noticeably higher *y*-intercepts than all other *Synechococcus* strains (**Table 2**; **Figure 2**), perhaps because these strains are more resilient to lysis than other clades resulting in lower yields of extracted genomic DNA.

Regressions were used to convert ITS copies quantified in field samples to cells per ml. For the clade XV assay, the regression of all three calibrations (two replicate calibrations for strain UW69 and one for strain UW106) was used (**Table 2**). For clades I, II, III, VIII, and XVI, the regression values of each individual clade were

used in back-calculating cell concentrations. For clades for which calibrations were not done (clades IV, X, CRD1, and CRD2), it was assumed that these clades have similar calibration curves to the other *Synechococcus* clades (excluding clade XV), and the slope and y-intercept from the regression of clades I, II, III, VIII, and XVI together were used.

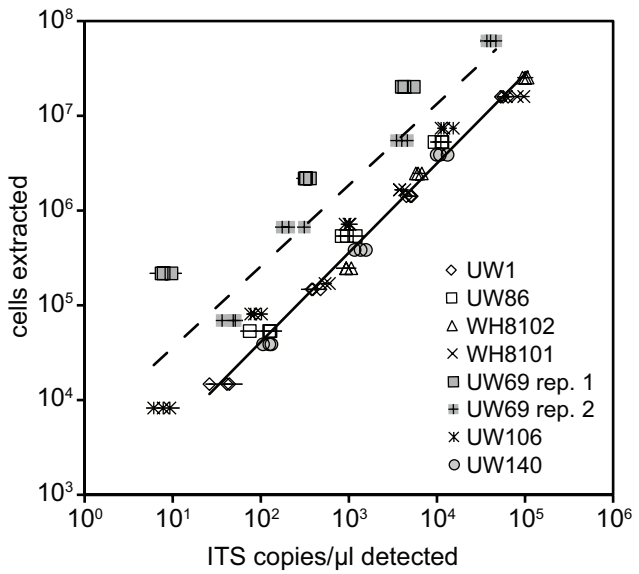

FIGURE 2 | Calibration of qPCR assays. Known amounts of cells from cultures were filtered and extracted for various strains. Extracted cells were plotted against the concentration of ITS copies/µl detected with qPCR using plasmid standards. Triplicate filters were made and extracted for each concentration of cells tested. Points represent averages of quadruplicate qPCR reactions performed on each extraction, and error bars represent the standard deviation. Log–log regression lines are shown for all clade XV strains tested (dashed line, UW69 both replicate filter sets and UW106) and all remaining strains together (solid line).

Table 2 | qPCR assay calibration curve statistics (see Figure 2).

Clade	Strain	Regression statistics[a]		
		R^2	Slope[b]	*y*-Intercept
I	UW1	0.99	0.94 ± 0.02	2.72
II	UW86	0.98	0.98 ± 0.05	2.79
III	WH8102	0.98	0.98 ± 0.05	2.56
VIII	WH8101	0.98	0.88 ± 0.05	2.92
XV	UW69 replicate 1	0.99	0.71 ± 0.03	4.64
XV	UW69 replicate 2	0.98	0.95 ± 0.04	3.41
XV	UW106	1.00	0.91 ± 0.02	3.13
XVI	UW140	0.99	1.01 ± 0.03	2.47
	All clade XV strains together	0.83	0.88 ± 0.07	3.65
	All other *Synechococcus* strains (excludes clade XV)	0.99	0.93 ± 0.02	2.76

[a] *Log-log regressions of cells extracted versus ITS copies/µl detected by qPCR (see **Figure 2**).*

[b] *95% confidence interval of slope is reported.*

APPLICATION OF qPCR ASSAYS IN THE SARGASSO SEA

Samples were collected on a transect off of the eastern United States in March of 2002 which traversed from the Sargasso Sea (station 8) through the Gulf Stream (station 16) and into coastal waters south of Massachusetts (stations 17, 19; **Figure 3**). The water column in the Sargasso Sea was well mixed to at least 175 m (**Figure 4**), as is typical for spring (DuRand et al., 2001). The Gulf Stream exhibited a warm surface layer (24°C) and a small chlorophyll maximum just below the surface mixed layer at 40 m. Station 17 was fairly uniform in temperature, but showed a subsurface peak in chlorophyll fluorescence twice as large as the maximum seen at other stations. Station 19 was located over the continental shelf and the water column was well mixed with chlorophyll fluorescence levels slightly higher than the Gulf Stream and Sargasso Sea. Water temperature at station 17 (14°C) was significantly colder than at the off-shore stations, and the drop in temperature from station 17 to station 19 (6°C) was just as large as the shift from off-shore to near-shore stations.

SYNECHOCOCCUS AND *PROCHLOROCOCCUS* POPULATION STRUCTURE

Total *Synechococcus* concentrations measured by flow cytometry decreased along the transect from the Sargasso Sea to the coast (**Figure 4**). Typical for this time of year, *Synechococcus* concentrations in the Sargasso Sea (14,000–36,000 cells/ml) outnumbered *Prochlorococcus* by 1.5- to 2-fold (DuRand et al., 2001). In contrast, *Prochlorococcus* concentrations in the Gulf Stream

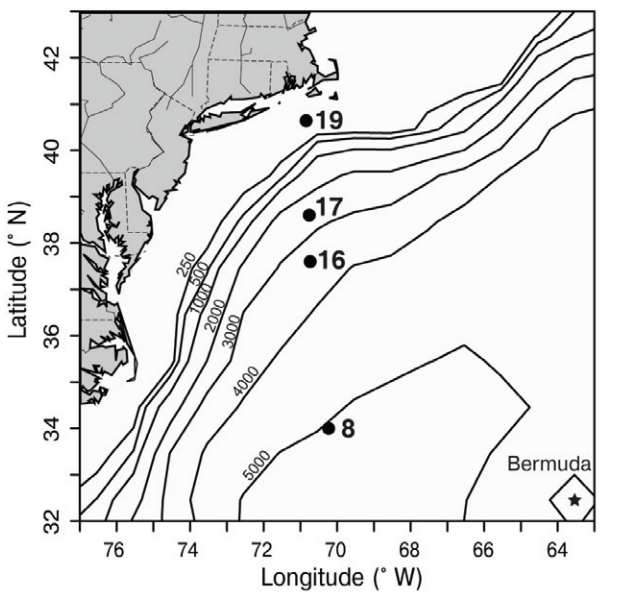

FIGURE 3 | Map depicting sampling locations (black dots) along a transect in the northwest Atlantic, south of Massachusetts in March 2002. Bathymetric contours (black lines, depth in m) are shown, and the location of Bermuda is marked with a star. Station 8 was located in the Sargasso Sea and station 16 was located in the Gulf Stream (based on satellite sea surface temperature, data not shown). Stations 17 and 19 represent coastal stations.

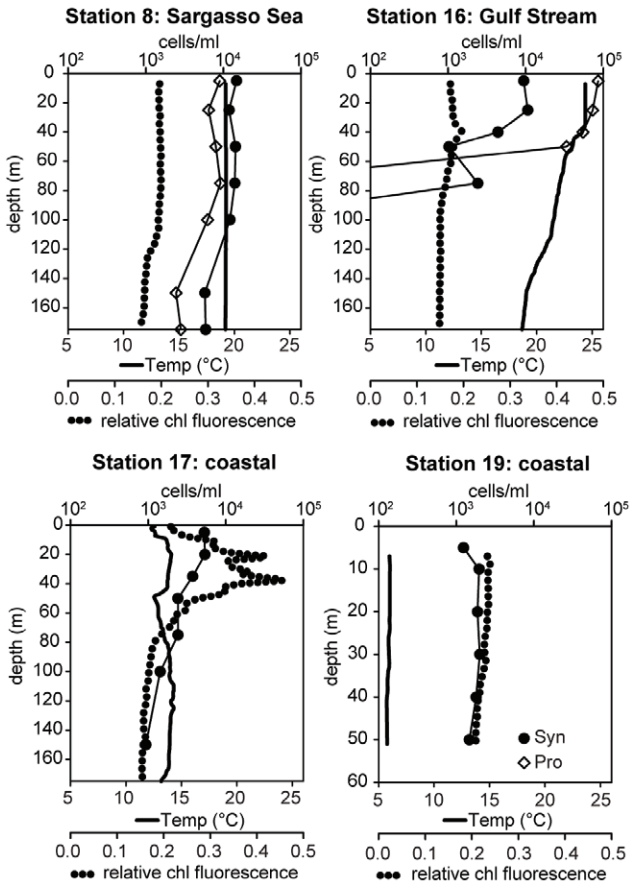

FIGURE 4 | Water column properties of field samples and total *Synechococcus* (Syn, filled circles) and *Prochlorococcus* (Pro, open diamonds) concentrations determined by flow cytometry. Water temperature is depicted with solid lines and relative chlorophyll (chl) fluorescence with dotted lines.

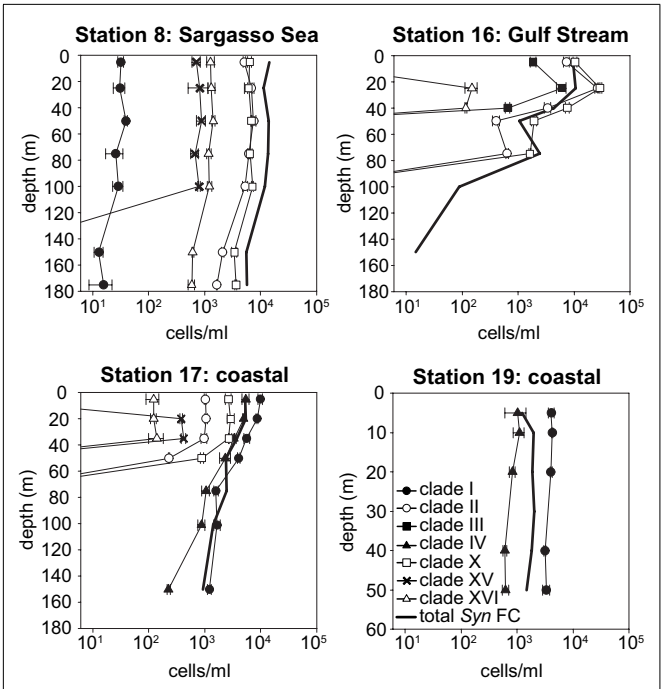

FIGURE 5 | Clade abundances determined by qPCR, and total *Synechococcus* concentrations determined by flow cytometry (FC). Error bars represent the standard deviation of triplicate qPCR reactions.

were $>3 \times 10^4$ cells/ml, 5- to 10-fold more abundant than *Synechococcus*. Neither genus was seen below 75 m in the Gulf Stream. *Synechococcus* concentrations at station 17 decreased slightly with depth ranging from 5,400 cells/ml at the surface to 934 cells/ml at 150 m. *Synechococcus* concentrations were fairly uniform (1,200–2,000 cells/ml) at the coastal station 19. No *Prochlorococcus* were observed at stations 17 and 19.

Synechococcus qPCR assays were applied to samples from these water columns. Amplicons of environmental samples had melt curves very similar to those of the plasmid standards for all clades detected (data not shown), further supporting the specificity of these assays. The abundance of the various clades reveal drastic shifts in community structure across the transect (**Figures 5** and **6**). Most significant was the shift in dominance of clades II and X in the warmer Sargasso Sea and Gulf Stream stations to clades I and IV at the colder coastal stations (stations 17 and 19). Only clades I and IV were detected at the coldest coastal station 19, but at station 17 several other clades (II, X, XV, and XVI) were detected at low abundance. Clades II, X, XV, and XVI were also present in the Sargasso Sea station. The Gulf Stream station was unique in that clade III was detected there and nowhere else. Clade II, X, and XVI were also detected in the Gulf Stream.

Total *Synechococcus* cell abundances determined by flow cytometry were compared to the sum of clade concentrations determined by qPCR (**Figure 6**). In the Sargasso Sea, the sum of qPCR results were very similar to total *Synechococcus* densities determined by flow cytometry at all depths (ratio of 0.95–1.3), but the sum of qPCR abundances were greater than flow cytometry numbers for the remaining three stations (ratio of 1.1–5.7).

DISCUSSION

A variety of loci (e.g., 16S, ITS, *cpeA*, *narB*, *ntcA*, *petB*, *rbcL*, *rpoC1*) have been used to assess and classify the diversity of marine *Synechococcus*. A MLSA using seven core genes found phylogenetic congruence between loci, reflecting relatively infrequent recombination between clades and general clonality in *Synechococcus* populations (Mazard et al., 2012). Consistent with this, the individual phylogenies determined here show congruence among five loci commonly used in diversity studies. Because our phylogenies included *ntcA* and the 5′ portion of *rpoC1* not covered in the prior MLSA study (Mazard et al., 2012), we were able to show that previously unassigned *rpoC1* sequences belong to clade XVI and that clade XIII defined by *ntcA* is synonymous with clade VII. We also assigned previously unclassified strains to appropriate clades (e.g., strain M16.17). However, there are still many clades across the various loci that are defined only by environmental sequences [e.g., clade XI and XII from *ntcA* (**Figure A4** in Appendix) or clade CRD2 in the ITS (**Figure A2** in Appendix)], and it is possible that some of these clades correspond to one another. Obtaining new

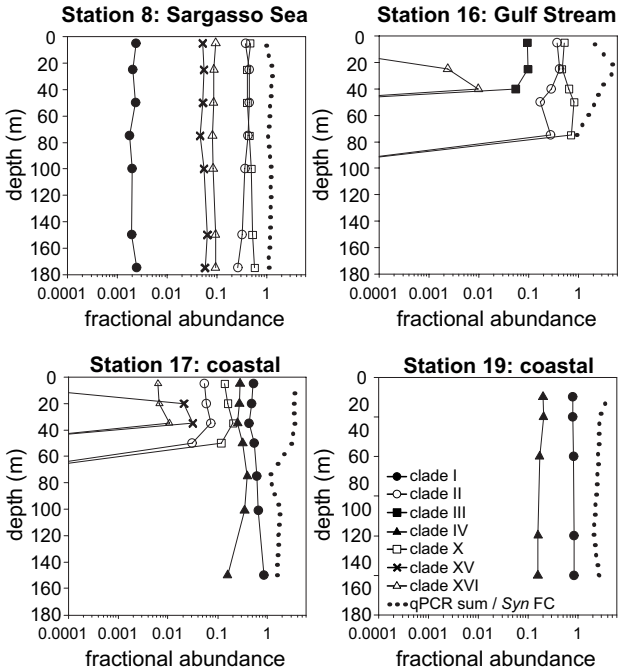

FIGURE 6 | Relative abundances of *Synechococcus* clades and the ratio of summed abundances to total *Synechococcus* abundance determined by flow cytometry. Relative abundances of clades were calculated by dividing the abundance of each clade by the sum of all clades detected by qPCR. Dotted lines depict the ratios of summed qPCR abundances to total *Synechococcus* abundances determined by flow cytometry (qPCR sum/*Syn* FC).

isolates and determining relevant sequences is necessary to further resolve if any of the clades defined by different loci are in fact synonymous.

Establishing that commonly used loci define congruent clades enables comparison of clade abundances measured by molecular assays that use different target loci such as the ITS, as here, *rpoC1* (Tai and Palenik, 2009) and 16S rDNA (Fuller et al., 2003) providing a better global picture of the biogeography of *Synechococcus*. One small caveat in these comparisons is that clade VII as defined by 16S rDNA sequences actually comprises two distinct clades (Ahlgren and Rocap, 2006; Mazard et al., 2012). Here we clarify the assignment of strains to clades VII and CRD1 and establish an independent assay for clade CRD1. However, it is not possible to compare quantitative data from assays currently designed for *narB* (Paerl et al., 2011) with the 16S rDNA, *rpoC1*, and ITS based assays. The *narB* qPCR primers detect sequences assigned to phylogenetic groups, named "A" through "G," that do not follow the conventional classification of clades established by previous studies (Paerl et al., 2008, 2011) and in many cases these groups include multiple clades as defined here and elsewhere. The *narB* primers also have mismatches to the majority of sequences within their putative target groups (**Figure A3** in Appendix). We suggest that these assays probably do not measure biologically relevant groups of sequences.

Phylogenomic analyses have divided marine *Synechococcus* clades into two larger phylogenetic groups (subclusters 5.1A and 5.1B; Dufresne et al., 2008). These subclusters were generally supported in our four gene concatenated tree, but individual gene phylogenies could not resolve the deeper evolutionary history of clades, consistent with other analyses of individual core genes (Mazard et al., 2012). The apparent rapid diversification of *Synechococcus* (Urbach et al., 1998) combined with low phylogenetic signal from the relatively short sequences used in single locus trees makes it difficult to resolve the higher branching order of the clades. Thus, although most individual loci are not adequate for resolving evolutionary relationships between clades, they contain enough variation to resolve fine-scale classification of *Synechococcus* diversity (placement of strains into clades), and can direct the selection of particular strains for genome sequencing to further resolve deeper evolutionary histories.

It has been suggested that subclusters 5.1A and 5.1B may reflect ecologically coherent groups that share common lifestyle strategies (Dufresne et al., 2008; Scanlan et al., 2009). Specifically 5.1A has been labeled as "open-ocean/specialists" and 5.1B as "coastal/opportunists". However, the idea of ecological coherence within groups 5.1A and 5.1B is in conflict with the fact that clade I and IV have nearly identical habitat ranges and appear to be specialized for cold, coastal, and mesotrophic habitats (Zwirglmaier et al., 2007, 2008; Tai and Palenik, 2009; and this study) yet belong two different subclusters, 5.1B and 5.1A respectively. Similarly, clade II appears to be more like an "opportunist" or "generalist" type, but it belongs to subcluster 5.1A that is claimed to contain specialist types. Clade II is found in a variety of habitats, in both oligotrophic and upwelling regions as well as coastal and open-ocean habitats (Zwirglmaier et al., 2008; Huang et al., 2012; this study). We suggest an alternative hypothesis wherein clades with similar lifestyle strategies have arisen independently via parallel evolution since the divergence of the 5.1A and 5.1B lineages. Additional data on clade biogeography and phylogenomics are needed to corroborate this hypothesis and elucidate the mechanism by which disparate lineages may arrive at common adaptive solutions to life in the oceans.

Having established congruency in clade phylogeny among multiple loci, we developed a new comprehensive set of ITS qPCR assays that detect 10 clades of marine *Synechococcus* and tested them in the Western Atlantic. We chose the ITS as a sequence target because it is much more variable than the 16S rDNA, allowing better resolution of closely related clades. Because the ITS has been widely used in diversity studies in the past 10 years, it is the locus with the largest number of sequences available for primer design. Despite its overall sequence variability, the ITS retains conserved regions, likely with structural function (Rocap et al., 2002), that enable robust clade-specific primer design. This is in contrast to protein coding genes where third codon position variability requires either the use of degenerate primers (Tai and Palenik, 2009) or acceptance of a high percentage of mismatches to the target sequences (Paerl et al., 2011). The ITS assays quantify most of the clades detected by previous 16S rDNA based probe methods (I–IV, VIII, X; Fuller et al., 2003) and all clades detected by *rpoC1* qPCR assays (I–IV; Tai and Palenik, 2009). Our new qPCR assays also detect newly characterized clades not covered by previous

methods (XV, XVI, CRD1, and CRD2; Saito et al., 2005; Ahlgren and Rocap, 2006). Overall, the assays are extremely sensitive, able to detect, in some cases, concentrations as little as tens of cells per ml (**Table 1**). In all but one case, these assays are highly specific with little or no cross-amplification of other clades. The one exception is the clade CRD1 primer set which exhibits significant cross-amplification with clade XVI (at a ratio of 1:25), but clade CRD1 can still be reliably quantified when clade XVI is present at low concentrations.

High-throughput sequence analysis methods provide new approaches to quantifying genetic types from field samples. Mazard et al. (2012) have recently utilized sequencing and RFLP analysis of many sequences from *petB* clone libraries to characterize communities, and Post et al. (2011) have used high depth pyrosequencing of the 16S rDNA to track the abundance of *Synechococcus* clades over time. qPCR assays can still provide an advantage over sequence analysis methods in their ability to quantitatively measure abundance over several orders of magnitude and in particular to sensitively measure minority clades (e.g., see **Figure 6**). Less abundant types (i.e., those less than 0.1% of the population, as we have detected here, see **Figure 6**) may be missed or misrepresented by PCR or clone library based methods that require enormous depths of sampling to quantitatively measure rare taxa. There is growing interest in the significance of rare types as potential reservoirs of genomic diversity (Sogin et al., 2006), and indeed rare bacteria can contribute significantly to the metabolic function of ecosystems (Musat et al., 2008).

The new *Synechococcus* qPCR assays successfully detected seven clades in Atlantic water samples, including recently described clades XV and XVI. Clades XV and XVI were detected in the same waters from which we previously discovered these two new clades using both culture isolation and cyanobacterial clone libraries (Ahlgren and Rocap, 2006), as were most of the other clades observed in that previous study. Clade VIII was not detected by qPCR in any samples. This is not surprising since clade VIII appears to be most prevalent in hypersaline habitats (Zwirglmaier et al., 2008; Huang et al., 2012). Clades CRD1 and CRD2 also were not seen in the Atlantic, but the ITS qPCR assays can successfully detect these clades in the Pacific (Ahlgren and Rocap, unpub. data), consistent with their detection using clone libraries in Pacific waters (Saito et al., 2005; Huang et al., 2012).

Summed *Synechococcus* concentrations of clades determined by qPCR were often greater than those determined by flow cytometry. Application of the *rpoC1* qPCR assays to field samples has also produced a similar overestimation of total *Synechococcus* populations (Tai and Palenik, 2009). Those authors speculate that this discrepancy is due to the presence of dividing cells that possess multiple genome copies but that are counted as only one cell by flow cytometry. Although most *Synechococcus* genomes contain two identical copies of the ITS, normalization of plasmid standards to cell cultures takes into account this fact. Some *Synechococcus* strains are known to possess multiple genome copies, and in some cases cells in culture maintain multiple genome equivalents at all times over the light:dark cycle even though field populations typically exhibit cyclical changes in ploidy level due to synchronization of cell cycle to the diel cycle (Binder and Chisholm, 1995; Vaulot et al., 1996; Liu et al., 1998; Jacquet et al., 2001; Holtzendorff et al., 2008; Griese et al., 2011). Natural *Synechococcus* populations can contain cells that contain >2 genome equivalents per cell, and the proportion of the population that has multiple genome copies varies between samples (Liu et al., 1998). Thus variability in ploidy level in natural populations across habitats and possible differences between laboratory cultures and natural populations could potentially explain overestimation of total cell number. Because overestimation by qPCR is typically threefold or less, we contend that significant ecological conclusions can still be drawn from the order of magnitude differences in clade abundances seen across the different sites sampled here.

The significant shift in *Synechococcus* community structure that we see in our Atlantic samples (**Figures 5** and **6**) is consistent with major patterns of clade biogeography inferred by previous studies. We find clade II highly abundant in warmer, off-shore stations, as seen in quantitative assays (Zwirglmaier et al., 2007, 2008) and diversity studies (Huang et al., 2012; Mazard et al., 2012). We found clade III only in surface waters in the Gulf Stream, the warmest station sampled (**Figure 5**). Clade III is typically found in warm oligotrophic water masses, such as the Mediterranean and the Red Sea only during summer (Fuller et al., 2005; Zwirglmaier et al., 2008; Post et al., 2011). Clade III has therefore been classified as an "oligotroph" (Zwirglmaier et al., 2008).

Our qPCR assays also confirm that clades I and IV dominate *Synechococcus* populations in cold, coastal waters (Zwirglmaier et al., 2007, 2008; Tai and Palenik, 2009; Tai et al., 2011; Huang et al., 2012; Mazard et al., 2012). The relative ratio of these clades shifts over seasonal cycles in California coastal waters and between different high latitude locales. In our samples, clade I was always more abundant than clade IV (1.7- to 6.5-fold), similar to observations in the spring off of California (Tai and Palenik, 2009). However in the Arctic, South Pacific, and Eastern Atlantic, clade IV is consistently more abundant than or on par with clade I concentrations (Zwirglmaier et al., 2008). These differences probably point to distinct adaptations between these two cold-adapted clades. Further application of qPCR assays to field samples or in lab competition experiments could provide insight into what controls the co-existence and relative abundance of clades I and IV in colder, coastal habitats.

Results from this Atlantic transect also provide insights into *Synechococcus* community structure that contrast from previous work. Here, clade X together with clade II dominated the warmer off-shore stations, but in previous 16S rDNA surveys, clade X was only rarely detected and never exceeded 10% of total cyanobacterial DNA amplified (Zwirglmaier et al., 2007, 2008). The prevalence of sequences from clades 5.3-I/X, 5.3-II, and 5.3-III in clone libraries constructed from open-ocean locations (e.g., sites UTK211, UTK262 from Huang et al., 2012) together with our data strongly suggests that these clades are adapted to open-ocean habitats.

We detected as many as six clades in a single sample (at coastal station 17, **Figures 5** and **6**) confirming the oft observed pattern that multiple clades of *Synechococcus* co-exist. For example, both here and in other studies, although clade I and IV are dominant in colder coastal waters, they are also present in warmer off-shore waters, albeit at low densities (**Figures 5** and **6**; Zwirglmaier et al., 2008). In addition, several clades such as IX, XV, and XVI have still

only been seen to comprise minor portions of total *Synechococcus* populations. These clades may occur at higher concentrations only under particular conditions. For example in the Red Sea, clade III remains at low concentrations at most times of the year but peaks in abundance during summer, stratified conditions (Fuller et al., 2005; Post et al., 2011).

The qPCR assays developed in this study provide valuable tools to further identify the specific adaptations and niches of *Synechococcus* clades. Statistical analysis of clade abundance and concurrently measured environmental parameters suggests factors such as temperature, depth, light level, and macronutrient concentrations only explain a portion of the variance in clade abundance (Johnson et al., 2006; Zwirglmaier et al., 2008). Other factors not measured, such as trace metal availability and top-down pressure from grazers or phage are likely to be important in the adaptation and ecology of cyanobacterial ecotypes (Mann et al., 2002; Sullivan et al., 2003; Zwirglmaier et al., 2009; Apple et al., 2011; Strom et al., 2011). Only one study has simultaneously followed the diversity of *Synechococcus* and their infecting phage, and although clade abundances were not measured, significant covariation of host and phage diversity was observed, strongly suggesting that phage impact community structure (Muhling et al., 2005). Coupling qPCR assays with measurement of these other factors will help illuminate the ecology of *Synechococcus* clades. A mechanistic understanding of clade dynamics within this one group of marine cyanobacteria will enrich our broader understanding of the important drivers that control microbial community structure in the oceans and the mechanisms of co-existence for bacteria in general. Relatively small differences in nutrient utilization or adaptation to temperature between *Prochlorococcus* ecotypes can impact ocean basin-scale distributions (Johnson et al., 2006). Therefore understanding the structure of microbial populations at the ecotype scale of diversity is critical to assessing metabolic functioning of the oceans on a global scale (Follows et al., 2007).

ACKNOWLEDGMENTS

We thank the captain and crew of the R/V Oceanus as well as E. V. Armbrust and R. Olson (chief scientists). We also thank D. Scanlan for cell pellets for strains RS9911 and RS9920 and B. Palenik for cell pellets from strain CC9803 and K. Peterson and C. Williams for assistance with sequencing. This work was supported by NSF grants OCE-0220826 and OCE-0352190 to G. Rocap and a NDSEG fellowship to N. Ahlgren.

REFERENCES

Ahlgren, N. A., and Rocap, G. (2006). Culture isolation and culture-independent clone libraries reveal new marine *Synechococcus* ecotypes with distinctive light and N physiologies. *Appl. Environ. Microbiol.* 72, 7193–7204.

Ahlgren, N. A., Rocap, G., and Chisholm, S. W. (2006). Measurement of *Prochlorococcus* ecotypes using real-time polymerase chain reaction reveals different abundances of genotypes with similar light physiologies. *Environ. Microbiol.* 8, 441–454.

Apple, J., Strom, S., Palenik, B., and Brahamsha, B. (2011). Variability in protist grazing and growth on different marine *Synechococcus* isolates. *Appl. Environ. Microbiol.* 77, 3074–3084.

Bar, T., Stahlberg, A., Muszta, A., and Kubista, M. (2003). Kinetic outlier detection (KOD) in real-time PCR. *Nucleic Acids Res.* 31, e105.

Beja, O., Suzuki, M. T., Koonin, E. V., Aravind, L., Hadd, A., Nguyen, L. P., Villacorta, R., Amjadi, M., Garrigues, C., Jovanovich, S. B., Feldman, R. A., and DeLong, E. F. (2000). Construction and analysis of bacterial artificial chromosome libraries from a marine microbial assemblage. *Environ. Microbiol.* 2, 516–529.

Binder, B. J., and Chisholm, S. W. (1995). Cell cycle regulation in marine *Synechococcus* sp. strains. *Appl. Environ. Microbiol.* 61, 708–717.

Cai, H., Wang, K., Huang, S., Jiao, N., and Chen, F. (2010). Distinct patterns of picocyanobacterial communities in winter and summer in the Chesapeake Bay. *Appl. Environ. Microbiol.* 76, 2955–2960.

Chen, F., Wang, K., Kan, J., Bachoon, D., Lu, J., Lau, S., and Campbell, L. (2004). Phylogenetic diversity of *Synechococcus* in the Chesapeake Bay revealed by ribulose-1,5-bisphosphate carboxylase-oxygenase (RuBisCO) large subunit gene (rbcL) sequences. *Aquat. Microb. Ecol.* 36, 153–164.

Chen, F., Wang, K., Kan, J., Suzuki, M., and Wommack, K. (2006). Diverse and unique picocyanobacteria in Chesapeake Bay, revealed by 16S-23S rRNA internal transcribed spacer sequences. *Appl. Environ. Microbiol.* 72, 2239–2243.

Choi, D., and Noh, J. (2009). Phylogenetic diversity of *Synechococcus* strains isolated from the East China Sea and the East Sea. *FEMS Microbiol. Ecol.* 69, 439–448.

Choi, D., Noh, J., Hahn, M., and Lee, C. (2011). Picocyanobacterial abundances and diversity in surface water of the northwestern Pacific Ocean. *Ocean Sci. J.* 46, 265–271.

Dufresne, A., Ostrowski, M., Scanlan, D., Garczarek, L., Mazard, S., Palenik, B., Paulsen, I., de Marsac, N., Wincker, P., Dossat, C., Ferriera, S., Johnson, J., Post, A., Hess, W., and Partensky, F. (2008). Unraveling the genomic mosaic of a ubiquitous genus of marine cyanobacteria. *Genome Biol.* 9, R90.

DuRand, M. D., Olson, R. J., and Chisholm, S. W. (2001). Phytoplankton population dynamics at the Bermuda Atlantic Time-series station in the Sargasso Sea. *Deep Sea Res. Part II Top. Stud. Oceanogr.* 48, 1983–2003.

Everroad, C., Six, C., Partensky, F., Thomas, J., Holtzendorff, J., and Wood, A. (2006). Biochemical bases of type IV chromatic adaptation in marine *Synechococcus* spp. *J. Bacteriol.* 188, 3345–3356.

Ferris, M. J., and Palenik, B. (1998). Niche adaptation in ocean cyanobacteria. *Nature* 396, 226–228.

Follows, M., Dutkiewicz, S., Grant, S., and Chisholm, S. (2007). Emergent biogeography of microbial communities in a model ocean. *Science* 315, 1843–1846.

Fuller, N. J., Marie, D., Partensky, F., Vaulot, D., Post, A. F., and Scanlan, D. J. (2003). Clade-specific 16S ribosomal DNA oligonucleotides reveal the predominance of a single marine *Synechococcus* clade throughout a stratified water column in the Red Sea. *Appl. Environ. Microbiol.* 69, 2430–2443.

Fuller, N. J., West, N. J., Marie, D., Yallop, M., Rivlin, T., Post, A. F., and Scanlan, D. J. (2005). Dynamics of community structure and phosphate status of picocyanobacterial populations in the Gulf of Aqaba, Red Sea. *Limnol. Oceanogr.* 50, 363–375.

Giovannoni, S., Britschgi, T., Moyer, C., and Field, K. (1990). Genetic diversity in Sargasso Sea bacterioplankton. *Nature* 345, 60–63.

Griese, M., Lange, C., and Soppa, J. (2011). Ploidy in cyanobacteria. *FEMS Microbiol. Lett.* 323, 124–131.

Herdman, M., Castenholz, R. W., Waterbury, J. B., and Rippka, R. (2001). "Form-genus XIII. *Synechococcus*," in *Bergey's Manual of Systematic Bacteriology*, eds D. R. Boone and R. W. Castenholz (New York, NY: Springer-Verlag), 508–512.

Holtzendorff, J., Partensky, F., Mella, D., Lennon, J. F., Hess, W. R., and Garczarek, L. (2008). Genome streamlining results in loss of robustness of the circadian clock in the marine cyanobacterium *Prochlorococcus marinus* PCC 9511. *J. Biol. Rhythms* 23, 187–199.

Huang, S., Wilhelm, S. W., Harvey, H. R., Taylor, K., Jiao, N., and Chen, F. (2012). Novel lineages of *Prochlorococcus* and *Synechococcus* in the global oceans. *ISME J.* 6, 285–297.

Jacquet, S., Partensky, F., Lennon, J. F., and Vaulot, D. (2001). Diel patterns of growth and division in marine picoplankton in culture. *J. Phycol.* 37, 357–369.

Jardillier, L., Zubkov, M. V., Pearman, J., and Scanlan, D. J. (2010). Significant CO(2) fixation by small prymnesiophytes in the subtropical and tropical northeast Atlantic Ocean. *ISME J.* 4, 1180–1192.

Jenkins, B., Zehr, J., Gibson, A., and Campbell, L. (2006). Cyanobacterial assimilatory nitrate reductase gene diversity in coastal and oligotrophic marine environments. *Environ. Microbiol.* 8, 2083–2095.

Johnson, Z. I., Zinser, E. R., Coe, A., McNulty, N. P., Woodward, E. M. S., and Chisholm, S. W. (2006). Niche partitioning among *Prochlorococcus* ecotypes along ocean-scale environmental gradients. *Science* 311, 1737–1740.

Kan, J., Evans, S., Chen, F., and Suzuki, M. (2008). Novel estuarine bacterioplankton in rRNA operon libraries from the Chesapeake Bay. *Aquat. Microb. Ecol.* 51, 55–66.

Li, W. K. W. (1994). Primary production of prochlorophytes, cyanobacteria, and eukaryotic ultraphytoplankton – measurements from flow cytometric sorting. *Limnol. Oceanogr.* 39, 169–175.

Lindell, D., and Post, A. F. (2001). Ecological aspects of ntcA gene expression and its use as an indicator of the nitrogen status of marine *Synechococcus* spp. *Appl. Environ. Microbiol.* 67, 3340–3349.

Liu, H., Campbell, L., Landry, M. R., Nolla, H. A., Brown, S. L., and Constantinou, J. (1998). *Prochlorococcus* and *Synechococcus* growth rates and contributions to production in the Arabian Sea during the 1995 Southwest and Northeast Monsoons. *Deep Sea Res. Part II Top. Stud. Oceanogr.* 45, 2327–2352.

Liu, H. B., Nolla, H. A., and Campbell, L. (1997). Prochlorococcus growth rate and contribution to primary production in the equatorial and subtropical North Pacific Ocean. *Aquat. Microb. Ecol.* 12, 39–47.

Ludwig, W., Strunk, O., Westram, R., Richter, L., Meier, H., Yadhukumar, L., Buchner, A., Lai, T., Steppi, S., Jobb, G., Forster, W., Brettske, I., Gerber, S., Ginhart, A. W., Gross, O., Grumann, S., Hermann, S., Jost, R., Konig, A., Liss, T., Lussmann, R., May, M., Nonhoff, B., Reichel, B., Strehlow, R., Stamatakis, A., Stuckmann, N., Vilbig, A., Lenke, M., Ludwig, T., Bode, A., and Schleifer, K. H. (2004). ARB: a software environment for sequence data. *Nucleic Acids Res.* 32, 1363–1371.

Mann, E. L., Ahlgren, N., Moffett, J. W., and Chisholm, S. W. (2002). Copper toxicity and cyanobacteria ecology in the Sargasso Sea. *Limnol. Oceanogr.* 47, 976–988.

Marie, D., Simon, N., and Vaulot, D. (2004). "Phytoplankton cell counting by flow cytometry," in *Algal Culturing Techniques*, ed. R. A. Anderson (London: Academic Press), 253–267.

Mazard, S., Ostrowski, M., Partensky, F., and Scanlan, D. J. (2012). Multi-locus sequence analysis, taxonomic resolution and biogeography of marine *Synechococcus*. *Environ. Microbiol.* 14, 372–386.

Mella-Flores, D., Mazard, S., Humily, F., Partensky, F., Mahe, F., Bariat, L., Courties, C., Marie, D., Ras, J., Mauriac, R., Jeanthon, C., Bendif, E. M., Ostrowski, M., Scanlan, D. J., and Garczarek, L. (2011). Is the distribution of *Prochlorococcus* and *Synechococcus* ecotypes in the Mediterranean Sea affected by global warming? *Biogeosciences* 8, 2785–2804.

Moore, L. R., and Chisholm, S. W. (1999). Photophysiology of the marine cyanobacterium *Prochlorococcus*: ecotypic differences among cultured isolates. *Limnol. Oceanogr.* 44, 628–638.

Moore, L. R., Post, A. F., Rocap, G., and Chisholm, S. W. (2002). Utilization of different nitrogen sources by the marine cyanobacteria *Prochlorococcus* and *Synechococcus*. *Limnol. Oceanogr.* 47, 989–996.

Moore, L. R., Rocap, G., and Chisholm, S. W. (1998). Physiology and molecular phylogeny of coexisting *Prochlorococcus* ecotypes. *Nature* 393, 464–467.

Muhling, M., Fuller, N. J., Millard, A., Somerfield, P. J., Marie, D., Wilson, W. H., Scanlan, D. J., Post, A. F., Joint, I., and Mann, N. H. (2005). Genetic diversity of marine *Synechococcus* and co-occurring cyanophage communities: evidence for viral control of phytoplankton. *Environ. Microbiol.* 7, 499–508.

Muhling, M., Fuller, N. J., Somerfield, P. J., Post, A. F., Wilson, W. H., Scanlan, D. J., Joint, I., and Mann, N. H. (2006). High resolution genetic diversity studies of marine *Synechococcus* isolates using rpoC1-based restriction fragment length polymorphism. *Aquat. Microb. Ecol.* 45, 263–275.

Musat, N., Halm, H., Winterholler, B., Hoppe, P., Peduzzi, S., Hillion, F., Horreard, F., Amann, R., Jorgensen, B. B., and Kuypers, M. M. M. (2008). A single-cell view on the ecophysiology of anaerobic phototrophic bacteria. *Proc. Natl. Acad. Sci. U.S.A.* 105, 17861–17866.

Paerl, R., Foster, R., Jenkins, B., Montoya, J., and Zehr, J. (2008). Phylogenetic diversity of cyanobacterial narB genes from various marine habitats. *Environ. Microbiol.* 10, 3377–3387.

Paerl, R. W., Johnson, K. S., Welsh, R. M., Worden, A. Z., Chavez, F. P., and Zehr, J. P. (2011). Differential distributions of *Synechococcus* subgroups across the California current system. *Front. Microbiol.* 2:59. doi:10.3389/fmicb.2011.00059

Paerl, R. W., Turk, K. A., Beinart, R. A., Chavez, F. P., and Zehr, J. P. (2012). Seasonal change in the abundance of *Synechococcus* and multiple distinct phylotypes in Monterey Bay determined by rbcL and narB quantitative PCR. *Environ. Microbiol.* 14, 580–593.

Palenik, B. (1994). Cyanobacterial community structure as seen from RNA-polymerase gene sequence-analysis. *Appl. Environ. Microbiol.* 60, 3212–3219.

Palenik, B. (2001). Chromatic adaptation in marine *Synechococcus* strains. *Appl. Environ. Microbiol.* 67, 991–994.

Partensky, F., Hess, W. R., and Vaulot, D. (1999). *Prochlorococcus*, a marine photosynthetic prokaryote of global significance. *Microbiol. Mol. Biol. Rev.* 63, 106–127.

Penno, S., Lindell, D., and Post, A. (2006). Diversity of *Synechococcus* and *Prochlorococcus* populations determined from DNA sequences of the N-regulatory gene ntcA. *Environ. Microbiol.* 8, 1200–1211.

Posada, D., and Crandall, K. A. (1998). MODELTEST: testing the model of DNA substitution. *Bioinformatics* 14, 817–818.

Post, A. F., Penno, S., Zandbank, K., Paytan, A., Huse, S. M., and Welch, D. M. (2011). Long term seasonal dynamics of *Synechococcus* population structure in the Gulf of Aqaba, Northern Red Sea. *Front. Microbiol.* 2:131. doi:10.3389/fmicb.2011.00131

Rocap, G., Distel, D. L., Waterbury, J. B., and Chisholm, S. W. (2002). Resolution of *Prochlorococcus* and *Synechococcus* ecotypes by using 16S-23S ribosomal DNA internal transcribed spacer sequences. *Appl. Environ. Microbiol.* 68, 1180–1191.

Saito, M. A., Rocap, G., and Moffett, J. W. (2005). Production of cobalt binding ligands in a *Synechococcus* feature at the Costa Rica upwelling dome. *Limnol. Oceanogr.* 50, 279–290.

Scanlan, D., Ostrowski, M., Mazard, S., Dufresne, A., Garczarek, L., Hess, W., Post, A., Hagemann, M., Paulsen, I., and Partensky, F. (2009). Ecological genomics of marine picocyanobacteria. *Microbiol. Mol. Biol. Rev.* 73, 249–299.

Scanlan, D. J., and West, N. J. (2002). Molecular ecology of the marine cyanobacterial genera *Prochlorococcus* and *Synechococcus*. *FEMS Microbiol. Ecol.* 40, 1–12.

Six, C., Thomas, J., Garczarek, L., Ostrowski, M., Dufresne, A., Blot, N., Scanlan, D., and Partensky, F. (2007). Diversity and evolution of phycobilisomes in marine Synechococcus spp.: a comparative genomics study. *Genome Biol.* 8, R259.

Sogin, M. L., Morrison, H. G., Huber, J. A., Mark Welch, D., Huse, S. M., Neal, P. R., Arrieta, J. M., and Herndl, G. J. (2006). Microbial diversity in the deep sea and the underexplored "rare biosphere." *Proc. Natl. Acad. Sci. U.S.A.* 103, 12115–12120.

Stamatakis, A. (2006). RAxML-VI-HPC: maximum likelihood-based phylogenetic analyses with thousands of taxa and mixed models. *Bioinformatics* 22, 2688–2690.

Steglich, C., Post, A. F., and Hess, W. R. (2003). Analysis of natural populations of *Prochlorococcus* spp. in the northern Red Sea using phycoerythrin gene sequences. *Environ. Microbiol.* 5, 681–690.

Strom, S., Brahamsha, B., Fredrickson, K., Apple, J., and Gutierrez-Rodriguez, A. (2011). Constitutive defense in the microbial plankton: a giant cell surface protein in *Synechococcus* WH8102 inhibits feeding by a model dinoflagellate predator. *J. Phycol.* 47, S49.

Sullivan, M. B., Waterbury, J. B., and Chisholm, S. W. (2003). Cyanophages infecting the oceanic cyanobacterium *Prochlorococcus*. *Nature* 424, 1047–1051.

Suzuki, M. T., Beja, O., Taylor, L. T., and DeLong, E. F. (2001). Phylogenetic analysis of ribosomal RNA operons from uncultivated coastal marine bacterioplankton. *Environ. Microbiol.* 3, 323–331.

Swofford, D. L. (1999). *PAUP*: Phylogenetic Analysis Using Parsimony (* and Other Methods)*. Sunderland, MA: Sinauer Associates.

Tai, V., Burton, R., and Palenik, B. (2011). Temporal and spatial distributions of marine *Synechococcus* in the Southern California Bight assessed by hybridization to bead-arrays. *Mar. Ecol. Prog. Ser.* 426, 133–147.

Tai, V., and Palenik, B. (2009). Temporal variation of *Synechococcus* clades at a coastal Pacific Ocean monitoring site. *ISME J.* 3, 903–915.

Toledo, G., and Palenik, B. (1997). *Synechococcus* diversity in the California current as seen by RNA polymerase (rpoC1) gene sequences of isolated strains. *Appl. Environ. Microbiol.* 63, 4298–4303.

Toledo, G., Palenik, B., and Brahamsha, B. (1999). Swimming marine *Synechococcus* strains with widely different photosynthetic pigment ratios form a monophyletic

group. *Appl. Environ. Microbiol.* 65, 5247–5251.

Urbach, E., Scanlan, D. J., Distel, D. L., Waterbury, J. B., and Chisholm, S. W. (1998). Rapid diversification of marine picophytoplankton with dissimilar light-harvesting structures inferred from sequences of *Prochlorococcus* and *Synechococcus* (Cyanobacteria). *J. Mol. Evol.* 46, 188–201.

Vaulot, D., LeBot, N., Marie, D., and Fukai, E. (1996). Effect of phosphorus on the *Synechococcus* cell cycle in surface Mediterranean waters during summer. *Appl. Environ. Microbiol.* 62, 2527–2533.

Waterbury, J. B., Watson, S. W., Valois, F. W., and Franks, D. G. (1986). Biological and ecological characterization of the marine unicellular cyanobacteria *Synechococcus*. *Can. J. Fish. Aquat. Sci.* 214, 71–120.

Waterbury, J. B., Willey, J. M., Franks, D. G., Valois, F. W., and Watson, S. W. (1985). A Cyanobacterium capable of swimming motility. *Science* 230, 74–76.

West, N. J., and Scanlan, D. J. (1999). Niche-partitioning of *Prochlorococcus* populations in a stratified water column in the eastern North Atlantic Ocean. *Appl. Environ. Microbiol.* 65, 2585–2591.

West, N. J., Schonhuber, W. A., Fuller, N. J., Amann, R. I., Rippka, R., Post, A. F., and Scanlan, D. J. (2001). Closely related *Prochlorococcus* genotypes show remarkably different depth distributions in two oceanic regions as revealed by in situ hybridization using 16S rRNA-targeted oligonucleotides. *Microbiology* 147, 1731–1744.

Zeidner, G., Preston, C. M., Delong, E. F., Massana, R., Post, A. F., Scanlan, D. J., and Beja, O. (2003). Molecular diversity among marine picophytoplankton as revealed by psbA analyses. *Environ. Microbiol.* 5, 212–216.

Zinser, E. R., Coe, A., Johnson, Z. I., Martiny, A. C., Fuller, N. J., Scanlan, D. J., and Chisholm, S. W. (2006). *Prochlorococcus* ecotype abundances in the North Atlantic Ocean as revealed by an improved quantitative PCR method. *Appl. Environ. Microbiol.* 72, 723–732.

Zuker, M. (2003). MFOLD web server for nucleic acid folding and hybridization prediction. *Nucleic Acids Res.* 31, 3406–3415.

Zwirglmaier, K., Heywood, J. L., Chamberlain, K., Woodward, E. M., Zubkov, M. V., and Scanlan, D. J. (2007). Basin-scale distribution patterns of picocyanobacterial lineages in the Atlantic Ocean. *Environ. Microbiol.* 9, 1278–1290.

Zwirglmaier, K., Jardillier, L., Ostrowski, M., Mazard, S., Garczarek, L., Vaulot, D., Not, F., Massana, R., Ulloa, O., and Scanlan, D. J. (2008). Global phylogeography of marine *Synechococcus* and *Prochlorococcus* reveals a distinct partitioning of lineages among oceanic biomes. *Environ. Microbiol.* 10, 147–161.

Zwirglmaier, K., Spence, E., Zubkov, M. V., Scanlan, D. J., and Mann, N. H. (2009). Differential grazing of two heterotrophic nanoflagellates on marine *Synechococcus* strains. *Environ. Microbiol.* 11, 1767–1776.

Conflict of Interest Statement: The authors declare that the research was conducted in the absence of any commercial or financial relationships that could be construed as a potential conflict of interest.

Received: 14 February 2012; accepted: 24 May 2012; published online: 19 June 2012.

Citation: Ahlgren NA and Rocap G (2012) Diversity and distribution of marine Synechococcus: multiple gene phylogenies for consensus classification and development of qPCR assays for sensitive measurement of clades in the ocean. Front. Microbio. ***3****:213. doi: 10.3389/fmicb.2012.00213*

This article was submitted to Frontiers in Aquatic Microbiology, a specialty of Frontiers in Microbiology.

APPENDIX

Table A1 | Primers and PCR conditions used to amplify and sequence five loci from *Synechococcus* strains.

Gene	PCR primers (listed 5′ to 3′)	Mg^{2+} conc. (mM)	Primer concentration (μM)	Thermocycling conditions	Internal sequencing primers (listed 5′ to 3′)
16S rDNA	OXY107F, ggacgggtgagtaacgcgtg; OXY1313R, cttcaygyaggcgagttgcagc (West et al., 2001)	1.5	0.2	30 cycles: 95°C 1 min; 55°C 1 min; 72°C 1 min	16S-515F, gtgccagcagccgcggtaa; 16S-907R, ccgtcaattcctttragttt
16S–23S rDNA ITS	16S-1247F, cgtactacaatgctacgg; 23S-241R, ttcgctcgccrctact (Rocap et al., 2002)	2.5	0.5	30 cycles: 95°C 30 s; 55°C 30 s; 72°C 1.5 min	ITS-AlaF, twtagctcagttggtagag; ITS-AlaR, ttcgctcgccrctact (Rocap et al., 2002)
narB	*narB*1F, gaaggcaayccgatgtgga; *narB*degR1, gcccctactgcggtgtnggctgygg (Ahlgren and Rocap, 2006)	3.5	1 (*narB*1F); 5 (*narB*degR1)	40 cycles: 95°C 1 min; 58°C 1 min; 72°C 2.5 min	narBseq1F, gacatccacttgccgattg; narBseq1R, caatcggcaagtggatgtc; narBseq2F, cccartggagygagaaggc; narBseq2R, gccttctcrctccaytggg; narBseq3F, aacaattcagcttcgattcag; narBseq3R, ctgaatcgaagctgaattgtt; narBseq4F, agcagrtsgaagcratgga; narBseq4R, tccatygcttcsayctgct; narBseqAF, attgcwccrggcagcg; narBseqAR, cgctgccyggwgcaat (Ahlgren and Rocap, 2006)
ntcA	*ntcA*1F, athttyttyccbggggayccdgc; *ntcA*4R, atggcytcggckatggcytgrt (Lindell and Post, 2001)	2	2.5	30 cycles: 95°C 1 min; 55°C 30 s; 72°C 30 s	n/a
rpoC1	*rpoC1*F1, cgcaccctgaagcccgaratggaygg; *rpoC1*R1, cgcttgatcagcttggcgcgyttytgncc (this study)	2.5	0.5	95°C 30 s; 60°C 30 s; 72°C 1 min	n/a

Table A2 | Classification of cultured strains and GenBank accession numbers of sequences used for multiple gene phylogenies.

Clade	Strain	16S rDNA	16S-23S ITS	*narB*	*ntcA*	*rpoC1*
I	CC9311[g]	CP000435	CP000435	CP000435	CP000435	CP000435
I	CC9617					AF154562
I	PS843					AF448093
I	taiyo					AF448105
I	UW1		JQ421038			
I	UW76		DQ351295			
I	WH8015		AF397717			
I	WH8020	AY172835	AF397719	DQ069073	AY885116	AF323594
I	WH9908		AF397720			
II	58E8					AF448101
II	CC9605[g]	CP000110	CP000110	CP000110	CP000110	CP000110
II	CC9701					AF155131
II	CC9705					AF308806
II	miyar					AF448102
II	RS9902	AJ621004			DQ204778	AJ621004
II	RS9903	AJ621005			DQ204779	AJ621005
II	RS9904	AJ621013				AJ621013
II	RS9907	AJ621007				AJ621007
II	RS9908	AJ621008				AJ621008
II	RS9911	AY172821	JF306822		DQ204781	**JQ421057**
II	RS9912	AY172822				AJ621010
II	SS9401					AF154563
II	UW122	**JQ421035**	DQ351300	DQ351338		**JQ421064**
II	UW86		DQ351301			
II	UW90		DQ351297			
II	UW93		DQ351298			
II	UW95		DQ351299			
II	UW96		DQ351296			
II	UW98		DQ351302			
II	WH6501		AF397706	DQ069071		AF448106
II	WH8002		AF397707			
II	WH8005		AF397708			
II	WH8009			DQ069078		
II	WH8012	**JQ421027**	AF397709	DQ351334	**JQ421049**	**JQ421062**
II	WH8104			DQ069080		
II	WH8108			DQ069082		
II	WH8109				AY885117	
III	C129	AY210409			AY885102	AF153339
III	C8015				AY885103	
III	CC9301					AF153332
III	CC9702					AF153337
III	CC9702					AF153337
III	CC9703					AF153338
III	Max42	AY172805				AJ621017
III	Minos11	AJ621021				AY172807
III	Minos12	AY172808				AJ621019
III	RS8015		AF397711			
III	RS9905	AY172815			DQ204780	AJ621006
III	WH8011					AF153334
III	WH8102[g]	NC_005070	NC_005070	NC_005070	NC_005070	NC_005070
III	WH8103	AF001479	AF397713	**JQ421045**	AY885101	L34063

(Continued)

Table A2 | Continued

Clade	Strain	16S rDNA	16S-23S ITS	*narB*	*ntcA*	*rpoC1*
III	WH8112		AF397714			AF153333
III	WH8113		AF397715			AF153335
III	WH8406		AF397716			
IV	BL107[g]	AATZ01000000	AATZ01000000	AATZ01000000	AATZ01000000	AATZ01000000
IV	CC9902[g]	CP000097	CP000097	CP000097	CP000097	CP000097
IV	EBAC392		AF268237			
IV	MB11A04		AY033297			
IV	MB11E09		AY033308			
V	RS9705	AF397725	AF397725			
V	RS9708	AF397726	AF397726		AY885106	
V	UW01					AJ621020
V	WH7803[g]	CT971583	CT971583	CT971583	CT971583	CT971583
VI	1002	AF448060				AF448082
VI	WH7805[g]	AAOK01000000	AAOK01000000	AAOK01000000	AAOK01000000	AAOK01000000
VI	WH8008		AF397722	DQ069076		
VI	WH8017	**JQ421036**	AF397723			
VI	WH8018	AF311292	AF397724		AY885115	AJ621015
VII	RS9920	AY172830	**JQ421037**	**JQ421043**		**JQ421056**
VII	UW92	**JQ421031**	DQ351314	DQ075325	**JQ421048**	**JQ421053**
VIII	RS9906	AY172816				**JQ421058**
VIII	RS9914	AY172824				AJ621011
VIII	RS9917[g]	NC_009482	NC_009482		NC_009482	NC_009482
VIII	WH8101	AF001480	AF397728	DQ069092	DQ204777	**JQ421065**
IX	RS9901	AY172811				AJ621003
IX	RS9916[g]	AAUA01000000	AAUA01000000	AAUA01000000	AAUA01000000	AAUA01000000
X, 5.3-?	Minos01	AY172806				AJ621022
X, 5.3-?	Minos02	AY172809				AJ621016
X, 5.3-I	RCC307[g]	NC_009482	NC_009482	NC_009482	NC_009482	NC_009482
XV	CC9803		**JQ421040**			
XV	UW104		DQ351304	DQ351336		
XV	UW106	**JQ421029**	DQ351305	DQ351337	**JQ421047**	**JQ421054**
XV	UW110		DQ351306			
XV	UW69	**JQ421028**	DQ351303	DQ351335	**JQ421051**	**JQ421063**
XVI	M16.7	DQ224203				
XVI	UW105	**JQ421034**	DQ351310	DQ069067	**JQ421046**	**JQ421055**
XVI	UW115		DQ351307			
XVI	UW117		DQ351308			
XVI	UW119		DQ351309			
XVI	UW140	**JQ421030**	DQ351315	**JQ421044**	**JQ421052**	**JQ421061**
XVI	UW146		DQ351312			
XVI	UW149		DQ351313			
XVI	UW158		DQ351311			
CRD1	CC9305				AY885107	AF013610
CRD1	Eum14	AY172804				AJ621023
CRD1	MITS9220	JCVI	AF397705		DQ204783	**JQ421059**
CRD1	Oli31	AY172810				AJ621018
CRD1	UW179	**JQ421033**	**JQ421041**	DQ069090	**JQ421050**	**JQ421060**
CRD1	UW180	**JQ421032**	**JQ421042**			
Unspecified	59					AF448100
Unspecified	CC9317					AF013609
Unspecified	CC9318					AF013608

(Continued)

Table A2 | Continued

Clade	Strain	16S rDNA	16S-23S ITS	*narB*	*ntcA*	*rpoC1*
Unspecified	CC9615					AF308804
Unspecified	CC9616					AF154561
Unspecified	CC9704					AF308805
Unspecified	M11.1	DQ224204				
Unspecified	miyav					AF448103
Unspecified	st235					AF448104
Subcluster 5.2	WH5701[g]	AANO01000000	AANO01000000	AANO01000000	AANO01000000	AANO01000000

Accession numbers of sequences generated in this study are in bold.

[g]The genomes of these strain have been sequenced.

"JCVI" – sequence retrieved from the J. Craig Venter Institute (https://research.venterinstitute.org/moore/).

Table A3 | Level of amplification when qPCR primer sets were challenged with non-specific template.

qPCR primer set tested	Template tested[a]												
	I	II	III	IV	V	VI	VII	VIII	X	XV	XVI	CRD1	CRD2
I	–	n.a.	n.a.	n.a.	n.a.	n.a.	n.a.	n.a.	n.a.	n.a.	n.a.	n.a.	n.a.
II	n.a.	–	n.a.	n.a.	n.a.	n.a.	n.a.	n.a.	n.a.	n.a.	n.a.	n.a.	n.a.
III	n.a.	n.a.	–	n.a.	n.a.	n.a.	n.a.	n.a.	n.a.	n.a.	n.a.	n.a.	n.a.
IV	n.a.	n.a.	n.a.	–	n.a.	n.a.	n.a.	n.a.	n.a.	n.a.	n.a.	n.a.	n.a.
VIII	n.a.	n.a.	n.a.	n.a.	n.a.	n.a.	n.a.	–	n.a.	n.a.	n.a.	n.a.	n.a.
X	n.a.	n.a.	n.a.	164	n.a.	n.a.	n.a.	n.a.	–	n.a.	n.a.	n.a.	n.a.
XV	n.a.	n.a.	n.a.	n.a.	n.a.	n.a.	n.a.	n.a.	n.a.	–	n.a.	n.a.	n.a.
XVI	n.a.	n.a.	n.a.	n.a.	n.a.	n.a.	n.a.	n.a.	n.a.	n.a.	–	n.a.	n.a.
CRD1	n.a.	n.a.	n.a.	n.a.	239	n.a.	134	n.a.	n.a.	n.a.	13,200[b]	–	103
CRD2	n.a.	n.a.	n.a.	n.a.	n.a.	n.a.	n.a.	n.a.	n.a.	n.a.	n.a.	n.a.	–

[a]Numbers indicate the degree of amplification in terms of copies/μl of the specific standards when qPCR primer sets were challenged with high concentrations (1.5×10^5 copies/μl) of the non-specific templates listed in ***Table 1*** *for each clade. Non-specific templates that did not amplify are indicated with "n.a." for no amplification.*

[b]Primer set CRD1 produced a high level of non-specific amplification, so lower concentrations of clade XVI plasmid oc175m12 were also tested. Challenging the CRD1 primer set with 3.5×10^4, 3.5×10^3, and 3.5×10^2 copies/μl of plasmid oc175m12 resulted in amplification to 1,280, 141, and 14.7 copies/μl respectively, or on average 25-fold less than the concentration of plasmid tested.

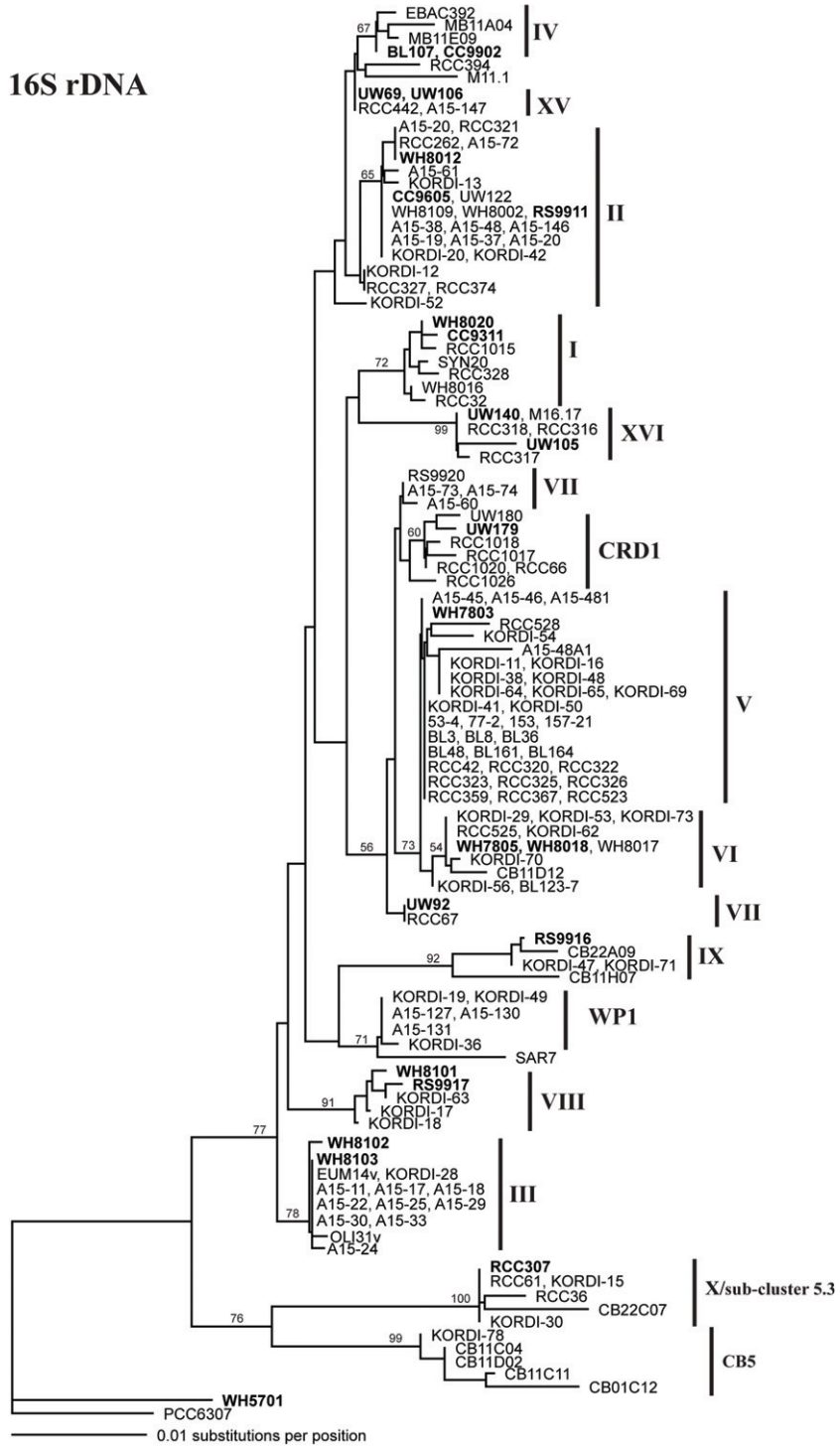

FIGURE A1 | Phylogenetic tree based on 1009 positions of the 16S rDNA gene. The trees were constructed in PAUP using the HKY + i + g model. Values at the nodes indicate the bootstrap support from 1000 trees found by neighbor joining and the HKY + i + g substitution model. The names of strains used in the four loci concatenated tree in **Figure A6** are in bold. Clade designations are indicated with solid vertical lines.

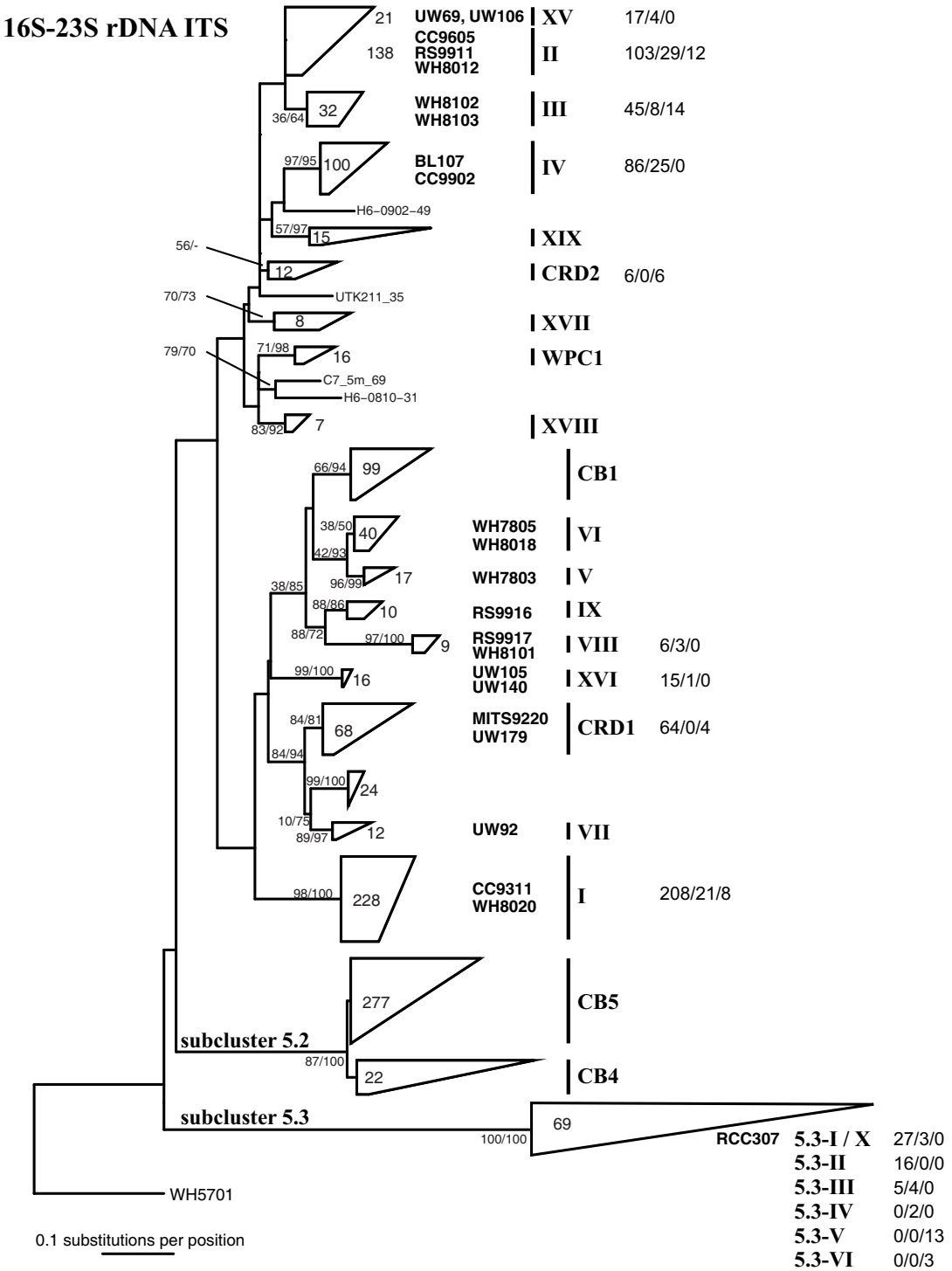

FIGURE A2 | Phylogenetic tree based on 322 positions of the 16S–23S rDNA ITS. The tree shown is the best scoring tree, as determined by maximum likelihood score, amongst 1000 neighbor joining trees constructed using the HKY + i + g substitution model and with randomized addition of taxa. Clade groupings shown in this neighbor joining tree are also supported by bootstrap analysis using maximum likelihood with the GTRGAMMA model in RAxML (1000 replicates) and neighbor joining and the HKY + i + g substitution model (1000 replicates). Nodes display bootstrap values (ML/NJ) where bootstrap support is >50% in at least one method. Clades were collapsed into groups represented by trapezoids. The number inside or to the right of the trapezoid indicates the number of sequences in that clade or subcluster. Clade designations are indicated with solid vertical lines, and representative strains within the clades are shown to the left of clade labels. Clade XV forms a monophyletic clade highly supported by bootstrap analysis (80/86, not shown on tree) and groups together with clade II strains. For clades for which qPCR assays were designed, numbers to the right of clade names show the number of sequences that have zero, one to two, or greater than two mismatches to both the forward and reverse qPCR primers combined (0 mismatches/1–2 mismatches/>2 mismatches).

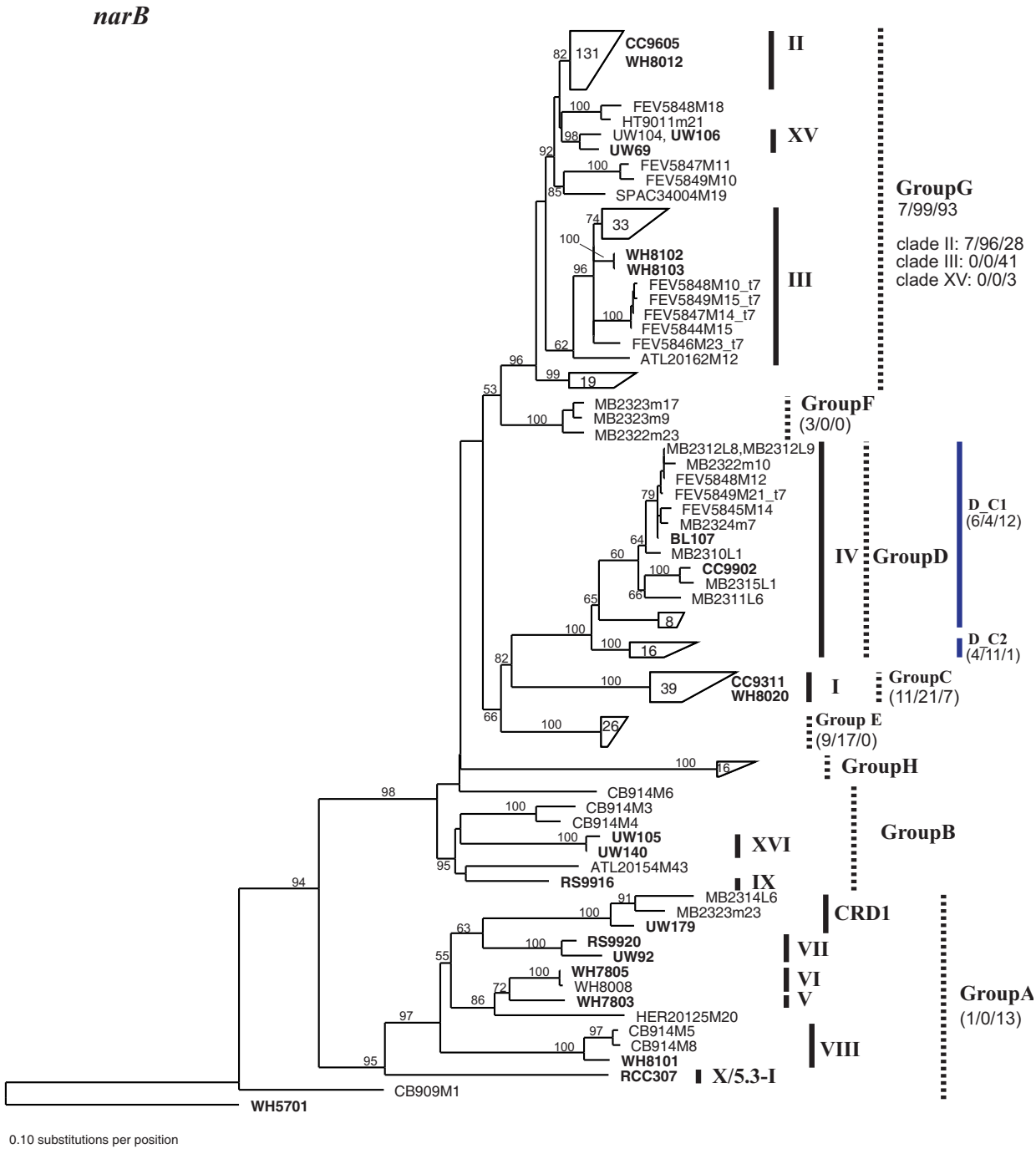

FIGURE A3 | Phylogenetic tree based on 648 nucleotide positions of the *narB* gene. Tree construction, bootstrap analysis, and taxa and clade labels as the same as described in **Figure A1**. Because of the large number of sequences, selected sequences are grouped together and represented by trapezoids. The number inside the trapezoid indicates the number of sequences in that group. Strains within those groups that have been used in the concatenated tree (**Figure A6**) are shown to the right of the trapezoids. The assignment of *narB* sequences to groups according to Paerl et al. (2011) is indicated with dashed lines. Group A, Group B, and Group G encompass multiple well-established clades as defined by phylogenies of other loci. Numbers below group names indicate the number of total mismatches that sequences within the group have to the primers and probe sets described in Paerl et al. (2011) (0 mismatches/1 or 2 total mismatches/>2 mismatches). For Group G which contains multiple clades as defined by other loci, the number of mismatches is also given for sequences belonging to clades II, III, and XV. Two primer and probe sets were designed to detect subgroups of Group D, D_C1, and D_C2 (designated with blue lines), and the number of mismatches that sequences have to their respective primer probe sets are given.

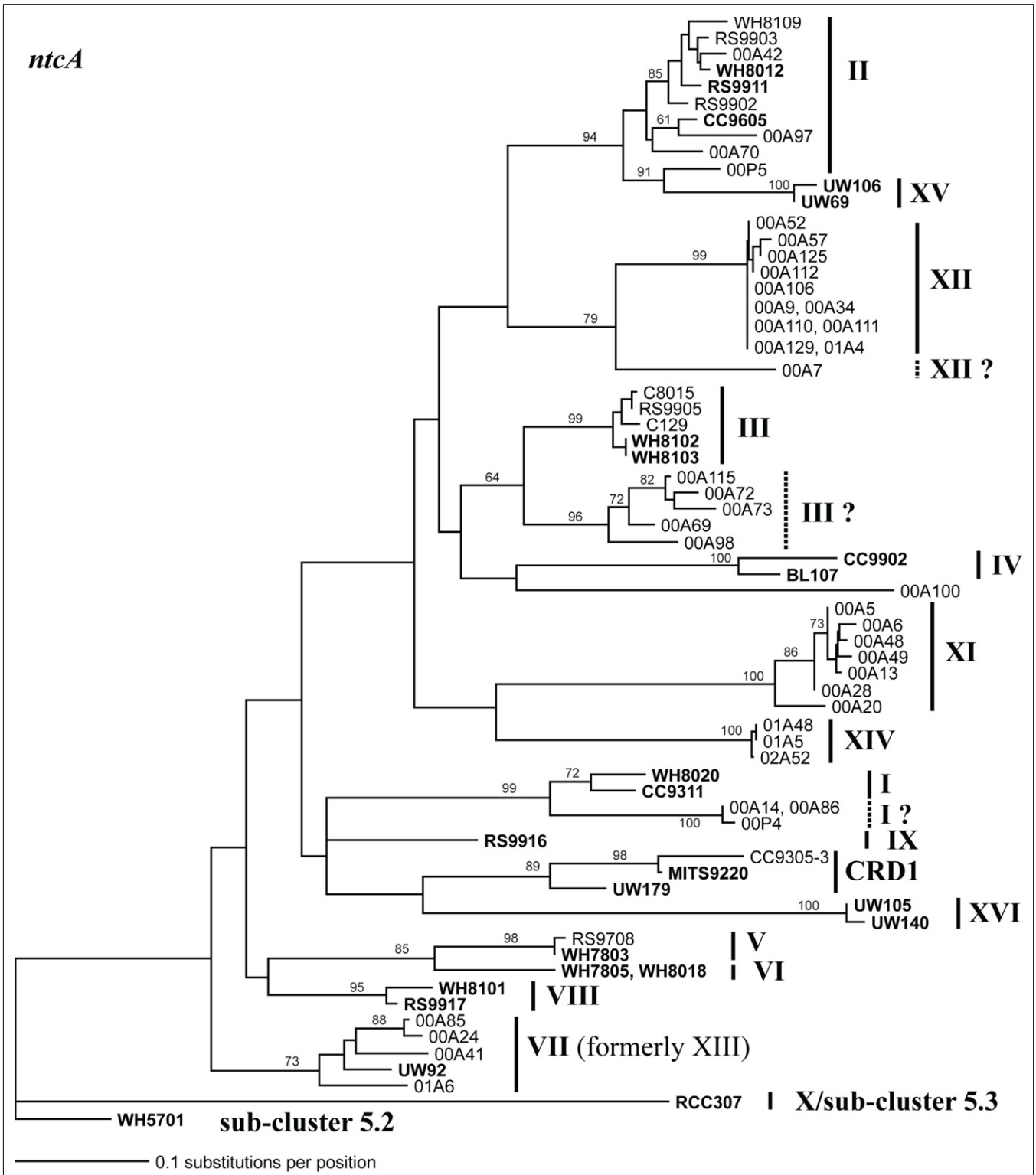

FIGURE A4 | Phylogenetic tree based on 297 nucleotide positions of the *ntcA* gene. Tree construction, bootstrap analysis, and taxa and clade labels are the same as described in **Figure A1**. Clade designations are listed as described in Penno et al. (2006) except that sequences formerly classified as clade XIII cluster with clade VII strain UW92 and these sequences have been reclassified to clade VII. Clades I, III, and XII contain groups of sequences that may warrant classification into new clades because they are as divergent from other sequences in their own clade as they are to other clades. These groups of sequences are labeled with a dashed line and a "?" following the clade name assigned by Penno et al.

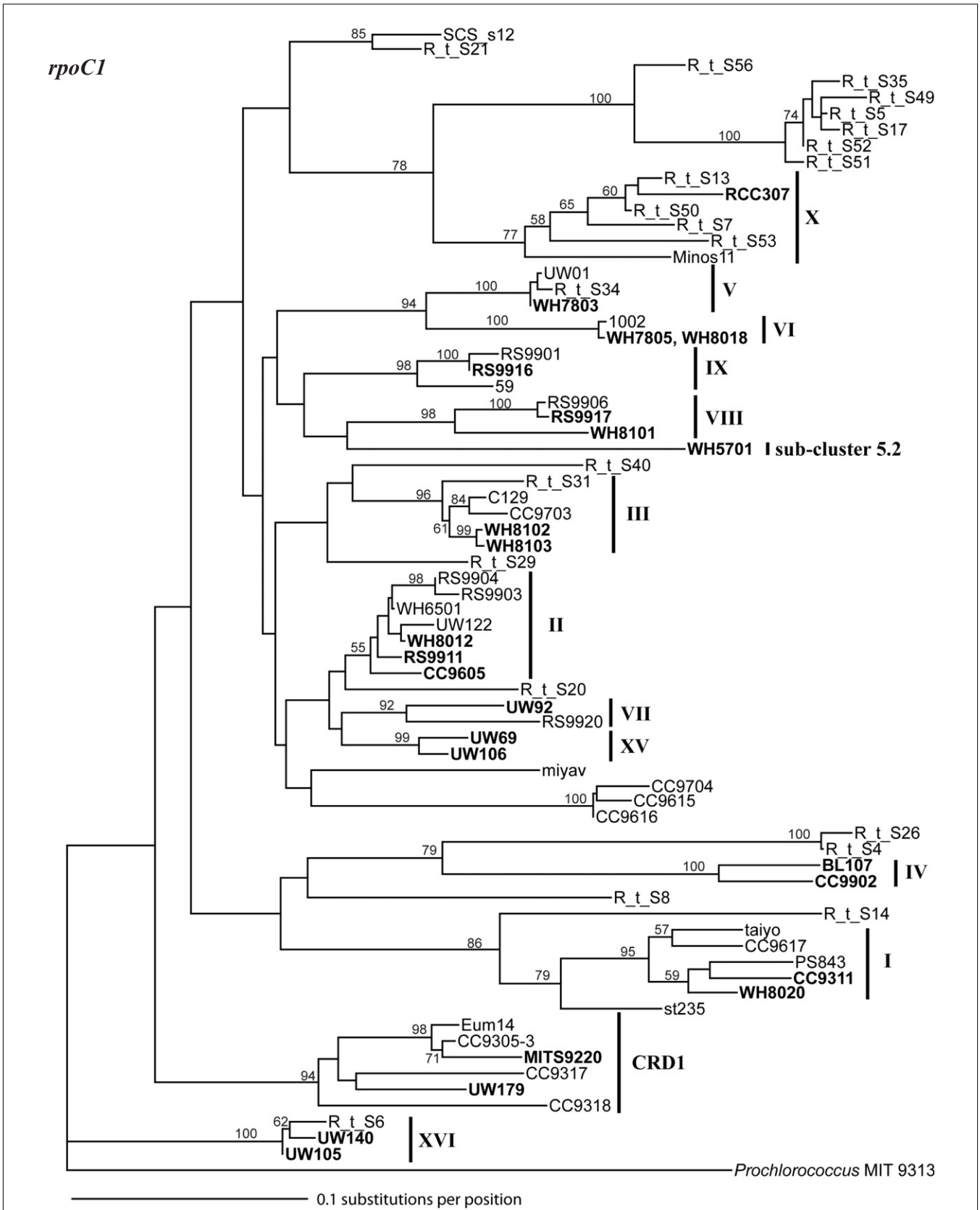

FIGURE A5 | Phylogenetic tree based on 460 nucleotide positions of the *rpoC1* gene. Tree construction, bootstrap analysis, and taxa and clade labels are the same as described in **Figure A1**. *Prochlorococcus* strain MIT 9313 was used as the outgroup.

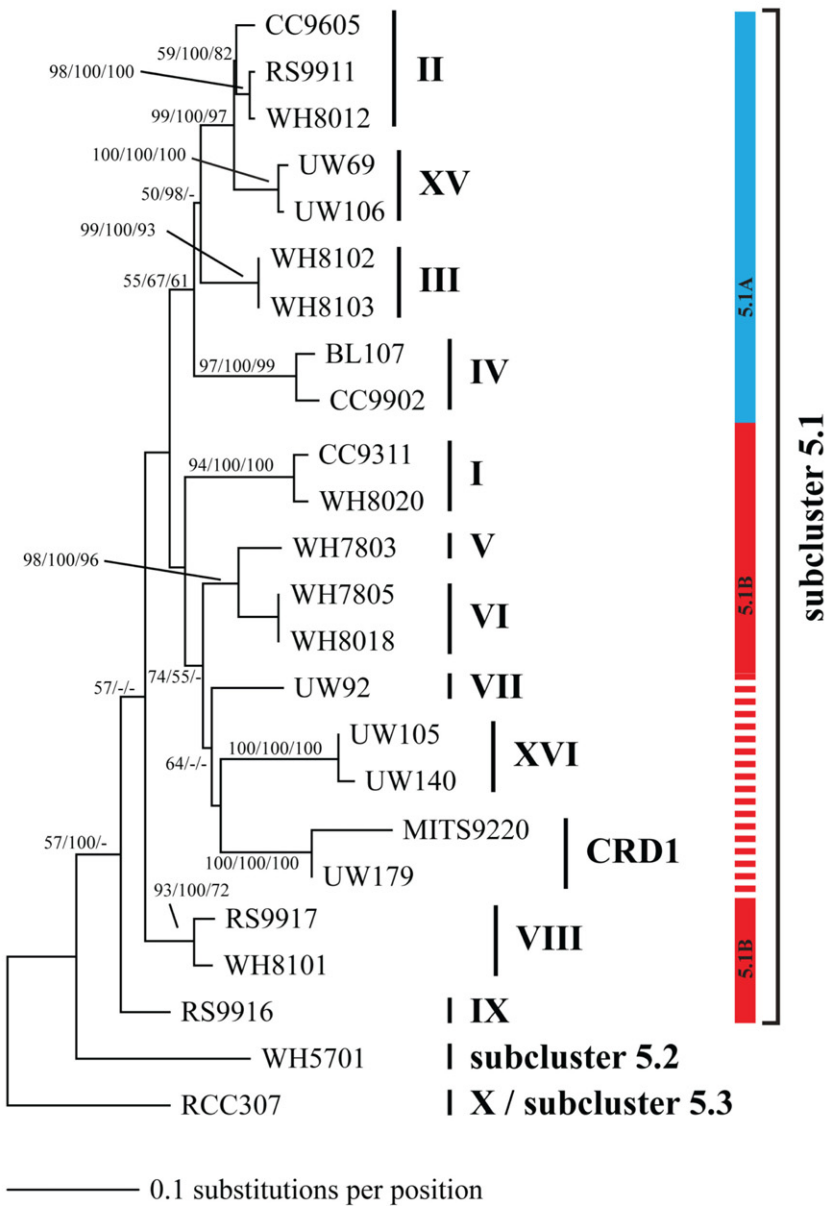

FIGURE A6 | Phylogenetic tree based on concatenation of four loci: the 16S rDNA gene, the ITS, *ntcA,* and *rpoC1.* Tree construction, bootstrap analysis, and taxa and clade labels as the same as described in **Figure A1** except that bootstrap values at the nodes were obtained using three methods: (neighbor joining, HKY + i + g model, 100 replicates/neighbor joining, Jukes–Cantor model, 1000 replicates/maximum likelihood, GTRGAMMA model, 1000 replicates). Phylogeny based on 1,129 core genes from strains with sequenced genomes support the division of strains subcluster 5.1 into two groups 5.1A (blue bar) and 5.1B (solid red bar) (Dufresne et al., 2008). The four loci concatenated phylogeny in **Figure A6** also supports the grouping of 5.1A strains, including clade XV. Strains in clades VII, CRD1, and XVI cluster with other 5.1B strains in clades V and VI with high bootstrap support, however it is unclear if these additional new strains without sequenced genomes form a single monophyletic cluster with all 5.1B strains (dashed red line).

frontiers in
MICROBIOLOGY

ORIGINAL RESEARCH ARTICLE
published: 15 November 2011
doi: 10.3389/fmicb.2011.00229

Constitutive extracellular polysaccharide (EPS) production by specific isolates of *Crocosphaera watsonii*

Jill A. Sohm, Bethanie R. Edwards, Brian G. Wilson and Eric A. Webb*

Department of Biological Sciences, University of Southern California, Los Angeles, CA, USA

Edited by:
Rex Malmstrom, DOE Joint Genome Institute, USA

Reviewed by:
Kathleen Scott, University of South Florida, USA
Hans Paerl, University of North Carolina–Chapel Hill, USA

***Correspondence:**
Eric A. Webb, Department of Biological Sciences, University of Southern California, 3616 Trousdale Parkway, AHF 107, Los Angeles, CA 90089-0371, USA.
e-mail: eawebb@usc.edu

Unicellular dinitrogen (N_2) fixing cyanobacteria have only recently been identified in the ocean and recognized as important contributors to global N_2 fixation. The only cultivated representatives of the open ocean unicellular diazotrophs are multiple isolates of *Crocosphaera watsonii*. Although constituents of the genus are nearly genetically identical, isolates have been described in two size classes, large ~5 μm and small ~3 μm cell diameters. We show here that the large size class constitutively produces substantial amounts of extracellular polysaccharides (EPS) during exponential growth, up to 10 times more than is seen in the small size class, and does so under both N_2 fixing and non-N_2 fixing conditions. The EPS production exceeds the amount produced by larger phytoplankton such as diatoms and coccolithophores by one to two orders of magnitude, is ~22% of the total particulate organic C in the culture, and is depleted in N compared to cellular material. The large difference in observed EPS production may be accounted for by consistently higher photochemical efficiency of photosystem II in the large (0.5) vs. small (~0.35) strains. While it is known that *Crocosphaera* plays an important role in driving the biological carbon (C) pump through the input of new nitrogen (N) to the open ocean, we hypothesize that this species may also contribute directly to the C cycle through the constitutive production of EPS. Indeed, at two stations in the North Pacific Subtropical Gyre, ~70% of large *Crocosphaera* cells observed were embedded in EPS. The evolutionary advantage of releasing such large amounts of fixed C is still unknown, but in regions where *Crocosphaera* can be abundant (i.e., the warm oligotrophic ocean) this material will likely have important biogeochemical consequences.

Keywords: *Crocosphaera*, extracellular polysaccharides, diazotroph

INTRODUCTION

Dinitrogen (N_2) fixation is the process by which diazotrophs can access the largest nitrogen (N) reservoir on earth, N_2 gas, and turn it into a biologically usable form. This process is exclusively prokaryotic, carried out by relatively few organisms, and represents an important source of new N to the N-starved open ocean (Capone et al., 2005). In the tropics and subtropics, the filamentous colony-forming cyanobacterium *Trichodesmium* is the most well studied diazotroph; however, it is now known that unicellular cyanobacteria also contribute significantly to N_2 fixation in these areas (Montoya et al., 2004). There are currently three groups of unicellular, diazotrophic cyanobacteria defined: UCYN-A, which is most closely related to *Cyanothece* ATCC 51142 but appears to be a photoheterotroph based on genomic research; group B, or *Crocosphaera watsonii*; and UCYN-C, a sister taxa to UCYN-A (Foster et al., 2007; Zehr et al., 2008; Tripp et al., 2010). Of these three marine groups, only *Crocosphaera* is represented in culture collections.

Crocosphaera appears to be widespread in the tropical and subtropical oceans; it has been identified by *nifH* abundance (a gene encoding for a subunit of the enzyme responsible for N_2 fixation) in large areas of the North Atlantic (Langlois et al., 2008), and the North Pacific (Church et al., 2008) and by flow cytometry and direct counting in the South Pacific (Campbell et al., 2005; Webb et al., 2009). In the North Atlantic, *Crocosphaera* is not always present; however, when it is, the abundance (determined as copies of *nifH*) can be quite high for an N_2-fixer, in the range of 10^4 L^{-1} (Langlois et al., 2008). In the North Pacific, *Crocosphaera nifH* abundance appears to be closer to 10^3 L^{-1}, but concentrations up to 10^4 L^{-1} have also been seen (Church et al., 2005, 2008), while in the warm pool of the South Pacific, concentrations up to 10^6 L^{-1} were recently shown (Moisander et al., 2010). Despite the potential biogeochemical importance of *Crocosphaera*, we are only just beginning to understand the ecology and physiology of this genus.

The type strain of group B is *C. watsonii* WH8501 and the laboratory isolates of this genus can be divided into two cell size classes, <4 and >4 μm, that are essentially phylogenetically indistinguishable (Zehr et al., 2007; Webb et al., 2009). Nevertheless, the bigger size class produces large amounts of extracellular material that becomes so abundant that it makes the media gel-like (Webb et al., 2009). Herein this material is identified as extracellular polysaccharides (EPS) that is similar in composition to transparent exopolymeric particles (TEP). The major difference between TEP and EPS is that TEP is defined as discrete particles of EPS, while EPS remains as a matrix around cells (Passow, 2002b). Past work suggests that the large *Crocosphaera*-like cells produce

this material in the field; cells of the large size class (~5–6 μm) are retained on an 8-μm pore size filter, and are seen in loose groupings (Webb et al., 2009). Presumably, these cells exist in a matrix of EPS and can therefore be caught on a filter with pore size larger than the cell diameter. Fitting with this hypothesis, similar groupings of *Crocosphaera*-like cells in a matrix were seen in a sample from a coral lagoon in the southwest Pacific Ocean (Biegala and Raimbault, 2008). These observations suggest that *Crocosphaera* produces this EPS *in situ* as well, however it is not known if this production is constitutive, confined to a specific growth phase or impacted by nutrient limitation.

The purpose of EPS production in *Crocosphaera* is unknown; however, in other phytoplankton, it appears that photosynthetically fixed carbon (C) is channeled into exopolymers during nutrient limited growth (Corzo et al., 2000). Many cyanobacteria have been reported to produce EPS, and some strains appear to produce this material exclusively under N_2-fixing conditions (Otero and Vincenzini, 2003). While TEP is mainly recognized as a diatom product, it is also produced by cyanobacteria, other phytoplankton, and bacteria (Passow, 2002a; Berman-Frank et al., 2007). These exopolymers are an important aspect of the global C cycle, as they comprise the matrix of marine snow particles that are a major contributor to C flux to the deep sea (Passow et al., 2001).

In this study we tracked exopolymer production in both large and small strains of *Crocosphaera* in culture and compared the values obtained with published data from other marine phytoplankton. Furthermore, we also investigated the controls of EPS production (i.e., could it be increased, reduced, or eliminated) by growing *Crocosphaera* in different nutrient and light regimes, and documented EPS production by *Crocosphaera*-like cells in the North Pacific Ocean.

MATERIALS AND METHODS

STRAINS AND CULTURE CONDITIONS

In this experiment, six strains of *C. watsonii* were tested for EPS production under diazotrophic growth conditions: three strains of the small size class (WH8501, WH0002, WH0401) and three strains of the large size class (WH0003, WH0005, WH0402). These cultures were isolated from diverse locations. These cultures are not currently available axenic and thus were not axenic for the experiments described here; however, EPS production was qualitatively observed when each strain was originally isolated and rendered axenic by John Waterbury. WH8501 was isolated in the South Atlantic, WH0002, WH0003, and WH0005 were isolated in the North Pacific and WH0401 and WH0402 were isolated in the North Atlantic (Webb et al., 2009). Thus, the strains used originate from many different areas, with both EPS and non-EPS producing strains from the same basin. All cultures were grown in triplicate batches on N free YBCII media (Chen et al., 1996), an artificial seawater media, in an incubator with a 14-h:10-h light:dark cycle at 27°C, and kept in constant motion on a shaker table (~100 RPM). With the exception of the light/N experiment (see below) all cultures were grown at 75–80 $\mu mol\ m^{-2}\ s^{-2}$ light intensity; the light/N experiment was carried out at 45 $\mu mol\ m^{-2}\ s^{-1}$. All cultures were tested for EPS production over the growth cycle, although only four strains (two large and two small) reached stationary phase before the termination of the experiments after about 3 weeks (these are shown in **Figure 2**). A number of additional experiments were also carried out with a representative of the large (WH0005) and small (WH0401) strains in order to answer the following questions: (1) is EPS production in the large strains controlled by light intensity or the presence of fixed N, as is seen in some other N_2-fixing cyanobacteria (Otero and Vincenzini, 2003), and (2) given previous work showing that nutrient limitation can induce EPS production in cyanobacteria (see Berman-Frank et al., 2007), can the levels of production seen in the large strains be induced in the small strains grown in nutrient deficient conditions? The following experiments were carried out to address these questions: (1) quantifying EPS production in WH0005 during exponential growth at a light intensity of half that used in the standard growth curves and on media with no N (−N) and with 1 mM NO_3^- (+N) added (named the light/N experiment), (2) measuring EPS production in a small strain (WH0401) grown on media with 1 mM NO_3^- for purposes of comparison to the experiment with WH0005, and (3) monitoring EPS production in WH0401 under low Fe and PO_4^{3-} conditions (20 and 25 times less than standard YBCII, respectively).

Sampling of cultures was carried out at the beginning of the light period. One sample for cell counts, chlorophyll (chl) *a* and EPS concentration was taken from each replicate culture over the exponential and stationary growth phase – values reported are the average of the three samples from the biological replicates. Cell numbers were counted with an epifluorescent microscope using a hemacytometer where replicate fields were counted until whichever came first: 10 fields or 200 cells. Chl *a* was determined in a fluorometer after samples were dissolved in acetone for 24 h at −20°C (Parsons et al., 1984). During early exponential growth, cell counts were the more accurate (less variable) way to quantify biomass and growth in the large strain cultures; however, in late log and stationary phase, the cells began to form large groupings (see **Figures 1A,B**) that could not be accurately counted with microscopy, as the distribution of cells in the field was not uniform. Therefore, growth of the large strain cultures was tracked with Chl *a* concentration only in experiments extending into stationary phase while both cell density and Chl *a* was used with the small size strains and in the light/N experiment where growth was tracked in early exponential phase only.

EPS QUANTIFICATION

To visualize and quantitatively measure the EPS, methods developed for staining and quantification of TEP were used (Passow and Alldredge, 1994, 1995b). Briefly, samples for microscopic evaluation of the EPS were filtered onto a 0.4-μm filter and stained for 2 s with a 0.02% Alcian Blue solution in 0.06% acetic acid, followed by rinsing with milli-Q water (Passow and Alldredge, 1994). The filter was mounted onto a slide and examined at 40× magnification on a Zeiss Axiostar plus microscope using light microscopy for the exopolymers and epifluorescent microscopy to visualize the location of the cells with relation to the EPS. Whole images were minimally adjusted in Adobe Photoshop CS4 for contrast, brightness, and hue in order to accentuate the borders of the cells and stained EPS. Samples for quantitative measurement of EPS were stained as above, placed dry into a glass test tube and stored

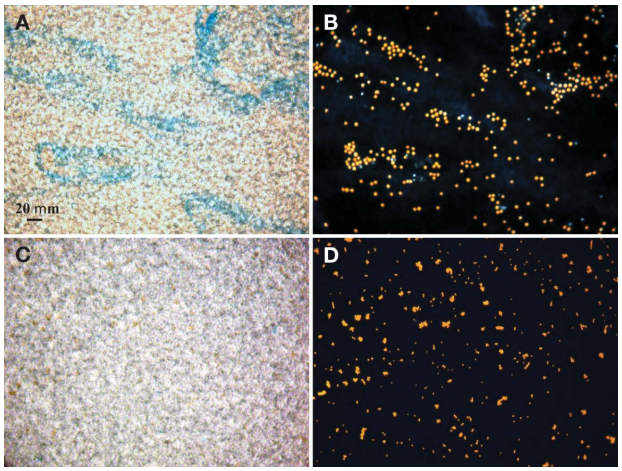

FIGURE 1 | Bright field microscopic images of EPS stained with Alcian Blue (A,C) and epifluorescence images of *Crocosphaera* cells under the DAPI longpass filter set (B,D). Stain and cell images show the same field of view of the large cell type WH0005 **(A,B)** and small cell type WH0401 **(C,D)** under 40× magnification.

in the dark for ∼3 weeks until processing. For quantification, the filters with stained samples were placed in 3 mL 80% H_2SO_4 for 2 h to dissolve the EPS, and the absorbance was read on a Bio-Rad SmartSpec 3000 spectrophotometer (Philadelphia, PA, USA) at 787 nm (Passow and Alldredge, 1995b). Xanthan gum standards were made in ethanol according to Claquin et al. (2008) and values are reported in microgram Xanthan gum equivalents per milliliter (abbreviated μg Xeq. mL^{-1}). The volume filtered was adjusted throughout the growth curve to account for the increase in EPS, 3–5 mL in the early stages of growth, down to 0.2–0.5 mL by the time late log or stationary phase were reached. Chl *a* and cell normalized EPS values for each strain are reported as the average of these values taken over the exponential growth period, as this is the period of active production.

ELEMENTAL ANALYSES

To assess the C and N content of the EPS, 30 mL of log phase WH0005 was centrifuged at 4000 × *g* for 10–15 min to separate the cells from the EPS. This strain was chosen, as it appears to be easier to separate from the EPS than the other isolates. The cell pellet and the supernatant containing the EPS were filtered separately onto pre-combusted GF/F filters and dried. These filters were then pressed into a pellet and analyzed on a Carlo Erba elemental CHN analyzer (Currently – CE Elantech, Lakewood, NJ, USA). The number of cells that did not separate from the EPS was determined by microscopy (as described above) using a subsample of the supernatant, and the final C and N values of the EPS reported were corrected for the C and N present as cells. The total particulate organic C or N (POC and PON) is defined as the C or N in EPS plus cells, as all this material is caught on a GF/F filter.

PHOTOSYNTHETIC EFFICIENCY

To test for intrinsic photosynthetic differences between the two size classes of *Crocosphaera*, the quantum yield of photosystem II (F_v/F_m) of the six strains was tested with 3-(3,4-dichlorophenyl)-1,1-dimethylurea (DCMU) as described in Samuelsson and Öquist (1977). Briefly, triplicate 30 mL cultures of each strain were grown in 50 mL glass tubes in YBCII medium at ∼75 μmol m^{-2} s^{-2} and the growth was followed with fluorescence. During acclimated exponential growth, the Chl *a* fluorescence was measured in dark adapted cells before (F_o) and after (F_m) the addition of DCMU to a final concentration of 10 μM using a Turner TD-700 fluorometer. The quantum yield of photosystem II was then calculated as $(F_m - F_o)/F_m$.

FIELD SAMPLING

Large *Crocosphaera*-like cells were investigated at two stations (27°19.19 N, 157°46.65 W, and 23°35.59 N, 157°40.24 W) in the North Pacific Subtropical Gyre (NPSG) in July 2010 on the R/V Kilo Moana, at depths of 5 and 25 m. About 100–150 mL samples were filtered onto 8 μm filters, stained with Alcian Blue as described above, and *Crocosphaera*-like cells and EPS were observed under epifluorescence and light microscopy, respectively. For the second station, the number of large cells on the filter was counted, noting the number that were embedded in stainable EPS.

RESULTS

CELL STAINING

Alcian Blue is a stain specific to acid mucopolysaccharides (Passow and Alldredge, 1995b). The large strains produced material that was stainable with Alcian Blue (**Figure 1**), therefore we conclude that it is chiefly composed of polysaccharides and is similar to the Alcian Blue stainable exopolymers released by other phytoplankton (EPS and TEP; Passow, 2002b). Microscopic observations showed that large strains (e.g., WH0005) do not appear to be releasing particles of exopolymers (or TEP) into the media, but rather a matrix loosely bound to the cells (or EPS; **Figures 1A,B**). To be consistent with the literature, the previously designated ECM of *Crocosphaera* (Webb et al., 2009) will be referred to as EPS. Images of a small strain representative (WH0401) show little to no stainable material under microscopic observation during stationary phase (**Figures 1C,D**).

EPS PRODUCTION

To determine the timing and magnitude of EPS production in *Crocosphaera*, three strains each of the large and small size class were grown under N_2-fixing conditions (no N added) and EPS production was quantified. Two of the large strains, WH0005 and WH0402, grew at the same rate based on the increase in Chl *a*, 0.29 day^{-1}, while WH0003 grew somewhat slower in the same conditions, at a rate of 0.17 day^{-1}. Regardless of the difference in growth rate, all three large strains showed EPS production during exponential growth that increased exponentially at a rate similar to its growth rate: EPS increased in large cell cultures at a rate of 0.31, 0.26, and 0.20 day^{-1} in WH0005, WH0402, WH0003, respectively. The amount of EPS produced by the cells during exponential growth, normalized to Chl *a* content, averaged 374 ± 33 μg Xanthan gum equivalents (μg chl *a*)$^{-1}$ for WH0005, 209 ± 92 μg Xanthan gum equivalents (μg chl *a*)$^{-1}$ for WH0402, and 392 ± 116 μg Xanthan gum equivalents (μg chl *a*)$^{-1}$ for WH0003 (**Table 1**), and in the cultures of WH0005 and WH0003, plateaued just after cultures reached stationary phase (**Figure 2**). This pattern was also

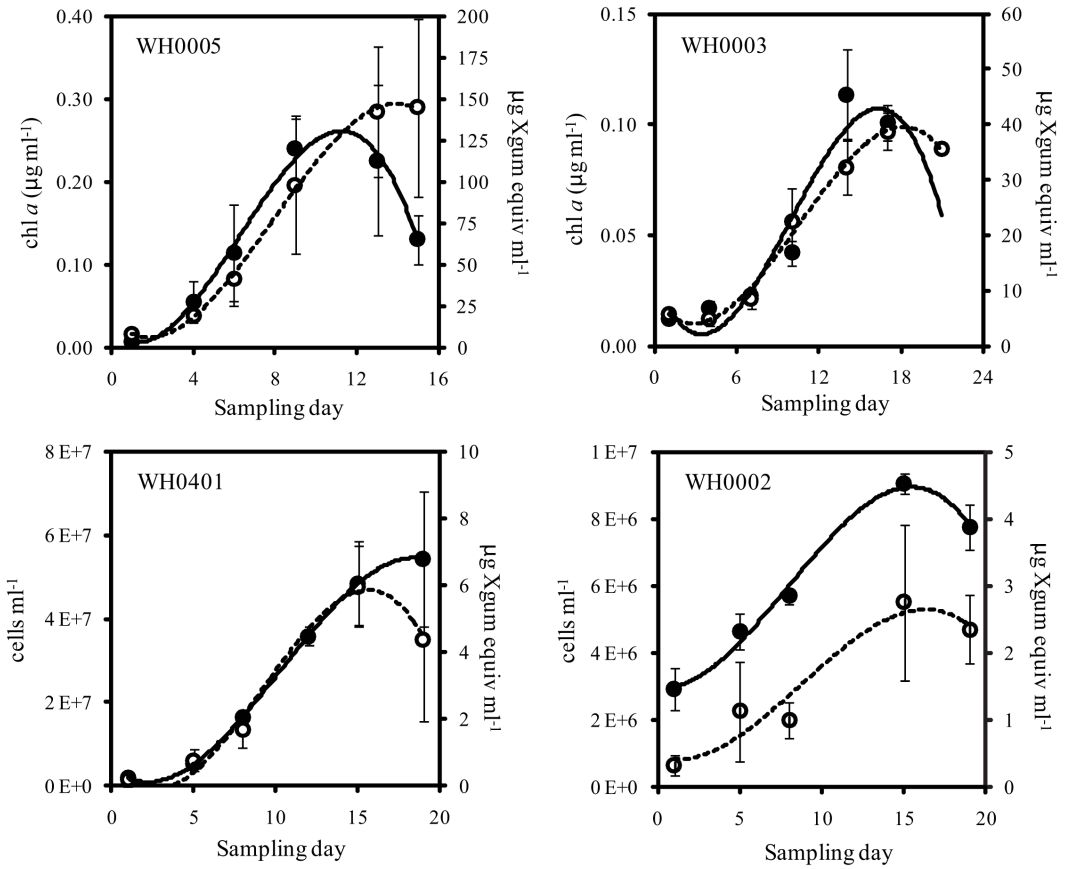

FIGURE 2 | Quantity of Chl *a* or cells (closed symbols, solid line) and EPS (open symbols, dashed line) from late log phase into stationary phase of large (top) and small (bottom) strains of *Crocosphaera*. Note that *y*-axis scales are different. Culture growth in the large strains is represented here with Chl *a* content, as it is difficult to accurately count cells in late log/stationary phase due to the growth of cells in large clusters. Error bars show SD.

seen in two of the small strains, WH0401 and WH0002 (**Figure 2**). This shows that EPS production occurs mainly in exponential phase in both large and small strains and stationary phase production is not a large contributor to EPS production in *Crocosphaera*. While visual observations indicated that the small size class strains were not producing EPS, when measured spectrophotometrically, all three small strains tested (WH8501, WH0002, and WH0401) did produced small amounts of EPS, ∼10 times less than is produced by the large size class. Accumulation rates were very similar to their growth rates of 0.1 (WH0401) and 0.28 day^{-1} (WH0002; **Table 1**; **Figure 2**).

While it is possible that differential cell lysis between large and small size classes could contribute to the order of magnitude difference in EPS production between the two classes, microscopic investigation of large and small strains determined that small, but similar, numbers of lysing cells were identifiable in cultures of both (data not shown). This is consistent with EPS being produced by living *Crocosphaera* cells.

NUTRIENT AND LIGHT EFFECTS ON EPS PRODUCTION

The addition and depletion of different nutrients in the media and growth on low light levels appeared to have little effect on the amount of EPS produced by representatives of the large and small strains. A comparison of EPS production in cultures of *Crocosphaera* WH0005 grown at low light (half the intensity of the growth curves described above) and with and without fixed N shows that lower light reduces the growth rates of the culture (from 0.29 to 0.20 day^{-1}) but the accumulation of EPS still occurs at a similar rate to growth (0.23 day^{-1}). The total amount of EPS produced per unit Chl *a* was somewhat reduced compared to cells grown on higher light (**Table 1**), but still an order of magnitude greater than produced by small cells. This may be due to higher Chl *a* production in cells grown under lower light conditions, rather than reduced EPS production; however, because cell counts were not possible through the entirety of the growth curve in standard conditions, these data are not available.

The addition of fixed N did not reduce the rate of EPS accumulation compared to the culture grown without fixed N (0.20 vs. 0.21 day^{-1}, respectively, $p = 0.80$). EPS was also produced in similar amounts in the +N and −N treatments (**Figure 3**, **Table 1**). WH0401, a small strain, also did not alter its EPS production when grown with fixed N, or when grown under Fe or PO_4^{3-} deficient conditions (**Table 1**). Chl *a* and cell normalized

Table 1 | Exopolymer production by batch cultures of *Crocosphaera* in log phase compared to other marine phytoplankton, normalized to both cellular volume and chl *a* content.

Species	Exopolymer production		Study
	Cell volume normalized (10^{-9} μg Xeq. μm^{-3})	Chl *a*-normalized (μg Xeq. [μg chl *a*]$^{-1}$)	
Chaetoceros affinis, CCMP 159	22	–	Passow (2002a)
Nitzchia angularis	0.9	–	Passow (2002a)
Pseudo-nitzschia fraudulenta	–	57[a]	Claquin et al. (2008)
Thalassiosira weissflogii	3	–	Passow (2002a)
Emiliana huxleyi (non-calcifying)	1	–	Passow (2002a)
Gonyaulax polyedra	20	–	Passow (2002a)
Anabaena flos-aquae	<1[b]	<1	Surosz et al. (2006)
Isochrysis galbana	–	13[a]	Claquin et al. (2008)
Phaeocystis antarctica	∼800[c]	148[d], 2720[c]	Hong et al. (1997)
DIAZOTROPHIC GROWTH			
Crocosphaera watsonii WH0005[e]	–	374 ± 33	This study
Crocosphaera watsonii WH0402[e]	–	209 ± 92	This study
Crocosphaera watsonii WH0003[e]	–	392 ± 116	This study
Crocosphaera watsonii WH8501[f]	Up to 17	–	This study
Crocosphaera watsonii WH0002[f]	12 ± 5	23 ± 2	This study
Crocosphaera watsonii WH0401[f]	11 ± 5	45 ± 14	This study
NUTRIENT EFFECTS ON SMALL STRAINS			
Crocosphaera watsonii WH0401 +N	13 ± 4	38 ± 13	This study
Crocosphaera watsonii WH0401 low P	17 ± 3	53 ± 16	This study
Crocosphaera watsonii WH0401 low Fe	13 ± 3	44 ± 1	This study
LIGHT/N EXPERIMENT			
Crocosphaera watsonii WH0005 −N	169 ± 48	233 ± 73	This study
Crocosphaera watsonii WH0005 +N	263 ± 70	213 ± 75	This study

[a] *At maximal growth in semi-continuous culture.*

[b] *Assuming a cell diameter of 5 μm and chl a content of 0.3 pg cell^{-1}.*

[c] *During stationary phase, 15–100 μmol m^{-2} s^{-1} light intensity. Assuming a cell diameter of 4 μm.*

[d] *Average during log phase.*

[e] *Large >4 μm cell type.*

[f] *Small <4 μm cell type.*

Error is shown as SD.

EPS concentrations in WH0401 were not significantly different between the three nutrient treatments and the control ($p > 0.05$).

ELEMENTAL ANALYSES

To determine the elemental composition of large *Crocosphaera* cells and the EPS they produce, a total of six separate culture replicates of WH0005 grown on YBCII with no fixed N added were analyzed for the C and N content. Cellular content of WH0005 averaged 6.4 ± 1.5 pg C cell^{-1} and 1.3 ± 0.4 pg N cell^{-1} while the EPS averaged 1.8 ± 0.3 pg EPS-C cell^{-1} and 0.12 ± 0.03 pg EPS-N cell^{-1} (**Table 2**). The contribution of EPS to total POC (EPS-C plus cellular C) was 22% during exponential growth. The contribution of EPS to total PON is much less than the contribution to POC (8.5%), as evidenced by an EPS C:N ratio of 25 compared to a cellular ratio of 7.2 (**Table 2**). Despite the possibility that heterotrophic bacteria are contributing N to the EPS value, the EPS C:N ratios determined show that the material is depleted in N relative to the cellular fraction and thus is an incomplete nutrient source.

Table 2 | Average carbon and nitrogen content of *Crocosphaera* WH0005 cells and EPS (normalized to cell number) and the average C:N ratio of cellular material and EPS.

	Cellular material	EPS
Carbon (pg/cell)	6.4 ± 1.5	1.8 ± 0.3
Nitrogen (pg/cell)	1.3 ± 0.4	0.12 ± 0.03
C:N[a]	7.2 ± 1.1	25 ± 7

[a] *Note that the C:N ratio is the average of the C:N of each sample, rather than the C:N of the average C and N content.*

Values are shown with SD.

PHOTOSYNTHETIC EFFICIENCY

The photochemical efficiency of photosystem II was determined for all six strains of *Crocosphaera* and it was found that the F_v/F_m of the large strains was ∼0.5, whereas the small strains were

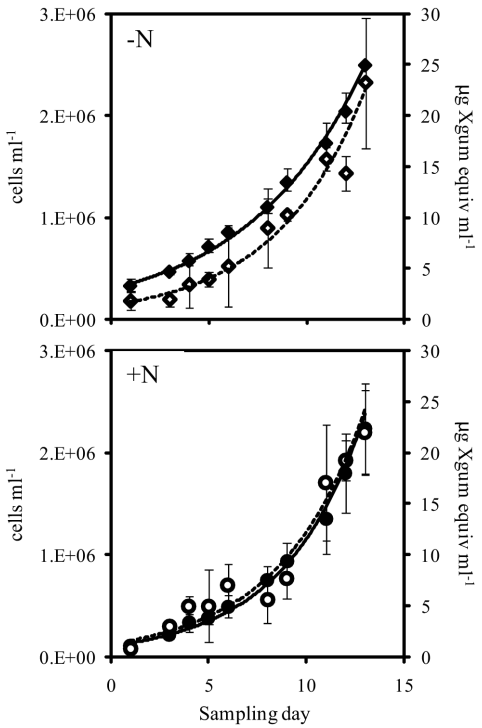

FIGURE 3 | Cell abundance (closed symbols, solid line) and EPS production (open symbols, dashed line) during exponential growth of the large cell class *Crocosphaera* strain WH0005 without N (top) and with 1 mM NO_3^- added (bottom). Error bars show SD.

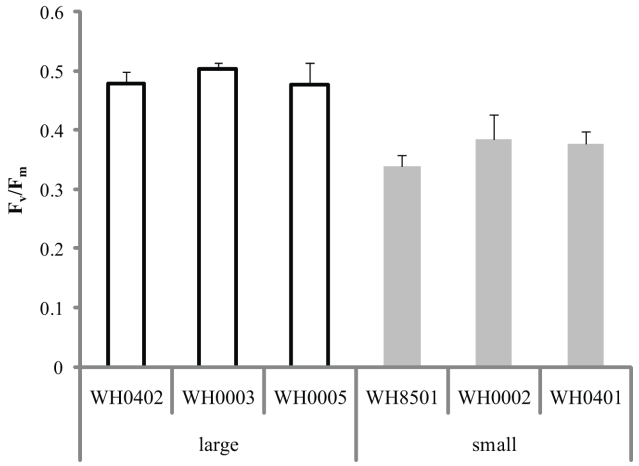

FIGURE 4 | Quantum yield of photosystem II (F_v/F_m) in replicate cultures of six *Crocosphaera* strains. All large strain samples were statistically significantly different than all small strain samples ($p < 0.05$), while among each size class, values were statistically indistinguishable. Error bars show SD.

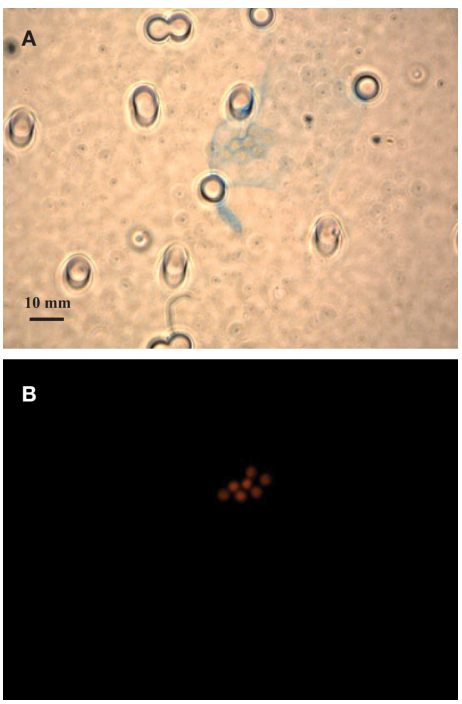

FIGURE 5 | Bright field microscopic images of EPS (A) and epifluorescence images of *Crocosphaera*-like cells under the DAPI longpass filter set (B) at 27°19.19 N, 157°46.65 W in the NPSG. Both images show the same field of view, at 63× magnification.

~0.35 (**Figure 4**). Comparisons among the large and small strains showed that F_v/F_m within each group was statistically indistinguishable ($p > 0.3$ and 0.1, respectively). Additionally, pairwise *t*-tests between all large and small strains showed that F_v/F_m was statistically significantly different between these two phenotypes ($p < 0.05$). Hence the large strains show a greater quantum yield of photosystem II than the small strains.

CROCOSPHAERA AND EPS IN THE FIELD

Extracellular polysaccharides production by field populations of large size class *Crocosphaera* was investigated using Alcian Blue staining and microscopy. Groupings of large *Crocosphaera*-like cells were observed at two stations in the North Pacific (**Figure 5**). Quantification at the second station showed that 74 and 65% of large *Crocosphaera*-like cells observed were embedded in stainable EPS at depths of 5 and 25 m, respectively. These observations support previous evidence that the large phenotype not only produces EPS in cultures, but in the field as well. These particles of *Crocosphaera*-like cells and EPS were also found in high abundance in a floating sediment trap deployed at 75 m for 24 h.

DISCUSSION

This study shows that *Crocosphaera* strains with cells >4 μm produce large amounts of EPS in exponential growth, which is consistent with the qualitative observation previously reported by Webb et al. (2009). However, small amounts of EPS were also measured in the three small strains tested. Therefore, the previous conclusion based on visual observations that the small strains produce no EPS, does not appear to be the case. Rather, the phenotypic difference between large and small strains is an order of magnitude

difference in EPS production, along with a previously described difference in chl *a*-normalized N_2 fixation rates (Webb et al., 2009). This result is remarkable considering that laboratory strains of *Crocosphaera* are nearly identical based on sequence divergence (Zehr et al., 2007; Webb et al., 2009) and that large metagenomic fragments isolated from the subtropical North Pacific showed 97–99% similarity to the WH8501 genome (Zehr et al., 2007). Thus, despite low apparent genomic diversity, there are two distinct phenotypic groups identified with different potential biogeochemical consequences, and this should be considered when quantifying *Crocosphaera* in the field by microscopy, flow cytometry, or *nifH* sequence abundance.

Early work on dissolved organic C (DOC) production by phytoplankton suggested that it is released in much greater quantities in stationary phase, compared to exponentially growing cultures (Berman and Holmhansen, 1974). However, like *Crocosphaera*, many phytoplankton have since been shown to produce EPS and TEP during the exponential growth phase, for example, the diatoms *Chaetoceros affinis*, *Thalassiosira weissflogii*, and *Nitzchia angularis*, the dinoflagellate *Gonyaulax polyedra* (Passow, 2002a) and the N_2-fixing cyanobacterium *Anabaena flos-aquae* (Surosz et al., 2006). Furthermore, Claquin et al. (2008) found that TEP was produced in semi-continuous cultures kept in log phase, and that maximal TEP production occurred at the optimal growth temperature in five out of seven marine phytoplankton species tested, indicating that for some species, TEP production is greatest when growth is optimal, rather than the more commonly held view that it is maximal in unbalanced growth (Nagata, 2000). The production of EPS in *Crocosphaera* fits with this model of extracellular release under optimal conditions and exponential growth. The timing of exopolymer release and response to environmental factors could depend on the function of exopolymers in different species (Passow, 2002a). In most cases, the purpose of these materials are not well understood, but some of the proposed functions of exopolymers are the absorption of nutrients (Sutherland, 1988), creation of a protective microenvironment (Reddy et al., 1996), and a sink of excess fixed C during growth imbalance (Otero and Vincenzini, 2004).

While *Crocosphaera* is not atypical in producing EPS during exponential growth, the amount that the large strains WH0005, WH0402, and WH0003 produce, compared to other tested species, is quite large. Conversely, the small strains (WH0002, WH8501, and WH0401) produced EPS quantities comparable to other phytoplankton (**Table 1**). Furthermore, the quantity of EPS produced by WH0005 by the end of the light/N experiment, normalized to cell volume, was 1–2 orders of magnitude greater than Passow (2002a) measured (as TEP) in nine species of marine phytoplankton from four phyla during both exponential and stationary growth (**Table 1**). Chl *a*-normalized EPS production varied somewhat among the three large strains; however WH0003, WH0005, and WH0402 all produced an order of magnitude more than other phytoplankton (**Table 1**). *Phaeocystis antarctica* is the only phytoplankton we found that produces an amount of exopolymeric material equal to or greater than that measured in the three large strains, but it does so in stationary and death phase (Hong et al., 1997), while *Crocosphaera* produces EPS mainly in exponential phase (**Figure 2**). However, the contribution of mucopolysaccharides to total POC of *Phaeocystis* is 2–11% in exponential phase (Alderkamp et al., 2007), compared to 22% that we found during exponential growth in WH0005. Thus, EPS production appears fundamentally different between these two species with high production values of exopolymers.

A number of strains of *Nostoc*, a freshwater, diazotrophic cyanobacterium, have been shown to produce EPS under N_2-fixing conditions, only to reduce or eliminate production when grown on an exogenous N source (Otero and Vincenzini, 2003). It is hypothesized that N_2-fixing *Nostoc* are N limited, leading to the fixation of extra CO_2 that is shunted to EPS, while growth on fixed N causes CO_2 limitation and cessation of EPS production (Otero and Vincenzini, 2004). In contrast, both the large (WH0005) and small (WH0401) strains produced similar amounts of EPS when grown with or without fixed N. This disparity between *Crocosphaera* and *Nostoc* suggests that neither WH0005 nor WH0401 are producing EPS as a sink of overflow production, and instead are producing it constitutively. Furthermore, nutrient depletion for P and Fe did not cause EPS production to increase in a small strain representative (WH0401, **Table 1**), data that stands in contrast to increases in exopolymer production under Fe stress observed in the diazotrophic cyanobacterium *Trichodesmium* (Berman-Frank et al., 2007). It remains to be seen if there are other conditions where EPS production in large or small strain *Crocosphaera* can be altered.

One potential explanation for the difference in EPS produced between the two size classes may be that large strains of *Crocosphaera* have more efficient CO_2 fixation mechanisms than small strains, leading them to fix more CO_2 than the small strains and release the excess as EPS. While it is not a direct measure of the efficiency of CO_2 fixation, the difference in the quantum yield of photosystem II (F_v/F_m) between the large and small strains (0.5 vs. 0.35 respectively) shows that the large strains are more efficient at using available photons for photochemistry (Falkowski and Raven, 2007). It is important to note, however, that the connection between quantum yield and EPS is shown here to be correlative, not causative. In fact, recent genomic study has revealed the presence of polysaccharide production genes in the genome of a large strain, but not a small strain (Bench et al., in press). The F_v/F_m values determined for the large strains were similar to those seen in other phycoerythrin-containing cyanobacterial cultures; *Trichodesmium* IMS101 and three *Synechococcus* strains have F_v/F_m values ∼0.55 (Berman-Frank et al., 2007; Six et al., 2007). Considering these data, the large *Crocosphaera* appear to have a "typical" efficiency for phycoerythrin-containing cyanobacteria, while the small strains have a low efficiency by comparison. It remains to be seen, however, why the smaller *Crocosphaera* isolates are less photochemically efficient.

The fact that EPS production has an associated energy cost suggests that it provides some benefit to the large cells. The lower surface area to volume ratio of the large size class could make them more susceptible to nutrient limitation than the small size class. There is evidence that these acidic polysaccharide exudates could act as metal chelators (Geesey et al., 1988), making micronutrients that are scarce in the open ocean more available to the large *Crocosphaera*. Another possibility is that the EPS production by large cells serves as a grazing deterrent to protistan grazers (Liu and Buskey, 2000).

Regardless, this EPS excretion has a number of hypothetical biogeochemical consequences in the field, as we have shown

that a majority of large cells produce EPS there. EPS could feed into the microbial loop by providing a C source for heterotrophic bacteria. Additionally, *Crocosphaera* EPS might have some nutritional value as appears to contain some N, but this amount would not likely provide complete N nutrition to organisms feeding on it. Alternatively, particles of EPS with *Crocosphaera* embedded could be grazed directly by larger zooplankton, short-circuiting the microbial loop. This would be a direct input of C and newly fixed N into the classical food chain and up into higher trophic levels. Calanoid copepods collected off coastal California were able to feed on TEP (Ling and Alldredge, 2003), and the cladoceran *Ceriodaphnia cornuta* showed better growth and reproductive performance when feeding on EPS of the freshwater N_2-fixing cyanobacterium *Anabaena spiroides* compared to feeding on seston (Choueri et al., 2007), suggesting particles of EPS containing *Crocosphaera* cells could be eaten successfully by larger zooplankton and sustain their growth.

The most well known characteristic of exopolymers is their role in the aggregation of phytoplankton into marine snow (Passow and Alldredge, 1995a). Since the sinking of marine snow is a major pathway of C flux to the deep sea (Passow et al., 2001), *Crocosphaera* produced EPS may provide a substrate for aggregation of smaller particles that could then sink out of the euphotic zone. We have observed large *Crocosphaera*-like cells in EPS in shallow sediment traps in the NPSG, providing evidence for the direct sinking of these particles, and showing that EPS production could have a biogeochemical impact in this way. However, more work on the *in situ* fate of the *Crocosphaera* produced EPS is needed to resolve its absolute biogeochemical impact.

ACKNOWLEDGMENTS

This work was supported by National Science Foundation grants OCE-0623499 and OCE-0825922 to Eric A. Webb, and the NSF USC Research Experience for Undergraduates grant OCE-0552988 for Bethanie R. Edwards. The authors would also like to thank Will Berelson and Lisa Collins for carrying out the elemental analysis, Linda Duguay, and the rest of USC REU program team for support and guidance, Chief Scientist Ben Van Mooy for providing the opportunity to collect field data, and the Captain and crew of the R/V Kilo Moana.

REFERENCES

Alderkamp, A. C., Buma, A. G. J., and Van Rijssel, M. (2007). The carbohydrates of Phaeocystis and their degradation in the microbial food web. *Biogeochemistry* 83, 99–118.

Bench, S. R., Ilikchyan, I. N., Tripp, H. J., and Zehr, J. P. (in press). Two strains of *crocosphaera watsonii* with highly conserved genomes are distinguished by strain-specific features. *Front. Aquat. Microbiol.*

Berman, T., and Holmhansen, O. (1974). Release of photoassimilated carbon as dissolved organic-matter by marine phytoplankton. *Mar. Biol.* 28, 305–310.

Berman-Frank, I., Rosenberg, G., Levitan, O., Haramaty, L., and Mari, X. (2007). Coupling between autocatalytic cell death and transparent exopolymeric particle production in the marine cyanobacterium *Trichodesmium*. *Environ. Microbiol.* 9, 1415–1422.

Biegala, I. C., and Raimbault, P. (2008). High abundance of diazotrophic picocyanobacteria (<3 μm) in a Southwest Pacific coral lagoon. *Aquat. Microb. Ecol.* 51, 45–53.

Campbell, L., Carpenter, E. J., Montoya, J. P., Kustka, A. B., and Capone, D. G. (2005). Picoplankton community structure within and outside a Trichodesmium bloom in the southwestern Pacific Ocean. *Vie et Milieu* 55, 185–195.

Capone, D. G., Burns, J. A., Montoya, J. P., Subramaniam, A., Mahaffey, C., Gunderson, T., Michaels, A. F., and Carpenter, E. J. (2005). Nitrogen fixation by *Trichodesmium* spp.: an important source of new nitrogen to the tropical and subtropical North Atlantic Ocean. *Global Biogeochem. Cycles* 19, GB2024.

Chen, Y., Zehr, J. P., and Mellon, M. (1996). Growth and nitrogen fixation of the diazotrophic filamentous nonheterocystous cyanobacterium *Trichodesmium* sp. IMSl01 in defined media: evidence for circadian rhythm. *J. Phycol.* 32, 916–923.

Choueri, R. B., Melao, M., Lombardi, A. T., and Vieira, A. A. H. (2007). Effects of cyanobacterium exopolysaccharides on life-history of *Ceriodaphnia cornuta* SARS. *J. Plankton Res.* 29, 339–345.

Church, M. J., Bjorkman, K. M., Karl, D. M., Saito, M. A., and Zehr, J. P. (2008). Regional distributions of nitrogen-fixing bacteria in the Pacific Ocean. *Limnol. Oceanogr.* 53, 63–77.

Church, M. J., Jenkins, B. D., Karl, D. M., and Zehr, J. P. (2005). Vertical distributions of nitrogen-fixing phylotypes at Stn ALOHA in the oligotrophic North Pacific Ocean. *Aquat. Microb. Ecol.* 38, 3–14.

Claquin, P., Probert, I., Lefebvre, S., and Veron, B. (2008). Effects of temperature on photosynthetic parameters and TEP production in eight species of marine microalgae. *Aquat. Microb. Ecol.* 51, 1–11.

Corzo, A., Morillo, J. A., and Rodriguez, S. (2000). Production of transparent exopolymer particles (TEP) in cultures of *Chaetoceros calcitrans* under nitrogen limitation. *Aquat. Microb. Ecol.* 23, 63–72.

Falkowski, P. G., and Raven, J. A. (2007). *Aquatic Photosynthesis*, 2nd Edn. Princeton: Princeton University Press.

Foster, R. A., Subramaniam, A., Mahaffey, C., Carpenter, E. J., Capone, D. G., and Zehr, J. P. (2007). Influence of the Amazon River plume on distributions of free-living and symbiotic cyanobacteria in the western tropical north Atlantic Ocean. *Limnol. Oceanogr.* 52, 517–532.

Geesey, G. G., Jang, L., Jolley, J. G., Hankins, M. R., Iwaoka, T., and Griffiths, P. R. (1988). Binding of metal-ions by extracellular polymers of biofilm bacteria. *Water Sci. Technol.* 20, 161–165.

Hong, Y., Smith, W. O., and White, A. M. (1997). Studies on transparent exopolymer particles (TEP) produced in the Ross Sea (Antarctica) and by *Phaeocystis antarctica* (Prymnesiophyceae). *J. Phycol.* 33, 368–376.

Langlois, R. J., Hummer, D., and Laroche, J. (2008). Abundances and distributions of the dominant nifH phylotypes in the Northern Atlantic Ocean. *Appl. Environ. Microbiol.* 74, 1922–1931.

Ling, S. C., and Alldredge, A. L. (2003). Does the marine copepod *Calanus pacificus* consume transparent exopolymer particles (TEP)? *J. Plankton Res.* 25, 507–515.

Liu, H., and Buskey, E. J. (2000). The exopolymer secretions (EPS) layer surrounding *Aureoumbra lagunensis* cells affects growth, grazing, and behavior of protozoa. *Limnol. Oceanogr.* 45, 1187–1191.

Moisander, P. H., Beinart, R. A., Hewson, I., White, A. E., Johnson, K. S., Carlson, C. A., Montoya, J. P., and Zehr, J. P. (2010). Unicellular cyanobacterial distributions broaden the oceanic N_2 fixation domain. *Science* 327, 1512–1514.

Montoya, J. P., Holl, C. M., Zehr, J. P., Hansen, A., Villareal, T. A., and Capone, D. G. (2004). High rates of N_2 fixation by unicellular diazotrophs in the oligotrophic Pacific Ocean. *Nature* 430, 1027–1031.

Nagata, T. (2000). "Production mechanisms of dissolved organic matter," in *Microbial Ecology of the Oceans*, ed. D. L. Kirchman (New York, NY: Wiley-Liss), 121–152.

Otero, A., and Vincenzini, M. (2003). Extracellular polysaccharide synthesis by *Nostoc* strains as affected by N source and light intensity. *J. Biotechnol.* 102, 143–152.

Otero, A., and Vincenzini, M. (2004). *Nostoc* (Cyanophyceae) goes nude: extracellular polysaccharides serve as a sink for reducing power under unbalanced C/N metabolism. *J. Phycol.* 40, 74–81.

Parsons, T. R., Maita, Y., and Lalli, C. M. (1984). *A Manual of Chemical and Biological Methods for Seawater Analysis*. Oxford: Pergamon Press, 173.

Passow, U. (2002a). Production of transparent exopolymer particles (TEP) by phyto- and bacterioplankton. *Mar. Ecol. Prog. Ser.* 236, 1–12.

Passow, U. (2002b). Transparent exopolymer particles (TEP) in aquatic environments. *Prog. Oceanogr.* 55, 287–333.

Passow, U., and Alldredge, A. L. (1994). Distribution, size and bacterial-colonization of transparent exopolymer particles (TEP) in the ocean. *Mar. Ecol. Prog. Ser.* 113, 185–198.

Passow, U., and Alldredge, A. L. (1995a). Aggregation of a diatom bloom in a mesocosm – the role of transparent exopolymer particles (TEP). *Deep Sea Res. Part II Top. Stud. Oceanogr.* 42, 99–109.

Passow, U., and Alldredge, A. L. (1995b). A dye-binding assay for the spectrophotometric measurement of transparent exopolymer particles (TEP). *Limnol. Oceanogr.* 40, 1326–1335.

Passow, U., Shipe, R. F., Murray, A., Pak, D. K., Brzezinski, M. A., and Alldredge, A. L. (2001). The origin of transparent exopolymer particles (TEP) and their role in the sedimentation of particulate matter. *Cont. Shelf Res.* 21, 327–346.

Reddy, K. J., Soper, B. W., Tang, J., and Bradley, R. L. (1996). Phenotypic variation in exopolysaccharide production in the marine, aerobic nitrogen-fixing unicellular cyanobacterium *Cyanothece* sp. *World J. Microbiol. Biotechnol.* 12, 311–318.

Samuelsson, G., and Öquist, G. (1977). A method for studying photosynthetic capacities of unicellular algae based on in vivo chlorophyll fluorescence. *Plant Physiol.* 40, 315–319.

Six, C., Finkel, Z. V., Irwin, A. J., and Campbell, D. A. (2007). Light variability illuminates niche-partitioning among marine picocyanobacteria. *PLoS ONE 2*, e1341. doi: 10.1371/journal.pone.0001341

Surosz, W., Palinska, K. A., and Rutkowska, A. (2006). Production of transparent exopolymer particles (TEP) in the nitrogen fixing cyanobacterium *Anabaena flos-aquae* OL-K10. *Oceanologia* 48, 385–394.

Sutherland, I. W. (1988). Bacterial surface polysaccharides: structure and function. *Int. Rev. Cytol.* 113, 187–231.

Tripp, H. J., Bench, S. R., Turk, K. A., Foster, R. A., Desany, B. A., Niazi, F., Affourtit, J. P., and Zehr, J. P. (2010). Metabolic streamlining in an open-ocean nitrogen fixing cyanobacterium. *Nature* 464, 90–94.

Webb, E. A., Ehrenreich, I. M., Brown, S. L., Valois, F. W., and Waterbury, J. B. (2009). Phenotypic and genotypic characterization of multiple strains of the diazotrophic cyanobacterium, *Crocosphaera watsonii*, isolated from the open ocean. *Environ. Microbiol.* 11, 338–348.

Zehr, J. P., Bench, S. R., Carter, B. J., Hewson, I., Niazi, F., Shi, T., Tripp, H. J., and Affourtit, J. P. (2008). Globally distributed uncultivated oceanic N_2-fixing cyanobacteria lack oxygenic photosystem II. *Nature* 322, 1110–1112.

Zehr, J. P., Bench, S. R., Mondragon, E. A., McCarren, J., and DeLong, E. F. (2007). Low genomic diversity in tropical oceanic N_2-fixing cyanobacteria. *Proc. Nat. Acad. Sci. U. S. A.* 104, 17807–17812.

Conflict of Interest Statement: The authors declare that the research was conducted in the absence of any commercial or financial relationships that could be construed as a potential conflict of interest.

Received: 20 September 2011; accepted: 28 October 2011; published online: 15 November 2011.

*Citation: Sohm JA, Edwards BR, Wilson BG and Webb EA (2011) Constitutive extracellular polysaccharide (EPS) production by specific isolates of Crocosphaera watsonii. Front. Microbio. **2**:229. doi: 10.3389/fmicb.2011.00229*

This article was submitted to Frontiers in Aquatic Microbiology, a specialty of Frontiers in Microbiology.

frontiers in
MICROBIOLOGY

ORIGINAL RESEARCH ARTICLE
published: 25 October 2011
doi: 10.3389/fmicb.2011.00214

Arsenate resistance in the unicellular marine diazotroph *Crocosphaera watsonii*

Sonya T. Dyhrman* and Sheean T. Haley

Department of Biology, Woods Hole Oceanographic Institution, Woods Hole, MA, USA

Edited by:
George S. Bullerjahn, Bowling Green State University, USA

Reviewed by:
Matthew Church, University of Hawaii at Manoa, USA
Lisa Moore, University of Southern Maine, USA
Eric A. Webb, University of Southern California, USA

****Correspondence:***
Sonya T. Dyhrman, Department of Biology MS#33, Woods Hole Oceanographic Institution, Woods Hole, MA 02543, USA.
e-mail: sdyhrman@whoi.edu

The toxic arsenate ion can behave as a phosphate analog, and this can result in arsenate toxicity especially in areas with elevated arsenate to phosphate ratios like the surface waters of the ocean gyres. In these systems, cellular arsenate resistance strategies would allow phytoplankton to ameliorate the effects of arsenate transport into the cell. Despite the potential coupling between arsenate and phosphate cycling in oligotrophic marine waters, relatively little is known about arsenate resistance in the nitrogen-fixing marine cyanobacteria that are key components of the microbial community in low nutrient systems. The unicellular diazotroph, *Crocosphaera watsonii* WH8501, was able to grow at reduced rates with arsenate additions up to 30 nM, and estimated arsenate to phosphate ratios of 6:1. The genome of strain WH8501 contains homologs for *arsA*, *arsH*, *arsB,* and *arsC*, allowing for the reduction of arsenate to arsenite and the pumping of arsenite out of the cell. The short-term addition of arsenate to the growth medium had no effect on nitrogen fixation. However, arsenate addition did result in the up-regulation of the *arsB* gene with increasing arsenate concentrations, indicating the induction of the arsenate detoxification response. The *arsB* gene was also up-regulated by phosphorus stress in concert with a gene encoding the high-affinity phosphate binding protein *pstS*. Both genes were down-regulated when phosphate was re-fed to phosphorus-stressed cells. A field survey of surface water from the low phosphate western North Atlantic detected expression of *C. watsonii arsB*, suggestive of the potential importance of arsenate resistance strategies in this and perhaps other systems.

Keywords: cyanobacteria, phosphorus, marine, arsenate, diazotroph, *Crocosphaera*

INTRODUCTION

Arsenic is prevalent in the marine environment, where it can occur as arsenite [As (III)] and arsenate [As (V)]. Both oxidation forms are toxic to the majority of living organisms, with arsenite interfering with enzyme function, and arsenate, the thermodynamically dominant form in most oxygenated surface waters (as AsO_4^{3-}), behaving as a phosphate analog (Apte et al., 1986) and disrupting phosphate uptake and utilization (Wängberg and Blanck, 1990; Bleeker et al., 2003).

In the surface ocean, arsenic has relatively high concentrations and follows a nutrient-like profile, with less arsenic at the surface than at depth suggestive of biological uptake and transport (Andreae, 1979; Cutter and Cutter, 1995). Due to the potential competitive inhibition between arsenate and phosphate (Smedley and Kinniburgh, 2002; Manomita et al., 2004), arsenate resistance, or detoxification pathways may be particularly important in low phosphate systems like the ocean gyres, including the western North Atlantic where surface phosphate levels are typically around 5 nM and can be sub-nanomolar (Wu et al., 2000; Lomas et al., 2010). Surface inorganic arsenic (arsenate and arsenite) concentrations in this region can be >12 nM (Cutter and Cutter, 1995) with an arsenic to phosphate ratio thus exceeding 2:1.

It has been proposed that under low phosphate conditions, microbial uptake of arsenate and its subsequent reduction to and excretion as arsenite is rapid (Andreae, 1979). There are relatively few studies of arsenic speciation in the ocean gyres, but of the studies that have been done, the speciation of dissolved arsenic (arsenite, arsenate, and methylated arsenic forms) was subtly controlled by the arsenate to phosphate ratio (Cutter and Cutter, 2006). The microbial detoxification products of arsenic including arsenite and methylated forms of arsenic have surface maxima, and in a study of profiles in the western Atlantic tracked closely with the chlorophyll*a* profile (Cutter and Cutter, 1995). These detoxification products have a short (days–months) residence time and their presence suggests active microbial arsenic detoxification in the surface ocean. Although some arsenic accumulation can occur in microbes (Statham et al., 1987), arsenic distributions suggest that the uptake of arsenic by phytoplankton primarily results in cycling between chemical forms within the euphotic zone and that the flux of arsenic into the deep ocean by particle transport is relatively minor (Andreae, 1979; Sanders and Windom, 1980).

Because of the prevalence of arsenic in the environment and its toxicity, many microbes carry well-described pathways for arsenate detoxification or resistance. The most common arsenate resistance system (*ars*) involves an arsenate reductase (ArsC), an arsenite efflux pump (ArsB or ACR3), and a transcriptional repressor (ArsR; Rosen, 1999; Mukhopadhyay et al., 2002; Busenlehner et al., 2003; López-Maury et al., 2003). Some bacteria also

possess other *ars* genes including *arsA*, an arsenite-stimulated ATPase that results in more efficient arsenite efflux through ArsB (Ordóñez et al., 2005; Silver and Phung, 2005). The presence of arsenate detoxification genes has been reported in a wide variety of picocyanobacteria (López-Maury et al., 2003; Scanlan et al., 2009). Furthermore, *Prochlorococcus* arsenate resistance genes are overrepresented in metagenome sequence from the surface North Atlantic with an elevated arsenate to phosphate ratio relative to the North Pacific (Coleman and Chisholm, 2010). This finding underscores the potential importance of arsenate detoxification, especially in the low phosphorus North Atlantic, yet arsenate resistance strategies have not been investigated in the unicellular marine nitrogen-fixing cyanobacteria.

In the oligotrophic oceans, nitrogen-fixing cyanobacteria are considered "keystone" species (Hewson et al., 2009a), because of their low relative abundance but significance to carbon and nitrogen fixation. Of these nitrogen-fixing cyanobacteria, unicellular diazotrophs are increasingly recognized as critically important to nitrogen cycling (Montoya et al., 2004), but are less well understood relative to larger filamentous nitrogen-fixing cyanobacteria like *Trichodesmium*. Phylogenetic analyses of the nitrogenase-encoding *nifH* sequences obtained from field surveys have shown that there are two distinct groups of the unicellular diazotrophs, one of which (group B) includes *Crocosphaera watsonii* WH8501 (Zehr et al., 2001; Falcón et al., 2002, 2004). *C. watsonii* is widely distributed through the surface waters of the tropical oceans (Church et al., 2005; Zehr et al., 2007), including low phosphate environments like the Sargasso Sea (Hewson et al., 2007). Recent work leveraging the whole genome sequence of *C. watsonii* WH8501 suggests that it has a robust capacity for scavenging phosphorus (e.g., presence of *pstSCAB*, a high-affinity phosphate transport system; Dyhrman and Haley, 2006), and as a diazotroph, it may drive down local phosphorus concentrations via nitrogen fixation. In these low phosphate scenarios there may be coupling between arsenate and phosphate cycling with the possible induction of arsenate detoxification or resistance strategies. Here we used a combination of genomic observations, physiological studies, and field analyses to examine arsenate resistance in *C. watsonii*.

MATERIALS AND METHODS

CULTURE CONDITIONS

Axenic *Crocosphaera watsonii* WH8501, previously designated as *Synechocystis* sp. strain WH8501, was obtained from John B. Waterbury at Woods Hole Oceanographic Institution. Cultures were grown at 27.5°C using a 14:10 h light dark cycle provided by cool white fluorescent bulbs with ~65 μmol quanta m^{-2} s^{-1}. Unless otherwise noted phosphorus replete (referred to as +P or Replete) cultures were grown in 2 L SO medium (Waterbury et al., 1986), made with a 0.2 μm filtered 75% Sargasso seawater base and 45 μM K_2HPO_4. Continued sterility was confirmed by testing for growth of contaminating organisms with a tryptone-fortified medium (Andersen et al., 1991). Growth was monitored by *in vivo* fluorescence on a Turner Designs TD-700 fluorometer.

ARSENATE AND PHOSPHATE GROWTH EXPERIMENT

Crocosphaera watsonii WH8501 was grown in triplicate on different concentrations of added arsenate and phosphate in SO medium made as above and amended with no added phosphate (NoP), 500 nM phosphate (LowP), and 45 μM phosphate (Replete). Sterile-filtered (0.2 μm) arsenate was added as ACS-grade sodium arsenate, $Na_2HAsO_4 \cdot 7H_2O$ (Chem Service, West Chester, PA, USA) in appropriate quantities to yield the following final concentrations in the NoP treatments: 0, 15, 30, 150, 500, 1000, and 5000 nM. Arsenate was added to the LowP treatments to yield the following final concentrations: 0, 500, 1000, and 5000 nM. No arsenate was added to the Replete cultures as a control. Cells used as the inoculum for all treatments were centrifuged initially for 10 min at 7000 rpm and resuspended in medium without added phosphate to restrict carryover. Where no arsenate or phosphate was added to the cultures, As:P ratios were estimated based on literature values for ambient arsenate (12 nM; Cutter and Cutter, 1995) and phosphate concentrations (5 nM; Jakuba et al., 2008) for the region where the water was collected.

ARSENATE ADDITION EXPERIMENTS

Crocosphaera watsonii was grown in 500 mL +P SO medium (as described above) to mid log phase and then equal volumes (25 mL) were dispensed into glass culture tubes. Arsenate was added to triplicate cultures at final concentrations of 0, 15, 30, 150, and 500 nM. The triplicate treatments were pooled and harvested by filtration (0.2 μm, 25 mm polycarbonate filters) after a 24 h incubation under the growth conditions detailed above. Samples were flash frozen immediately and later stored in liquid nitrogen for subsequent gene expression analyses. In similar experiments to assay nitrogen fixation, 30 mL of exponentially growing +P *C. watsonii* WH8501 cells were dispensed into 75-mL square polycarbonate culturing bottles. Arsenate was added to triplicate culture bottles at final concentrations of 0, 15, 30, 150, 500, and 1000 nM arsenate.

PHOSPHORUS MANIPULATION EXPERIMENTS

Triplicate +P (45 μM) cultures were grown as a scale up as described above and harvested at late log phase by centrifugation (7000 rpm). The cell pellets were pooled and split into two equal volumes, washed twice in either +P or −P (−P; 1 μM K_2HPO_4) medium to restrict carryover and resuspended in 25 mL of the same medium. The resulting +P and −P cell suspensions were divided among 3–500 mL flasks of like medium. Whole flasks were harvested onto polycarbonate filters (47 mm, 0.2 μm) at 0, 24, 72, and 120 h after resuspension and flash frozen in liquid nitrogen for subsequent analyses. In an additional experiment, triplicate +P and −P cultures were inoculated each with 2 mL P replete stock that had been centrifuged, split into two equal volumes, washed twice in either +P or −P medium and resuspended in 2 mL of the same medium. Cultures were harvested from mid log phase +P cultures. When growth had ceased in −P cultures, the triplicate cultures were pooled and split into six flasks. Triplicate cultures were re-fed with phosphate to replete P levels (45 μM) and the remaining three were unchanged. Flasks were subsampled at 0, 24, 48, 72, 120, and 168 h after phosphate addition, harvested onto polycarbonate filters (25 mm, 0.2 μm), and flash frozen in liquid nitrogen for subsequent analyses.

NITROGEN FIXATION

Nitrogen fixation was assayed 24 h after the addition of arsenate (as described above), over the midpoint of the dark period

in the incubator by the acetylene reduction assay described by Capone and Montoya (2001). Briefly, all culture bottle caps were replaced with silicone septa. Acetylene was produced by mixing 50 mL of MilliQ water with 15 g calcium carbide and stored in a bladder. Six milliliters of acetylene were injected into the bottles. At times 0, 30, 60, 90, and 120 min after injection, duplicate 0.4-mL samples were removed from the headspace of the bottles and 0.3-mL samples were injected into a Shimadzu GC-8A gas chromatograph and integrated by a Shimadzu CR8A Chromatopac to measure the ethylene peaks. Standards of 9.1 ppm ethylene were used to calibrate the peak heights. Ethylene formed was calculated according to Capone and Montoya (2001) with Bunsen coefficients calculated for a 75% seawater/25% MilliQ water mixture and ambient temperature according to Breitbarth et al. (2004). Nitrogenase activity was calculated as the average rate of ethylene production per volume (nmol C_2H_4 h^{-1} mL^{-1}) with a ratio of 3:1. Growth of cultures was monitored by relative fluorescence with a Turner Designs Aquafluor fluorometer. The nitrogen fixation rate calculated for the control (no arsenate added) was set to one and the nitrogen fixation rates for different arsenate concentrations were compared as a proportion above or below the control.

FIELD SAMPLE COLLECTION

Samples were collected on board the *R/V Bank of Bermuda Atlantic Explorer* in the western North Atlantic (**Figure 1**) in 2006 on the BVAL37 transect from Bermuda to Puerto Rico. At each station, 12 L of near surface (∼5 m) seawater was collected via a Niskin bottle and filtered through 0.2 μm Sterivex cartridge filters (Millipore) under low pressure. Samples were flash frozen and stored in liquid nitrogen prior to analyses. Total processing time from water to liquid nitrogen was roughly 20 min. Dissolved inorganic phosphate (DIP) concentration was determined on Niskin-collected water from the same depth and analyzed as described elsewhere with a typical detection limit of 0.5 nM (Lomas et al., 2010).

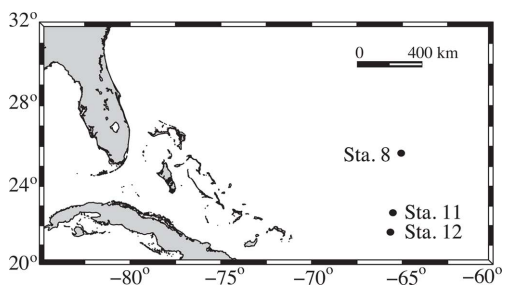

FIGURE 1 | Station locations for field samples collected from an October 2006 transect from north to south in the Sargasso Sea.

TOTAL RNA EXTRACTION FROM CULTURE AND FIELD SAMPLES

RNA extractions were performed on cultured *C. watsonii* WH8501 cells with the RNeasy Mini Kit (Qiagen, Valencia, CA, USA) with a small modification to the lysis procedure. Lysis was performed by adding ∼500 μl zirconium/silica beads (0.5 mm) and vortexing for 10 min at 250 rpm. The RNA was then treated with Turbo DNase (Ambion, Austin, TX, USA) following the rigorous protocol to remove genomic DNA. RNA was quantified spectrophotometrically, and a total of 60 ng of RNA was transcribed into cDNA using random hexamers included in the iScript cDNA Synthesis kit (Bio-Rad, Hercules, CA, USA), according to the instructions. Additional reactions for each sample were set up without reverse transcriptase (RT) to ensure the absence of genomic DNA in no-RT controls.

RNA was extracted from field samples using the RNeasy Mini Kit (Qiagen) with minor modifications in the lysis procedure. Lysis was performed by adding ∼500 μl zirconium/silica beads (0.5 mm), TE/lysozyme buffer (15 mg mL^{-1}), and Buffer RLT (Qiagen) to the Sterivex cartridge. Cartridges were vortexed for 10 min at 250 rpm. The resulting lysate was removed through the Sterivex inlet with a syringe, transferred into a 15-mL conical tube, and processed as per the remaining steps of the RNeasy protocol. Nucleic acid concentrations were quantified using a NanoDrop® ND-1000 spectrophotometer (NanoDrop Technologies, Wilmington, DE, USA). Field samples typically yielded ∼35 ng total RNA. For the field samples, RNA was transcribed and amplified in one step (see below) using gene-specific primers (**Table 1**).

GENE EXPRESSION

Crocosphaera watsonii WH8501 culture samples were quantitatively assayed by qRT-PCR while field samples were qualitatively assayed by RT-PCR. Primer sets for *arsB*, *pstS*, and *rotA* (**Table 1**)

Table 1 | Primers and amplification conditions for the genes used in qRT-PCR and RT-PCR.

Gene	Primer sequence	Accession number	Annealing temperature (°C)	Amplicon size (bp)
arsB	5′ AACAATGGTTTGCCAGGGAAC	ZP_00514915	59.5°C	116
	3′ GTCATACTTTGGTGATGGTTGCG			
pstS	5′ TTGTGCAACTCAACACAGCA	ZP_00514993	59.5°C	127
	3′ TCTGTCATGGCCACATCACT			
rotA	5′ GAGAAGATGCTCCTATTACCGCC	ZP_00514036	59.5°C	243
	3′ GTTGACCCAATGCTTTGCTGTAG			
phnD[a]	5′ TCGGNGCMATYCCSGATCAGAACCCSG		65°C[b]	620
	3′ TTGGGCTGSGCGASCCAGTGGTARTC			
	3′ GGNCGNGCCACCCAGTGGTARTC			

[a] *Primers were designed by Ilikchyan et al. (2009).*

[b] *Decreased by 0.5°C each cycle until 55°C was reached, after Ilikchyan et al. (2009).*

were designed based on the sequenced genome of *C. watsonii* WH8501[1]. Primers, designed and utilized by Ilikchyan et al. (2009), were used to amplify the *Synechococcus* spp. *phnD* gene encoding a putative phosphonate binding protein (**Table 1**). All analyses were performed in triplicate in an iCycler iQ Real-time PCR detection system (Bio-Rad) in a total volume of 25 μl. The reaction mix contained 12.5 μl iQ SYBR Green Supermix (Bio-Rad), 0.2 μM primer concentrations, and 1 μl template cDNA (diluted 1:10). Reactions were cycled using a temperature profile of 95°C for 5 min (1×), 95°C for 30 s (1×), and 59.5°C for 30 s (45×). The temperature profile also included a melt curve protocol at the end of the program. In all cases, melt curves were used to confirm single amplification products for the different reactions. In addition, for each sample and primer pair no-RT controls and no template controls were run to test for DNA contamination and specificity of amplification. These negative controls did not typically amplify, but in the rare cases where there was any amplification the measured template concentration was at least two orders of magnitude less than the sample template concentration.

The comparative, or ΔΔCt, method was used to normalize the expression of each gene for the qRT-PCR. The amplification efficiency and validation of the ΔΔCt method were tested for each primer set on cDNA. Amplification efficiency was determined to be acceptable if it fell between 90 and 110% with an r^2 of 0.98 or higher. Each primer pair was considered acceptable if the ΔCt of the two slopes was less than 0.1. Samples were normalized to the constitutively expressed *rotA* (ZP_00514036), encoding a peptidyl–prolyl *cis*-trans isomerase (Hassidim et al., 1992; Thellin et al., 1999). This gene has previously been used as a reference gene with the marine diazotroph *Trichodesmium erythraeum* (Orchard et al., 2009), and the Ct of this reference gene did not vary with plate or treatment in samples normalized to total RNA. Fold changes were calculated using the Relative Expression Software Tool, which accounts for differences in efficiency in its fold change calculation[2]. For each experiment a single T_0 time point sample was used as a calibrator for calculating fold changes. The *p*-values were calculated using a pair-wise fixed reallocation randomization analysis as noted (Pfaffl et al., 2002).

RT-PCR of environmental samples was performed using a OneStep-RT-PCR kit (Qiagen) according to the manufacturer's instructions. Briefly, the reaction mix contained RNase-free water, 5× OneStep-RT-PCR buffer, dNTP mix (containing 10 mM of each dNTP), 0.6 μM gene-specific primer concentrations (final), OneStep-RT-PCR enzyme mix, and template RNA (∼10 ng) for a total reaction volume of 20 μl. Reactions were cycled with a temperature profile of 50°C for 30 min (1×), 95°C for 15 min (1×), 94°C for 30 s, 59.5°C for 30 s, and 72°C for 1 min (40×), and 72°C for 10 min. To validate the integrity of the extracted RNA, *Synechococcus* spp. *phnD* amplification was included for each environmental sample. The temperature profile was the same for the reverse transcription and initial PCR activation steps. However, the temperature profile for amplification was modified to 95°C for 5 min (1×), 95°C for 1 min, an initial annealing temperature of 65°C for 1 min decreasing by 0.5°C each cycle until 55°C was reached, and 72°C for 1 min (40×), and extension at 72°C for 20 min (Ilikchyan et al., 2009). Additionally, reactions were performed without RT to ensure the absence of genomic DNA in the RNA samples. RT-PCR products were resolved on 2% agarose gels. Selected bands were identified, excised, and gel purified using the QIAquick gel extraction kit (Qiagen). Sequencing of PCR products was performed at the University of Maine Sequencing Facility (Orono, ME). All sequence data were analyzed manually using the programs Sequencher (Gene Codes Corporation, Ann Arbor, MI, USA), MacVector (Accelrys, Burlington, MA, USA), and BLASTN[3]. The sequence of the field amplicon has been deposited in the EMBL Nucleotide Sequence Database[4] with accession number FR873108.

RESULTS

GENOMIC OBSERVATIONS

The genome of *C. watsonii* WH8501 contains homologs for genes involved in the reduction of arsenate to arsenite and the pumping of arsenite out of the cell (**Figure 2**). A homolog of an arsenite efflux pump, *arsB* (ZP_00514915) and an arsenate reductase, *arsC* (ZP_00514912), are present in the *C. watsonii* genome (**Figure 2**). These genes are separated by two genes, *arsH* and *arsH′*, encoding proteins of unknown function (**Figure 2**). The *arsA* (ZP_00516616) gene, an arsenical pump-driving ATPase, is 87.82% identical to *Synechococcus* PCC 6803. In both *Synechococcus* PCC 6803 and *C. watsonii* WH8501 *arsA* is not contiguous to the other *ars* genes, and in *C. watsonii* WH8501 it is isolated on a relatively small contig. The *C. watsonii* WH8501 genome also contains the *pstSCAB* genes that encode a high-affinity P transport system and an additional putative low affinity phosphate permease (Dyhrman and Haley, 2006).

ARSENATE ADDITION EFFECTS ON GROWTH AND NITROGEN FIXATION

Different concentrations of arsenate were added to *C. watsonii* WH8501 cultures to measure the effect on growth in combination with two different phosphate concentrations. Growth rates were calculated for each biological replicate (e.g., each flask) and then averaged within a treatment. The growth rate calculated for the

[1]http://img.jgi.doe.gov/pub/main.cgi
[2]http://www.gene-quantification.de/download.html
[3]http://www.ncbi.nlm.nih.gov/BLAST
[4]http://www.ebi.ac.uk/embl/

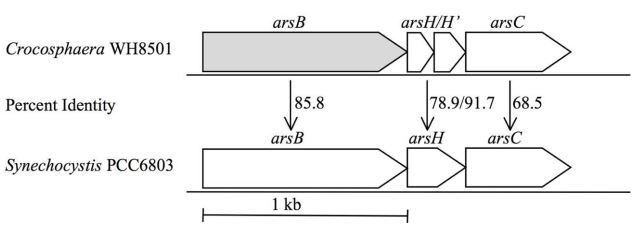

FIGURE 2 | The gene topology of *C. watsonii* WH8501 *arsCHB* and percent identity to *Synechocystis* PCC6803. Genes shaded gray have been shown to be up-regulated by phosphorus stress, or arsenate addition in this study.

Replete control (no arsenate added, 45 μM phosphate) was set to one and the growth rate for different arsenate and phosphate concentrations were normalized to the Replete growth rate. Significant differences in normalized growth rates were found in different treatments (**Figure 3A**, one-way ANOVA, $p < 0.0001$). *Post hoc* testing at the $p < 0.05$ level (Student Newman–Keuls) found no significant differences in normalized growth rate between the Replete and the cultures grown with no added arsenate, regardless of added phosphate concentration, although yield on day 8 of the experiment was highest in the Replete treatment (**Figure 3B**). All treatments with added arsenate had normalized growth rates significantly lower than the Replete. Four arsenate addition levels were replicated with and without added phosphate; a 2-way ANOVA using these arsenate and phosphate concentrations as factors found no significant effect of phosphate concentration on normalized growth rate ($p = 0.3341$; **Figure 3A**). However, increasing arsenate concentration had a highly significant effect on normalized growth rate ($p < 0.0001$; **Figure 3A**). There was no significant interaction effect between phosphate and arsenate ($p = 0.9051$). For the cultures with NoP (0 nM – typically ∼5 nM residual phosphate in culture medium), growth rates were depressed in the 15- and 30-nM treatments (**Figure 3A**). The transition from positive growth to negative growth occurred with an arsenate addition between 30 and 150 nM (**Figure 3A**). Short-term (24 h) additions of arsenate in concentrations of 0, 15, 30, 150, 500, and 1000 nM had no affect on *in vivo* fluorescence (data not shown). Further, these same arsenate additions had no acute effect (one-way ANOVA, $p = 0.9816$) on nitrogen fixation rate after 24 h (**Figure 4**).

GENE EXPRESSION PATTERNS

In +P cultures of *C. watsonii* WH8501, expression of *arsB* was higher, and statistically different from the no addition control with the addition of 30 nM ($p = 0.000$; **Figure 5**). In this experiment, fold changes increased as a function of increasing arsenate (**Figure 5**). The expression of *arsB* was higher in −P cultures of *C. watsonii* WH8501 relative to the +P control by 72 h ($p = 0.000$), and further increased by 120 h (**Figure 6**). Consistent with previous work (Dyhrman and Haley, 2006), the expression of *pstS* in the −P cultures was statistically higher than in the +P cultures by 120 h ($p = 0.000$), although overall expression levels of *pstS* were low relative to *arsB* (**Figure 6**). When P was re-supplied to P-stressed cultures, *arsB* ($p = 0.000$), and *pstS* ($p = 0.012$; data not shown) were statistically lower within 48 h and remained low (*arsB*; $p = 0.013$ and *pstS*; $p = 0.044$) over the course of the 168-h experiment (**Figure 7**).

FIELD DETECTION OF *C. watsonii ARSB*

Three near surface samples were examined for the expression of the *C. watsonii arsB* gene in an oligotrophic region of the western North Atlantic during a transect from Bermuda to Puerto Rico in October 2006 (BVAL 37). The field stations examined had DIP concentrations <10 nM (**Table 2**). A *C. watsonii arsB* transcript was detected at station 12, and confirmed with sequencing of the amplicon, which was 100% identical to the *arsB* WH8501 genome sequence. *C. watsonii arsB* transcripts were not detected at stations 8 and 11. Amplification was not observed in the no-RT controls for the stations tested, and expression of the *Synechococcus* sp. *phnD* transcript was detected at all stations (**Table 2**).

DISCUSSION

Arsenate is common in the ocean with surface water concentrations from approximately 5–20 nM (Andreae, 1979; Cutter and Cutter, 1995). Arsenate and phosphate share the same oxidative state and as a consequence, enzymes, and proteins may bind arsenate and move it into the cell by phosphate transport systems with little selectivity (Tawfik and Viola, 2011). Although some microbes thrive in high arsenate (Brunskill et al., 1980; Thiel, 1988; López-Maury et al., 2003), marine microorganisms, which must take up phosphate to supply their metabolic needs, face a unique problem in oligotrophic regimes, where phosphate concentrations are low and arsenate may equal or exceed the phosphate concentration

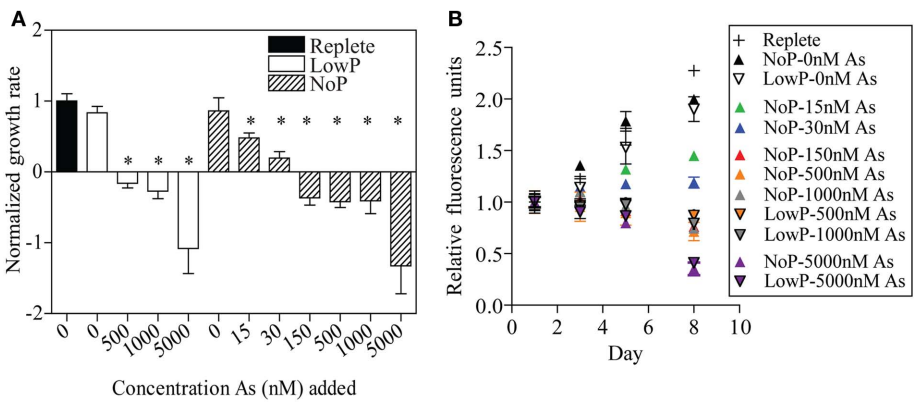

FIGURE 3 | *C. watsonii* WH8501 growth responses to arsenate (As). **(A)** Growth rate of *C. watsonii* WH8501 normalized to the Replete control with 45 μM phosphate (P) and no added As. Treatments consisted of different concentrations of As added to medium with either LowP (500 nM) or NoP. Error bars are the SE of the mean ($n = 3$). Significantly lower growth rates from the Replete control ($p < 0.05$) are indicated (*) for each treatment using a 1-way ANOVA. **(B)** *C. watsonii* WH8501 relative fluorescence as a function of day in growth curves for each P and as treatment. Treatment key is ordered by the yield on day 8. Error bars are the SE of the mean ($n = 3$).

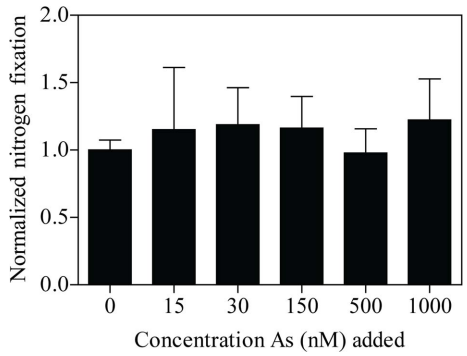

FIGURE 4 | Nitrogenase activity of *C. watsonii* WH8501 normalized to the control with no added arsenate. Treatments consisted of different concentrations of added arsenate as indicated. Error bars indicate the SE of the mean ($n = 3$).

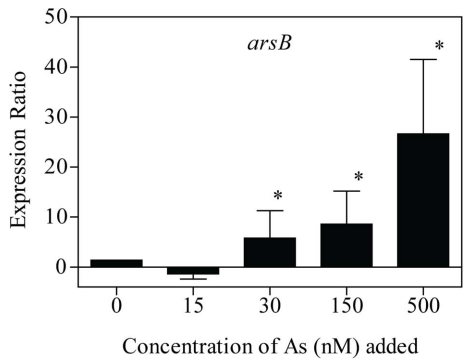

FIGURE 5 | Expression pattern for *arsB* as a function of arsenate additions. The expression ratio is the fold change of triplicate measurements between the sample expression and the calibrator expression (e.g., the zero time point). Error bars indicate the SE of triplicate measurements of the expression ratio. Significance ($p < 0.05$) is indicated (*) for each arsenate addition treatment relative to the no addition control using a pair-wise fixed reallocation randomization analysis.

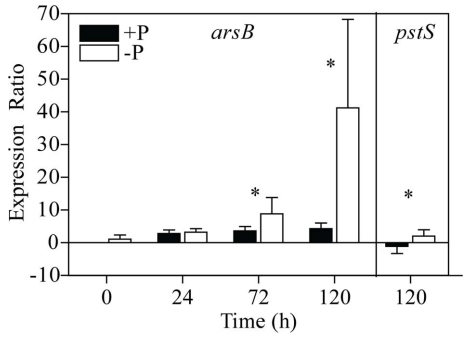

FIGURE 6 | Expression patterns for *arsB* and *pstS* in cultures transferred into either phosphate replete (+P) or no added P (−P) medium. The expression ratio is the fold change of triplicate measurements between the sample expression and the calibrator expression (e.g., the zero time point). Error bars indicate the SE of triplicate measurements of the expression ratio. Significance ($p < 0.05$) is indicated (*) for the −P versus the +P culture at a single time point for pair-wise fixed reallocation randomization analysis.

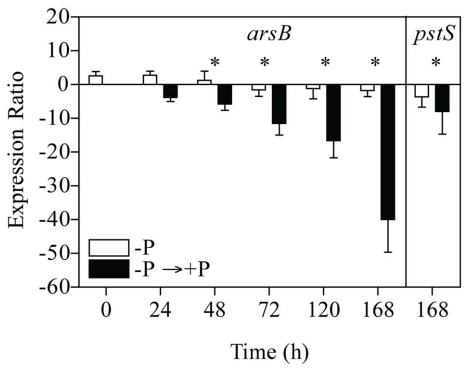

FIGURE 7 | Expression patterns for *arsB* and *pstS* in phosphate deficient cultures (−P) re-fed with phosphate (+P). The expression ratio is the fold change of triplicate measurements between the sample expression and the calibrator expression (e.g., the zero time point). Error bars indicate the SE of triplicate measurements of the expression ratio. Significance ($p < 0.05$) is indicated (*) for the −P versus the re-fed culture at a single time point for pair-wise fixed reallocation randomization analysis.

(Johnson and Pilson, 1972). Nitrogen-fixing marine cyanobacteria are often present in low phosphate environments, and exhibit evidence of P stress-induced adaptations in some regions like the western North Atlantic (Dyhrman et al., 2002, 2007; Dyhrman and Haley, 2006). It has also been hypothesized that they may draw down phosphate to the extent that they induce phosphate deficiency in local microbial populations (Hewson et al., 2009b). In these systems, cellular arsenate resistance strategies would allow diazotrophs to ameliorate the effects of arsenate transport into the cell.

Despite the potential coupling between arsenate and phosphate cycling in marine waters, relatively little is known about arsenate resistance in the nitrogen-fixing marine cyanobacteria that are common in oligotrophic systems. The unicellular diazotroph, *C. watsonii* WH8501, was able to grow, but with reduced rates, with arsenate additions up to 30 nM, and estimated arsenate to phosphate ratios up to 6:1. Cell abundance declined rapidly in treatments with 500 nM arsenate and phosphate together at a 1:1 ratio, suggesting that *C. watsonii* is sensitive to the absolute concentration of arsenate and not simply the arsenate to phosphate ratio. Several cyanobacterial species, such as *Anabaena variabilis* and *Synechocystis* strain PCC6803 are able to grow in the presence of high concentrations of arsenate (up to 75 mM) and in low-millimolar concentrations of arsenite, respectively (Thiel, 1988; López-Maury et al., 2003). At this juncture, *C. watsonii* WH8501 appears to be more sensitive to arsenate additions, ceasing net growth with additions of 500 nM arsenate in medium with 500 nM phosphate, and with additions of only 30 nM arsenate in medium made from low phosphate Sargasso Sea seawater with no added P. The selectivity of phosphate transporters for phosphate relative to arsenate can be variable (Budd and Craig, 1981; Takahashi et al., 2001; Tawfik and Viola, 2011) and was not examined herein, but

Table 2 | Presence or absence of *Crocosphaera watsonii arsB, arsB* no-RT, and *Synechococcus* spp. *phnD* in field samples.

Cruise-station ID	*arsB*	*arsB* no-RT	*phnD*	DIP (nM)
BVAL37–8	−	−	+	5.4
BVAL37–11	−	ND	+	2.7
BVAL37–12	+	−	+	BLD

ND, not determined – there was not enough template for this sample to perform a no-RT reaction for arsB; DIP, Dissolved inorganic phosphate; BLD, Below detection limit.

these growth data suggest that arsenate is able to enter the cell and effect net growth rate in both 0 nM added and 500 nM added phosphate treatments. Phosphate may be transported by *C. watsonii* WH8501 using a low affinity phosphate permease system under high phosphate, and via the canonical *pstSCAB* high-affinity system under low phosphate (Dyhrman and Haley, 2006). These growth data are consistent with this hypothesis, given that the arsenate exhibited toxic effects on growth and was likely transported into the cells in both the 500- and 0-nM treatments. This is also consistent with the sensitivity of *C. watsonii* to arsenate compared to other cyanobacteria, as the putative low affinity phosphate permease transport system is not common in the other marine cyanobacteria (Dyhrman and Haley, 2006).

Arsenate metabolism and the related genes are well studied in a diverse array of microbes (Stolz et al., 2006). A conserved strategy for arsenate detoxification among the marine picocyanobacteria examined to date is the reduction of arsenate to arsenite within the cell by means of an arsenate reductase and subsequent removal by an arsenite efflux pump (ArsB; Scanlan et al., 2009). The required genes are broadly distributed in the marine picocyanobacteria *Prochlorococcus* and *Synechococcus* (Scanlan et al., 2009). The arsenate resistance genes are also present in *C. watsonii* WH8501, which has homologs for *arsA* and *arsCHH′B*. The *arsA* gene is not contiguous with the other ars genes in the genome. It encodes an arsenical pump-driving ATPase, *arsC* encodes a putative arsenate reductase, and *arsB* encodes the arsenite efflux pump. The ArsH protein has been shown to be required for resistance to arsenite and arsenate in some bacteria, such as *Yersinia enterocolitica* (Neyt et al., 1997), and *arsH* is present in the *arsBHC* operon involved in arsenic resistance in the cyanobacteria *Synechocystis* sp. PCC6803 (López-Maury et al., 2003), but its role in detoxification is unknown.

The short-term addition of arsenate to high phosphate cultures of *C. watsonii* WH8501 resulted in the up-regulation of the *arsB* gene, demonstrating its responsiveness to arsenate. Expression levels were titered to increasing arsenate concentration, indicating the induction of an arsenate detoxification response that is sensitive to absolute concentration of arsenate. Although *arsB* was significantly induced with arsenate additions of 30 nM or greater, arsenate did not result in acute effect on growth or nitrogen fixation over the 24-h incubation. In fact, there may be no acute effect on nitrogen fixation because *C. watsonii* WH8501 is able to detoxify arsenate. Given the growth responses to longer-term arsenate exposure highlighted above, there is likely an effect on nitrogen fixation in scenarios of chronic exposure, or where the arsenate resistance system is unable to compensate. This could be the result of arsenic accumulation in the cell, which has been shown to occur with chronic exposure in other phytoplankton (Sanders and Windom, 1980). As such, arsenate toxicity could be a controlling factor on nitrogen fixation in areas where the arsenate to phosphate ratio, or the absolute arsenate concentration, is chronically high. Regardless, *C. watsonii* WH8501 clearly induces *arsB* in response to even low arsenate additions, which underscores the sensitivity of the resistance response to arsenate.

The *arsB* expression patterns examined herein demonstrate that the gene is concomitantly expressed during P stress with *pstS*. The differences in the *arsB* and *pstS* expression ratios, are consistent with the heterogeneity observed between P-responsive genes in *T. erythraeum* (Orchard et al., 2009), and likely reflect different transcript abundances. Expression levels of both genes decline upon P addition to phosphate deficient cells within 48 h. This is somewhat slower than what is observed with *Prochlorococcus* strains (Martiny et al., 2006), and the diazotroph *T. erythraeum* (Orchard et al., 2009), which may be related to the relatively slow doubling times (∼40–60 h) reported for *C. watsonii* strains (Webb et al., 2009). Although the arsB gene is clearly induced in concert with pstS, a known phosphate-responsive phosphate binding protein gene, the arsB in this case may be responsive to the changing arsenate uptake dynamics driven by changes in the expression of the high-affinity phosphate transport system, and the arsenate to phosphate ratio in the medium, rather than as a direct response to phosphate supply.

Unicellular diazotrophs such as *C. watsonii* are increasingly recognized for their contribution to oceanic nitrogen fixation (Zehr et al., 2001; Montoya et al., 2004), despite their low abundance. This low abundance makes tracking *C. watsonii* gene expression patterns in the field a challenge relative to more abundant picocyanobacteria. For example, even at its highest cell densities in *C. watsonii* bloom scenarios, relatively few *C. watsonii* transcripts could be detected in metadata sets (Hewson et al., 2009a). Low field abundances have thus, in part, restricted transcriptomic studies of this diazotroph in the field to surveys of *nifH* transcripts and the one metatranscriptomic study in a high density population highlighted above (Hewson et al., 2009a). Herein, we observed expression of *C. watsonii arsB* in the near surface waters of the tropical western North Atlantic. The likely explanation for why two of the three stations did not have a detectable *C. watsonii arsB* amplicon is low cell abundance, since estimated cell density in this general region of the western North Atlantic is both spatially variable and low; ranging from undetectable to about seven *C. watsonii nifH* copies L^{-1} (Langolis et al., 2008; Moisander et al., 2010). *C. watsonii* abundance was not examined on the transect, but *Synechococcus* abundances in this region averaged 10^4 cells mL^{-1} in surface waters (Casey et al., 2009), much higher than

typical *C. watsonii* abundances ($<<10^3$ cells mL^{-1}). The fact that the samples amplified for *Synechococcus* sp. *phnD* suggests that the RNA was of good quality, and either *C. watsonii arsB* was not expressed, or *C. watsonii* was not present at abundances where *arsB* transcripts could be detected. Despite these challenges, the *arsB* transcript detected at station 12 was clearly from *C. watsonii*. Without quantitative data we are unable to ascertain if this transcript was induced to levels that would suggest substantial arsenate detoxification, however, the expression of *arsB* is consistent with the detection of the arsenite detoxification product in the North Atlantic (Andreae and Klumpp, 1979; Sanders and Windom, 1980).

The expression of arsenate detoxification genes has not been comprehensively examined in marine microbial populations, although expression of arsenate reductase, *arsA*, and *arsB* were detected in metatranscriptome data from a *Trichodesmium* consortium collected from the South Pacific (Hewson et al., 2009b). In this case, the *arsA* was from *Trichodesmium*, and the other signals were from other heterotrophic bacteria present in the sample (Hewson et al., 2009b). The presence of these transcripts in the relatively high phosphate environment of the South Pacific may be attributed to changes in P cycling driven by a dense population of diazotrophs (Hewson et al., 2009b), and/or differences in the sensitivity of different microbes to arsenate toxicity. Of the very few *C. watsonii* transcripts detected in this study, none were related to arsenate detoxification (Hewson et al., 2009b). The *arsB* transcript was also not detected in the metatranscriptome of a bloom of *C. watsonii* in the South Pacific (Hewson et al., 2009a). The detection of *C. watsonii arsB* in the western North Atlantic and not the South Pacific is consistent with the relatively high phosphate environment of the South Pacific relative to the western North Atlantic. However it is difficult to cross-compare between PCR and metatranscriptome studies because of differences in the sensitivities of the two methods, and the lack of quantitative data. Regardless, the field detection *arsB* in the western North Atlantic is permissive of the induction of *C. watsonii* arsenate detoxification strategies in this low phosphate environment.

More detailed, quantitative studies that track the expression of *arsB*, and rates of arsenate reduction are required to examine coupling between the cycling of phosphate and arsenate in diazotrophs like *C. watsonii* in the field, and to determine the impact of phosphate and arsenate supply on *C. watsonii* growth and nitrogen fixation *in situ*. However, the data presented herein are a first step toward these more detailed characterization studies. Taken together, these data identify that *C. watsonii* has an arsenate resistance strategy that is sensitive to changes in arsenate, and phosphate concentration. Chronic arsenate exposure may reduce growth rates despite the presence of a detoxification mechanism in this group of diazotrophs, and the expression of *C. watsonii arsB* in the western North Atlantic suggests that the coupling of the arsenate and phosphate cycles should be examined in greater detail in oligotrophic marine systems.

ACKNOWLEDGMENTS

The authors thank Dr. Elizabeth Orchard (WHOI), Dr. Mike Lomas (BIOS), Dr. Andrew Juhl (LDEO), and Dr. Louie Wurch (WHOI) for helpful discussions and assistance. The authors also thank the captain and crew of the *R/V Bank of Bermuda Atlantic Explorer* for assistance at sea, as well as Harriet Alexander (WHOI) for generating the cruise transect map. Special thanks are due to Abigail Heithoff (WHOI) for conducting nitrogen fixation measurements. This research was funded in part by the National Science Foundation #OCE-0451419, and the Center for Microbial Oceanography: Research and Education.

REFERENCES

Andersen, R. A., Jacobson, D. M., and Sexton, J. P. (1991). *Provasoli-Guillard Center for Culture of Marine Phytoplankton: catalogue of strains.* Provasoli-Guillard Center for Culture of Marine Phytoplankton: West Boothbay Harbor, ME.

Andreae, M. O. (1979). Arsenic speciation in seawater and interstitial waters: the influence of biological-chemical interactions on the chemistry of a trace element. *Limnol. Oceanogr.* 24, 440–452.

Andreae, M. O., and Klumpp, D. W. (1979). Biosynthesis and release of organoarsenic compounds by marine algae. *Environ. Sci. Technol.* 13, 738–741.

Apte, S. C., Howard, A. G., Morris, R. J., and McCartney, M. J. (1986). Arsenic, antimony and selenium speciation during a spring phytoplankton bloom in a closed experimental ecosystem. *Mar. Chem.* 20, 119–130.

Bleeker, P. M., Schat, H., Vooijs, R., Verkleij, J. A. C., and Ernst, W. H. O. (2003). Mechanisms of arsenate tolerance in *Cytisus striatus*. *New Phytol.* 157, 33–38.

Breitbarth, E., Mills, M. M., Friedrichs, G., and LaRoche, J. (2004). The Bunsen gas solubility coefficient of ethylene as a function of temperature and salinity and its importance for nitrogen fixation assays. *Limnol. Oceanogr. Methods* 2, 282–288.

Brunskill, G. J., Graham, B. W., and Rudd, J. W. M. (1980). Experimental studies on the effect of arsenic on microbial degradation of organic matter and algal growth. *Can. J. Fish. Aquat. Sci.* 37, 415–423.

Budd, K., and Craig, S. R. (1981). Resistance to arsenate toxicity in the blue-green alga *Synechococcus leopoliensis*. *Can. J. Bot.* 59, 1518–1521.

Busenlehner, L. S., Pennella, M. A., and Giedroc, D. P. (2003). The Smt/ArsR family of metalloregulatory transcriptional repressors: structural insights into prokaryotic metal resistance. *FEMS Microbiol. Rev.* 27, 131–143.

Capone, D. G., and Montoya, J. P. (2001). "Nitrogen fixation and denitrification," in *Methods in Microbiology,* ed. J. Paul (San Diego, CA: Academic), 501–515.

Casey, J. R., Lomas, M. W., Michelou, V. K., Dyhrman, S. T., Orchard, E. D., Ammerman, J. W., and Sylvan, J. B. (2009). Phytoplankton taxon-specific orthophosphate (Pi) and ATP utilization in the western subtropical North Atlantic. *Aquat. Microb. Ecol.* 58, 31–44.

Church, M. J., Jenkins, B. D., Karl, D. M., and Zehr, J. P. (2005). Vertical distributions of nitrogen-fixing phylotypes at Stn ALOHA in the oligotrophic North Pacific Ocean. *Aquat. Microb. Ecol.* 38, 3–14.

Coleman, M. L., and Chisholm, S. W. (2010). Ecosystem-specific selection pressures revealed through comparative population genomics. *Proc. Natl. Acad. Sci. U.S.A.* 107, 18634–18639.

Cutter, G. A., and Cutter, L. S. (1995). Behavior of dissolved antimony, arsenic, and selenium in the Atlantic Ocean. *Mar. Chem.* 49, 295–306.

Cutter, G. A., and Cutter, L. S. (2006). Biogeochemistry of arsenic and antimony in the North Pacific Ocean. *Geochem. Geophys. Geosy.* 7, Q05M08.

Dyhrman, S. T., Ammerman, J. W., and Van Mooy, B. A. S. (2007). Microbes and the marine phosphorus cycle. *Oceanography* 20, 110–116.

Dyhrman, S. T., and Haley, S. T. (2006). Phosphorus scavenging in the unicellular marine diazotroph *Crocosphaera watsonii*. *Appl. Environ. Microbiol.* 72, 1452–1458.

Dyhrman, S. T., Webb, E. A., Anderson, D. M. A., Moffett, J. W., and Waterbury, J. B. (2002). Cell-specific detection of phosphorus stress in *Trichodesmium* from the Western North Atlantic. *Limnol. Oceanogr.* 47, 1832–1836.

Falcón, L. I., Carpenter, E. J., Cipriano, F., Bergman, B., and Capone, D. G. (2004). N2-fixation by unicellular bacterioplankton from the Atlantic and Pacific Oceans: phylogeny and in situ rates. *Appl. Environ. Microbiol.* 70, 765–770.

Falcón, L. I., Cipriano, F., Chistoserdov, A. Y., and Carpenter, E. J. (2002). Diversity of diazotrophic unicellular cyanobacteria in the tropical North Atlantic Ocean. *Appl. Environ. Microbiol.* 68, 5760–5764.

Hassidim, M., Schwarz, R., Lieman-Hurwitz, J., Marco, E., Ronen-Tarazi, M., and Kaplan, A. (1992). A cyanobacterial gene encoding peptidyl-prolyl cis-trans isomerase. *Plant Physiol.* 100, 1982–1986.

Hewson, I., Moisander, P. H., Achilles, K. M., Carlson, C. A., Jenkins, B. D., Mondragon, E. A., Morrison, A. E., and Zehr, J. P. (2007). Characteristics of diazotrophs in surface to abyssopelagic waters of the Sargasso Sea. *Aquat. Microb. Ecol.* 46, 15–30.

Hewson, I., Poretsky, R. S., Beinhart, R. A., White, A. E., Shi, T., Bench, S. R., Moisander, P. H., Paerl, R. W., Tripp, H. J., Montoya, J. P., Moran, M. A., and Zehr, J. P. (2009a). In situ transcriptomic analysis of the globally important keystone N_2-fixing taxon *Crocosphaera watsonii. ISME J.* 3, 618–631.

Hewson, I., Poretsky, R. S., Dyhrman, S. T., Zielinski, B., White, A. E., Tripp, H. J., Montoya, J. P., and Zehr, J. P. (2009b). Microbial community gene expression within colonies of the diazotroph, *Trichodesmium*, from the Southwest Pacific Ocean. *ISME J.* 3, 1286–1300.

Ilikchyan, I. N., McKay, R. M. L., Zehr, J. P., Dyhrman, S. T., and Bullerjahn, G. S. (2009). Detection and expression of the phosphonate transporter gene *phnD* in marine and freshwater picocyanobacteria. *Environ. Microbiol.* 11, 1314–1324.

Jakuba, R. W., Moffett, J. W., and Dyhrman, S. T. (2008). Evidence for the linked biogeochemical cycling of zinc, cobalt, and phosphorus in the western North Atlantic Ocean. *Global Biogeochem. Cycles* 22, GB4012.

Johnson, D. L., and Pilson, M. E. Q. (1972). Arsenate in the Western North Atlantic and adjacent regions. *J. Mar. Res.* 30, 140–148.

Langolis, R. J., Hümmer, D., and LaRoche, J. (2008). Abundances and distributions of the dominant nifH phylotypes in the Northern Atlantic Ocean. *Appl. Environ. Microbiol.* 74, 1922–1931.

Lomas, M. W., Burkel, A. L., Lomas, D. A., Bell, D. W., Shen, C., Dyhrman, S. T., and Ammerman, J. W. (2010). Sargasso Sea phosphorus biogeochemistry: an important role for dissolved organic phosphorus (DOP). *Biogeosciences* 7, 695–710.

López-Maury, L., Florencio, F. J., and Reyes, J. C. (2003). Arsenic sensing and resistance system in the cyanobacterium *Synechocystis* sp. strain PCC 6803. *J. Bacteriol.* 185, 5363–5371.

Manomita, P. M., Bhowmik, N., Bandopadhyay, B., and Sharma, A. (2004). Comparison of mercury, lead and arsenic with respect to genotoxic effects on plant systems and the development of genetic tolerance. *Environ. Exp. Bot.* 52, 199–223.

Martiny, A. C., Coleman, M. L., and Chisholm, S. W. (2006). Phosphate acquisition genes in *Prochlorococcus* ecotypes: evidence for genome-wide adaptation. *Proc. Natl. Acad. Sci. U.S.A.* 103, 12552–12557.

Moisander, P. H., Beinhart, R. A., Hewson, I., White, A. E., Johnson, K. S., Carlson, C. A., Montoya, J. P., and Zehr, J. P. (2010). Unicellular cyanobacterial distributions broaden the oceanic N_2 fixation domain. *Science* 327, 1512–1514.

Montoya, J. P., Holl, C. M., Zehr, J. P., Hansen, A., Villareal, T., and Capone, D. G. (2004). High rates of N_2 fixation by unicellular diazotrophs in the oligotrophic Pacific Ocean. *Nature* 430, 1027–1031.

Mukhopadhyay, R., Rosen, B. P., Phung, L. T., and Silver, S. (2002). Microbial arsenic: from geocycles to genes and enzymes. *FEMS Microbiol. Rev.* 26, 311–325.

Neyt, C., Iriarte, M., Thi, V. H., and Cornelis, G. R. (1997). Virulence and arsenic resistance in *Yersinia. J. Bacteriol.* 79, 612–619.

Orchard, E. D., Webb, E. A., and Dyhrman, S. T. (2009). Molecular analysis of the phosphorus starvation response in *Trichodesmium* spp. *Environ. Microbiol.* 11, 2400–2411.

Ordóñez, E., Letek, M., Valbuena, N., Gil, J. A., and Mateos, L. M. (2005). Analysis of genes involved in arsenic resistance in *Corynebacterium glutamicum* ATCC 13032. *Appl. Environ. Microbiol.* 71, 6206–6215.

Pfaffl, M. W., Horgan, G., and Leo, D. (2002). Relative expression software tool (REST) for group wise comparison and statistical analysis of relative expression results in real-time PCR. *Nucleic Acids Res.* 30, E36.

Rosen, B. P. (1999). Families of arsenic transporters. *Trends Microbiol.* 7, 207–212.

Sanders, J. G., and Windom, H. L. (1980). The uptake and reduction of arsenic species by marine algae. *Estuarine Coastal Mar. Sci.* 10, 555–567.

Scanlan, D. J., Ostrowski, M., Mazard, S., Dufresne, A., Garczarek, L., Hess, W. R., Post, A. F., Hagemann, M., Paulsen, I., and Partensky, F. (2009). Ecological genomics of marine picocyanobacteria. *Microbiol. Mol. Biol. Rev.* 73, 249–299.

Silver, S., and Phung, L. T. (2005). Genes and enzymes involved in bacterial oxidation and reduction of inorganic arsenic. *Appl. Environ. Microbiol.* 71, 599–608.

Smedley, P. L., and Kinniburgh, D. G. (2002). Phosphate transport and arsenate resistance in the cyanobacterium *Anabaena variabilis. Appl. Geochem.* 17, 517–568.

Statham, P. J., Burton, J. D., and Maher, W. A. (1987). Dissolved arsenic in waters of the Cape Basin. *Deep Sea Res. A* 34, 1353–1359.

Stolz, J. F., Basu, P., Santini, J. M., and Oremland, R. S. (2006). Arsenic and selenium microbial metabolism. *Annu. Rev. Microbiol.* 60, 107–130.

Takahashi, A., Kawakami, H., Iwakiri, K., and Matsuto, S. (2001). Some characteristics of arsenate transport in a marine cyanobacterium, *Synechococcus* sp. *Appl. Organomet. Chem.* 15, 291–298.

Tawfik, D. S., and Viola, R. E. (2011). Arsenate placing phosphate: alternative life chemistries and ion promiscuity. *Biochemistry* 50, 1128–1134.

Thellin, O., Zorzi, W., Lakaye, B., De Borman, B., Coumans, B., Hennen, G., Grisar, T., Igout, A., and Heinen, E. (1999). Housekeeping genes as internal standards: use and limits. *J. Biotechnol.* 75, 291–295.

Thiel, T. (1988). Phosphate transport and arsenate resistance in the cyanobacterium *Anabaena variabilis. J. Bacteriol.* 170, 1143–1147.

Wängberg, S.-Å., and Blanck, H. (1990). Arsenate sensitivity in marine periphyton communities established under various nutrient regimes. *J. Exp. Mar. Biol. Ecol.* 139, 119–134.

Waterbury, J. B., Valois, F. W., and Franks, D. G. (1986). "Biological and ecological characterization of the marine unicellular cyanobacterium *Synechococcus*," in *Photosynthetic Picoplankton,* eds T. Platt and W. K. W. Li (Ottawa: Canadian Department of Fisheries and Oceans), 71–120.

Webb, E. A., Ehrenreich, I. M., Brown, S. L., Valois, F. W., and Waterbury, J. B. (2009). Phenotypic and genotypic characterization of multiple strains of the diazotrophic cyanobacterium, *Crocosphaera watsonii*, isolated from the open ocean. *Environ. Microbiol.* 11, 338–348.

Wu, J., Sunda, W., Boyle, E. A., and Karl, D. M. (2000). Phosphate depletion in the western North Atlantic Ocean. *Science* 289, 759–762.

Zehr, J. P., Montoya, J. P., Jenkins, B. D., Hewson, I., Mondragon, E., Short, C. M., Church, M. J., Hansen, A., and Karl, D. M. (2007). Experiments linking nitrogenase gene expression to nitrogen fixation in the North Pacific subtropical gyre. *Limnol. Oceanogr.* 52, 169–183.

Zehr, J. P., Waterbury, J., Turner, P. J., Montoya, J. P., Omoregie, E., Steward, G. F., Hansen, A., and Karl, D. M. (2001). Unicellular cyanobacteria fix N_2 in the subtropical North Pacific Ocean. *Nature* 412, 635–638.

Conflict of Interest Statement: The authors declare that the research was conducted in the absence of any commercial or financial relationships that could be construed as a potential conflict of interest.

Received: 09 August 2011; paper pending published: 27 August 2011; accepted: 06 October 2011; published online: 25 October 2011.

Citation: Dyhrman ST and Haley ST (2011) Arsenate resistance in the unicellular marine diazotroph Crocosphaera watsonii. Front. Microbio. ***2****:214. doi: 10.3389/fmicb.2011.00214*

This article was submitted to Frontiers in Aquatic Microbiology, a specialty of Frontiers in Microbiology.

frontiers in
MICROBIOLOGY

ORIGINAL RESEARCH ARTICLE
published: 26 April 2012
doi: 10.3389/fmicb.2012.00140

Benthic cyanobacterial mats in the high Arctic: multi-layer structure and fluorescence responses to osmotic stress

Marie Lionard [1,2,3]*, ***Bérangère Péquin*** [1,2,4,5], ***Connie Lovejoy*** [1,2,4,5] ***and Warwick F. Vincent*** [1,2,3]

[1] *Département de Biologie, Université Laval, Québec, QC, Canada*
[2] *Takuvik Joint International Laboratory, Université Laval – CNRS, QC, Canada*
[3] *Centre d'Études Nordiques, Université Laval, Québec, QC, Canada*
[4] *Québec-Océan, Québec, QC, Canada*
[5] *Institut de Biologie Intégrative et des Systèmes, Québec, QC, Canada*

Edited by:
George S. Bullerjahn, Bowling Green State University, USA

Reviewed by:
Michael R. Twiss, Clarkson University, USA
Rachael Marie Morgan-Kiss, Miami University, USA

***Correspondence:**
Marie Lionard, Département de Biologie, Université Laval, Québec, QC, Canada G1V 0A6.
e-mail: marie.lionard@bio.ulaval.ca

Cyanobacterial mats are often a major biological component of extreme aquatic ecosystems, and in polar lakes and streams they may account for the dominant fraction of total ecosystem biomass and productivity. In this study we examined the vertical structure and physiology of Arctic microbial mats relative to the question of how these communities may respond to ongoing environmental change. The mats were sampled from Ward Hunt Lake (83˚5.297′N, 74˚9.985′W) at the northern coast of Arctic Canada, and were composed of three visibly distinct layers. Microsensor profiling showed that there were strong gradients in oxygen within each layer, with an overall decrease from 100% saturation at the mat surface to 0%, at the bottom, accompanied by an increase of 0.6 pH units down the profile. Gene clone libraries (16S rRNA) revealed the presence of Oscillatorian sequences throughout the mat, while *Nostoc* related species dominated the two upper layers, and Nostocales and Synechococcales sequences were common in the bottom layer. High performance liquid chromatography analyses showed a parallel gradient in pigments, from high concentrations of UV-screening scytonemin in the upper layer to increasing zeaxanthin and myxoxanthin in the bottom layer, and an overall shift from photoprotective to photosynthetic carotenoids down the profile. Climate change is likely to be accompanied by lake level fluctuations and evaporative concentration of salts, and thus increased osmotic stress of the littoral mat communities. To assess the cellular capacity to tolerate increasing osmolarity on physiology and cell membrane integrity, mat sections were exposed to a gradient of increasing salinities, and PAM measurements of *in vivo* chlorophyll fluorescence were made to assess changes in maximum quantum yield. The results showed that the mats were tolerant of up to a 46-fold increase in salinity. These features imply that cyanobacterial mats are resilient to ongoing climate change, and that in the absence of major biological perturbations, these vertically structured communities will continue to be a prominent feature of polar aquatic ecosystems.

Keywords: microbial mats, cyanobacteria, polar lake, pigments, molecular phylogeny

INTRODUCTION

Cyanobacterial mats are well known for their ecological success in extreme environments (Stal and Krumbein, 1985). Some of the most striking examples occur in the polar regions where cyanobacterial mats often dominate the biomass and productivity of freshwater ecosystems (Vincent, 2000). This ubiquitous and abundant distribution has been attributed to the ability of Arctic and Antarctic cyanobacterial communities to withstand extreme conditions of the polar environment including continuous solar radiation (UV and photosynthetically active radiation, PAR) during summer, persistent cold temperatures, and freeze–thaw cycles (Zakhia et al., 2008). These ambient conditions of the Arctic are currently being modified by the impacts of global climate change. Observations and models show faster climatic changes in the Arctic than at other latitudes, with a rate of atmospheric warming over the last four decades that has been up to three times greater than the global average (Serreze and Francis, 2006), and this trend is likely to continue in the future (IPCC, 2007).

Two major impacts of warming on Arctic lakes are reduced thickness and duration ice cover, and a shift toward an increasingly negative precipitation minus evaporation balance. The latter is favored by increased evaporation at warmer lake water temperatures, as well as the increasing exposure of the lakes to the atmosphere during a longer ice-free season. For some High Arctic lakes this has led to increased salinities, and in some cases, complete evaporation to dryness (Smol and Douglas, 2007). Cyanobacterial mats living in these shallow water ecosystems will be increasingly subject to the osmotic stresses of solute concentration and desiccation. These effects may be further compounded by salt-exclusion during freeze-up of shallow water lakes (Schmidt et al., 1991) and the littoral zone of deeper lakes. Cyanobacteria have long

been known to be tolerant of salinity fluctuations, but to a variable extent among taxa (Mackay et al., 1984), and osmotic effects have not been assessed in the Arctic where the physiological stress may be exacerbated by cold ambient temperatures. Both evaporation and salt-exclusion contribute to high salinity and the polar microbial mats are exposed to higher salinities in liquid water compared to microbial mats at lower latitudes. Reduced ice cover (and its associated snow; Belzile et al., 2001) also results in greater exposure to solar UV radiation, which is increasing over the Arctic as a result of stratospheric ozone depletion (Manney et al., 2011).

The phylogenetic composition of temperate latitude microbial mats has been extensively studied (e.g., Balskus et al., 2011; Bolhuis and Stal, 2011) and these communities contain diverse cyanobacteria, other Bacteria, and some eukaryotes. However, despite their ubiquitous distribution throughout the Arctic, in lakes, ponds and streams, the community composition, and structure of microbial mats in northern Polar Regions is much less studied. Initial surveys of bacteria (Bottos et al., 2008), cyanobacteria (Jungblut et al., 2010), and one metagenomic study of mats on Arctic ice shelves, has confirmed the diversity of cyanobacteria along with other Bacteria, notably Proteobacteria, and Archaea (Varin et al., 2010). The ice shelf mats also provide a protected habitat for eukaryotes including diatoms, chlorophytes, flagellates, ciliates, and microinvertebrates (Vincent, 2000).

Most studies to date on high latitude microbial mats have focused on their bulk taxonomic, pigment, and physiological characteristics; however there is also evidence of strong vertical gradients in these properties within such communities (e.g., Quesada et al., 1999; Hawes and Schwarz, 2001). Such gradients are also well known from temperate latitude mats. For example, a study conducted on microbial mats of the intertidal zone showed major vertical changes down the mat profile in coloration, pigment content, and phylogenetic composition (Balskus et al., 2011).

Our aims in the present study were to characterize cyanobacterial mats growing at the northern limit of the terrestrial High Arctic, and to evaluate the hypothesis that these communities have a high tolerance to the osmotic stresses that may be increasingly common in the future. We determined the oxygen and pH gradients in mat samples by way of microsensor profiling in two successive years of sampling. We partitioned the mats into their component layers distinguishable by color, and examined the molecular phylogeny (by 16S rRNA gene analysis) and pigment composition (by high performance liquid chromatography, HPLC) of each stratum to evaluate the vertical structure of these communities that thrive in the extreme High Arctic environment.

MATERIALS AND METHODS

STUDY SITE

Sampling took place in July 2010 and 2011 at Ward Hunt Lake (WHL; 83°05.297′N, 74°09.985′W), as part of the program "Northern Ellesmere Island in the Global Environment" (NEIGE). This lake is on Ward Hunt Island off the northern coast of Ellesmere Island in the Canadian High Arctic and within Quttinirpaaq National Park. The total area is of the lake is 0.37 km^2, with a maximum recorded depth of 7.5 m. At this extreme latitude, ice covers the lake for at least 9 months of the year and there are 147 days of continuous light during summer (Mueller et al., 2005). Microbial mats occur in the seasonally ice-free littoral zone along the northern and western sides of the lake. Although, phytoplankton in this oligotrophic lake are strongly nutrient limited, high concentrations of nutrients have been recorded in the interstitial waters of the mats (Villeneuve et al., 2001), and in 2-week bioassays the mat phototrophs showed no response to nutrient enrichment (Bonilla et al., 2005).

FIELD SAMPLING

Temperature, oxygen, and conductivity of lake water in the littoral zone were measured on July 10, 2011 using a Hydrolab DS5X profiler (Loveland, CO, USA).

The mats were sampled from 10 to 20 cm water depth in July 2010 and 2011. The samples were placed in a cooler with lake water and taken directly to a field laboratory. Microenvironmental gradients within the mats were assessed within 20–40 min of collection using micromanipulator-controlled, 10 μm diameter Unisense microsensors for oxygen and pH (Unisense, Aarhus, Denmark), with accurate positioning to within 10 μm. The microsensor measurements were made at 100 μm intervals to obtain vertical profiles through the mats.

The cyanobacterial mats samples were separated at the field laboratory into three layers: surface black colonies, an upper pink layer, and a lower green layer (**Figure 1**). Subsamples for HPLC analysis of the three layers were placed into a dry-shipper (previously cooled with liquid nitrogen) in the field and transferred to −80°C storage until pigment analysis. Samples for DNA extraction were stored in 1.5 mL of buffer (1.8 mL of 40 mmol L^{-1} EDTA; 50 mmol L^{-1} Tris pH = 8.3; 0.75 mol L^{-1} sucrose) and kept frozen in the dry-shipper in the field and transferred to −80°C storage until analysis.

FIGURE 1 | Photograph of the Ward Hunt Lake microbial mats. The mats were photographed 30 min after sampling, on July 7, 2010. The mat on the left shows the view from the top, with black colonies distributed over the pink surface. The mat on the right has been turned upside down to show the green layer, which extended down into interstices of the underlying rocky substrate. The black colonies were up to 5 mm in diameter.

PIGMENT ANALYSIS

Within 1 month of collection, samples from the three layers of the microbial mat destined for pigment analysis were freeze-dried using a Labconco Freezone 12 (Labconco, Kansas City, USA). Mat subsamples were then weighed and extracted in the dark by grinding for 2 min followed by two sonication treatments for 30 s each at 17 W in 4 mL 90% acetone:water (vol/vol). The samples were then left overnight at −20°C under an argon gas atmosphere, and the supernatant recovered after vortexing and centrifugation (4150 rpm for 15 min at 4°C). This was filtered through a 0.2-μm pore size PTFE Acrodisc filter (PALL Corporation, Ann Arbor, MI, USA) and placed in a 2-mL amber vial with an argon gas atmosphere for immediate analysis by HPLC. Each layer of the mat was extracted three more times to ensure the full recovery of all material. Four vials were thus analyzed for each mat sample, and the results summed.

High performance liquid chromatography analysis was performed using a ProStar HPLC system (Varian, Palo Alto, CA, USA) with a Symmetry C8 column (3.5 μm pore size, 4.6 mm × 150 mm; Waters Corporation, Milford, MA, USA) at 25°C, with a C8 guard column (5 μm pore size, 3.9 mm × 20 mm; Waters Corporation). Carotenoids were quantified by their absorbance at 450 nm in a Diode Array Detector (350–750 nm) and chlorophylls were detected by fluorescence (excitation at 400 nm and emission at 650 nm). The HPLC separation method was as in Zapata et al. (2000). Pigments were identified based on retention time and spectral comparisons with standards from DHI (Water & Environments, Horsholm, Denmark).

MOLECULAR ANALYSIS

Mat samples for DNA analysis were extracted using a modified salt-based protocol as in Harding et al. (2011). Cyanobacteria-specific primers 27F1 and 809R (Jungblut et al., 2005, 2010) were used to amplify 16S rRNA gene fragments using the polymerase chain reactions (PCR) with Phusion® High-Fidelity Polymerase, buffer, and dNTPs (New England BioLabs, Pickering, ON, Canada) on the iCyclerTM Thermal Cycler (Bio-Rad Laboratories, Inc., Hercules, CA, USA). Denaturation was for 30 s at 98°C, followed by 29 cycles of 10 s at 98°C, 30 s at 55°C, 30 s at 72°C, and a final extension time of 5 min at 72°C.

Amplified PCR products were verified by gel electrophoresis then purified with a QIAquick PCR Purification kit (Qiagen, Mississauga, ON, Canada). Amplicons were cloned using a StrataClone PCR Cloning Kit (Stratagene, Agilent Technologies, Santa Clara, CA, USA). Positive clones were transferred to 96-well plates containing Luria Bertani medium with 7% glycerol. The target cloned fragments were amplified using the vector-specific primers M13F and M13R. PCR products were verified by gel electrophoresis and the results visualized using the Bio-Rad Gel Doc imaging system and Quantity One Software (Bio-Rad Laboratories, Hercules, CA, USA). For each library 30–50 clones were sequenced using the vector-specific T7 universal primer (single read) at the Centre Hospitalier de l'Université Laval (CHUL, QC, Canada) using an ABI 3730xl system (Applied Biosystems, Foster City, CA, USA), after purification.

A total of 108 high quality sequences were retained and manually checked using the BioEdit program (Hall, 1999 – version 7.0.5.3). Suspect sequences were checked manually to detect chimeras by separate nBLAST searches of short fragments. The closest matches for each ribotype based on nBLAST searches (Altschul et al., 1990) of the nr/nt GenBank database were selected as reference sequences, additional sequences of cultured species were also added in an attempt to increase the phylogenetic resolution. If the closest match was to an uncultured clone, the closest isolated strain sequence was retrieved and included in our phylogenetic analysis. Following our microscopy identification (see below) of the morphological genus *Dichothrix* we directly sequenced several filaments from one colony, which were picked under a stereo microscope. Four samples were amplified directly using cyanobacterial specific primers 27F1 and 809R and sequenced in both directions using the same primers. The eight separate sequencing reactions yielded the same sequence (CBS4-C1). The phylogenetic tree was constructed following, initial alignment with multiple alignment using fast Fourier transform (MAFFT, Katoh and Toh, 2008) on the EMBL-EBI portal (http://www.ebi.ac.uk/Tools/msa/mafft/), all sequences were then trimmed to 754 nt and realigned using first MAFFT and then ClustalW2, both provided similar arrangements and Nexus guide trees with the 16S rRNA gene sequence of *E. coli* DP170 as the outgroup. The final tree was constructed and bootstrapped (1000 replicates) using the Maximum Likelihood in RAxML program (Version 7.3.0; Stamatakis, 2006; Stamatakis et al., 2008). The evolutionary model used was GTR +i+ gamma (Tavaré, 1986). The sequences are deposited in GenBank (accession numbers JQ249752–JQ249830).

MICROSCOPY ANALYSIS

The microbial mat samples were preserved with a 10% (final concentration) glutaraldehyde–paraformaldehyde solution (Lovejoy et al., 1993) and maintained in the dark at 4°C until analysis. Samples were dispersed prior to enumeration and diluted in purified water (milliQ water, Millipore, Billerica, USA) to be sedimented in 15 mL cylindrical counting chambers (Villeneuve et al., 2001); and observed by Fluorescence, Nomarski, Utermöhl (FNU) microscopy (Lovejoy et al., 1993). Samples were examined using an Olympus IX71 inverted microscope (Olympus Canada, Richmond Hill, ON, Canada) at 200× and 400× magnification under UV, green, or blue excitation as well as under bright field (Köhler) illumination.

Another microbial mat sample for taxonomic analysis was kept frozen at −20°C without fixatives. This sample was thawed and dispersed in water prior to examination with an Olympus IX71 inverted microscope at 200× magnification under visible light.

SALINITY TOLERANCE EXPERIMENT

Twelve 150 mL beakers were filled with 100 mL of water sampled from WHL on July 7, 2010, and these lake water samples were then adjusted to the following conductivities with a NaCl solution: 0.25 (original lake water, no salt addition) 0.5, 1, 2.5, 5, 10, 30, 100, 150, 200, 250, and 300 mS cm^{-1}. NaCl solution was used as sodium and chloride are the most abundant dissolved ions in seawater, and the marine aerosols that reach this coastal lake. The experiment was repeated the next year (July 7, 2011) with the same range of salinities, plus an additional treatment of 50 mS cm^{-1}. A 1.3-cm^2

sample of freshly collected microbial mat was placed in each beaker, and the active fluorescence parameters F_0 (minimum fluorescence) and F_m (maximum fluorescence) were then measured over the subsequent 24 h using a PAM 2000 (Walz, Germany). Photochemical quantum yield $[F_v/F_m = (F_m - F_0)/F_m]$ was calculated according to Butler (1978) to assess the physiological state of the photosynthetic communities within the microbial mats. The measurements were made placing the fluorescence detector at a distance of 6 mm from black communities of the surface. In the 2010 experiment, the mats were also inverted to measure the response of the bottom community.

RESULTS

MICROSENSOR PROFILES

On July 10, 2010, the lake water at the mat sampling site had a measured conductivity of 250 µS cm^{-1}, the pH was 7.45, the water temperature was 5.2°C, and the oxygen concentration was at 107% of saturation. The microbial mat was composed of three distinct layers: the black layer from the surface to 2.2 mm depth in 2010 and to 1.5 mm in 2011; the pink layer to 4 mm depth; and the green layer to the bottom at 5.5 mm in 2010 and 4.8 mm depth in 2011 (**Figure 2**). Within the mat, the *in situ* percentage of oxygen saturation decreased from 100% at the surface to 56% within the upper black layer, further decreasing to 19% through the middle pink layer and to 0% at the bottom of the green layer. There was a steep gradient within each layer, as indicated by the high coefficients of variation (**Table 1**). The pH slightly increased down the mat profile from 7.45 to 7.52 in the upper black layer, to 7.80 through the pink layer, and to 7.93 in the bottom green layer, with peaks in pH at the midpoint of each layer (**Figure 2A**; **Table 1**). The oxygen and pH profiles were similar in 2011, but oxygen did not fall completely to zero at the bottom of the profile (**Figure 2B**).

PIGMENT ANALYSES

The major pigments as shown by HPLC analysis were scytonemin and its decomposition product reduced-scytonemin, 4-ketomyxol-2′-methylpentoside (keto-mmp), fucoxanthin, myxoxanthin, alloxanthin, zeaxanthin, lutein, canthaxanthin, echinenone, Chlorophyll *a* (Chl *a*), and β-carotene (**Table 2**). Chl *a* concentrations were similar in the pink and black layers, and increased eightfold in the lower layer, from 55 (pink) to 430 µg Chl *a* g^{-1} dry weight (green). The black and pink layers had similar ratios of pigments per unit Chl *a*, with high ratios of scytonemin, red-scytonemin, keto-mmp, canthaxanthin, echinenone, and β-carotene. Canthaxanthin, echinenone, and β-carotene were still present in the green layer, along with myxoxanthin and zeaxanthin and trace amounts of reduced-scytonemin, scytonemin, and keto-mmp. The eukaryotic pigments fucoxanthin, alloxanthin, and lutein were also recovered from this bottom layer. The concentrations of photoprotective carotenoids (echinenone, zeaxanthin, lutein, and canthaxanthin) and photosynthetic carotenoids (fucoxanthin and alloxanthin) varied among layers. Myxoxanthin and β-carotene have more than one role in the cell and were therefore excluded from this analysis. Photoprotective carotenoids per unit Chl *a* were twofold higher in the black and pink layers relative to the bottom green layer, while the two photosynthetic carotenoids were only detected in the green layer (**Table 2**).

MOLECULAR ANALYSIS

A clone library was generated for each layer. We obtained 26, 41, and 41 high quality sequences for the black, pink, and green layer respectively for a final number of 108 sequences The cyanobacteria sequences from the three layers were diverse and while several of the sequences had good matches to cultured species for example *Snowella* spp. and *Synechococcus* sp. PC7502, the majority had best matches to other environmental clones, notably those

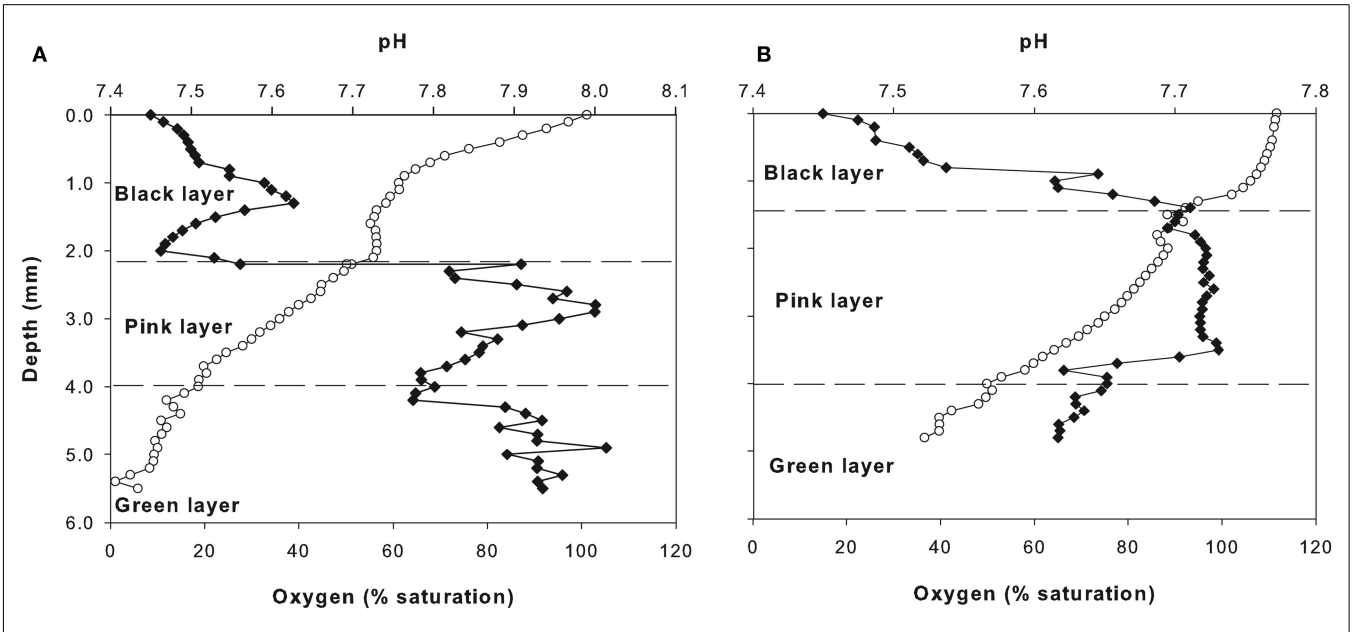

FIGURE 2 | Unisense microsensor oxygen (white circles) and pH (black diamonds) profiles down through the microbial mat in 2010 (A) and 2011 (B).

Table 1 | pH and oxygen, SD; coefficient of variation (CV) within the three layers of cyanobacterial mats from Ward Hunt Lake, July 7, 2010.

Layer	pH		Oxygen (% saturation)	
	Mean ± SD	CV (%)	Mean ± SD	CV (%)
Black	7.7 ± 0.1	1.7	66.2 ± 14.9	22.5
Pink	7.8 ± 0.1	0.7	47.4 ± 8.2	17.2
Green	7.9 ± 0.0	0.6	14.1 ± 7.6	53.7

Black, Pink, and Green designate the upper, middle, and bottom layers of the mat.

Table 2 | Pigment characteristics of the microbial mat layers as defined in Table 1.

	Black layer	Pink layer	Green layer
CONCENTRATION (μg g^{-1} DRY WEIGHT)			
Chlorophyll *a*	62.5	54.7	429.8
PIGMENT RATIOS			
Red-scytonemin	0.14	0.06	<0.01
Scytonemin	0.17	0.06	<0.01
Keto-mmp	0.28	0.41	<0.01
Fucoxanthin	n.d.	n.d.	0.06
Myxoxanthin	n.d.	n.d.	0.03
Alloxanthin	n.d.	n.d.	0.01
Zeaxanthin	n.d.	n.d.	0.06
Lutein	n.d.	n.d.	0.01
Canthaxanthin	0.13	0.17	0.02
Echinenone	0.14	0.12	0.04
β-carotene	0.16	0.14	0.18
Photoprotective carotenoids	0.27	0.29	0.14
Photosynthetic carotenoids	n.d.	n.d.	0.39
Total carotenoids	0.72	0.84	0.42

The pigment ratios are per unit by weight. The photoprotective carotenoids values are for summation of echinenone, zeaxanthin, lutein, and canthaxanthin. The photosynthetic carotenoids are for fucoxanthin and alloxanthin. The abbreviations used are: keto-mmp, 4-ketomyxol-2′-methylpentoside; n.d., not detectable.

recovered previously form WHL sequences (**Figure 3**) reported in Jungblut et al. (2010). Three environmental clusters accounted for the majority of the clones and these were named after the original WHL sequences (WHL-82, WHL-87, and WHL-69). Nearest cultured matches to other sequences included *Nostoc*, *Leptolyngbya*, *Phormidium*, *Oscillatoria*, *Chamaesiphon*, and *Gloeobacter* (**Figure 3**). Oscillatorian sequences were found in all three layers, but in different proportions. The black layer sequences were mostly *Nostoc*, which accounted for 65% of the sequences. *Synechococcus* and *Leptolyngbya* were the second and third most frequent followed by *Pseudanabaena* and *Gloeobacter*. The pink layer was similar to the black layer with *Nostoc* accounting for 50% of sequences, but the second most common sequences were closest to *Pseudanabaena* with 22%, followed by *Gloeobacter*, *Synechococcus*, *Phormidium*, and *Leptolyngbya* and *Chamaesiphon*. The green layer was quite different with lower representation by *Nostoc* (29% of sequences). *Snowella* sequences accounted for 22% and *Synechococcus* for 27% of the sequences, and taxa with sequences closest to *Pseudanabaena*, *Leptolyngbya*, *Phormidium*, *Oscillatoria*, and *Gloeobacter* were also present in this layer (**Figure 4**). The sequence of *Dichothrix* morphospecies aligned most closely to *Leptolyngbya* in the Oscillatoriales.

MICROSCOPIC ANALYSIS

Diverse morphospecies were observed within the microbial mat. In the black and pink layers, heterocystous *Dichothrix* sp. was well represented, with its usual associated fine filaments. *Nostoc* sp., mostly in small colonies, were also noted. The pink layer contained various Oscillatoriales of diverse filament diameters, within the morpho-genera *Lyngbya*, *Oscillatoria*, *Phormidium*, *Pseudanabaena*, and *Leptolyngbya*. In the lower green layer, the order Synechococcales was represented, specifically, the colonial genera *Snowella* and *Aphanocapsa*. Other than cyanobacteria, pennate diatoms occurred throughout the microbial mat and included the genera *Achnanthes*, *Caloneis*, *Cymbella*, *Denticula*, *Eunotia*, *Navicula*, and *Nitzschia*. Nematodes were observed in the green layer.

SALINITY RESPONSES

The initial F_v/F_m of the microbial mat in 2010 ranged from 0.35 to 0.39. For the upper black layer, the F_v/F_m values immediately after the salt amendments defined as T_0 remained above 0.25 up to 150 mS cm^{-1}, and fell to less than 0.1 at conductivities of 200 mS cm^{-1} and above. After 8 and 24 h of incubation, high F_v/F_m values (>0.2) were maintained up to 30 mS cm^{-1} (**Figure 5A**). A similar set of responses was recorded for the green layer, with high F_v/F_m values (>0.2) up to 100 mS cm^{-1} at T_0 and to 30 mS cm^{-1} at 8 and 24 h (**Figure 5B**). This experiment was repeated in 2011 for the upper black layer, and the results were similar to those in 2010. F_v/F_m values above 0.2 were recorded at conductivities up to 50 mS cm^{-1} over 4 h. After 2 days of incubation, F_v/F_m values >0.29 were maintained up to 30 mS cm^{-1} and there was a decline to <0.1 at 50 mS cm^{-1} (**Figure 5C**).

To test the capacity of the photosynthetic communities to recover from the salinity increase, all mat sections at the end of the first experiment were placed back into lake water with its natural conductivity of 0.25 mS cm^{-1}. The mats that had been previously exposed to conductivities of less than 50 mS cm^{-1} showed ongoing F_v/F_m ratios above 0.2 and values above 0.3 were recorded for prior exposures of up to 10 mS cm^{-1}. There was some evidence of partial recovery in the two most extreme salinities (150 and 200 mS cm^{-1}), where F_v/F_m values rose from zero to around 0.2 after 4 h (**Figure 6**).

DISCUSSION

COMMUNITY COMPOSITION

Cyanobacteria dominated the microbial mats from WHL, as in many lakes of the polar regions (e.g., Vincent, 2000; Zakhia et al., 2008). Previous studies on this lake have reported taxa from the Nostocales, Oscillatoriales, and Synechococcales (Villeneuve et al., 2001; Bonilla et al., 2005; Jungblut et al., 2010), consistent with our analyses. *Nostoc* was found throughout the mat, producing black globular colonies at the surface. The sequence from filaments of the "*Dichothrix*" sample was found to be within the Oscillatoriales, rather than the Nostocales as expected. Reliably classified

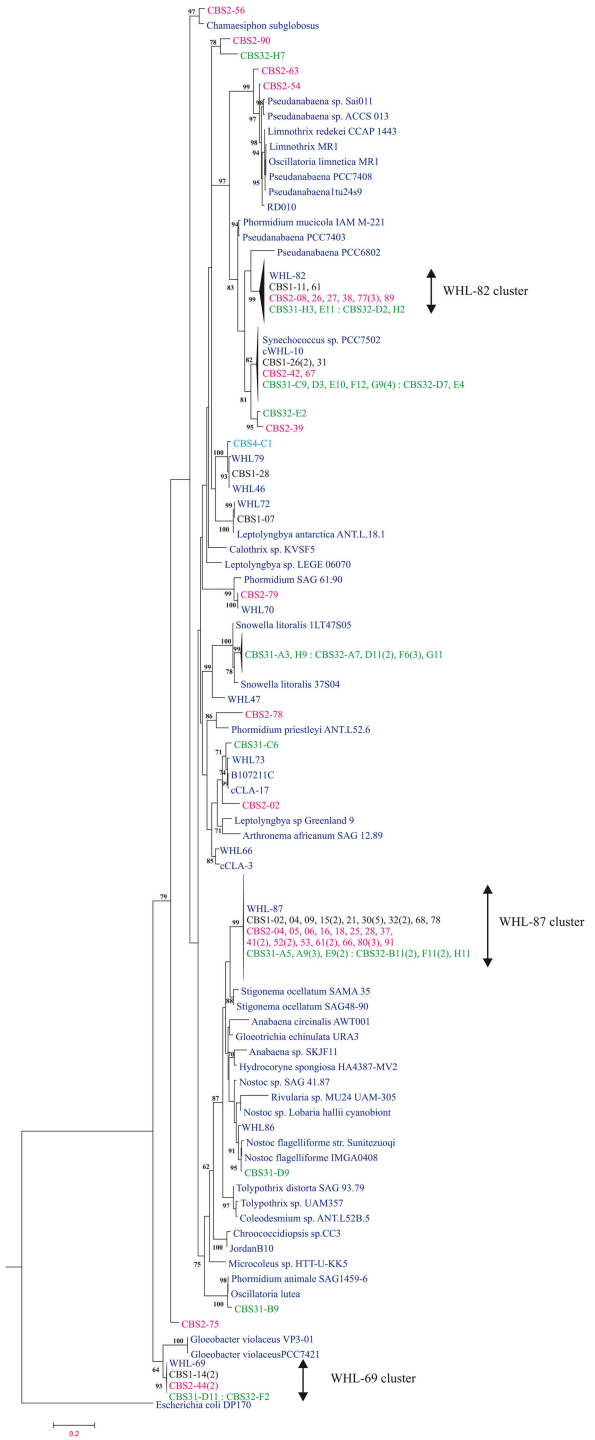

FIGURE 3 | Phylogenetic tree from clone library and reference sequences. Sequences from the black (CBS1), pink (CBS2), and green (CBS31 and CBS32) layers are in black, pink, and green respectively. The different sequence designations from the libraries follow the dash, and the numbers of identical sequences are given in parenthesis. The *Dichothrix* filaments CBS4-C1 direct PCR sequence is light blue. Reference sequences are dark blue. WHL sequences are from Jungblut et al. (2010) and cCLA sequences from Harding et al. (2011). Bootstraps values ≥60% based on maximum likelihood are indicated at the nodes.

Dichothrix species are not as yet represented in GenBank and further investigation is required to determine if this *Dichothrix*, which had heterocysts and therefore is morphologically a heterocystous Nostocales, has affinities to the non-heterocystis Oscillatoriales. Alternatively, the thin trichomes that appear on the tips of *Dichothrix* colonies may be a separate oscillatorian taxon, which we amplified from our single trichome. Deeper within the mat matrix there were no macroscopic colonies, suggesting a shift toward the uniseriate, filamentous form of *Nostoc* that is often found in association with *Oscillatoria* (Potts, 2000). The ability of *Nostoc* to fix nitrogen, resist desiccation (Mataloni et al., 2000), and form UV-screening pigments (see below) would make it well suited to life at the mat surface in the shallow littoral waters of the lake. While not observed in the present study, *Nostoc* also produces motile hormogones (Broady, 1979), enabling vertical migration to optimize UV-protection deeper within the mat, light-harvesting toward the mat surface, and access to nutrient resources in the mat interior.

In the green layer of the mat, there was an increased presence of taxa that had their closest 16S rRNA gene sequence matches to *Snowella* and *Synechococcus*. These mostly planktonic taxa have previously been reported as metaphyton (Komárek and Komárková-Legnerova, 1992). *Synechococcus* mats are known from hot spring environments (Stal, 2000), but have been less reported from the polar regions.

Gloeobacter-like sequences (WHL-69 cluster, **Figure 3**) were found throughout the mat, and have been reported previously from WHL and a pond mat from Ellesmere Island (Jungblut et al., 2010). The sequences in the present study also closely match a set of Gloeobacterales sequences from an epilithic biofilm of a Spanish high mountain lake (GenBank accession number FR667281 and associated sequences). The Gloeobacterales lineage is divergent from other cyanobacteria in a variety of striking ways, including the absence of thylakoids and unique genes for carotenoid biosynthesis (Tsuchiya et al., 2005). However the GenBank reference *Gloeobacter* in culture (strain PCC 7421) is only 93% similar to our sequences, the Jungblut et al. (2010) sequences, and those from the Spanish alpine lakes, implying that this phylogenetically unusual component of the cold biosphere may prove to be a new genus.

Oscillatorian cyanobacteria were found through the mat profile and are well known from Arctic and Antarctic mats. These organisms in culture have an ability to acclimate via pigment shifts to large variations in ambient irradiance including UV radiation (Quesada and Vincent, 1997). Most are cold-tolerant rather than psychrophiles (Tang et al., 1997). The oscillatorians recorded here had close matches to those previously reported in this region of the High Arctic (Jungblut et al., 2010; Harding et al., 2011) and included those that remain distance from cultured groups (WHL-82 clade and WHL-87 clade). Overall our phylogenies highlighted the poor concordance between morphospecies and 16S rRNA gene sequences as previously noted by Jungblut et al. (2010) and others. The limited morphological repertoire of cyanobacteria likely contributes to this poor phylogeny and suggests that this group requires major careful taxonomic revision. The 16S rRNA gene may also lack resolution at higher taxonomic ranks and additional genes need to be included in such revisions. However, despite these shortcomings, at the level of 99–100% similarity many of the

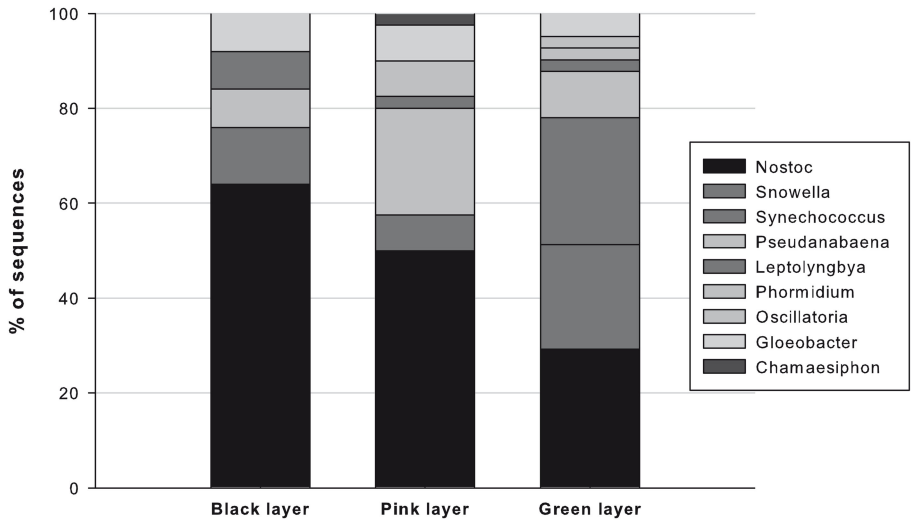

FIGURE 4 | The percentage of each taxonomic group in the black, pink, and green layers of the Ward Hunt Lake microbial mat. The nearest matches are given to the following reference taxa: *Gloeobacter*, accession number FR798924.1, 93% similarity; *Leptolyngbya*, AY493607.1, 88–99%; *Synechococcus*, AF448080.1, 95–99%; *Pseudanabaena*, AB039019.1, 86–94%; *Snowella*, AJ781041.1, 97%; *Nostoc*, EU178143.1, 90–95%.

sequences were previously recovered from the same lake and all of their nearest environmental matches were to other cold regions as earlier reported by Jungblut et al. (2010).

PIGMENT COMPOSITION

The HPLC analyses showed clear differences in pigment concentration and composition through the mat profile, and this vertical structure may reflect both species differences as well as physiological differences among the layers (Quesada et al., 1999). Reduced-scytonemin and scytonemin were major pigments of the black layer of the microbial mat, and are well known in the Nostocales. The decrease in scytonemin and reduced-scytonemin with an increase in keto-mmp was consistent with *Pseudanabaena* and other oscillatorians in the pink layer. The photoprotective carotenoids were in highest concentration, both in absolute terms and per unit Chl *a* in the upper two layers where irradiance and oxygen levels were highest, consistent with their role as quenching agents of reactive oxygen species.

The pigment signature of the green layer was in accordance with the appearance of myxoxanthin and zeaxanthin, which are typical for Synechococcales, and the presence of three pigments that are characteristic of eukaryotic taxa: fucoxanthin (found in diatoms and other chrysophytes), alloxanthin (found in cryptophytes), and lutein (characteristic of green algae). Our observations as well as previous taxonomic analyses of these mats have observed pennate diatoms, notably *Cymbella* spp. and *Achnanthes* spp., as well as chlorophytes, notably *Mougeotia* sp. and *Zygnema* sp. (Villeneuve et al., 2001). Canthaxanthin, echinenone, and β-carotene are found in all cyanobacteria, and were detected in all three layers, as expected.

Scytonemin and its reduced derivative (Garcia-Pichel and Castenholz, 1991) contributed the dominant fraction of the total pigment content of the mat, collectively accounting for 2% of the dry weight of the surface community, 0.6% of the pink layer, and 0.2% of the bottom layer. In cultured organisms, scytonemin has been recorded up to 5% of dry weight, and can similarly accumulate to high levels in natural assemblages (Karsten et al., 1998). This pigment has a broad absorbance maximum that peaks in the UV-A waveband but that also extends into the UV-B and PAR wavebands (Proteau et al., 1993). It can absorb up to 90% of incident radiation (Castenholz and Garcia-Pichel, 2000), and thereby acts as an effective sunscreen for the entire community. The Ward Hunt communities therefore seem well protected from any future increases in UV exposure as a result of stratospheric ozone depletion or increased duration of ice-free conditions.

OXYGEN AND pH PROFILES

The oxygen content of the mats dropped from 100% saturation, to 0% at the bottom of the green layer in 2010, and to below 40% in 2011. This implies that the mat consortia have a strong respiratory demand for oxygen as a result of the bottom layer phototrophs growing under shaded conditions, as well as the high concentration of bacterial heterotrophs typically found in polar microbial mats (e.g., Varin et al., 2010). It may also reflect the strong oxygen sink conditions immediately beneath the mats, where heterotrophic bacteria would dominate. The low photosynthesis/respiration (P/R) balance is likely to extend upward through the mat later in the season when the lake becomes covered by ice and snow and the day length shortens, eventually to continuous winter darkness. In shallow Antarctic ponds, the bottom waters become anoxic during winter-freeze-up, and the mats experience continuous reducing conditions through much of the year (Schmidt et al., 1991). Similar conditions are likely to prevail in WHL during late Arctic autumn and winter.

The pH profiles of the Ward Hunt mats showed an increase with depth, contrary to the decreasing P/R ratios down the profile as inferred from the oxygen data. However the shifts were relatively small, in accordance with the high dissolved inorganic

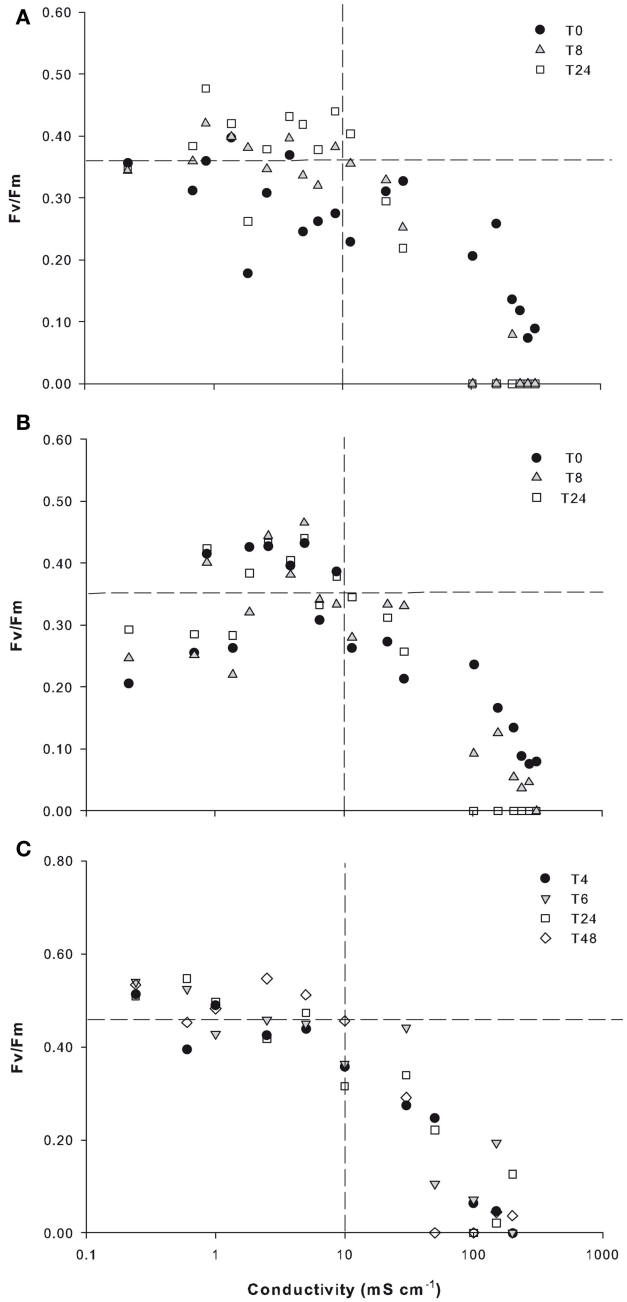

FIGURE 5 | Photophysiological responses by Ward Hunt Lake mats to osmotic stress. The mats were incubated at a range of increasing salinities, and the quantum yield ratio (F_v/F_m) was measured immediately (T_0), and after 8 and 24 h in 2010 and immediately (T_0) and after 4, 6, 24, and 48 h in 2011. The 2010 data are for the surface black layer **(A)** and the bottom green layer **(B)**, and the 2011 data are for the surface black layer only **(C)**. The horizontal dashed lines are for the mean F_v/F_m values calculated for all time intervals at salinity up to 10 mS cm^{-1} (vertical dashed lines).

carbon concentrations, and thus buffering capacity, that have been observed in the interstitial waters of these mats. Up to 141 mg C L^{-1} were measured in the mats, while the concentrations in the overlying water were around 16 mg C L^{-1} (Villeneuve et al., 2001). The pH peaks in each layer might reflect a depth optimum for oxygenic photosynthesis in each community, with the equivalent peak in oxygen obliterated by its rapid diffusive flux downward as a result of the strong vertical gradient in concentration. Although rare, 16S rRNA gene sequences of green sulfur bacteria have been recorded from these microbial mats (Lionard and Lovejoy, unpublished data). However, no marker pigments (bacteriochlorophylls) for photosynthetic sulfur bacteria were detected in the HPLC analyses, implying that any anoxygenic photosynthesis was likely minimal. The pH values throughout the mat were within the neutral to alkaline range in which cyanobacteria are commonly found (Castenholz, 2009).

SALINITY TOLERANCE

The Ward Hunt mats tolerated increased salinity up to a conductivity of 10 mS cm^{-1}, 46 times ambient salinities of the lake water, with little change in photophysiological state as measured by the active fluorescence parameter F_v/F_m. For the mats previously exposed to high salinities and then placed in freshwater, this quantum yield ratio returned within hours to the range 0.35–0.39, indicative of excellent physiological conditions for *Nostoc* (Bowker et al., 2002). The mucilaginous, exopolysaccharide sheath enveloping *Nostoc* colonies, is known to provide a buffer from external variations in salinity (Webb et al., 2003; Hall-Stoodley et al., 2004). However, salinity tolerance varies widely among cyanobacteria, which range from species of relatively narrow tolerance (Stal and Krumbein, 1985) to euryhaline species (Nübel et al., 1999). The broad tolerances measured here for both the surface and bottom communities imply that cyanobacteria species in the mats continue to be metabolically active despite large and rapid fluctuations in salinity, effectively increasing the range of environmental conditions where active photosynthesis can occur, with implications for the energy budget within the microbial mats. These results are consistent with measurements of photosynthesis by microbial mats from Arctic (Mueller et al., 2005) and Antarctic ice shelves (Hawes et al., 1992); and Antarctic lakes (Sabbe et al., 2004), which have shown acclimation to greatly increased salinities.

CONCLUSION

The cyanobacterial mats of WHL were suited to resist the major fluctuations in environmental conditions that occur at present in the High Arctic. The layered community structure, with UV-screening pigments and photoprotective carotenoids at the surface, allows a more diverse community including eukaryotes to grow in the bottom green communities of the mats. These bottom communities must contend with low oxygen tensions in summer, and the entire mat community is likely to experience anoxia during winter-freeze-up. The salinity responses measured here indicate broad tolerances and no loss of photosynthetic function under high and fluctuating osmolarities. Previous work on polar microbial mats has shown their tolerance of desiccation (Hawes et al., 1992), and that cyanobacterial isolates from Arctic and Antarctic mats grow faster at temperatures that are well above the present day ambient conditions (Tang et al., 1997). In combination, these results imply that cyanobacterial communities will continue to dominate polar aquatic ecosystems despite ongoing variations in water balance, increased UV radiation, and

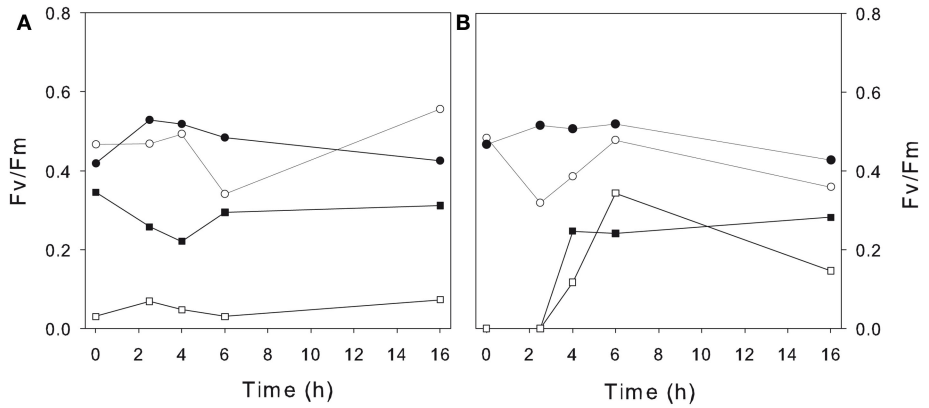

FIGURE 6 | Photophysiological activity of Ward Hunt Lake mats during their recovery from osmotic stress. The mats that were incubated under increased salinities for 48 h (as in **Figure 5**) were transferred back to the original Ward Hunt Lake water (conductivity of 0.25 mS cm^{-1}), and their photosynthetic quantum yields (F_v/F_m) were then monitored during the subsequent 16 h. **(A)** Pre-incubation conditions of 0.25 (control; solid circles), 5 (open circles), 30 (closed squares), and 100 mS cm^{-1} (open squares). **(B)** Pre-incubation conditions of 2.5 (control; solid circles), 10 (open circles), 150 (closed squares), and 200 mS cm^{-1} (open squares).

prolongation of ice-free conditions. However, these slow-growing mat communities currently experience little grazing pressure, and their persistence may be less assured if the northward expansion of invasive species accompanying climate change (Vincent et al., 2011 and references therein) includes arthropod grazers that feed on these large stocks of benthic microbial biomass.

ACKNOWLEDGMENTS

We acknowledge financial support from the Canada Research Chair in Aquatic Ecosystem Studies, the Network of Centers of Excellence program ArcticNet, and Natural Sciences and Engineering Council of Canada. Logistical support was supplied by the Polar Continental Shelf Project (PCSP publication number) and we are also grateful to Parks Canada for access to their facilities in Quttinirpaaq "top of the world" National Park. We also thank Denis Sarrazin and Sébastien Bourget for field assistance, Marie-Josée Martineau for laboratory assistance, and Anne-Dorothée Jungblut for advice on the molecular analyses. We also thank the two referees for their insightful review comments and suggestions on the submitted manuscript.

REFERENCES

Altschul, S. F., Warren, G., Webb, M., Myers, E. W., and Lipman, D. J. (1990). Basic local alignment search tool. *J. Mol. Biol.* 215, 403–410.

Balskus, E. P., Case, R. J., and Walsh, C. T. (2011). The biosynthesis of cyanobacterial sunscreen scytonemin in intertidal microbial mat communities. *FEMS Microbiol. Ecol.* 77, 322–332.

Belzile, C., Vincent, W. F., Gibson, J. A. E., and Van Hove, P. (2001). Bio-optical characteristics of the snow, ice and water column of a perennially ice-covered lake in the high Arctic. *Can. J. Fish. Aquat. Sci.* 58, 2405–2418.

Bolhuis, H., and Stal, L. J. (2011). Analysis of bacterial and archaeal diversity in coastal microbial mats using massive parallel 16S rRNA gene tag sequencing. *ISME J.* 5, 1701–1712.

Bonilla, S., Villeneuve, V., and Vincent, W. F. (2005). Benthic and planktonic algal communities in a high Arctic lake: pigment structure and contrasting responses to nutrient enrichment. *J. Phycol.* 41, 1120–1130.

Bottos, E. M., Vincent, W. F., Greer, C. W., and Whyte, L. G. (2008). Prokaryotic diversity of arctic ice shelf microbial mats. *Environ. Microbiol.* 10, 950–966.

Bowker, M. A., Reed, S. C., Belnap, J., and Phillips, S. L. (2002). Temporal variation in community composition, pigmentation, and Fv/Fm of desert cyanobacterial soil crusts. *Microb. Ecol.* 43, 13–25.

Broady, P. A. (1979). The Signy Island terrestrial reference sites: IX. The ecology of the algae of Site 2, a moss carpet. *Antarct. Sci.* 47, 13–29.

Butler, W. L. (1978). Energy distribution in the photochemical apparatus of photosynthesis. *Annu. Rev. Plant Physiol.* 29, 345–378.

Castenholz, R. W., and Garcia-Pichel, F. (2000). "Cyanobacteria responses to UV-radiation," in *The Ecology of Cyanobacteria: Their Diversity in Time and Space*, eds B. A. Whitton and M. Potts (Dordrecht: Kluwer Acad. Publ.), 591–611.

Castenholz, R. W. (2009). Mats, microbial. *Environ. Microbiol. Ecol.* 14, 278–292.

Garcia-Pichel, F., and Castenholz, R. W. (1991). Characterization and biological implications of scytonemin, a cyanobacterial sheath pigment. *J. Phycol.* 27, 395–409.

Hall, T. A. (1999). BioEdit: a user-friendly biological sequences alignment editor and analysis program for Windows 95/98/NT. *Nucleic Acids Symp. Ser.* 41, 95–98.

Hall-Stoodley, L., Costerton, J. W., and Stoodley, P. (2004). Bacterial biofilms: from the natural environment to infectious diseases. *Nat. Rev. Microbiol.* 2, 95–108.

Harding, T., Jungblut, A.-D., Lovejoy, C., and Vincent, W. F. (2011). Microbes in high Arctic snow and implications for the cold biosphere. *Appl. Environ. Microbiol.* 77, 3234.

Hawes, I., Howard-Williams, C., and Vincent, W. F. (1992). Desiccation and recovery of Antarctic cyanobacterial mats. *Polar Biol.* 12, 587–594.

Hawes, I., and Schwarz, A.-M. (2001). Absorption and utilization of low irradiance by cyanobacterial mats in two ice-covered Antarctic lakes. *J. Phycol.* 37, 5–15.

IPCC. (2007). "IPCC Summary for policymakers," in *Climate Change 2007: The Physical Science Basis. Contribution of Working Group I to the Fourth Assessment Report of the Intergovernmental Panel on Climate Change*, eds S. Solomon, D. Qin, M. Manning, Z. Chen, M. Marquis, K. B. Averyt, M. Tignor, and H. L. Miller (Cambridge: Cambridge University Press), 1–18.

Jungblut, A.-D., Hawes, I., Mountfort, D., Hitzfeld, B., Dietrich, D. R., Burns, B. P., and Neilan, B. A. (2005). Diversity within cyanobacterial mat communities in variable salinity meltwater ponds of McMurdo Ice Shelf, Antarctica. *Environ. Microbiol.* 7, 519–529.

Jungblut, A.-D., Lovejoy, C., and Vincent, W. F. (2010). Global distribution of cyanobacterial ecotypes in the cold biosphere. *ISME J.* 4, 191–202.

Karsten, U., Maier, J., and Garcia-Pichel, F. (1998). Seasonality in UV-absorbing compounds of cyanobacterial mat communities from an intertidal mangrove flat. *Aquat. Microb. Ecol.* 16, 37–44.

Katoh, K., and Toh, H. (2008). Recent developments in the MAFFT multiple sequence alignment program. *Brief. Bioinformatics* 9, 286–298.

Komárek, J., and Komárková-Legnerova, J. (1992). Variability of some planktonic gomphosphaerioid cyanoprokaryotes in northern lakes. *Nord. J. Bot.* 12, 513–524.

Lovejoy, C., Vincent, W. F., Frenette, J.-J., and Dodson, J. J. (1993). Microbial gradients in a turbid estuary: application of a new method for protozoan community analysis. *Limnol. Oceanogr.* 38, 1295–1303.

Mackay, M. A., Norton, R. S., and Borowitzka, L. J. (1984). Organic osmoregulatory solutes in cyanobacteria. *Microbiology* 130, 2177–2191.

Manney, G. L., Santee1, M. L, Rex, M., Livesey, N. J., Pitts, M. C., Veefkind, P., Nash, E. R., Wohltmann, I., Lehmann, R., Froidevaux, L., Poole, L. R., Schoeberl, M. R., Haffner, D. P., Davies, J., Dorokhov, V., Gernandt, H., Johnson, B., Kivi, R., Kyro, E., Larsen, N., Levelt, P. F., Makshtas, A., McElroy, C. T., Nakajima, H., Concepción Parrondo, M., Tarasick, D. W., von der Gathen, P., Walker, K. A., and Zinoviev, N. S. (2011). Unprecedented Arctic ozone loss in 2011. *Nature* 478, 469–477.

Mataloni, G., Tell, G., and Wynn-Williams, D. D. (2000). Structure and diversity of soil algal communities from Cierva Point (Antarctic Peninsula). *Polar Biol.* 23, 205–211.

Mueller, D. R, Vincent, W. F., Bonilla, S., and Laurion, I. (2005). Extremotrophs, extremophiles and broadband pigmentation strategies in a high arctic ice shelf ecosystem. *FEMS Microbiol. Ecol.* 53, 73–87.

Nübel, U., Garcia-Pichel, F., Kühl, M., and Muyzer, G. (1999). Quantifying microbial diversity: morphotypes, 16S rRNA genes, and carotenoids of oxygenic phototrophs in microbial mats. *Appl. Environ. Microbiol.* 65, 422–430.

Potts, M. (2000). '*Nostoc*,' in *The Ecology of Cyanobacteria*, eds B. A. Whitton and M. Potts (Netherlands: Kluwer Academic Publishers), 465–504.

Proteau, P. J., Gerwick, W. H., Garcia-Pichel, F., and Castenholz, R. (1993). The structure of scytonemin, an ultraviolet sunscreen pigment from the sheaths of cyanobacteria. *Experientia* 49, 825–829.

Quesada, A., and Vincent, W. F. (1997). Strategies of adaptation by Antarctic cyanobacteria to ultraviolet radiation. *Eur. J. Phycol.* 32, 335–342.

Quesada, A., Vincent, W. F., and Lean, D. R. S. (1999). Community and pigment structure of Arctic cyanobacterial assemblages: the occurrence and distribution of UV-absorbing compounds. *FEMS Microbiol. Ecol.* 28, 315–323.

Sabbe, K., Hodgson, D. A., Verleyen, E., Taton, A., Wilmotte, A., Vanhoutte, K., and Vyverman, W. (2004). Salinity, depth and the structure and composition of microbial mats in continental Antarctic lakes. *Freshw. Biol.* 49, 296–319.

Schmidt, S., Moskal, W., De Mora, S. J., Howard-Williams, C., and Vincent, W. F. (1991). Limnological properties of Antarctic ponds during winter freezing. *Antarct. Sci.* 3, 379–388.

Serreze, M. C., and Francis, J. A. (2006). The Arctic amplification debate. *Climate Change* 76, 241–264.

Smol, J. P., and Douglas, M. S. V. (2007). Crossing the final ecological threshold in high Arctic ponds. *Proc. Natl. Acad. Sci. U.S.A.* 104, 12395–12397.

Stal, L. J. (2000). "Cyanobacterial mats and stromatolites," in *The Ecology of Cyanobacteria: Their Diversity in Time and Space*, eds B. A. Whitton and M. Potts (Dordrecht: Kluwer), 61–120.

Stal, L. J., and Krumbein, W. E. (1985). Isolation and characterization of cyanobacteria from a marine microbial mat. *Botanica Marina* 28, 351–366.

Stamatakis, A. (2006). RAxML – VI-HPLC: maximum likelihood- based phylogenetic analyses with thousands of taxa and mixed models. *Bioinformatics* 22, 2688–2690.

Stamatakis, A., Hoover, P., and Rougemont, J. (2008). A rapid bootstrap algorithm for the RAxML web servers. *Syst. Biol.* 57, 758–771.

Tang, E. P. Y., Tremblay, R., and Vincent, W. F. (1997). Cyanobacterial dominance of polar freshwater ecosystems: are high latitude mat-formers adapted to the low temperature environment? *J. Phycol.* 33, 171–181.

Tavaré, S. (1986). Some probabilistic and statistical problems in the analysis of DNA sequences. *Lect. Math. Life Sci.* 17, 57–86.

Tsuchiya, T., Takaichi, S., Misawa, N., Maoka, T., Miyashita, H., and Mimuro, M. (2005). The cyanobacterium *Gloeobacter violaceus* PCC 7421 uses bacterial-type phytoene desaturase in carotenoid biosynthesis. *FEBS Lett.* 579, 2125–2129.

Varin, T., Lovejoy, C., Jungblut, A.-D., Vincent, W. F., and Corbeil, J. (2010). Metagenomic profiling of Arctic microbial mat communities as nutrient scavenging and recycling systems. *Limnol. Oceanogr.* 55, 1901–1911.

Villeneuve, V., Vincent, W. F., and Komarek, J. (2001). Community structure and microhabitat characteristics of cyanobacterial mats in an extreme High Arctic environment: Ward Hunt Lake. *Nova Hedwigia* 123, 199–224.

Vincent, W. F. (2000). "Cyanobacterial dominance in the Polar regions," in *The Ecology of Cyanobacteria*, eds B. A. Whitton and M. Potts (Netherlands: Kluwer Academic Publishers), 321–340.

Vincent, W. F., Callaghan, T. V., Dahl-Jensen, D., Johansson, M., Kovacs, K. M., Michel, C., Prowse, T., Reist, J. D., and Sharp, M. (2011). Ecological implications of changes in the Arctic cryosphere. *Ambio* 40, 87–99.

Webb, J. S., Givskov, M., and Kjelleberg, S. (2003). Bacterial biofilms: prokaryotic adventures in multicellularity. *Curr. Opin. Microbiol.* 6, 578–585.

Zakhia, F., Jungblut, A.-D., Taton, A., Vincent, W. F., and Wilmotte, A. (2008). "Cyanobacteria in cold ecosystems," in *Psychrophiles: From Biodiversity to Biotechnology*, eds R. Margesin, F. Schinner, J.-C. Marx, and C. Gerday (Berlin: Springer–Verlag), 121–135.

Zapata, M., Rodríguez, F., and Garrido, J. L. (2000). Separation of chlorophylls and carotenoids from marine phytoplankton: a new HPLC method using a reversed phase C8 column and pyridine-containing mobile phases. *Mar. Ecol. Prog. Ser.* 195, 29–45.

Conflict of Interest Statement: The authors declare that the research was conducted in the absence of any commercial or financial relationships that could be construed as a potential conflict of interest.

Received: 29 January 2012; paper pending published: 17 February 2012; accepted: 24 March 2012; published online: 26 April 2012.

Citation: Lionard M, Péquin B, Lovejoy C and Vincent WF (2012) Benthic cyanobacterial mats in the high Arctic: multi-layer structure and fluorescence responses to osmotic stress. Front. Microbio. ***3****:140. doi: 10.3389/fmicb.2012.00140*

This article was submitted to Frontiers in Aquatic Microbiology, a specialty of Frontiers in Microbiology.

frontiers in
MICROBIOLOGY

REVIEW ARTICLE
published: 21 May 2012
doi: 10.3389/fmicb.2012.00173

Cyanobacteria of the genus *Prochlorothrix*†

Alexander Pinevich*, Natalia Velichko and Natalia Ivanikova

Microbiology Department, Faculty of Biology and Soil Science, St. Petersburg State University, St. Petersburg, Russia

Edited by:
George S. Bullerjahn, Bowling Green State University, USA

Reviewed by:
George S. Bullerjahn, Bowling Green State University, USA
Edward Hall, United States Geological Survey, USA

****Correspondence:***
Alexander Pinevich, Microbiology Department, Faculty of Biology and Soil Science, St. Petersburg State University, 29, Lane 16 Vasilievskii island, St. Petersburg, Russia
e-mail: pinevich.a@mail.ru

Green cyanobacteria differ from the blue–green cyanobacteria by the possession of a chlorophyll-containing light-harvesting antenna. Three genera of the green cyanobacteria namely *Acaryochloris*, *Prochlorococcus,* and *Prochloron* are unicellular and inhabit marine environments. *Prochlorococcus marinus* attracts most attention due to its prominent role in marine primary productivity. The fourth genus *Prochlorothrix* is represented by the filamentous freshwater strains. Unlike the other green cyanobacteria, *Prochlorothrix* strains are remarkably rare: to date, living isolates have been limited to two European locations. Taking into account fluctuating blooms, morphological resemblance to *Planktothrix* and *Pseudanabaena*, and unsuccessful attempts to obtain enrichments of *Prochlorothrix*, the most successful strategy to search for this cyanobacterium involves PCR with environmental DNA and *Prochlorothrix*-specific primers. This approach has revealed a broader distribution of *Prochlorothrix*. Marker genes have been found in at least two additional locations. Despite of the growing evidence for naturally occurring *Prochlorothrix*, there are only a few cultured strains with one of them (PCC 9006) being claimed to be axenic. In multixenic cultures, *Prochlorothrix* is accompanied by heterotrophic bacteria indicating a consortium-type association. The genus *Prochlorothrix* includes two species: *P. hollandica* and *P. scandica* based on distinctions in genomic DNA, cell size, temperature optimum, and fatty acid composition of membrane lipids. In this short review the properties of cyanobacteria of the genus *Prochlorothrix* are described. In addition, the evolutionary scenario for green cyanobacteria is suggested taking into account their possible role in the origin of simple chloroplast.

Keywords: cyanobacteria, *Prochlorothrix*, Prochlorophytes

INTRODUCTION

Oxygenic photosynthetic bacteria are represented by blue–green cyanobacteria and green cyanobacteria. This distinction is analogous to that between green chlorosome-containing and purple non-chlorosome-containing anoxygenic photosynthetic bacteria and is based on the supramolecular organization of the light-harvesting complex rather than cell color (certain blue–green cyanobacteria are blue, green, red, violet, or brownish). Blue–green cyanobacteria are characterized by a constantly expressed phycobiliprotein light-harvesting antenna, or phycobilisome, with the exception of inducible mutants and terminally differentiated wild type cells called heterocysts. In contrast, green cyanobacteria have a constitutive chlorophyll-protein light-harvesting antenna instead of the phycobilisome (the former is expressed in some blue–green cyanobacteria in stress conditions). In terms of pigments, green cyanobacteria possess accessory chlorophyll(s), whereas blue–green cyanobacteria have only *chl a* (Partensky and Garczarek, 2003).

Green cyanobacteria are worth interest primarily for two reasons. First of all, *Prochlorococcus marinus* dominates pelagic environments for large regions of the world's oceans. Secondly, the remaining four species (*Acaryochloris marina*, *Prochloron didemni*, *Prochlorothrix hollandica*, and *Prochlorothrix scandica*) are limited to specific eutrophic habitats, in contrast to ubiquitously distributed *P. marinus* and blue–green cyanobacteria (Partensky et al., 1999).

Cyanobacteria of the genus *Prochlorothrix* are unique among green cyanobacteria being filamentous and freshwater, as opposed to the other three marine unicellular species.

In this review, the properties of cyanobacteria of the genus *Prochlorothrix* are summarized, and the phylogeny of green cyanobacteria is reconsidered in the light of their role in the origin of simple chloroplast.

SCOPE OF OBJECTS

CIRCUMSTANCES OF DISCOVERY

Green cyanobacteria were initially discovered by the chromatographic detection of the accessory *chl b* and/or other accessory chlorophylls (a_2, b_2, *c*, etc) in collected samples. This approach lead to the discovery of two unicellular species *P. didemni* (Lewin, 1981) and *A. marina* (Miyashita et al., 1996), as well as the filamentous species *P. hollandica* (Burger-Wiersma et al., 1989) and *P. scandica* (Pinevich et al., 1999). The third unicellular species,

†The GenBank accession number for the 16S rRNA gene sequence of *Prochlorothrix* sp. NIVA-8/90 is HQ316169. The accession number for the sequences of the single 16S–23S-ITS, *psbO* and *PsaF* genes in *P. hollandica* PCC 9006 are JQ739143, JQ739144, and HQ316172 respectively. The accession numbers for the sequences of two 16S–23S-ITS in *Prochlorothrix* sp. NIVA-8/90 are HQ316170 and HQ316171 respectively. The accession number for the partial 16S rRNA sequence of the uncultured *Prochlorothrix* of the Finnish Bay is JQ739142.

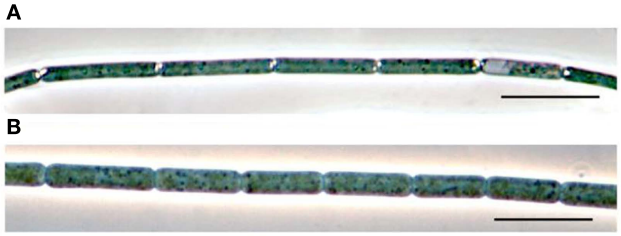

FIGURE 1 | Light micrographs of *Prochlorothrix hollandica* PCC 9006 (A) and *P. scandica* NIVA 8/90 (B). Bar, 10 μm.

P. marinus, was revealed by flow cytometry in oceanic picoplankton (Chisholm et al., 1988). Later on, pigment-based methods were supplemented with or gave way to PCR detection of the 16S rRNA gene with specific primers (Castiglioni et al., 2004). In order to increase the sensitivity of detection, as well as for a better separation of gene clusters, internal transcribed spacers of 16S–23S-rRNA were also tested (Laloui et al., 2002; Rocap et al., 2002). Screening for green cyanobacteria is also performed using other primers which help amplify genes which code for photosynthetic proteins, e.g., Pcb proteins of *chl a*/*b* antenna distinct from CAB proteins in green algae, euglenae, and higher plants (Geiß et al., 2003).

REPRESENTATIVES

The first member of the genus *Prochlorothrix*, the type species *P. hollandica* (**Figure 1A**) was validly described according to the rules of Bacteriological Code (Burger-Wiersma et al., 1989). In the modern taxonomic system, it is ascribed to Subsection III of Phylum X. *Cyanobacteria* (Oxygenic Photosynthetic Bacteria) or the order "*Oscillatoriales*" (Castenholz, 2001).

The second member of the genus *Prochlorothrix* is *Prochlorothrix* sp. NIVA 8/90 (**Figure 1B**). This strain was named *P. scandica* (Pinevich et al., 1999) legitimized under the rules of Botanical Code (Skulberg, 2008).

Prochlorothrix sp. NIVA 8/90 is considered as separate species primarily based on genomic DNA differences with *P. hollandica* (**Table 1**). Noteworthy, the previous demand for 3% dissimilarity of 16S rRNA is now considered to be not obligatory in species delimitation (Wayne et al., 1987). *Prochlorothrix hollandica* and *P. scandica* also differ in 16S–23S-ITS, and have one (1,100 bp) and two (1,100 and 620 bp) 16S–23S-ITS, respectively. The larger ITS in *Prochlorothrix* sp. NIVA 8/90 is 99% identical to the single ITS in *P. hollandica*. At the same time, the two ITS in *Prochlorothrix* sp. NIVA 8/90 demonstrate low mutual similarity (Velichko et al., unpublished). In addition, these two cyanobacteria differ by another genetic criterion: the electrophoretic profile of PCR-amplified highly iterated palindromic sequences (HIP-1; Robinson et al., 1995; Smith et al., 1998; Velichko et al., unpublished).

Phenotypic criteria for the species difference between *P. hollandica* and *P. scandica* are cell size, temperature optimum (see below), and fatty acid composition of the membrane lipids (**Table 2**).

Due to the presence of $C_{16:2}$ and $C_{18:2}$ fatty acids both species should be categorized as group 5 cyanobacteria (Cohen et al., 1995). In both species, $C_{14:0}$, $C_{16:0}$, $C_{14:1}$, and $C_{16:1}$ fatty acids are among the major components. The profile of saturated (straight-chain and branched) fatty acids is comparable in the two species, except for a double amount of $C_{18:0}$ stearic acid in *P. scandica*. At the same time, cellular content of unsaturated fatty acids is species-specific. The most prominent differences of *P. scandica* from *P. hollandica* are a twofold increase (8.7% vs 5.0%) in the amount of the $C_{16:1}\omega5$ isomer palmitoleic acid, sevenfold increase (3.4% vs 0.5%) in the amount of $C_{18:1}\omega9$ oleic acid, and a twofold decrease (11.9% vs 21.4%) in the amount of the $C_{16:1}\omega7$ isomer palmitoleic acid. In addition, the trace amounts of dienoic $C_{16:2}\omega4$ and trienoic $C_{16:3}\omega3$ acids are 1.8% vs 1.0% and 1.5% vs 0.7% in *P. scandica* and *P. hollandica*, respectively.

Table 1 | Genetic distinction between *P. hollandica* and *P. scandica*.

Criteria of distinction	Measure of assignment to different species (%)	
	Conventional	Actual
Δ Mol% GC	>5	6.6
DNA–DNA hybridization degree	<30	17.9
Positional matches in the complete sequence of 16S rRNA gene	>3	2

Table 2 | Cellular fatty acid composition (%) of *P. scandica* and *P. hollandica* grown under identical conditions.

Fatty acid	*P. scandica* NIVA-8/90	*P. hollandica* CCAP 1490/1
STRAIGHT-CHAIN		
$C_{12:0}$	0.5	0.6
$C_{14:0}$	10.7	8.7
$C_{15:0}$	0.8	1.1
$C_{16:0}$	18.1	17.7
$C_{18:0}$	**1.2**	**0.5**
BRANCHED		
Iso-$C_{16:1}$*	1.4	2.0
Anteiso-$C_{16:1}$*	6.7	6.0
UNSATURATED		
$C_{12:1}$*	1.3	0.8
$C_{14:1}$*	14.3	17.0
$C_{15:1}$*	8.0	9.6
$C_{16:1}\omega9$*	5.5	3.7
$C_{16:1}\omega7$*	**11.9**	**21.4**
$C_{16:1}\omega5$*	**8.7**	**5.0**
$C_{16:2}\omega4$*	**1.8**	**1.0**
$C_{16:3}\omega3$*	**1.5**	**0.7**
$C_{18:1}\omega9$*	**3.4**	**0.5**
$C_{18:1}\omega11$*	0.7	0.5
$C_{18:2}\omega6$*	0.2	0.3
Unknown	4.0	2.2

**The position(s) of double-bond(s) is not thoroughly determined; trans-cis isomeric state of unsaturated fatty acids is not determined. The most prominent differences between the two species are in bold.*

DISTRIBUTION

Evidence for the presence of the genus *Prochlorothrix* has been restricted to eutrophic freshwater or brackish habitats of North Europe (**Figure 2**). *Prochlorothrix hollandica* was accidentally encountered during a routine study of cyanobacterial blooms in the Loosdrecht lake system near Amsterdam (The Netherlands; Burger-Wiersma et al., 1989). These polymictic and highly eutrophic (∼60 mg m^{-3} *chl a*) water pools of average depth ∼2 m originate from a flooded turf pit, with phytoplankton represented mostly by blue–green filamentous cyanobacteria of the group *Limnothrix*/*Pseudanabaena* (Zwart et al., 2005). In addition, "Dutch" green cyanobacteria were also found in a shallow eutrophic Lake Tjeukemeer (van Liere et al., 1989). Finally, according to personal communication by J. van der Does (van Liere et al., 1989), the presence of filamentous green cyanobacteria was registered in other shallow eutrophic Dutch lakes by fluorescence microscopy.

The second representative of the genus *Prochlorothrix*, *P. scandica* was isolated from Lake Mälaren (1,140 km^2, medium depth ∼13 m) near Stockholm, Sweden (Skulberg, 2008).

Based on these discoveries, the representatives of the genus *Prochlorothrix* are common in eutrophic lakes occupied mainly by cyanobacteria (Lewin et al., 1980; van Liere et al., 1989).

In addition to direct evidence for the presence of these cyanobacteria in eutrophic lakes, they have been indirectly detected by the PCR-amplification of 16S rRNA gene and *pcb* genes (Geiß et al., 2003). Natural DNA was obtained from water samples of estuary Darss-Zingst located near the South-West coast of the Baltic Sea between the cities Rostock and Stralsund (Germany). This polymictic and eutrophic water body is represented by a chain of lagoons fed by the mouth of Prerow River, separated from the Baltic Sea by the Peninsula Frischland/Darss, and is characterized by opposite gradients of dissolved organic substances and salinity (Geiß et al., 2004). It is reasonable to expect that dynamic combination of these (a)biotic factors favors the development of cyanobacteria from the genus *Prochlorothrix*.

In summer 2011 *Prochlorothrix*-like 16S rRNA nucleotide sequences were detected in the brackish waters of the Finnish Bay in the environs of St. Petersburg, Russia (Velichko et al., unpublished data). Also, we came across an environmental *Prochlorothrix*-like 16S RNA gene sequence revealed during the metagenomic screening of New Orleans area water systems after Hurricanes Katrina and Rita (Amaral-Zettler et al., 2008).

Phylogenetic reconstruction of all available *Prochlorothrix* 16S rRNA gene sequences demonstrates close clustering of the environmental sequences from different regions of the world within the *Prochlorothrix* group (**Figure 3**). In fact, within the *Prochlorothrix* group sequences of the 16S rRNA gene are 98–99% similar.

In seems that the strains of *Prochlorothrix* detected in brackish coastal waters are merely temporary invaders from the mainland, and they could even sporadically occur in open waters of the Baltic

FIGURE 2 | Sampling location of *Prochlorothrix* strains and *Prochlorothrix*-type environmental DNA.

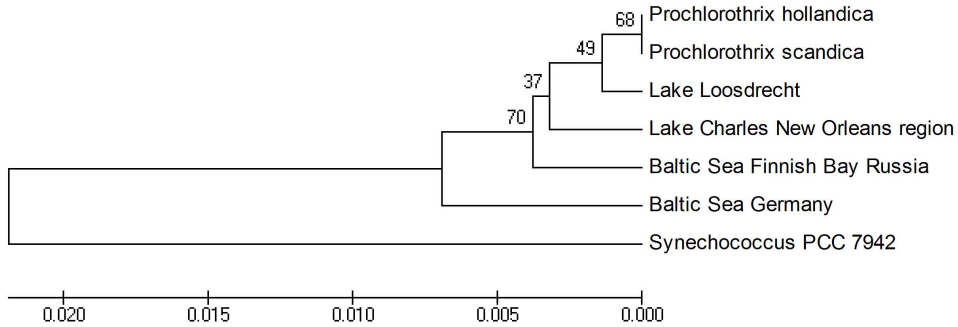

FIGURE 3 | Unrooted dendrogram of a 375-bp fragment of *Prochlorothrix* 16S rDNA sequences obtained by the UPGMA method using MEGA version 4 (Tamura et al., 2007). Bootstrap values based on 1,000 replications are shown at the nodes.

Sea (Geiß et al., 2003). At the same time, there is no indication of their presence in any oligotrophic lake.

FUNCTIONAL ECOLOGY

Filamentous green cyanobacteria never dominate the phytoplankton of small polymictic lakes. Growth rate of natural populations of *P. hollandica* is usually 30–40% that of *Oscillatoria*-like blue–green cyanobacteria (0.02–0.14 day^{-1}; see Pel et al., 2004). This is possibly the reason why these blue–green cyanobacteria dominate and even suppress green cyanobacteria in natural environment.

PRIMARY PRODUCTIVITY

The biomass of *Prochlorothrix* which reaches its maximum during the bloom season can be used as a principal nutrient by the zooplankton. In particular, the number of *Euchlanis dilatata* (Rotatoria, Nemathelminthes) which is among the main primary suppliers in the Loosdrecht Lakes (Gulati et al., 1993), is increased in late summer and in early spring which coincides with mass development of *Prochlorothrix*. The intensity of *Prochlorothrix* biomass consumption by this invertebrate is commeasurable with that of the blue–green cyanobacterium *Aphanizomenon flos-aquae* (Gulati et al., 1993).

PHOTOACCLIMATION

Genes *pcbABC* in *P. hollandica* constitute an operon (Nikolaitchik and Bullerjahn, 1998; van der Staay et al., 1998). The antenna proteins pcbAB selectively associate with PSII, while the antenna protein PcbC is attached to PSI (Bumba et al., 2005). Photosystems I and II in *P. hollandica* have the peripheral antennae which produce a 18-meric ring around the PSI trimer and a 14-meric ring around the PSII dimer (Boichenko et al., 2007). *Prochlorothrix hollandica* is the only green cyanobacterium in which a shift of photosynthetic States 1 ↔ 2 (i.e., preferential light channeling) was demonstrated. However, the details of the structural/functional association between the *chl a/b* antenna with photosystems remain obscure. According to one of the two conflicting models, in State 1 the main *chl a/b* antenna (which consists of proteins PcbB and PcbC) transiently associates both PS. In State 2, the minor *chl a/b* antenna (which consists of PcbA protein) dissociates from the super complex of the main *chl a/b* antenna and PSII (Post et al., 1992). In another model (van der Staay and Staehelin, 1994), in State 1 the stacked thylakoids are enriched with the super complex of *chl a/b* antenna and PSII, whereas unstacked thylakoids contain PSI.

Later experimental data suggest a compromise model (Partensky and Garczarek, 2003) based on the spatial redistribution of (de)phosphorylated Pcb proteins.

TEMPERATURE

The culture optimum growth of *P. hollandica* PCC 9006 and *P. scandica* NIVA-8/90 is 20 and 24°C respectively (Pinevich et al., 1999; Skulberg, 2008). However, in nature they were shown to grow at lower temperatures. Compared to other green cyanobacteria, *Prochlorothrix* occupies a narrow geographic range characterized by significant seasonal changes in temperature, as well as by the episodic formation of ice cover in winter time. For instance in July 1984 when *P. hollandica* PCC 9006 was discovered in Lake Loosdrecht the water temperature was 18°C (Burger-Wiersma et al., 1989), whereas in April 1998 it was only 8°C (Zwart et al., 2005). As a rule, mass development of *Prochlorothrix* in this lake occurs in the end of summer when water temperature is 15–18°C (Post and Bullerjahn, 1994).

Water sampling from Lake Mälaren, where *P. scandica* NIVA-8/90 was detected was performed in October 1990. During this period, the temperature is 10–13°C throughout the water column due to the active mixing (Skulberg, 2008).

SALINITY RESPONSE

Cyanobacteria of the genus *Prochlorothrix* are traditionally considered to inhabit freshwater pools, and they are sensitive even to a small increase in salinity. *Prochlorothrix hollandica* PCC 9006 demonstrated poor growth in the presence of 25 mM NaCl, and the growth was fully suppressed at 100 mM or after the addition of sea water equivalent (Burger-Wiersma et al., 1989). Our data on the comparative salt resistance in *P. hollandica* PCC 9006 and *P. scandica* NIVA-8/90 confirm the inhibitory effect of 50–100 mM NaCl (Pinevich et al., unpublished data). Increased salinity provoked morphological changes in both species: cells were elongated, and the filaments became zigzag. At >200 mM NaCl, the filaments of both species degraded after a week growth.

Although high sensitivity to salt can be easily explained by the inability to synthesize osmotic protectors, salt adaptation

may depend on the local ion climate. In particular, *P. hollandica* was resistant to 170 mM NaCl when grown in a semi-synthetic medium supplied with water from the estuary Darss-Zingst. Under these conditions, an increase in the cellular content of sucrose was registered (Bergmann et al., 2008). This data are in agreement with the detection of *Prochlorothrix*-like marker genes in the phytoplankton of the Baltic Sea open waters (Geiß et al., 2003).

INVOLVEMENT IN SYMBIOSES

In contrast to the rest of green cyanobacteria, the strains of *Prochlorothrix* are easily cultured on liquid mineral media (see below). However, most attempts to obtain pure cultures on solid medium proved unsuccessful. Cultures ceased to grow, when attempts to get rid of heterotrophic contaminants were made by the authors. FISH hybridization with taxon-specific probes EUB338II, EUB338III, ALF968, BET42a, GAM42a, and DELTA495a revealed a vast diversity of heterotrophic bacteria associated with *P. hollandica* PCC 9006 and *P. scandica* NIVA-8/90. In case of *P. hollandica* PCC 9006, a positive signal was obtained with probes specific to alpha-, beta-, and gammaproteobacteria. On the other hand, heterotrophic epiphytes of *P. scandica* NIVA-8/90 belong to alpha- and betaproteobacteria (Velichko et al., unpublished data).

These data, along with the fact that bacteria-free filaments of *P. hollandica* PCC 9006 demonstrated negligible growth in liquid culture (Schyns et al., 1997), indicate a mutually favorable consortium-type association between the filamentous green cyanobacteria and their heterotrophic satellites.

CULTIVATION

MEDIA AND STRAINS

Cyanobacteria of the genus *Prochlorothrix* are grown in mineral media FPG, BG-11, and Z8 which contain relatively low amounts of inorganic salts and are routinely used for the cultivation of freshwater blue–green cyanobacteria (**Table 3**). Double-distilled water is necessary. Otherwise, unidentified contaminating chemicals inhibit growth. For slant cultivation, semisolid agar ($\leq$0.5%) is recommended, since $\geq$1% inhibits growth. In addition to double-distilled water and mineral salts of high quality, purified agar (e.g., Difco) is needed. Cell growth is suppressed by elevated concentrations of NaCl, and the degree of salt resistance depends on ion content of the medium (Burger-Wiersma et al., 1989; Bergmann et al., 2008). Since *Prochlorothrix* sp. is unable to fix nitrogen even in microaerobic conditions, an addition of combined nitrogen is necessary.

In collections *Prochlorothrix* sp. is represented by several cultured strains. One of them, isolated in the Netherlands and validly described as *P. hollandica* (Burger-Wiersma et al., 1989), is maintained under different strain identifiers (CALU 1027, CCAP 1490/1, NIVA-5/89, PCC 9006, and SAG 10.89). Several multixenic strains isolated in Sweden are stored in the Norwegian Institute for Water Research (Oslo, Norway) collection, namely NIVA 8/90, 9/90, and 16/90 (Skulberg, 2008). Strain *P. hollandica* PCC 9006 (CALU 1027) and strain *P. scandica* NIVA-8/90 (CALU 1205) are stored at the collection of St. Petersburg University (St. Petersburg, Russia). Various methods of axenization were attempted including streaking, repeated washing, and micromanipulation, as well as differential sensitivity to antibiotics (Burger-Wiersma et al., 1989; Pinevich et al., 1999; Skulberg, 2008). All of them proved unsuccessful because of the loss of viability in both liquid and solid medium. In the latter case, filaments grow not as colonies, but rather as films surrounded by dim layer of colorless heterotrophic bacteria.

Table 3 | Nutrition media for the cultivation of *Prochlorothrix*.

Component	Medium		
	FPG*	BG-11**	Z8***
MACRO NUTRIENTS (mg L^{-1})			
$NaHCO_3$	100.0	–	–
Na_2CO_3	–	20.0	20.0
$NaNO_3$	500.0	1500.0 (300.0)	467.0
NH_4Cl	–	–	31.0
K_2HPO_4	25.0	40.0	–
$MgSO_4 \cdot 7H_2O$	50.0	75.0	250.0
$CaCl_2 \cdot 2H_2O$	13.0	36.0	–
$Ca(NO_3)_2 \cdot 4H_2O$	–	–	59.0
MICRO NUTRIENTS (mg L^{-1})			
$FeCl_3 \cdot 2H_2O$	0.3	–	2.8
H_3BO_3	2.68	2.86	3.1
$MnC1_2 \cdot 4H_2O$	1.81	1.81	–
$MnSO_4 \cdot 4H_2O$	–	–	2.23
$ZnSO_4 \cdot 7H_2O$	0.22	0.22	0.22
$(NH_4)_6Mo_7O_{24} \cdot 4H_2O$	0.002	–	0.08
$Na_2MoO_4 \cdot 2H_2O$	–	0.39	–
$CuSO_4 \cdot 5H_2O$	–	0.079	–
$Co(NO_3)_2 \cdot 6H_2O$	0.08	0.05	0.146
NH_4VO_3	0.01	–	–
$VOSO_4 \cdot 6H_2O$	–	–	0.054
$Al_2(SO_4)_3 \cdot K_2SO_4 \cdot 2H_2O$	–	–	0.474
$NiSO_4 \cdot (NH_4)_2SO_4 \cdot 6H_2O$	–	–	0.198
$Cr(NO_3)_3 \cdot 7H_2O$	–	–	0.037
$Cd(NO_3)_2 \cdot 4H_2O$	–	–	0.154
$Na_2WO_4 \cdot 2H_2O$	–	–	0.033
KBr	–	–	0.119
KI	–	–	0.083
CHELATORS (mg L^{-1})			
Citric acid	–	6.0	–
EDTA	0.3	1.0	3.7

**Extracted from Burger-Wiersma et al. (1989); **Rippka et al. (1979); ***Kotai (1972). Double-distilled water is generally used.*

GROWTH PARAMETERS

Batch cultures of *P. hollandica* PCC 9006 in FPG medium at 40 μE m^{-2} s^{-1} and 20°C grew at a maximum rate of 0.02 h^{-1} (Burger-Wiersma et al., 1989). When the BG-11 medium was used, grow rate varied from 0.007 h^{-1} (Burger-Wiersma et al., 1989) to 0.026 h^{-1} (Bergmann et al., 2008). Optimum growth temperature for *P. hollandica* PCC 9006 is 20°C (Burger-Wiersma et al., 1989; Pinevich et al., 1999), while that for *P. scandica* is 24°C (Pinevich et al., 1999). Stirring or air bubbling failed to stimulate growth and even resulted in decreased viability due to mechanical damage of the filaments.

MORPHOLOGY

Immotile, non-branching filaments of *Prochlorothrix* sp. grow by equal binary fission of intercalary cells and multiply by fortuitous fragmentation. Hormogonia or other types of differentiated structures are never observed.

Filaments of *P. hollandica* PCC 9006 and *P. scandica* NIVA-8/90 (**Figure 1**) are ≤250 μm long. Mean cell size of *P. hollandica* PCC 9006 is $11.8 \pm 0.9 \times 1.6 \pm 0.1$ μm (length vs width, 7.4:1), while that of *P. scandica* NIVA-8/90 being $7.4 \pm 0.7 \times 2.1 \pm 0.1$ μm (3.5:1). In both cases, the width of cell-to-cell junction is 1/8–1/5 of filament diameter. In this respect, the filaments of *Prochlorothrix* more closely resemble those of *Limnothrix* than those of *Pseudanabaena*. In the latter case, the width of cell-to-cell junction is 1/2 of filament diameter (Castenholz, 2001).

SELECTED FEATURES OF ULTRASTRUCTURE

THYLAKOID STACKING

In addition to unstacked thylakoids which are typical of blue–green cyanobacteria, *P. hollandica* PCC 9006 contains stacked thylakoids vaguely resembling grana thylakoids in chloroplasts (Giddings et al., 1980; Schuster et al., 1984; Miller et al., 1988; Golecki and Jürgens, 1989). In both cases, membrane adhesion is maintained by the PSII proteins and *chl a*/*b* antenna proteins (van der Staay and Staehelin, 1994).

Thylakoids in freeze-fractured cells of *P. hollandica* PCC 9006 were shown to be laterally heterogeneous (van der Staay and Staehelin, 1994). Similarly to chloroplasts, stacked regions are enriched with globular particles which correspond to the super complexes of PSII with *chl a*/*b* antenna. By contrast, PSI and ATP synthase are preferentially localized in the unstacked regions (Schuster et al., 1984; van der Staay and Staehelin, 1994).

Membranes of stacked thylakoids in *P. scandica* NIVA-8/90 are covered with particles (viridosomes) which are 10.0 ± 2.3 nm diameter and are located with the periodicity of 20.0 ± 5.6 nm. These are suggested to correspond to the epimembrane domain of *chl a*/*b* antenna (Pinevich et al., 1999). The analogous particles (xanthosomes) are present in both the chromophyte algae (e.g., *Bacillariophyceae* and *Phaeophyceae*) and *Dinozoa* (Katoh et al., 1993; Green and Durnford, 1996).

Thylakoid stacking in *Prochlorothrix* may help redistribute excitation energy between the adjoining thylakoids (Dekker and Boekema, 2005). Alternatively, it may be a functionless result of segregation of PSII centers in thylakoid membranes (Bullerjahn and Post, 1993; see Functional Ecology and Photoacclimation).

THYLAKOID CENTERS

An intriguing detail of ultrastructure in *P. hollandica* PCC 9006 and *P. scandica* NIVA-8/90, also rarely observed in blue–green cyanobacteria, is the thylakoid center. The latter corresponds to a ∼200-nm electron dense zone between cell membrane and two to four radiating thylakoids (Pinevich et al., 1996). These metastable structures possibly channel the molecules of *chl-ide* a_{GG} (the precursor of *chl* a) from the sites of synthesis in cell membrane to the functional sites in thylakoids (Nierzwicki-Bauer et al., 1983; Bryant, 1986; Hinterstoisser et al., 1993).

GAS VESICLES

Similarly to many planktonic filamentous blue–green cyanobacteria, *P. hollandica* PCC 9006 contains honeycomb-like aggregates of gas vesicles. An individual vesicle is a cylinder of 50 nm diameter with conical ends. Its 125–265 nm length mirrors different stages of self-assembly (Golecki and Jürgens, 1989; Pinevich et al., 1999).

CARBOXYSOMES

Similarly to blue–green cyanobacteria, the carboxysomes of *P. hollandica* PCC 9006 are enveloped in a non-unit membrane. However, the carboxysomes of *P. scandica* NIVA-8/90 lack this shell resembling the pyrenoid of green algae and higher plants (McKay and Gibbs, 1990; Morden and Golden, 1991; Pinevich et al., 1996). According to the immune electron microscopy data, all RuBisCO of *P. hollandica* PCC 9006 is associated with carboxysomes. Whereas, the RuBisCO in *P. scandica* NIVA-8/90 exists in both the immobilized and soluble form (Pinevich et al., 1996). Carboxysomes in *Prochlorothrix* were shown to contact thylakoids (Pinevich et al., 1999), which is not the case in blue–green cyanobacteria. This association may promote phosphorylation of ribulose-5-phosphate, as well as the activity of carbonic anhydrase (Pinevich et al., 1999).

GENETICS

Genome size of *Prochlorothrix* is ∼5.5 Mb (Post and Bullerjahn, 1994; Schyns et al., 1997) which is within the range of most cyanobacteria. The G + C Mol% of genomic DNA is 51–53 (Herdman, 1981; Coleman and Lewin, 1983; Burger-Wiersma et al., 1989; Dufresne et al., 2003).

GENOME SEQUENCING

Genome sequencing of *P. hollandica* PCC 9006 is currently performed by the authors. Automatic annotation using The RAST Server (Rapid Annotations using Subsystems Technology; Aziz et al., 2008) was performed on the draft sequence, and the manual curation of automatically annotated genes is being done. We are focusing primarily on photosynthetic genes. Phylogenetic affiliation for two of them, namely *psbO* and *psaF*, are given below (see Phylogeny).

ENERGY ASSIMILATION

In contrast to unicellular green cyanobacteria, *Prochlorothrix* has not been tested for dark chemotrophy; the only studied mode of energy assimilation in this case is phototrophy.

PHOTOSYNTHETIC PIGMENTS

Prochlorothrix hollandica PCC 9006 contains accessory *chl b* (Burger-Wiersma et al., 1989). It is suggested to be synthesized from *chl* b_2 in one stage using 4-vinyl-reductase (Helfrich et al., 1999). The alternative way involves *chl a* oxygenase which was the enzyme also found in *Prochloron didemni* and higher plants (Tanaka et al., 1998; Tomitani et al., 1999; Nagata et al., 2005).

Among the carotenoids in *P. hollandica* PCC 9006 are β-carotene and zeaxanthin (van der Staay et al., 1992). The content of β-carotene in *P. hollandica* PCC 9006 is four times that of zeaxanthin. The former preferentially associates with PSI, while the latter complexes with 56/58 kDa proteins integrated in the cell membrane (Omata et al., 1985; Engle et al., 1991).

LIGHT-HARVESTING ANTENNA

In contrast to blue–green cyanobacteria, *P. hollandica* PCC 9006 and *P. scandica* NIVA 8/90 possess the light-harvesting antenna

containing both *chl a* and *chl b* (Bryant, 1986; Burger-Wiersma and Post, 1989; Hess et al., 1996; Marquardt et al., 1998). Although it was originally thought that Pcb proteins of this antenna share the origin with CAB proteins in chloroplasts, in fact they have no similarity (La Roche et al., 1996; van der Staay et al., 1998). In particular, Pcb proteins of *P. hollandica* PCC 9006 do not react with antibodies raised against CAB proteins of green algae and higher plants (Hiller and Larkum, 1985; Bullerjahn et al., 1990; van der Staay and Staehelin, 1994). At the same time, Pcb proteins of *P. hollandica* PCC 9006 are similar to PsbB and PsbC (CP43) proteins of PSII core antenna. In addition, they share similarity with *IsiA* (CP43′) protein of PSI stress antenna which is formed in blue–green cyanobacteria under iron starvation (Bullerjahn et al., 1987, 1990; van der Staay and Staehelin, 1994; Nikolaitchik and Bullerjahn, 1998; van der Staay et al., 1998; Partensky et al., 1999). Hexadomain proteins Pcb/Cp43/*IsiA* vary in the length of the loop exposed at the thylakoid exoplasmic surface between helices V and VI (Herbstová et al., 2010).

Genes *pcbABC* of *P. hollandica* PCC 9006 form an operon (Nikolaitchik and Bullerjahn, 1998; van der Staay et al., 1998). The genes *pcbA* and *pcbB* genes belong to the evolutionary lineage of *IsiA* and code for polypeptides of 32 and 33 kDa. The third gene, *pcbC*, belongs to a separate lineage and codes for a polypeptide of 38 kDa (van der Staay and Staehelin, 1994; van der Staay et al., 1998; Garczarek et al., 2000).

Pcb proteins aggregate in multimeric super complexes (Bibby et al., 2001, 2003; Chen et al., 2002, 2005; Partensky and Garczarek, 2003) which surround the oligomers of PSI and PSII (Bibby et al., 2003; Boichenko et al., 2007). PcbA/PcbB proteins build up the mobile antenna of both photosystems, while the PcbC proteins associate with a portion of antenna tightly bound to PSI (Herbstová et al., 2010).

PHOTOSYSTEMS

PSI polypeptides of *P. hollandica* PCC 9006 are the same as in blue–green cyanobacteria (Schuster et al., 1984; Bullerjahn et al., 1987; van der Staay et al., 1998; Garczarek et al., 2000). They include major PsaA/PsaB proteins (66 kDa) and 6 minor proteins PsaC–F, I–M (20 kDa; Burger-Wiersma and Post, 1989; van der Staay et al., 1993). PSII proteins of *P. hollandica* PCC 9006 include CP43/CP47, D1/D2, PsbH, and PsbO, as well as low molecular weight polypeptides PsbJ and PsbK (Greer, 1991; Greer and Golden, 1992; Mor et al., 1993; Post and Bullerjahn, 1994). Interestingly, *psbA* gene has a 3′-terminal 21-nucleotide deletion; the same deletion is present in the chloroplast ortholog (Morden and Golden, 1991).

The oxygen evolving complex (OEC) in *P. hollandica* PCC 9006 lacks proteins PsbP (17 kDa) and PsbQ (23 kDa) typical of chloroplasts (Mor et al., 1993). The interaction of OEC with Cl− and Ca2+ is provided by the hydrophobic Mn-stabilizing protein PsbO (37 kDa) different from the more amphiphilic analog in blue–green cyanobacteria (26.5 kDa; Mor et al., 1993; Barber and Kühlbrandt, 1999).

FACULTATIVE ANOXYGENIC PHOTOSYNTHESIS

Among green cyanobacteria, P. *hollandica* PCC 9006 is uniquely capable of photosynthesis with sulfide as electron donor and, respectively, without dioxygen production (Post and Arieli, 1997). OEC of this cyanobacterium retains activity at $\leq$1 mM sulfide. High resistance to sulfide stress is provided by the PsbO protein which protects the catalytic site of OEC (Mor et al., 1993; Post and Arieli, 1997). The transition to anoxygenic photosynthesis occurs at >1 mM sulfide when this substance inhibits both the biogenesis and activity of PSII, especially that of OEC.

A relative resistance to sulfide allows *P. hollandica* dominate the phytoplankton of water bodies with sulfide accumulating in warm seasons (Post and Arieli, 1997). Given the trophic state of shallow waters harboring *Prochlorothrix*, sulfide production in the anoxic sediments may mix with surface waters. Thus, sulfide resistance may be an essential adaptation in this habitat.

SUBSTRATE ASSIMILATION AND ENZYMOLOGY

CARBON ASSIMILATION

Data on the ability to use organic substrates (photomixotrophy or photoheterotrophy, in the light; chemoheterotrophy, in darkness) in *Prochlorothrix* is absent. Similarly to most blue–green cyanobacteria, *Prochlorothrix* demonstrates photoautoptrophy based on Calvin cycle with RuBisCO as key enzyme. *Prochlorothrix hollandica* PCC 9006 contains IB-subform of RuBisCO which clusters together with RuBisCO of blue–green β-cyanobacteria from the so-called "green" phylogenetic branch of the enzyme (Morden and Golden, 1991; Shimada et al., 1995; Chen et al., 2004; Badger et al., 2006).

RuBisCO of *P. hollandica* PCC 9006 is encoded by the dicistronic operon *rbcLS* which consists of genes for the large (L, 57 kDa) and small (S, 13 kDa) subunits, respectively. The holoenzyme (560 kDa) belongs to the L_8S_8-type (Hawthornthwaite et al., 1990; Morden and Golden, 1991). Enzymatic activity is maximum at 30°C and pH 8; Mg^{2+} is used as a cofactor (Hawthornthwaite et al., 1990).

NITROGEN ASSIMILATION

There are no data on the ability of *P. hollandica* PCC 9006 for aerobic nitrogen fixation. Initial attempts to induce nitrogenase under the conditions of nitrogen starvation proved unsuccessful (Burger-Wiersma et al., 1989). Furthermore, there are no *nif* genes sequences in the partially reconstructed genome of this cyanobacterium (Pinevich et al., unpublished data).

At the same time, *P. hollandica* PCC 9006 assimilates both ammonium and nitrate. Maximum growth rate in culture conditions is observed at 0.75 mM NH_4^+, whereas growth is inhibited at 3 mM. Growth is also absent if 1.5 mM urea substitutes for nitrate, indicating lack of the urease enzyme (Burger-Wiersma et al., 1989).

PHOSPHORUS ASSIMILATION

According to field experiments, the most extensive growth of *P. hollandica* PCC 9006 takes place in those parts of water bodies where phytoplankton is limited by phosphorus deficiency (Burger-Wiersma et al., 1989). *Prochlorothrix hollandica* PCC 9006 is characterized by higher maximum rate of phosphorus uptake and by lower saturation constant for this substrate as compared to other filamentous cyanobacteria, in particular *Planktothrix* sp. (Ducobu et al., 2002; Dignum et al., 2005).

Special enzymology: RNAse P

This enzyme performs the maturation of 5′-end of tRNA and is ubiquitous in prokaryotes including plastids and mitochondria. *Prochlorothrix hollandica* PCC 9006 contains a rare type of this RNAse characterized by long domain P15/16, as well as by a GGU motif which binds 3′-CCA of pre-tRNA and is absent from the ribozymes of other cyanobacteria (Fingerhut and Schön, 1998).

PHYLOGENY

Tracing phylogeny of green cyanobacteria raises the questions regarding: (i) relations within the green cyanobacteria group; (ii) relations between green and blue–green cyanobacteria; (iii) relations between green cyanobacteria and simple plastids; (iv) the ancestor of green cyanobacteria; and (v) the origin of chlorophyll light-harvesting antenna.

Here, two phylogenies are involved. One of them is the general evolution of cyanobacteria reconstructed by the comparative analysis of the major informational (in particular, 16S rNNA gene and *rpoS*) and photosynthetic genes (in particular, *psbA* and *petE*). Secondly, it is the evolution of green cyanobacteria traced by the analysis of the *pcb* genes coding for the chlorophyll light-harvesting antenna.

16S rRNA GENE

According to this evolutionary criterion, green cyanobacteria are polyphyletic (Urbach et al., 1992). Paradoxically, *P. hollandica* PCC 9006 clusters close to the unicellular strain *Synechococcus* PCC 6301 (Pinevich et al., 2010). Detailed dendrograms showing the distribution of green cyanobacteria between separate clades of cyanobacterial tree, as well as mutual subordination of strains from the same genus, are presented elsewhere (Turner, 1997; Moore et al., 1998; Partensky et al., 1999; Miyashita et al., 2003; Partensky and Garczarek, 2003; Rocap et al., 2003; de los Rios et al., 2007; Münchhoff et al., 2007; Scanlan et al., 2009).

RpoC GENE

Another informational gene which helps reconstruct the evolutionary history of cyanobacteria is *rpoC1* coding for a subunit of the DNA dependent RNA polymerase. Here, again, green cyanobacteria were shown to be polyphyletic, and *P. hollandica* PCC 9006 groups with *Synechococcus* PCC 6301 (Palenik and Haselkorn, 1992).

The phylogenies of the major photosynthesis genes [*psaF*, coding for the conservative PsaF protein, a 21-kDa three-domain component of the reaction center complex; *psbA*, coding for the 32 kDa core PSII protein; *psbO*, coding for the Mn-stabilizing protein PsbO; and *petE*, coding for the copper-containing soluble protein plastocyanin (∼11 kDa), which donates electrons to PSI] repeat that of the 16S rRNA gene with green cyanobacteria being polyphyletic and *P. hollandica* PCC 9006 clustering with *Synechococcus* PCC 6301 (**Figures 4** and **5**; Pinevich et al., 2010).

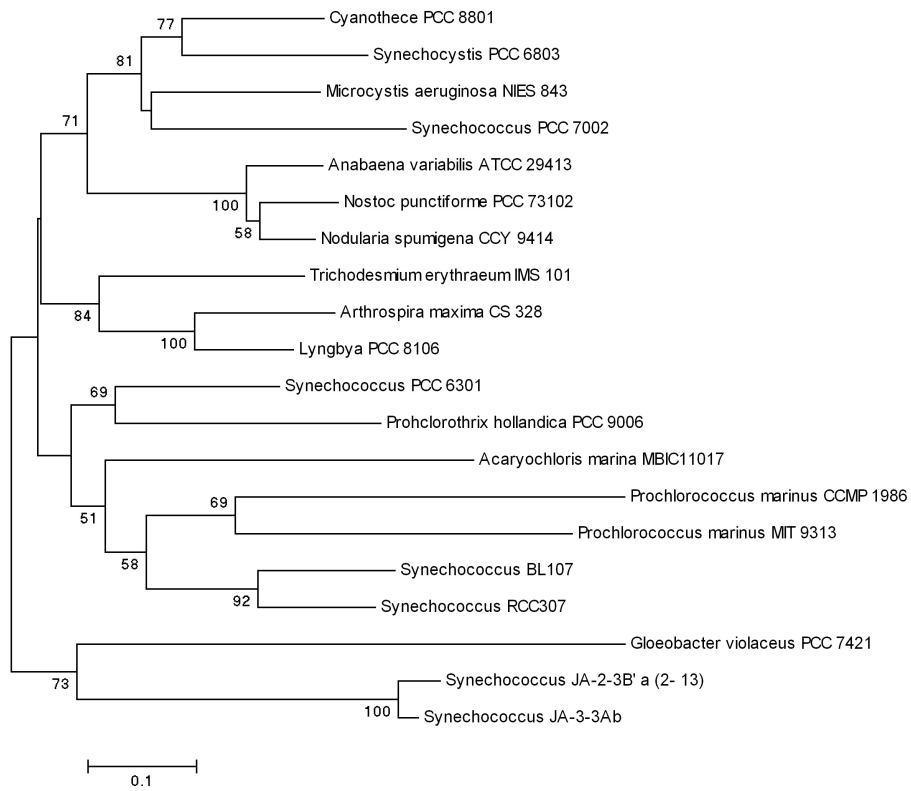

FIGURE 4 | Phylogenetic relationship of the PsaF protein constructed by neighbor-joining method using MEGA version 4 (Tamura et al., 2007). Selected bootstrap values (greater than 50%) based on 1,000 replications are shown at nodes.

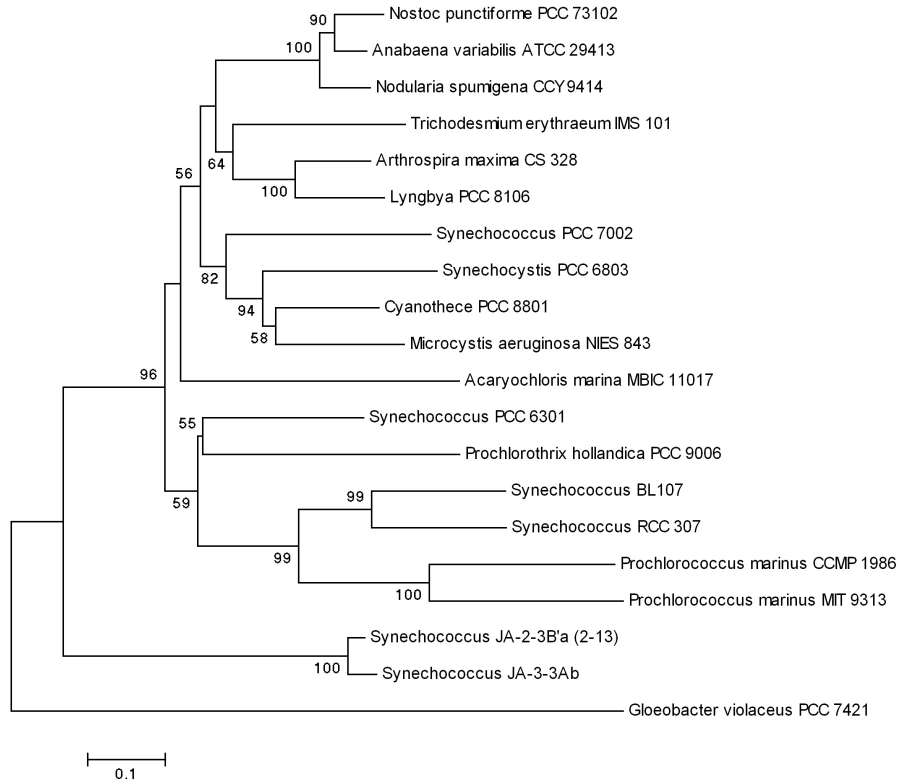

FIGURE 5 | Phylogenetic relationship of PsbO protein constructed by neighbor-joining method using MEGA version 4 (Tamura et al., 2007). Selected bootstrap values (greater than 50%) based on 1,000 replications are shown at nodes.

Pcb GENES

The *pcbABC* genes of *P. hollandica* PCC 9006 which code for the antenna proteins of family Pcb/*IsiA*/CP43 cluster together with their counterparts in unicellular green cyanobacteria from the genera *Acaryochloris* and *Prochloron* (Pinevich et al., 2010). The highly conserved proteins of Pcb/*IsiA*/CP43 family are thought to be inherited from a common ancestor of cyanobacteria. They might evolve according to two scenarios.

According to the first scenario, these proteins may have appeared in *Synechococcus*-like ancestor of *P. marinus* which inhabited oceanic systems poor in iron (Ting et al., 2002). In these stress conditions, they constitutively expressed both the *IsiA* (CP43′) protein and the phycobilisome. Among the descendants of this hypothetical cyanobacterium were phycoerythrin-rich strains of *Synechococcus*, as well as phycobiliprotein free or phycobiliprotein-poor (phycobilisome free) strains of *P. marinus*.

By the second scenario, *pcb* and *isiA* genes evolved independently by duplication and subsequent specialization of the copied *psbC*-like gene in a protocyanobacterium (Chen et al., 2005). This scenario is more plausible since it explains the existence of a set of *chl*-binding proteins in blue–green and green cyanobacteria.

Both scenarios assume a transient coexistence of the *chl*-based antenna with the phycobiliprotein-based antenna (Shimada et al., 2003).

GENES CODING FOR ENZYMES OF THE CHROMOPHORE BIOSYNTHESIS

The evolution of these genes is distinct from that of the *pcb* genes. In fact, presence of the conservative His residues in Pcb proteins is only a prerequisite of *chl* binding. In other words, the formation of *chl*-containing antennae, in particular the *chl a*/*b* antenna, needs biosynthetic enzymes for the respective chromatophores. Since the ancestor of Pcb proteins is thought to be *chl a*-binding protein (see above), the incorporation of *chl b*, a_2, b_2, and *d* in antennae of different green cyanobacteria suggests the formation of these pigments as byproducts in the metabolic pathway of *chl a*. In fact, monovinyl *chls* are synthesized from divinyl precursors by reductases, whereas *chl b* and *chl d* are formed by oxygenases (Beale, 2008).

The *cao* genes coding for *chl a* oxygenase in *P. hollandica* PCC 9006 and *P. didemni* are highly similar (Tomitani et al., 1999). Correspondingly, these green cyanobacteria did not acquire this gene independently, but rather the ability to synthesize *chl b* was a trait of common ancestor of cyanobactetria.

The evolutionary loss of phycobilins resulted in the appearance of green cyanobacteria like *P. hollandica* PCC 9006 and *P. didemni*, while the loss of *chl b* resulted in the lineage of blue–green cyanobacteria, which allows to consider both these green cyanobacteria as a model for the protocyanobacterium (Tomitani et al., 1999).

RELATION OF GREEN CYANOBACTERIA TO THE ORIGIN OF THE SIMPLE CHLOROPLAST

Although cyanobacterial origin of the simple chloroplast is beyond doubt (Morden et al., 1992; McFadden, 1996), the specific nature of ancestry is debatable.

The *Prochloron*-type green cyanobacteria were rejected as a candidate, since Pcb proteins are dissimilar with the members of CAB family (La Roche et al., 1996; van der Staay et al., 1998). This conclusion prematurely deprived green cyanobacteria of any role in the origin of the simple chloroplast.

However, it should be noted that Pcb proteins cluster with PsbC/*IsiA*(CP43′) proteins (Bullerjahn et al., 1987, 1990; van der Staay and Staehelin, 1994; Nikolaitchik and Bullerjahn, 1998; van der Staay et al., 1998; Partensky et al., 1999). This finding, as well as data on the relationships between green cyanobacteria and their blue–green relatives (see above) help restore the role of the former as both the ancestor of the chloroplast, as well as the ancestor of oxygenic phototrophic bacteria.

CHLOROPLAST ORIGINS

The ancestor of chloroplasts is hypothesized to possess both the *pcb* genes, coding for *chl*-binding antenna proteins, and the *pbp* genes coding for phycobilisome (Tomitani et al., 1999). This cyanobacterium, engulfed by a non-photosynthetic protist, became a precursor of three lineages of the simple chloroplasts (**Figure 6**).

One lineage is represented by the chloroplast of *Chlorophyceae*/*Charophyceae*/*Plantae* which lost the ancestral *pcb* and *pbp* genes. The loss of "old" *chl a*/*b*-binding Pcb proteins was compensated by the acquisition of convergent "new" *chl a*/*b*-binding CAB proteins.

Two other lineages are represented by the chloroplasts of *Glaucocystophyceae* and *Rhodophyceae* which lost the ancestral *pcb* genes but retained the ancestral *pbp* genes.

CYANOBACTERIAL ORIGINS

Cyanobacteria are hypothesized to share the ancestor with chloroplasts, i.e., the primordial cyanobacterium had both the *pcb* genes, coding for *chl*-binding antenna proteins, and the *pbp* genes coding for phycobilisome (Tomitani et al., 1999). This cyanobacterium became a precursor of two lineages of cyanobacteria (**Figure 6**).

One lineage, resulting from the loss of ancestral *pcb* genes is represented by blue–green cyanobacteria. The other lineage originating from the complete or partial loss of ancestral *pbp* genes is represented by green cyanobacteria. Noteworthy, the latter were not chloroplast ancestors.

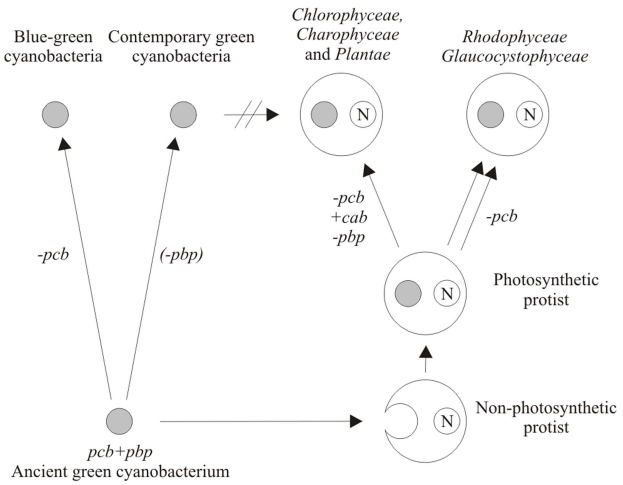

FIGURE 6 | A possible phylogenetic scenario for the origin of green cyanobacteria, blue–green cyanobacteria, and simple plastids. See text for the explanation. N denotes cell nucleus.

Interestingly, the genes responsible for *chl b* synthesis were divergently inherited by green cyanobacteria and chloroplasts.

GENERAL CONCLUSION

The primordial cyanobacterium which possessed both the *pcb* and *pbp* genes is by definition a green cyanobacterium Therefore, the ancient green bacteria should be reconsidered as key players of the evolutionary process which resulted in the biodiversity of cyanobacteria and plastids.

CONCLUDING REMARKS

Cyanobacteria of the genus *Prochlorothrix*, in contrast to the other cyanobacteria, are both very rare and largely incapable of axenic growth. They combine trivial features (primarily, oxygenic photosynthesis) with specific, yet obscure aspects of homeostasis and competitive potential. The analysis of their environmental and symbiotic ecology can help better understand this uniqueness. Thereby, the complete annotation of *P. hollandica* PCC 9006 genome is important, as well as search and isolation of new strains of the genus.

ACKNOWLEDGMENTS

We are grateful to Dr. Svetlana Averina and Dr. Olga Gavrilova for fruitful collaboration. Our thanks are due toYaroslav Borisov who participated in the annotation of *P. hollandica* PCC 9006 genes.

REFERENCES

Amaral-Zettler, L. A., Rocca, J. D., Lamontagne, M. G., Dennett, M. R., and Gast, R. J. (2008). Changes in microbial community structure in the wake of Hurricanes Katrina and Rita. *Environ. Sci. Technol.* 42, 9072–9078.

Aziz, R. K, Bartels, D., Best, A. A., DeJongh, M., Disz, T., Edwards, R. A., Formsma, K., Gerdes, S., Glass, E. M., Kubal, M., Meyer, F., Olsen, G. J., Olson, R., Osterman, A. L., Overbeek, R. A., McNeil, L. K., Paarmann, D., Paczian, T., Parrello, B., Pusch, G. D., Reich, C., Stevens, R., Vassieva, O., Vonstein, V., Wilke, A., and Zagnitko, O. (2008). The RAST Server: rapid annotations using subsystems technology. *BMC Genomics* 9, 75.

Badger, M. R., Price, G. D., Long, B. M., and Woodger, F. J. (2006). The environmental plasticity and ecological genomics of the cyanobacterial CO2 concentrating mechanism. *J. Exp. Bot.* 57, 249–265.

Barber, J., and Kühlbrandt, W. (1999). Photosystem II. *Curr. Opin. Struct. Biol.* 9, 469–475.

Beale, S. I. (2008). Photosynthetic pigments: perplexing persistent prevalence of "superfluous" pigment production. *Curr. Biol.* 18, 342–343.

Bergmann, I., Geiß-Brunschweiger, U., Hagemann, M., and Schoor, A. (2008). Salinity tolerance of the chlorophyll b-synthesizing cyanobacterium Prochlorothrix

hollandica strain SAG 10.89. *Microbiol. Ecol.* 55, 685–696.

Bibby, T. S., Nield, J., and Barber, J. (2001). Three-dimensional model and characterization of the iron stress-induced CP43'-photosystem I supercomplex isolated from the cyanobacterium Synechocystis PCC 6803. *J. Biol. Chem.* 276, 43246–43252.

Bibby, T. S., Nield, J., Chen, M., Larkum, A. W., and Barber, J. (2003). Structure of a photosystem II supercomplex isolated from Prochloron didemni retaining its chlorophyll a/b light-harvesting system. *Proc. Natl. Acad. Sci.* 100, 9050–9054.

Boichenko, V. A., Pinevich, A. V., and Stadnichuk, I. N. (2007). Association of chlorophyll a/b-binding Pcb proteins with photosystems I and II in Prochlorothrix hollandica. *Biochim. Biophys. Acta* 1767, 801–806.

Bryant, D. A. (1986). The cyanobacterial photosynthetic apparatus: comparison to those of higher plants and photosynthetic bacteria. *Can. Bull. Fish. Aquat. Res.* 214, 423–500.

Bullerjahn, G. S., Jensen, T. S., Sherman, D. M., and Sherman, L. A. (1990). Immunological characterization of the P proteins from chlorophyll a/b antenna in Prochlorothrix hollandica and Prochloron sp. *FEMS Microbiol. Lett.* 67, 99–106.

Bullerjahn, G. S., Matthijs, H. C. P., Mur, L. R., and Sherman, L. A. (1987). Chlorophyll-protein composition of the thylakoid membrane from Prochlorothrix hollandica, a prokaryote containing chlorophyll b. *Eur. J. Biochem.* 168, 295–300.

Bullerjahn, G. S., and Post, A. F. (1993). The prochlorophytes: are they more than just chlorophyll a/b cyanobacteria? CRC Crit. *Rev. Microbiol.* 19, 43–59.

Bumba, L., Prasil, O., and Vacha, F. (2005). Antenna ring around trimeric photosystem I in chlorophyll b containing cyanobacterium Prochlorothrix hollandica. *Biochim. Biophys. Acta* 1708, 1–5.

Burger-Wiersma, T., and Post, A. F. (1989). Functional analysis of the photosynthetic apparatus of Prochlorothrix hollandica (Prochlorales), a chlorophyll b containing prokaryote. *Plant Physiol.* 91, 770–774.

Burger-Wiersma, T., Stal, L. J., and Mur, L. R. (1989). *Prochlorothrix hollandicagen.* nov., sp. nov., a filamentous oxygenic photoautotrophic procaryote containing chlorophylls a and b: assignment to *Prochlovotrichaceae* fam. nov. and order Prochlorales Florenzano, Balloni, and Materassi 1986, with emendation of the ordinal description. *Int. J. Syst. Bacteriol.* 39, 250–257.

Castenholz, R. W. (2001). "Phylum BX Cyanobacteria," in *Bergey's Manual of Systematic Bacteriology*, eds D. R. Boone, R. W. Castenholz, and G. M. Garrity (New York: Springer-Verlag), 473–599.

Castiglioni, B., Rizzi, E., Frosini, A., Sivonen, K., Rajaniemi, P., Rantala, A., Mugnai, M. A., Ventura, S., Wilmotte, A., Boutte, C., Grubisic, S., Balthasart, P., Consolandi, C., Bordoni R., Mezzelani A., Battaglia, C., and De Bellis, G. (2004). Development of a universal microarray based on the ligation detection reaction and 16S rRNA gene polymorphism to target diversity of Cyanobacteria. *Appl. Environ. Microbiol.* 70, 7161–7172.

Chen, F., Wang, K., Kan, J., Suzuki, M. T. and Wommack, K. E. (2004). Phylogenetic diversity of Synechococcus in the Chesapeake Bay revealed by ribulose-1,5-bisphosphate carboxylase-oxygenase (RuBisCO) large subunit gene (rbcL) sequences. *Aquat. Microb. Ecol.* 36, 153–164.

Chen, M., Hiller, R. G., Howe, C. J., and Larkum, A. W.D. (2005). Unique origin and lateral transfer of prokaryotic chlorophyll-b and chlorophyll-d light-harvesting systems. *Mol. Biol. Evol.* 22, 21–28.

Chen, M., Quinnell, R. G., and Larkum, A. W. D. (2002). The major light-harvesting pigment protein of Acaryochloris marina. *FEBS Lett.* 514, 149–152.

Chisholm, S. W., Olson, R. J., Zettler, E. R., Goericke, R., Waterbury, J. B., and Welschmeyer, N. A. (1988). A novel free-living prochlorophyte abundant in the oceanic euphotic zone. *Nature* 334, 340–343.

Cohen, Z., Margheri, M., and Tomaselli, L. (1995). Chemotaxonomy of cyanobacteria. *Phytochemistry* 40, 1155–1158.

Coleman, A. W., and Lewin, R. A. (1983). The disposition of DNA in Prochloron (Prochlorophyta). *Phycologia* 22, 209–212.

Dekker, J. P., and Boekema, E. J. (2005). Supramolecular organization of thylakoid membrane proteins in green plants. *Biochim. Biophys. Acta* 1706, 12−−39.

de los Rios, A., Grube, M., Sancho, L. G., and Ascaso, C. (2007). Ultrastructural and genetic characteristics of endolithic cyanobacterial biofilms colonizing Antarctic granite rocks. *FEMS Microbiol. Ecol.* 59, 386–395.

Dignum, M., Matthijs, H. C. P., Pel, R., Laanbroek, H. J., and Mur, L.R. (2005). "Nutrient limitation of freshwater cyanobacteria," in *Harmful Cyanobacteria*, eds J. Huisman, H. C. P. Matthijs, P. M. Visser (Dordrecht: Kluwer Academic Publishers), 65–86.

Ducobu, H., Huisman, J., Jonker, R. R., and Mur, L. R. (2002). Competition between a prochlorophyte and a cyanobacterium under various phosphorus regimes: comparison with the Dropp model. *J. Phycol.* 34, 467–476.

Dufresne, A., Salanoubat, M., Parnensky, F., Artiguenave, F., Axmann, I. M., Barbe, V., Duprat, S., Galperin, M. Y., Koonin, E. V., Le Gall, F., Makarova, K. S., Ostrowski, M., Oztas, S., Robert, C., Rogozin, I. B., Scanlan, D. J., Tandeau de Marsac, N., Weissenbach, J., Wincker, P., Wolf, Y. I., and Hess, W. R. (2003). Genome sequence of the cyanobacterium Prochlorococcus marinus SS120, a nearly minimal oxyphototrophic genome. *Proc. Natl. Acad. Sci. U.S.A.* 100, 10020–10025.

Engle, J. M., Burkhart,W., Sherman, D. M., and Bullerjahn, G. S. (1991). Purification and characterization of a surface-associated carotenoid-binding complex from the photosynthetic prokaryote, Prochlorothrix hollandica. *Arch. Microbiol.* 155, 453–458.

Fingerhut, C., and Schön, A. (1998). Sequence and functional characterization of RNAse P RNA from the chl a/b containing cyanobacterium Prochlorothrix hollandica. *FEBS Lett.* 428,161–164.

Garczarek, L., Hess, W. R., Holzendorff, J., van der Staay, G. W. M., and Partensky, F. (2000). Multiplication of antenna genes as a major adaptation to low light in a marine prokaryote. *Proc. Natl. Acad. Sci. U.S.A.* 97, 4098–4101.

Geiß, U., Bergmann, I., Blank, M., Schumann, R., Hagemann, M., and Schoor, A. (2003). Detection of Prochlorothrix in brackish waters by specific amplifications of pcb genes. *Appl. Environ. Microbiol.* 69, 6243–6249.

Geiß, U., Selig, U., Schumann, R., Steinbruch, R., Bastrop, R., Hagemann, M., and Schoor, A. (2004). Investigations on cyanobacterial diversity in a shallow estuary (Southern Baltic Sea) including genes relevant to salinity resistance and iron starvation acclimation. *Environ. Microbiol.* 6, 377–387.

Giddings, T. H, Withers, N. W., and Staehelin, L. A. (1980). Supramolecular structure of stacked and unstacked regions of the photosynthetic membranes of Prochloron sp., a prokaryote. *Proc. Natl. Acad. Sci. U.S.A.* 77, 352–356.

Golecki, J. R., and Jürgens, U. J. (1989). Ultrastructural studies on the membrane systems and cell inclusions of the filamentous prochlorophyte Prochlorothrix hollandica. *Arch. Microbiol.* 152, 77–82.

Green, B. R., and Durnford, D. G. (1996).The chlorophyll-carotenoid proteins of oxygenic photosynthesis. *Annu. Rev. Plant Physiol. Plant Mol. Biol.* 47, 685–714.

Greer, K. L. (1991). Nucleotide sequence of psbB from Prochlorothrix hollandica. *Plant Mol. Biol.* 17, 915–917.

Greer, K. L., and Golden, S. S. (1992). Conserved relationship between psbH and petBD genes: presence of a shared upstream element in Prochlorothrix hollandica. *Plant Mol. Biol.* 19, 355–365.

Gulati, R. D., Ejsmont-Karabin, J., and Postema, G. (1993). Feeding in Euchlanis dilatata lucksiana Hauer on filamentous cyanobacteria and a prochlorophyte. *Hydrobiologia* 255/256, 269–274.

Hawthornthwaite, A. M., Beanland, T. J., Howe, C. J., and Codd, G. A. (1990). The ribulose bisphosphate carboxylase/oxygenase of Prochlorothrix hollandica: purification, subunit structure and partial N-terminal sequence analysis of the large subunit. *Z. Naturforsch.* 45S, 733–738.

Helfrich, M., Ross, A., and King, G. C. (1999). Identification of 8-vinyl-prochlorophyllide a in phototrophic prokaryotes and algae: chemical and spectroscopic properties. *Biochim. Biophys. Acta.* 1410, 262–272.

Herbstová, M., Litvin, R., Gardian, Z., Komenda, J., and Vácha, F. (2010). Localization of Pcb antenna complexes in the photosynthetic prokaryote Prochlorothrix hollandica. *Biochim. Biophys. Acta* 1797, 89–97.

Herdman, M. (1981). Deoxyribonucleic acid base composition and genome size of Prochloron. *Arch. Microbiol.* 129, 314–316.

Hess, W. R., Parnensky, F., van der Staay, G. W. M., Garcia-Fernandez, J. M., Börner, T., and Vaulot, D. (1996). Coexistence of phycoerythrin and chlorophyll a/b antenna in a marine prokaryote. *Proc. Natl. Acad. Sci. U.S.A.* 93, 11126–11130.

Hiller, R. G., and Larkum, A. W. D. (1985). The chlorophyll-protein complexes of Prochloron sp.

Prochlorophyta). *Biochim. Biophys. Acta* 806, 107–115.

Hinterstoisser, B., Cichna, M., Kunter, O., and Peschek, G. A. (1993). Cooperation of plasma and thylakoid membranes for the biosynthesis of chlorophyll in cyanobacteria: the role of the thylakoid centers. *J. Plant Physiol.* 142, 407–413.

Katoh, T., Tanaka, A., and Mimuro, M. (1993). Xanthosomes: supramolecular assemblies of xanthophyll-chlorophyll a/c-protein complexes. *Meth. Enzymol.* 214, 402–412.

Kotai, J. (1972). *Instructions for Preparation of Modified Nutrient Solution Z8 for Algae.* Oslo: Norwegian Institute for Water Research, B11–B69.

Laloui, W., Palinska, K., Rippka, R., Partensky, F., De Marsac, N. T., Herdman, M., and Iteman, I. (2002). Genotyping of axenic and non-axenic isolates of the genus Prochlorococcus and the OMGF-"Synechococcus" clade by size, sequence analysis or RFLP of the Internal Transcribed Spacer of the ribosomal operon. *Microbiology* 148, 453–465.

La Roche, J., van der Staay, G. W. M., Partensky, F., Ducret, A., Aebersold, R., Li, R., Golden, S. S., Hiller, R. G., Wrench, P. M., Larkum, A. W., and Green, B. R. (1996). Independent evolution of the prochlorophyte and green plant chlorophyll a/b light-harvesting proteins. *Proc. Natl. Acad. Sci. U.S.A.* 93, 15244–15248.

Lewin, R.A. (1981). "The Prochlorophytes," in *The Prokaryotes. A Handbook on Habitats, Isolation, and Identification of Bacteria*, eds M. P. Starr, H. Stolp, H. G. Trüper, A. Balows, and H. G. Schlegel (Berlin: Springer-Verlag), 257–266.

Lewin, R. A., Cheng, L., and Lafargue, F. (1980). Prochlorophytes in the Caribbean. *Bull. Mar. Sci.* 30, 744–745.

Marquardt, J., Hu, Q., Iwasaki, I., Miyashita, H., Kurano, N., Miyachi, S., and Mörschel, E. (1998). "The structure of the biliprotein aggregates of the chl d-containing prokaryote Acaryochloris marina" in *Photosynthesis: Mechanism and Effects,* ed. G. Garab (Dordrecht: Kluwer Academic Publisher), 217–220.

McFadden, G. I. (1996). Endosymbiosis and evolution of the plant cell. *Curr. Opin. Plant Biol.* 2, 513–519.

McKay, R. M. L., and Gibbs, S. P. (1990). Composition and function of pyrenoids: cytochemical and immunocytochemical approaches. *Can. J. Bot.* 69, 1040–1052.

Miller, K. R., Jacob, J. S., Burger-Wiersma, T., and Matthijs, H. C. (1988). Supramolecular structure of the thylakoid membrane of Prochlorothrix hollandica: a chlorophyll b-containing prokaryote. *J. Cell Sci.* 91, 577–586.

Miyashita, H., Adachi, K., Kurano, N., Ikemoto, H., Chihara, M., and Miyachi, S. (1996). Chlorophyll d as a major pigment. *Nature* 383, 402.

Miyashita, H., Ikemoto, H., Kurano, N., Miyachi, S., and Chihara, M. (2003). Acaryochloris marina gen. et sp. nov. (Cyanobacteria), an oxygenic photosynthetic prokaryote containing chl d as a major pigment. *J. Phycol.* 39, 1247–1253.

Moore, L. R., Rocap, G., and Chisholm, S. W. (1998). Physiology and molecular phylogeny of coexisting Prochlorococcus ecotypes. *Nature* 393, 464–467.

Mor, T. S., Post, A. F., and Ohad, I. (1993). The manganese stabilizing protein (MSP) of Prochlorothrix hollandica is a hydrophobic membrane-bound protein. *Biochim. Biophys. Acta* 1141, 206–212.

Morden, C. W., Delwiche, C. F., Kuhsel, M., and Palmer, J. D. (1992). Gene phylogenies and the endosymbiotic origin of plastids. *BioSystems* 28, 75–90.

Morden, C. W., and Golden, S. S. (1991). Sequence analysis and phylogenetic reconstruction of the genes encoding the large and small subunits of the ribulose-1,5-bisphosphate carboxylase/oxygenase from the chlorophyll-containing prokaryote Prochlorothrix hollandica. *J. Mol. Evol.* 32, 379–395.

Münchhoff, J., Hirose, E., Maruyama, T., Sunairi, M., Burns, B. P., and Neilan, B. A. (2007). Host specificity and phylogeography of the prochlorophyte Prochloron sp., an obligate symbiont in didemnid ascidians. *Environ. Microbiol.* 9, 890–899.

Nagata, N., Tanaka, R., Satoh, S., and Tanaka, A. (2005). Identification of a vinyl reductase gene for chlorophyll synthesis in Arabidopsis thaliana and implications for the evolution of Prochlorococcus Species. *Plant Cell* 17, 233–240.

Nierzwicki-Bauer, S. A., Balkwill, D. L., and Stevens, S. E. (1983). Three-dimensional ultrastructure of a unicellular cyanobacterium. *J. Cell Biol.* 97, 713–722.

Nikolaitchik, O. A., and Bullerjahn, G. S. (1998). Transcript analysis of the pcbABC genes encoding the antenna apoproteins in the photosynthetic prokaryote Prochlorothrix hollandica. *FEMS Microbiol. Lett.* 68, 187–194.

Omata, T., Okada, M., and Murata, N. (1985). Separation and partial characterization of membranes from Prochloron sp. *Plant Cell Physiol.* 26, 579–584.

Palenik, B., and Haselkorn, R. (1992). Multiple evolutionary origins of prochlorophytes, the chlorophyll b-containing prokaryotes. *Nature* 55, 265–267.

Partensky, F., and Garczarek, L. (2003). "The photosynthetic apparatus of chlorophyll b- and d-containing cyanobacteria," in *Photosynthesis in Algae*, eds A. W. Larkum, S. E. Douglas, and J. A. Raven (Dordrecht: Kluwer Academic Publishers), 29–62.

Partensky, F., Hess, W. R., and Vaulot, D. (1999). Prochlorococcus, a marine photosynthetic prokaryote of global significance. *Microbiol. Mol. Biol. Rev.* 63, 106–127.

Pel, R., Floris ,V., Gons, H., and Hoogveld, H. L. (2004). Linking flow cytometric sorting and compound-specific 13C-analysis to determine population-specific isotopic signatures and growth rates in cyanobacteria-dominated lake plankton. *J. Phycol.* 40, 857–866.

Pinevich, A. V., Averina, S. G., and Velichko, N. V. (2010). Essays in the biology of prochlorophytes (in Russian, with English Table of Contents and Summary). St. Petersburg: Publishing House of St. Petersburg University.

Pinevich, A. V., Matthijs, H. C. P., Gavrilova O. V., Averina, S. G., and Velichko, N. V. (1996). New ultrastructural aspects of membranes and cell inclusions in Prochlorothrix hollandica (Prochlorales, Cyanobacteria). *Microbios* 87, 217–225.

Pinevich, A. V., Skulberg, O., Matthijs, H. C. P., Schubert, H., Willen, E., Gavrilova, O. V., and Velichko, N. (1999). Characterization of a novel chlorophyll b-containing Prochlorothrix species (Prochlorophyta) and its photosynthetic apparatus. *Microbios* 100, 159–174.

Post, A. F., and Arieli, B. (1997). Photosynthesis of Prochlorothrix hollandica under sulfide-rich anoxic conditions. *Appl. Environ. Microbiol.* 63, 3507–3511.

Post, A. F., and Bullerjahn, G. S. (1994). The photosynthetic machinery in prochlorophytes: structural properties and ecological significance. *FEMS Microbiol. Rev.* 13, 393–414.

Post, A. F., Gal, A., and Ohad, I. (1992). Characterization of light-activated reversible phosphorylation of a chlorophyll a/b antenna apoprotein in the photosynthetic prokaryote Prochlorothrix hollandica. *Biochim. Biophys. Acta* 1110, 75–82.

Rippka, R., Deruelles, J., Waterbury, J. B., Herdman, M., and Stanier, R. Y. (1979). Generic assignments, strain histories and properties of pure cultures of cyanobacteria. *Gen. Microbiol.* 111, 1–61.

Robinson, N. J., Robinson, J., Gupta, A., Bleasby, A. J., Whitton, B. A., and Morby, A. P. (1995). Singular over-representation of an octameric palindrome, HIP1, in DNA from many cyanobacteria. *Nucleic Acids Res.* 23, 729–735.

Rocap, G., Dispel, D. L., Waterbury, J. B., and Chisholm, S. W. (2002). Resolution of Prochlorococcus and Synechococcus ecotypes by using 16S–23S ribosomal DNA internal transcribed spacer sequences. *Appl. Environ. Microbiol.* 68, 1180–1191.

Rocap, G., Larimer, F. W., Lamerdin, J., Malfatti, S., Chain, P., Ahlgren, N. A., Arellano, A., Coleman, M., Hauser, L., Hess, W. R., Johnson, Z. I., Land, M., Lindell, D., Post, A. F., Regala, W., Shah, M., Shaw, S. L., Steglich, C., Sullivan, M. B., Ting, C. S., Tolonen, A., Webb, E. A., Zinser, E. R., and Chisholm, S. W. (2003). Genome divergence in two Prochlorococcus ecotypes reflects oceanic niche differentiation. *Nature* 424, 1042–1047.

Scanlan, D. J., Ostrowski, M., Mazard, S., Dufresne, A., Garczarek, L., Hess, W. R., Post, A. F., Hagemann, M., Paulsen, I., and Partensky, F. (2009). Ecological genomics of marine picocyanobacteria. *Microbiol. Mol. Biol. Rev.* 73, 249–299.

Schuster, G., Owens, D. C., Cohen, Y., and Ohad, I. (1984). Thylakoid polypeptide composition and light-independent phosphorylation of the chlorophyll a/b-protein in Prochloron, a prokaryote exhibiting oxygenic photosynthesis. *Biochim. Biophys. Acta.* 767, 596–605.

Schyns, G., Rippka, R., Namane, A., Campbell, D., Herdman, M., and Houmard, J. (1997). Prochlorothrix hollandica PCC 9006: genomic properties of an axenic representative of the chlorophyll a/b-containing oxyphotobacteria. *Res. Microbiol.* 148, 345–354.

Shimada, A., Yano, N., Kanai, S., Lewin, R. A., and Maruyama, T. (2003). Molecular phylogenetic relatioship between two symbiotic photo-oxygenic prokaryotes, Prochloron sp. and Synechocystis trididemni. *Phycologia* 42, 193–197.

Shimada, A. S., Kanai, T., and Maruyama, T. (1995). Partial

sequence of ribulose-1,5-bisphosphate carboxylase/oxygenase and the physiology of Prochloron and Prochlorococcus (Prochlorales). *J. Mol. Evol.* 40, 671–677.

Skulberg, O. (2008). Species of Prochlorothrix: a retrospective view with attention on taxonomy // Algol. *Studies* 126, 87–101.

Smith, J. K., Parry, J. D., Day, J. G., and Smith, R. J. (1998). A PCR technique based on the Hip1 interspersed repetitive, sequence distinguishes cyanobacterial species and strains. *Microbiology* 144, 2791–2801.

Tamura, K., Dudley, J., Nei, M., and Kumar, S. (2007). MEGA4: Molecular Evolutionary Genetics Analysis (MEGA) software version 4.0. *Mol. Biol. Evol.* 24, 1596–1599.

Tanaka, A., Ito, H., Tanaka, R., Yoshida, K., and Okada, K. (1998). Chlorophyll a oxygenase (CAO) is involved in chlorophyll b formation from chlorophyll a. *Proc. Natl. Acad. Sci. U.S.A.* 95, 12719–12723.

Ting, C. S., Rocap, G., King, J., and Chisholm, S. W. (2002). Cyanobacterial photosynthesis in the oceans: the origins and significance of divergent light-harvesting strategies. *Trends Microbiol.* 10, 134–142.

Tomitani, A., Okada, K., Miyashita H., Matthijs, H. C. P., Ohno, T., and Tanaka, A. (1999). Chlorophyll b and phycobilins in the common ancestor of cyanobacteria and chloroplasts. *Nature* 400, 159–162.

Turner, S. (1997). Molecular systematics of oxygenic photosynthetic bacteria. *Plant Syst. Evol.* 11, 13–52.

Urbach, E., Robertson, D. L., and Chisholm, S. W. (1992). Multiple evolutionary origins of prochlorophytes within the cyanobacterial radiation. *Nature* 355, 267–269.

van der Staay, G. W. M., Boekema, E. J., Dekker, J. P., and Matthijs, H. C. P (1993). Characterization of trimeric photosystem I particles from the prochlorophyte Prochlorothrix hollandica by electron microscopy and image analysis. *Biochim. Biophys. Acta* 1142, 189–193.

van der Staay, G. W. M., Brouwer ,A., Baard, R. L., van Mourikb, F., and Matthij, H. C. P. (1992). Separation of photosystems I and II from the oxychlorobacterium (prochlorophyte) Prochlorothrix hollandica and association of chlorophyll b binding antennae with photosystem II. *Biochim. Biophys. Acta* 1102, 220–228.

van der Staay, G. W. M., and Staehelin, L. A. (1994). Biochemical characterization of protein composition and protein phosphorylation patterns in stacked and unstacked thylakoid membranes of the prochlorophyte Prochlorothrix hollandica. *J. Biol. Chem.* 269, 24834–24844.

van der Staay, G. W. M., Yurkova, N., and Green, B. R. (1998). The 38 kDa chlorophyll a/b protein of the rokaryote Prochlorothrix hollandica is encoded by a divergent pcb gene. *Plant Mol. Biol.* 36, 709–716.

van Liere, L., Breebaart, L., and Dullemont, Y. J. (1989). Determining the relative number of prochlorophytes in lake phytoplankton using epifluorescence microscopy. *Br. Phycol. J.* 24, 391–394.

Wayne, L. G., Brenner, D. J., Cowell, R. R., Grimont, P. A. D., Kandler, O., Krichevsky, M. I., Moore, L. H., Murray, R. G. E., Stackebrandt, E., Starr, M. P., and Truper, H. G. (1987). Report of the ad hoc committee on reconciliation of approaches to bacterial systematic. *Int. J. Syst. Bacteriol.* 37, 463–464.

Zwart, G., Kamst-van Agterveld, M. P., van der Werff-Stacerman, I., Hagen, F., Hoogveld, H. L., and Gons, H. J. (2005). Molecular characterization of cyanobacterial diversity in a shallow eutrophic lake. *Environ. Microbiol.* 7, 365–377.

Conflict of Interest Statement: The authors declare that the research was conducted in the absence of any commercial or financial relationships that could be construed as a potential conflict of interest.

Received: 30 January 2012; accepted: 19 April 2012; published online: 21 May 2012.

*Citation: Pinevich A, Velichko N and Ivanikova N (2012) Cyanobacteria of the genus Prochlorothrix. Front. Microbio. **3**:173. doi: 10.3389/fmicb.2012.00173*

This article was submitted to Frontiers in Aquatic Microbiology, a specialty of Frontiers in Microbiology.

frontiers in
MICROBIOLOGY

REVIEW ARTICLE
published: 18 April 2012
doi: 10.3389/fmicb.2012.00138

The languages spoken in the water body (or the biological role of cyanobacterial toxins)

Aaron Kaplan[1]*, Moshe Harel[1], Ruth N. Kaplan-Levy[2], Ora Hadas[2], Assaf Sukenik[2] and Elke Dittmann[3]

[1] Department of Plant and Environmental Sciences, The Hebrew University of Jerusalem, Jerusalem, Israel
[2] The Yigal Allon Kinneret Limnological Laboratory, Israel Oceanographic and Limnological Research, Migdal, Israel
[3] Institut für Biochemie und Biologie, Universität Potsdam, Potsdam, Germany

Edited by:
George S. Bullerjahn, Bowling Green State University, USA

Reviewed by:
Michael R. Twiss, Clarkson University, USA
Greg Boyer, State University of New York, USA

***Correspondence:**
Aaron Kaplan, Department of Plant and Environmental Sciences, The Hebrew University of Jerusalem, Edmond J. Safra Campus, Givat Ram, Jerusalem 91904, Israel.
e-mail: aaron.kaplan@mail.huji.ac.il

Although intensification of toxic cyanobacterial blooms over the last decade is a matter of growing concern due to bloom impact on water quality, the biological role of most of the toxins produced is not known. In this critical review we focus primarily on the biological role of two toxins, microcystins and cylindrospermopsin, in inter- and intra-species communication and in nutrient acquisition. We examine the experimental evidence supporting some of the dogmas in the field and raise several open questions to be dealt with in future research. We do not discuss the health and environmental implications of toxin presence in the water body.

Keywords: aoa, cylindrospermopsin, microcystin, cyr, mcy

INTRODUCTION

"What determines who is there?" is a long standing but nevertheless intriguing biological/environmental question. Numerous field and laboratory studies, and modeling of the data thereof, were performed in an attempt to reveal the effects of biotic and abiotic parameters on the temporal and spatial dynamics of phytoplankton populations (Ogawa, 1988; Walsby, 1997; Abraham, 1998). There is a growing body of evidence that secondary metabolites play an important part in the shaping of the community composition through inter- and intra-species communication but, for the most part, their biological role, mode of action, and regulation of their production are poorly understood. One example is the evolutionary drivers for the richness and large diversity of secondary metabolites produced by various cyanobacteria, a phenomenon that we know little about. It has been proposed that at least part of the richness observed in the case of a *Lyngbya* sp. is due to improper systematic analysis and that several strains are in fact involved (Engene et al., 2011) but, if any, this argument strengthens the message that a large diversity of secondary metabolites is formed in this genus (Liu and Rein, 2010). A comprehensive chemotyping, i.e., analysis of the array of secondary metabolites within a given organism (Sivonen, 2008), combined with the application of genetic approaches using various genomic tools are required and to some extent emerging (Mejean et al., 2010; Jones et al., 2011). In the long run it will provide us with a complete array of metabolites produced and enable recognition of the genetic potential and its expression particularly under changing environmental conditions.

Cyanobacteria are known to produce a wide variety of secondary metabolites including non-ribosomally made peptides, polyketides, and alkaloids. Naturally most of the research on cyanobacterial secondary metabolites focused on those that were classified as toxic to eukaryotes, mainly microcystin, nodularin, saxitoxin, and cylindrospermopsin (Pearson et al., 2010), since their presence may constitute a serious threat to water quality in many freshwater bodies worldwide (Carmichael, 1997; Griffiths and Saker, 2003; Zegura et al., 2011). There is a growing body of evidence that regional and global climatic change may benefit various species of harmful cyanobacteria by increasing their growth rates, dominance, persistence, geographic distributions, and activity (see Paerl and Huisman, 2009; Sukenik et al., this issue).

Numerous publications have described the implications of cyanobacterial toxin production on environmental and health aspects but this is beyond the scope of the present paper. Here we discuss the nature and biological role of two cyanobacterial toxins, microcystin and cylindrospermopsin, for which experimentally based information has recently been obtained.

MICROCYSTIN

OCCURRENCE AND TOXICITY

Microcystins are the most frequently reported cyanobacterial toxins in freshwater environments and are regarded as a major health hazard and challenge to the quality of drinking water (Dittmann and Wiegand, 2006). Microcystins are predominantly produced by freshwater strains including *Microcystis*, *Planktothrix*, and *Anabaena* (Welker and von Dohren, 2006) but were also incidentally reported from terrestrial environments. Toxic and non-toxic strains usually co-exist in natural bloom samples due to the sporadic distribution of toxin biosynthesis genes in the producing genera (Via-Ordorika et al., 2004). Microcystin penetrates the liver where it inhibits eukaryotic protein phosphatases type 1 and 2A, eventually leading to liver hemorrhage and death (Runnegar et al., 1995). The hepatotoxin was implicated in a number of animal and human intoxications, the

most fatal case being reported from a hemodialysis center in Brazil where patients died with symptoms of hepatotoxicity after exposure to water from a nearby reservoir contaminated with cyanobacteria (Jochimsen et al., 1998). The cyclic heptapeptide displays the general structure *cyclo*(D-Ala-X-D-MeAsp-Z-Adda-D-Glu-MdhA) in which X and Z represent variable L amino acids. D-MeAsp is D-erythro-β-methyl-aspartic acid, MdhA is *N*-methyldehydroalanine and Adda is (2*S*,3*S*,8*S*,9*S*)-3-amino-9-methoxy-2,6,8-trimethyl-10-phenyldeca-4,6 dienoic acid (Botes et al., 1984). Many variants have been described in the scientific literature, mostly differing in amino acid positions X and Z (Sivonen and Jones, 1999; Welker and von Dohren, 2006). The related nodularins are exclusively produced by *Nodularia* strains in brackish water environments and possess the general structure *cyclo*(D-MeAsp-L-arginine-Adda-D-Glu-Mdhb), in which Mdhb is 2-(methylamino)-2-dehydrobutyric acid (Annila et al., 1996).

PHYSIOLOGICAL STUDIES ON MICROCYSTIN PRODUCTION

Research toward an understanding of the biological role of microcystin started in the 1980s when several research groups began to study the impact of environmental factors on the cellular toxin content. Generally, the production of microcystin by a single strain seems to be rather consistent with variations usually not exceeding a factor of four (Sivonen and Jones, 1999). This led to the general notion that microcystin production is directly correlated to growth, perhaps showing a linear correlation between cell division and toxin production (Orr and Jones, 1998). This was further examined by the development of a model for the prediction of cellular microcystin contents from growth rates in N-limited cultures (Long et al., 2001). This model is in agreement with data obtained in several studies that have reported high microcystin production rates in cultures with high nitrogen and high phosphorus concentrations that are not limited in growth (Sivonen et al., 1990; Vezie et al., 2002). From their data, Orr and Jones (1998) concluded that microcystin is not a secondary metabolite but rather displays attributes of an essential intracellular compound. The fact that microcystin and many other cyanobacterial "secondary metabolites" are produced from the beginning of the logarithmic phase indeed distinguishes them from secondary metabolites of many other microorganisms.

However, a number of other studies have reported effects of specific environmental factors on microcystin production. Lukac and Aegerter (1993) correlated low iron concentrations with an increased toxin production, whereas Utkilen and Gjolme (1992), detected higher microcystin production at high iron conditions. Other authors have suggested the impact of light, temperature, and pH (Vanderwesthuizen and Eloff, 1985; Rapala et al., 1997; Wiedner et al., 2003). Interestingly, some of the environmental factors had a differential effect on various isoforms of the toxin (Rapala et al., 1997). Many of the observed effects on microcystin formation might be due to a limiting response of growth to the respective parameter. The largest problem for the interpretation and comparison of the different studies, however, is the observed strain-specific difference in toxin production under standard growth conditions. The environmentally induced changes are far less pronounced than the differences in toxin contents measured in individual strains. Physiological studies could thus provide an overview about the influence of abiotic factors on microcystin production but could not provide a clue about the role of the toxin in the producing cells.

BIOSYNTHESIS, REGULATION, AND EVOLUTION OF MICROCYSTIN

A new era of research toward understanding the biological role of microcystin became possible with the identification of the *mcy* genes encoding the non-ribosomal complex for microcystin biosynthesis. The *mcy* clusters were first described for two strains of *Microcystis aeruginosa* (Nishizawa et al., 1999, 2000; Tillett et al., 2000). The genomic locus in *Microcystis* spans 55 kb and comprises 10 bidirectionally organized genes encoding non-ribosomal peptide synthetases (NRPS), polyketide-synthases (PKS), tailoring enzymes, and an ABC transporter (McyA-J; Nishizawa et al., 1999, 2000; Tillett et al., 2000). The *mcy* gene cluster was later also characterized for *Planktothrix* and *Anabaena* (Christiansen et al., 2003; Rouhiainen et al., 2004), a closely related gene cluster that could be assigned to the biosynthesis of nodularin in *Nodularia* (Moffitt and Neilan, 2004).

Knowledge about the biosynthesis gene cluster ultimately permitted analysis of the impact of environmental stimuli on the transcription of the *mcy* genes and a possible interaction of the promoter region with transcription factors. Several studies revealed a clear impact of light and iron-limiting conditions on *mcy* transcript abundance. Kaebernick and co-workers used the RNAse protection assay to quantify *mcy* transcripts under various light intensities and qualities. They observed that *mcy* transcripts are elevated above a critical threshold of light of about 30 μmol photons m^{-2} s^{-1} (Kaebernick et al., 2000). In a follow-up study, the authors could show alternative transcriptional start sites for the *mcyA-C* and *mcyD-J* operons in *Microcystis* under low light and high light conditions, respectively (Kaebernick et al., 2002). An increased *mcy* transcript accumulation under high light conditions was also found in *Planktothrix agardhii* (Tonk et al., 2005). A significant rise in the *mcy* transcript accumulation and an increased toxin production was observed following iron starvation (Sevilla et al., 2008). In contrast, the effect of light on transcription could not be correlated with higher toxin content per cell. Studies on the transcription of *mcy* genes were thus not only answering questions but also raising new ones. For example, differential effects on the transcription of various *mcy* genes were observed following various stresses such as oxidative stress. The *mcy*B was only 20% up-regulated whereas *mcy*A, *mcy*H, and *mcy*D transcripts increased by 270, 330, and 370%, respectively, in agreement with published data (Straub et al., 2011).

Screening of the 750-bp long bidirectional *mcy* promoter region between *mcy*A and *mcy*D revealed the presence of transcription factor binding sites for the ferric uptake regulator Fur and the global nitrogen regulator NtcA (Kaebernick et al., 2002). For both factors, binding to the *mcy* promoter region could be confirmed *in vitro* (Martin-Luna et al., 2006; Ginn et al., 2010; **Figure 1**). The Fur binding suggests a response of *mcy* genes to iron availability and redox status of the cell, which could explain the effects of high light and iron-limiting conditions on transcript abundance. On the other hand, NtcA binding typically mediates a response of cyanobacterial cells to nitrogen-limiting conditions

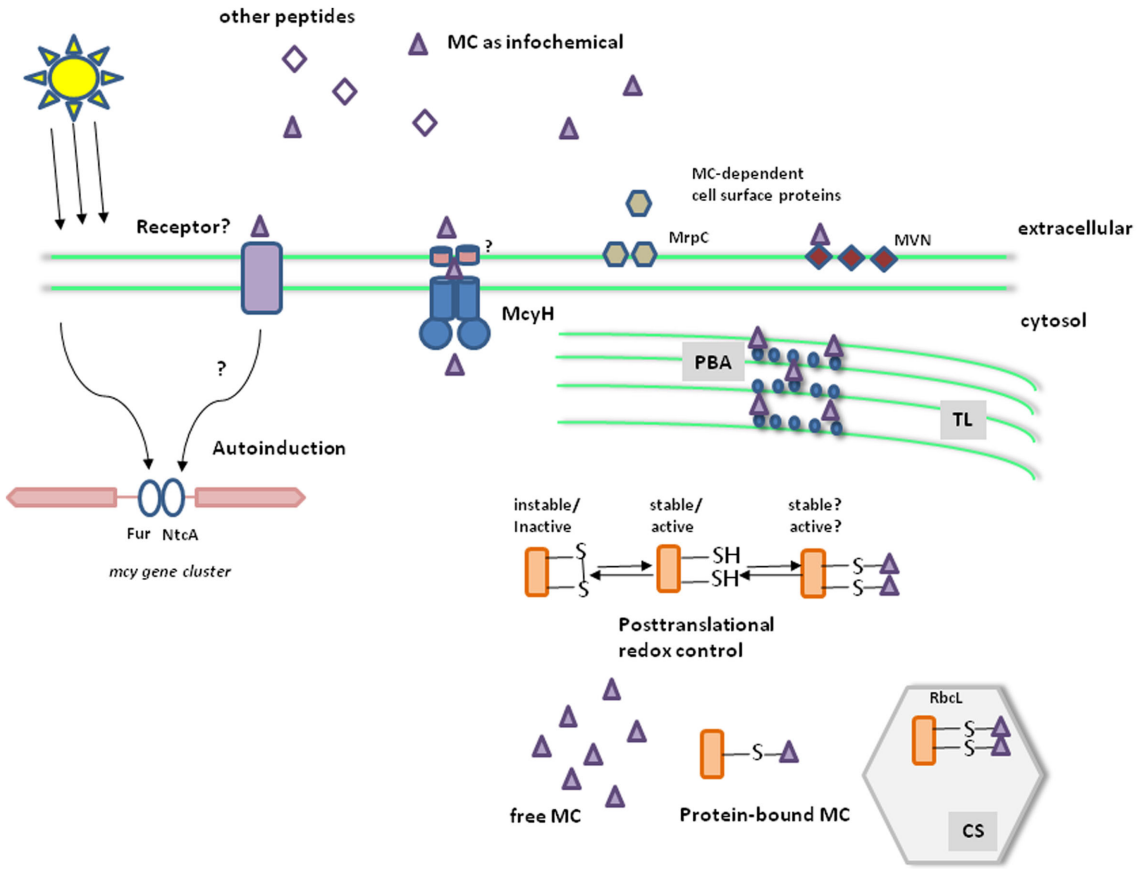

FIGURE 1 | Working model for the global role of microcystin in *M. aeruginosa*. Microcystin biosynthesis is up-regulated under high light and iron deficiency. Two transcriptional regulators, NtcA and Fur, were shown to bind to the bidirectional promoter region of the *mcy* operon (left). A fraction of the toxin is released from lysing cells and via the ABC transporter McyH, thereby acting as an infochemical for the neighboring cells (e.g., leading to an autoinduction of microcystin biosynthesis) and influencing extracellular proteins such as the lectin MVN and the glycoprotein MrpC. The microcystin receptor is still unknown (middle). Inside cells, microcystin is partly bound to proteins. Binding partners include proteins of the phycobilisomes (PBA) and the large subunit of Rubisco (RbcL). The covalent binding to cysteines is preferentially formed under highlight and oxidative stress conditions. Microcystin can thus interfere with the known redox control of proteins and affect their stability and/or activity (right). TL, thylakoids; CS, carboxysomes.

but the expected transcriptional changes (under different nitrogen concentrations) could not be confirmed (Sevilla et al., 2010). Considering the fact that the cellular redox state influences NtcA expression (Alfonso et al., 2001) and that NtcA and Fur regulons have been previously shown to overlap in cyanobacteria (Lopez-Gomollon et al., 2007), NtcA binding to the *mcy* promoter region may reflect the dependence of *mcy* transcription on the redox status of the cell rather than on nitrogen availability.

Elucidation of *mcy* genes in different genera also provided a basis for the reconstruction of the evolutionary history of these genes. Whereas the sporadic distribution of genes suggested an impact of horizontal gene transfer on *mcy* evolution, the comparison of *mcy* genes from various cyanobacterial genera with house-keeping genes could clearly rule out the possibility of a lateral transfer between different cyanobacterial genera. An evolutionary scenario has been proposed in which the ancestral *mcy* genes were already present in the last common ancestor of all present-day cyanobacteria (Rantala et al., 2004). The sporadic distribution was explained as a result of frequent gene losses. This hypothesis is supported by the observation of ongoing deletion events of partial or complete *mcy* gene clusters in natural and laboratory populations (Schatz et al., 2005; Christiansen et al., 2008). Prior to the phylogenetic analysis and related data showing dynamic changes in the mcy genes, a major role of microcystin as a feeding deterrent was widely accepted. However, since the last ancestor of all extant cyanobacteria preceded the appearance of the metazoans, a primary defense role of microcystin against eukaryote grazers is questionable. It was recently demonstrated that microcystin binds to thiol groups of various proteins (Zilliges et al., 2011; see below) similarly to its binding to certain eukaryotic protein phosphatases. It seems likely that the toxic effect of microcystin (due to inhibition of these phosphatases) reflects a recent evolution of these proteins rather than its primary role. In this respect it is worth mentioning that a recent bioinformatic study suggested that the *sxt* genes encoding saxitoxin, a cyanobacterial neurotoxin, are also ancient and that potassium rather than sodium channels was the original target of this toxin (Murray et al., 2011).

COMPARATIVE ANALYSIS OF *M. AERUGINOSA* AND MICROCYSTIN-DEFICIENT MUTANTS

As mentioned above, strain-specific differences in the rate of microcystin production are a major problem for the interpretation and comparison of studies on the impact of environmental stimuli. Moreover, comparative growth or feeding assays with toxic and non-toxic strains are biased by other strain-specific differences in addition to toxicity. The elucidation of microcystin biosynthesis genes provided the possibility to construct mutants that are deficient in microcystin production, but otherwise identical to the corresponding wild-type strains (Dittmann et al., 1997). The use of these mutants in comparative studies has significantly advanced our understanding about the biological role of microcystin.

The microcystin-deficient mutant Δ*mcy*B and the corresponding wild-type strain were used in feeding studies with *Daphnia*. These studies revealed that different *Daphnia* sp. could not distinguish between the wild-type and the microcystin-deficient mutant; both strains were ingested in similar rates (Rohrlack et al., 1999, 2001). These finding argued against a primary role as feeding deterrent as was widely accepted at the time. Wild-type and mutant were also compared for their growth and pigmentation under different light regimes (Hesse et al., 2001). The growth rates of the mutant and the WT were similar when grown at light intensities of 4–110 μmol photons m^{-2} s^{-1} but the absorption spectra in the range of photosynthetic active radiance varied significantly. The mutant cells possessed lower contents of chlorophyll a and of several carotenoids under these conditions (Hesse et al., 2001). Furthermore, a lower capability of mutant Δ*mcy*B to acclimate to low inorganic carbon concentrations was proposed (Jahnichen et al., 2007). These results were supported by growth competition studies using *M. aeruginosa* PCC7806 and mutant Δ*mcyB*. The microcystin-producing wild-type had a strong selective advantage under low CO_2 conditions (Van de Waal et al., 2011). A spontaneous *Microcystis* mutant, strain MG-J, bearing a deletion in mcy and unable to produce microcystins was isolated from a toxic wild-type strain MG-K (Schatz et al., 2005). Laboratory and field experiments comparing the wild-type with this spontaneous mutant indicated an advantage of the toxic strain over its non-toxic successor. When grown separated by a membrane, which allowed passage of the media but not the cells, MG-K severely inhibited the growth of MG-J. In addition, when MG strains were placed in dialysis bags in Lake Kinneret (Sea of Galilee), Israel, during the season in which *Microcystis* is often observed, cells of MG-J lysed but not MG-K (Schatz et al., 2005). Taken together, the data support the notion that microcystins play an important physiological role in the producing strains.

This, however, is difficult to accommodate with the observation that under natural conditions non-toxic colonies are present, sometimes in large proportion, together with toxic ones. What determines the proportion of microcystins-producing-cells in the natural *Microcystis* population is not clear. A thorough direct analysis of single colonies revealed that most of the colonies in the examined lake did not produce microcystins (Fastner et al., 2001).

TOWARD CLARIFICATION OF THE MECHANISTIC ROLE OF MICROCYSTIN-EXTRACELLULAR ROLE

The availability of the microcystin-deficient mutant also offered the possibility for a more detailed analysis of the role of microcystin at the molecular level. Proteomic comparisons between wild-type and mutant strains revealed the differential accumulation of a prominent protein spot. The protein identified by a reverse genetic approach was designated MrpA (microcystin-related protein A) and shows some similarity to the RhiA protein of the symbiotic strain *Rhizobium leguminosarum* biovar viciae (Dittmann et al., 2001). Moreover, the *mrpA* gene was co-transcribed with a second gene, *mrpB* that codes for a protein with high similarity to the RhiB protein encoded as part of the same *rhiABC* operon (Dittmann et al., 2001). The Rhi proteins were implicated in symbiotic nodule formation. Interestingly, the operon is under the control of extracellular acylhomoserine lactone (AHL) type signals in *Rhizobium* (Rodelas et al., 1999). This raised the possibility of a role of microcystin as an intercellular signal. Indeed, microcystin is released from *Microcystis* cells, in particular above a critical light threshold (Wiedner et al., 2003). Transport of microcystin through the inner membrane might be mediated by the activity of McyH, which shows homology to ABC transporter (**Figure 1**). A knock-out of the corresponding gene *mcyH*, however, leads to a complete loss of toxin production (Pearson et al., 2004) and thus the mutant could not be used to study the impact of McyH on internal microcystin level or assess a specific role in sensing of extracellular microcystin.

A possible extracellular role could nevertheless be assessed by an external addition of microcystin. Schatz et al. (2007) could show that addition of supernatants from cells lysed either mechanically or because of stress conditions leads to a strong upregulation of microcystin biosynthesis genes in the remaining cells. A less pronounced autoinduction effect could also be seen after addition of pure microcystin or other peptides, micropeptin, and microginin, produced by *Microcystis* which, together with microcystin, formed the stronger effect of the cell-free supernatant. Noticeably, the response of the remaining cells is strongly affected by the age of the culture but was hardly detected in older cultures. Analysis of the abundance of *mcy* transcripts clearly indicated a large accumulation at stationary phase thereby reducing the response to externally provided microcystin. On the other hand, *mcy* transcripts were hardly detected in cultures maintained in early log phase for several generations, but these cells responded strongly to the addition of microcystins or the cell-free supernatant by upregulating the expression of *mcy* genes. It was therefore suggested that microcystins serve as infochemicals; their release to the media by lysing cells due to various stressors is sensed by the rest of the *Microcystis* cells which upregulate *mcy* transcription (**Figure 1**; Schatz et al., 2007). Larger production of microcystin may promote the fitness of the *Microcystis* cells and their competitiveness with other phytoplankton species (reviewed by Pflugmacher, 2002; Babica et al., 2006).

Furthermore, several studies have supported a microcystin role in *Microcystis* colony formation. The expression pattern of two extracellular proteins, the lectin MVN (Kehr et al., 2006) and the glycoprotein MrpC (Zilliges et al., 2008) were strongly altered in

mutant strains lacking microcystin. MrpC is the dominant extracellular protein in *Microcystis* and directly implicated in cell–cell contacts between *Microcystis* cells (Zilliges et al., 2008). Both MVN and MrpC seem to be specific for certain *Microcystis* ecotypes. It is not clear yet, if microcystin is directly involved in morphotype formation and the mechanism whereby it influences the cell surface proteins (**Figure 1**).

EXPERIMENTAL SUPPORT FOR AN INTRACELLULAR ROLE OF MICROCYSTIN

As indicated, physiological experiments using wild-type and mutants suggested that the ability to produce microcystin is beneficial for the *Microcystis* cells. Elucidation of the *M. aeruginosa* PCC7806 genome enabled a more comprehensive analysis of molecular differences between wild-type and microcystin-deficient mutant such as via proteomic comparisons in cells maintained under various conditions such as high light and darkness (Zilliges et al., 2011). Remarkably, under all the conditions examined loss of microcystin led to considerable alteration in the protein pattern. Noticeably, a large number of spots could be assigned to Calvin–Benson cycle proteins, the phycobilisome, to redox-dependent reductases, and unidentified proteins (Zilliges et al., 2011). In particular, the differences in protein isoform formation were striking. Generally, the wild-type showed more protein isoforms than the microcystin-deficient mutant (Zilliges et al., 2011). In addition, it was shown that microcystin binds covalently to many of the differentially accumulating proteins *in vitro* and *in vivo* including phycobilisome antennae proteins and RbcL, the large subunit of Rubisco. This may at least partly explain the additional isoforms for proteins in the microcystin-producing wild-type (**Figure 1**; Zilliges et al., 2011) and the change in pigmentation during growth experiments (Hesse et al., 2001). Microcystin attachment to proteins was strongly enhanced under high light and oxidative stress conditions, raising the possibility of a consequent effect on their activity and stability. Many of the differentially accumulating proteins are indeed "cysteine-sensitive," i.e., subject to degradation upon oxidation of their cysteines following oxidative stress. A stabilizing effect of the microcystin binding was confirmed in the case of RbcL that was clearly more resistant to protease digestion in the wild-type (Zilliges et al., 2011). Moreover, growth experiments performed under oxidative stress or very high light conditions revealed a clear advantage for the microcystin-producing wild-type (Zilliges et al., 2011) and electron microscopy showed the localization of microcystin in the thylakoid and carboxysome areas (Gerbersdorf, 2006). These data may explain the differences in pigmentation and adaptation to low inorganic carbon concentrations discussed above and explain some of the controversial issues in earlier physiological studies. The fact that high light conditions lead to an increase in *mcy* transcription but not microcystin production is likely due to strong bias in microcystin detection due to covalent binding to proteins.

Another proteomic study revealed similar differences in the protein patterns between six different natural toxic and non-toxic strains, particularly in nine spots differentially accumulated in all toxic strains. Those were assigned to carbon–nitrogen metabolism and redox maintenance (Alexova et al., 2011). Differences in the acclimation to changing redox or light or carbon conditions may therefore be the main biotic parameters distinguishing toxic from non-toxic strains. This is at least partly supported by growth experiments that revealed an advantage of natural toxic over non-toxic strains under low (Schatz et al., 2005) but not under high carbon concentrations (Van de Waal et al., 2011), and an advantage of toxic strains under elevated temperatures (Dziallas and Grossart, 2011).

CYLINDROSPERMOPSIN

OCCURRENCE AND TOXICITY

Cylindrospermopsin (CYN) is an alkaloid toxin produced by several filamentous cyanobacteria including *Aphanizomenon ovalisporum* (hereafter *Aphanizomenon*), *Cylindrospermopsis raciborskii*, *Oscillatoria* sp. PCC 6506, *Anabaena bergii*, *Umezkia nathans*, *Aphanizomenon flos-aquae*, and others (Banker et al., 1997; Kaebernick and Neilan, 2001; Schembri et al., 2001; Preussel et al., 2006; Mazmouz et al., 2010). CYN was shown to accumulate in the environment (Kinnear, 2010) and inhibit protein and glutathione synthesis leading to cell death (Runnegar and Lu, 1994; Runnegar et al., 1995, 2002; Froscio et al., 2001; Metcalf et al., 2004). Effects of genotoxicity and on cholesterol levels have also been reported (Humpage et al., 2000, 2005; Shen et al., 2002; Reisner et al., 2004). Activity of cytochrome P450 enzyme system is apparently essential for the development of CYN toxicity (Runnegar et al., 1995). Damage to DNA (Straser et al., 2011) and carcinogenic activity were also suggested (Humpage et al., 2000; Murphy and Thomas, 2001). The role of specific residues essential for CYN toxicity is emerging in that the uracil moiety and the hydroxyl at position C7 are essential (Banker et al., 2001).

Due to its practical importance, emphasis was placed on abiotic conditions under which blooms of CYN-forming organisms may occur (Hadas et al., 1999, 2002; Burford and Davis, 2011; De Figueiredo et al., 2011) and to assessment of the effect of abiotic parameters on CYN production under field and laboratory conditions such as S and P limiting conditions (Bacsi et al., 2006). A comprehensive description of the many excellent studies on bloom conditions in various water bodies is beyond the scope of this paper. One example is the case of *Aphanizomenon* population in Lake Kinneret that showed close agreement between the optimal conditions for its growth in the laboratory and those which occurred during its bloom in 1994 (Hadas et al., 2002). An important aspect is the size of the inoculum; formation of akinetes; and their germination thereby raising the new population is poorly understood and requires further research (Sukenik et al., 2007). Maximal CYN formation in *C. raciborskii* is observed under light intensity higher than required for optimal growth (Dyble et al., 2006), suggesting that the redox state of the cells is involved. Apparently the status of the *C. raciborskii* culture, logarithmic, or stationary, is also critical to the rate of CYN formation. In both diazotrophic and nitrate supplied log phase cultures, CYN accumulation is linear with the growth rate but decoupling between the two parameters is observed at stationary phase (Hawkins et al., 2001). Similarly, differential effects of temperature on growth and CYN production in various *C. raciborskii* strains were observed (Saker and Griffiths, 2000). Taken together, the bulk of the data indicate that little is known about the cellular mechanisms involved in the regulation of CYN formation

and their interaction with the abiotic conditions experienced by the cells. Furthermore, as in the case of microcystin discussed above, comparison of published data is rather difficult because of lack of information on the exact conditions and the very different conditions in field and laboratory experiments.

THE *aoa*/*cyr* GENE CLUSTERS AND CYN BIOSYNTHESIS

The mechanism of CYN biosynthesis was partly resolved by following production in *C. raciborskii* cultures that were supplemented with stable ^{13}C, ^{18}O, ^{15}N, and ^{3}H isotopes, suggesting that five molecules of acetate are catalytically condensed by a polyketide-synthase (PKS) to form the carbon skeleton of CYN. Two other carbons and one of the nitrogen atoms of the guanidine moiety are probably donated by glycine. Guanidinoacetic acid was proposed as a source for two nitrogen atoms of the guanidino moiety used as a starter unit that initiates the biosynthetic process. The guanidinoacetic acid is probably formed by amidination of glycine by amidinotransferase but the exact donor of the other N atoms in the guanidino moiety, most likely arginine, has not been resolved (Burgoyne et al., 2000; Murphy and Thomas, 2001; Shalev-Alon et al., 2002; Pearson et al., 2010). Following the recognition that PKS and amidinotransferase are involved, Shalev-Alon et al. (2002) identified a genomic region in *Aphanizomenon* likely involved in CYN biosynthesis; recognition of a similar genomic region in *C. raciborskii* (Mihali et al., 2008) and *Oscillatoria* sp. strain PCC 6506 (Mazmouz et al., 2010) followed (**Figure 2**). It should be noted, however, that we are missing unequivocal evidence that the *aoa*/*cyr* gene clusters in these organisms are engaged in CYN biosynthesis. Although genes essential for CYN biosynthesis are present in these clusters, since these organisms are, so far, not amenable to genetic manipulations it was not possible to inactivate these genes and thereby provide a critical evidence that we have been seeking.

Support to the notion that the aoa/cyr gene cluster is indeed involved in CYN biosynthesis rests on the observation that a sulfotransferase-encoding gene essential for CYN synthesis, *cyrJ*, is present only in CYN-producing *C. raciborskii* strains (Mihali et al., 2008; Alster et al., 2010). Similarly, *cyrJ* is detected in four CYN-producing *Oscillatoria* strains but lacking in a non-CYN-producing strain (Mazmouz et al., 2010). Finally, non-toxic *Aphanizomenon* isolated from Lake Kinneret possess *aoaA* and *aoaC* but is missing *aoaJ* (Ballot et al., 2011).

Following the identification of the gene clusters putatively involved in CYN biosynthesis (**Figure 2** and below), an attractive (and most likely) scheme of the cascade of events leading to CYN formation was proposed (Mihali et al., 2008; Pearson et al., 2010; the reader is referred to these publications for a comprehensive discussion of the proposed scheme). However, decisive evidence that this is indeed the case must await biochemical confirmation. Furthermore, the proposed scheme does not account for the formation of two CYN analogs, 7-deoxycylindrospermopsin (7-deoxy-CYN) and 7-epicylindrospermopsin (7-epi-CYN) whose relative abundance varies in different cyanobacterial species (see Mazmouz et al., 2011), suggesting alterations in the activity and regulation of various steps in CYN production. It was suggested that CyrI, a 2-oxoglutarate-dependent iron oxygenase performs the last step of CYN biosynthesis from 7-deoxy-CYN (Mazmouz et al., 2011). These authors raised the possibility that a relaxed stereospecificity of CyrI produces both stereoisomers at position 7. Alternatively, an unidentified hydroxylase produces the 7-epi-CYN from 7-deoxy-CYN. The levels of CyrI or its activity in various CYN-producing cyanobacteria should be examined to account for the variability in the abundance of 7-deoxy-CYN compared to CYN; 7-deoxy-CYN is a minor product in *C. raciborskii* and *Raphidiopsis curvata* (Li et al., 2001) but a major one in *Lyngbya wollei* (Seifert et al., 2007). On the other hand 7-epi-CYN was detected only in *Aphanizomenon* in small quantities.

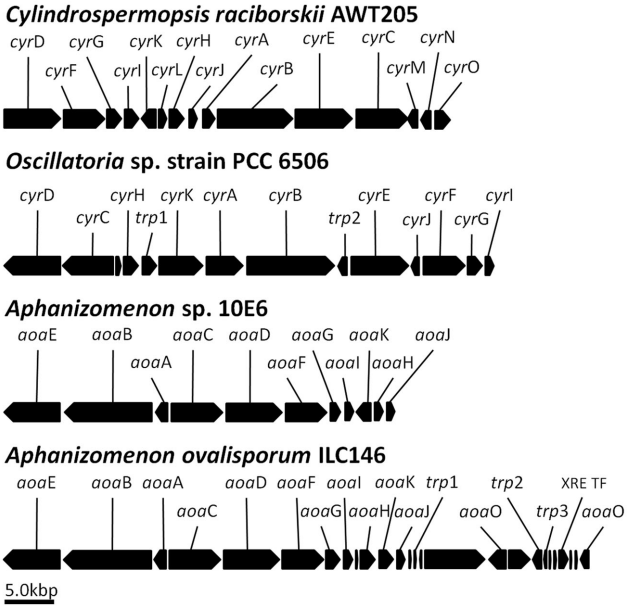

FIGURE 2 | The aoa/cyr clusters putatively involved in cylindrospermopsin biosynthesis in four cyanobacterial species. The scheme was constructed based on data for *Cylindrospermopsis raciborskii* (Mihali et al., 2008), *Oscillatoria* sp. PCC 6506C (Mazmouz et al., 2010), *Aphanizomenon* strain 10E6 (Accession Number, WOS, 000281239600017; Stuken and Jakobsen, 2010), and *Aphanizomenon ovalisporum* strain ILC146 (draft, yet unpublished sequence). Open reading frames without designation represent hypothetical proteins. Note the transposase (trp) genes and transcription factor (XRE TF) in the sequence of *Aphanizomenon* strain ILC146. The high sequence similarity between genes in the four species suggests a common ancestor but the significant differences in gene organization may indicate lateral gene transfers and transposases involvement (see text). Note that despite the presence of genes essential for CYN biosynthesis, we are still missing experimental evidence for the role of this cluster.

Figure 2 shows the genomic organization of the *aoa*/*cyr* in four CYN-producing cyanobacteria. In the absence of a detailed phylogenetic analysis it is hard to assess the development of these clusters but high similarity between the genes does indicate that they are evolutionarily related, possibly from a common ancestor, and that an horizontal gene transfer was involved (Stuken and Jakobsen, 2010). The differences in the gene organization clearly indicate divergence from this ancestor; shuffling of the aoa/*cyr* genes is substantial. The two *Aphanizomenon* clusters are quite similar but with two main exceptions. Two *aoaO* genes can be identified in strain ILC146 (draft, yet unpublished sequence) but we could not detect it in strain 10E6 (Accession Number, WOS, 000281239600017;

Stuken and Jakobsen, 2010). Altogether, the role of *aoaO*/*cyrO* in CYN production, if any, is not clear due to its low homology to other genes in the data bases. Again, a genetic approach could resolve this question. Compared with strain ILC146, the region of *aoaH-K* underwent reorganization in strain 10E6 with the *aoaK* encoded on the opposite strand and precedes *aoaH*. The presence of several transposase encoding genes is noted and they may be involved in the reorganizations.

REGULATION OF TRANSCRIPTION

Following the identification of the genomic regions putatively involved in CYN biosynthesis in *Aphanizomenon* (Shalev-Alon et al., 2002), *C. raciborskii* (see Neilan et al., 2008), and *Oscillatoria* strain PCC 6506 (Mazmouz et al., 2010), it became possible to study their regulation. In both *Aphanizomenon* species but not in *C. raciborskii* and *Oscillatoria* sp. (**Figure 2**) the amidinotransferase and polyketide-synthase encoding genes, *aoaA* and *aoaC*, respectively, are transcribed on the reverse strands. Analysis of the genomic region between them identified two transcription start points for each of these genes, differentially expressed under nitrogen and light-stress conditions (Shalev-Alon et al., 2002) and by phosphate availability (Bar-Yosef et al., 2010). Gel shift assays and DNA affinity columns isolated a protein that specifically binds to a 150-bp DNA fragment from the region between *aoaA* and *aoaC* in *Aphanizomenon* ILC146 and MS/MS analyses identified similarity to AbrB in other cyanobacteria and in *Bacillus* sp. Comparison of the native AbrB isolated from *A. ovalisporum* with that obtained after cloning and over-expression of *abrB* in *E. coli* identified specific post-translational modifications in the native cyanobacterial AbrB. This includes N-acetylation of residue T2 and methylation of specific residues, which are all missing in the protein expressed in *E. coli*. A gene encoding a putative acetylase was identified in the draft genomic sequence of *Aphanizomenon* ILC146 (yet unpublished) but, as mentioned with respect to the role of *aoa* genes, failure to genetically modify or inactivate genes in this organism does not enable recognition of the significance of these modifications to *aoaA*/*C* expression. The exact role of these post-translational modifications to the regulation of CYN formation is yet to be established. It is worth mentioning that AbrB-like proteins were thereafter recognized in various cyanobacteria. In *Synechocystis* sp. PCC6803 they were implicated in the regulation of several genes belonging to inorganic carbon uptake (Lieman-Hurwitz et al., 2009), nitrogen metabolism and C–N regulation (Yamauchi et al., 2011), the bidirectional hydrogenase (Oliveira and Lindblad, 2008), and in iron superoxide dismutase in *Nostoc* sp. strain PCC 7120 (Agervald et al., 2010). However, as much as information gained from these fields may contribute to our understanding of the involvement of these AbrB-like (designated CyAbrB) in CYN formation, a comprehensive analysis is beyond the scope of the present review.

THE BIOLOGICAL ROLE OF CYN

Laboratory and field experiments revealed the biological role and function of CYN (Bar-Yosef et al., 2010). Many microorganisms, from bacteria to yeast, respond to inorganic phosphate (Pi) limitation by expressing their PHO regulon and excretion of alkaline phosphatase (APase) thereby enhancing the supply of Pi from organic compounds and improving their competitiveness for resources and domination. Analysis of the abundance of *Aphanizomenon* and APase activity in Lake Kinneret during the summers of 1994–2009 showed strong correlation between these parameters, suggesting that APase emerged from Pi-limited filaments, but closer analysis clearly indicated this was not the case (Bar-Yosef et al., 2010). Application of enzyme labeled fluorescence (ELF) on lake samples showed APase in various organisms but not in *Aphanizomenon*, and staining by DAPI revealed high level of polyphosphate bodies (PPBs) in *Aphanizomenon*. ELF-APase signals were detected in *Aphanizomenon* only after it exploited the PPBs under prolonged Pi deprivation in laboratory cultures or toward the end of its natural bloom, in the autumn (Bar-Yosef et al., 2010). *Aphanizomenon* cultures respond to removal of external Pi by fast induction of CYN production and only part of its PHO regulon, including the high affinity Pi uptake system, PstS, and *phoD*, encoding an internal APase. In contrast, transcripts encoding extracellular APase and its activity were observed only after 5–7 days during which it consumes the internal Pi.

Addition of spent media from *Aphanizomenon* or CYN to various phytoplankton species (*Chlamydomonas reinhardtii* used as a model organism) led to induction of genes typically up-regulated by Pi-limitation (Bar-Yosef et al., 2010) and a large rise in the extracellular APase activity despite the presence of ample Pi in the medium. Using ELF-APase to stain mixed cultures of *Aphanizomenon* with *Chlamydomonas* or *Debarya* sp. showed APase in the latter two but not in *Aphanizomenon*. These data suggested that CYN induces the excretion of APase by *other* phytoplanktons in the water body. *Aphanizomenon* can then compete for the Pi released consequent to APase activity from other organisms. Apparently *Aphanizomenon* does it quite successfully, grows rapidly, and dominates in the seasonal bloom. CYN is used to "enslave" other organisms to fulfill the Pi demands of the "toxic" strains. It explains the observed rise in APase activity in the water body during the early phase of *Aphanizomenon* bloom and reveals a mechanism whereby it can form massive blooms despite limiting Pi conditions.

Noticeably, the response of target organisms to *Aphanizomenon* spent medium was greater than observed following application of purified CYN, although its concentration in the used media was considerably smaller. This suggests a synergistic involvement of other secondary metabolites in the used media, the nature of which is not known. It resembles the stronger induction of *mcy* genes in *Microcystis* sp. by its own spent medium rather than by isolated microcystin, discussed above.

Naturally we expect other CYN producers such as *C. raciborskii* to induce APase in other organisms. Lack of ELF-APase staining in lake samples of *Anabaena* sp., *Planktothrix* sp., and *Planktolyngbya* sp. (Rengefors et al., 2003) and delayed APase secretion in Pi-deprived *Trichodesmium* sp. (Orchard et al., 2009) may indicate similar capabilities in other cyanobacterial lineages that are not known to produce CYN.

Finally, there are numerous reports over the last decade showing a significant rise in the abundance of toxic filamentous N_2 fixing cyanobacteria in freshwater bodies (See Sukenik et al., this issue). The reason is not known, particularly as it occurs simultaneously with intensive efforts of lake management authorities to reduce

nutrient inflow from the watershed. The rise in cyanobacterial abundance has been attributed to various causes, including global warming, but in view of the role attributed to CYN we raise an alternative possibility that superior competitiveness for Pi enables these organisms to flourish in such lakes. In terms of competitiveness, it is worth mentioning that N allocation to produce CYN is cheaper for the cells than APase secretion (Bar-Yosef et al., 2010).

OUTLOOK: THE MAIN OPEN QUESTIONS

Here we focused on the biological role of two cyanobacterial toxins, microcystin and cylindrospermopsin, but many open questions need to be resolved. We proposed external and internal roles of microcystin and presented experimental evidence to support our view. Given the phylogenetic analysis that revealed that *mcy* (and *sxt*) are ancient but were lost in most of the present-day cyanobacterial strains, we raise the question what, if any, fulfills these biological roles in the other cyanobacterial strains lacking microcystin. What were the evolutional drivers that led to the deletion of *mcy* genes from most strains? We are missing an experiment whereby spent media, and/or supernatant from broken cells of one of the strains for which genetic information and tools (such as microarray) are available, will be applied to its own population. This will be followed by an analysis of the transcript abundances. Perhaps some other secondary metabolites perform these roles, as do micropeptin and microginin for the infochemical task in *Microcystis*. Furthermore, given the advantage of toxic over non-toxic *Microcystis* strains in growth competition experiments, why do we often find them inhabiting the same habitat, indoor as well as outdoor? Is it possible that while saving the resources necessary to produce microcystin, the non-toxic strains use microcystin produced by the toxic ones? What is in fact the role of McyH, which shows homology to ABC transporters but its inactivation blocks microcystin biosynthesis? Does it, like some other transporters, serve as the sensor for microcystin presence in the environment?

For CYN, with the emergence of more *aoa*/*cyr* sequences, it is becoming possible to perform a phylogenetic analysis for these gene clusters as well but the main task is to develop the means to make at least one of the CYN-producing strains amenable to genetic manipulations. We are still missing experimental evidence that this gene cluster is involved in CYN production. What are the mechanisms whereby presence of CYN induces the PHO regulon in other phytoplankton species even in the presence of ample Pi externally? What are the mechanisms enabling the differential expression of some of the PHO regulon genes in *Aphanizomenon* whereby external alkaline phosphatase is blocked as long as internal P is available in the form of polyphosphate bodies? What is the nature of the other components in the spent medium from *Aphanizomenon* that act synergistically with CYN? Is this ability to improve its own P supply by enslaving other organisms unique to *Aphanizomenon*? Can a similar mechanism be found in other organisms for P or other nutrients? These are just some of the open questions ensuring an exciting research period ahead of us.

ACKNOWLEDGMENTS

We thank Dr. R. Reinhardt and Dr. M. Kube from Max Planck Institute for Molecular Genetics, Berlin, for their guidance and support with the molecular analysis of *A. ovalisporum* genome. Research in our laboratories is supported by grants from the Israel Science Foundation to Aaron Kaplan; Israeli Science and Technology Ministry (MOST) to Aaron Kaplan and Assaf Sukenik; the German Research Foundation (Di910/3-1) to Elke Dittmann; the Hebrew University of Jerusalem to Aaron Kaplan; the Israel Water Authority to Assaf Sukenik and Aaron Kaplan; the Yohai Ben-Noon Foundation to Moshe Harel; and by the EU-NEST program to Assaf Sukenik, Ora Hadas, and Ruth N. Kaplan-Levy.

REFERENCES

Abraham, E. R. (1998). The generation of plankton patchiness by turbulent stirring. *Nature* 391, 577–580.

Agervald, A., Baebprasert, W., Zhang, X. H., Incharoensakdi, A., Lindblad, P., and Stensjo, K. (2010). The CyAbrB transcription factor CalA regulates the iron superoxide dismutase in *Nostoc* sp. strain PCC 7120. *Environ. Microbiol.* 12, 2826–2837.

Alexova, R., Haynes, P. A., Ferrari, B. C., and Neilan, B. A. (2011). Comparative protein expression in different strains of the bloom-forming cyanobacterium *Microcystis aeruginosa*. *Mol. Cell. Proteomics* 10, M110 003749.

Alfonso, M., Perewoska, I., and Kirilovsky, D. (2001). Redox control of ntcA gene expression in *Synechocystis* sp. PCC 6803: nitrogen availability and electron transport regulate the levels of the NtcA protein. *Plant Physiol.* 125, 969–981.

Alster, A., Kaplan-Levy, R. N., Sukenik, A., and Zohary, T. (2010). Morphology and phylogeny of a non-toxic invasive *Cylindrospermopsis raciborskii* from a Mediterranean Lake. *Hydrobiologia* 639, 115–128.

Annila, A., Lehtimaki, J., Mattila, K., Eriksson, J. E., Sivonen, K., Rantala, T. T., and Drakenberg, T. (1996). Solution structure of nodularin. An inhibitor of serine/threonine-specific protein phosphatases. *J. Biol. Chem.* 271, 16695–16702.

Babica, P., Blaha, L., and Marsalek, B. (2006). Exploring the natural role of microcystins – a review of effects on photoautotrophic organisms. *J. Phycol.* 42, 9–20.

Bacsi, I., Vasas, G., Suranyi, G., Hamvas, M., Mathe, C., Toth, E., Grigorszy, I., Gaspar, A., Toth, S., and Borbely, G. (2006). Alteration of cylindrospermopsin production in sulfate- or phosphate-starved cyanobacterium *Aphanizomenon ovalisporum*. *FEMS Microbiol. Lett.* 259, 303–310.

Ballot, A., Ramm, J., Rundberget, T., Kaplan-Levy, R. N., Hadas, O., Sukenik, A., and Wiedner, C. (2011). Occurrence of non-cylindrospermopsin-producing *Aphanizomenon ovalisporum* and *Anabaena bergii* in Lake Kinneret (Israel). *J. Plankton Res.* 33, 1736–1746.

Banker, R., Carmeli, S., Hadas, O., Teltsch, B., Porat, R., and Sukenik, A. (1997). Identification of cylindrospermopsin in the cyanobacterium *Aphanizomenon ovalisporum* (Cyanophyceae) isolated from Lake Kinneret, Israel. *J. Phycol.* 33, 613–616.

Banker, R., Carmeli, S., Werman, M., Teltsch, B., Porat, R., and Sukenik, A. (2001). Uracil moiety is required for toxicity of the cyanobacterial hepatotoxin cylindrospermopsin. *J. Toxicol. Environ. Health* 62, 281–288.

Bar-Yosef, Y., Sukenik, A., Hadas, O., Viner-Mozzini, Y., and Kaplan, A. (2010). Enslavement in the water body by toxic *Aphanizomenon ovalisporum*, inducing alkaline phosphatase in phytoplanktons. *Curr. Biol.* 20, 1557–1561.

Botes, D. P., Tuinman, A. A., Wessels, P. L., Viljoen, C. C., Kruger, H., Williams, D. H., Santikarn, S., Smith, R. J., and Hammond, S. J. (1984). The structure of cyanoginosin-LA, a cyclic heptapeptide toxin from the cyanobacterium *Microcystis aeruginosa*. *J. Chem. Soc. Perkin Trans. I* 1, 2311–2318.

Burford, M. A., and Davis, T. W. (2011). Physical and chemical processes promoting dominance of the toxic cyanobacterium *Cylindrospermopsis raciborskii*. *Chin. J. Oceanol. Limnol.* 29, 883–891.

Burgoyne, D. L., Hemscheidt, T. K., Moore, R. E., and Runnegar, M. T. C. (2000). Biosynthesis of cylindrospermopsin, *J. Org. Chem.* 65, 152–156.

Carmichael, W. W. (1997). The cyanotoxins. *Adv. Bot. Res.* 9, 211–256.

Christiansen, G., Fastner, J., Erhard, M., Borner, T., and Dittmann, E. (2003). Microcystin biosynthesis in *Planktothrix*: genes, evolution, and manipulation. *J. Bacteriol.* 185, 564–572.

Christiansen, G., Molitor, C., Philmus, B., and Kurmayer, R. (2008). Nontoxic strains of cyanobacteria are the result of major gene deletion events induced by a transposable element. *Mol. Biol. Evol.* 25, 1695–1704.

De Figueiredo, D. R., Goncalves, A. M. M., Castro, B. B., Goncalves, F., Pereira, M. J., and Correia, A. (2011). Differential inter- and intra-specific responses of *Aphanizomenon* strains to nutrient limitation and algal growth inhibition. *J. Plankton Res.* 33, 1606–1616.

Dittmann, E., Neilan, B. A., and Borner, T. (2001). Molecular biology of peptide and polyketide biosynthesis in cyanobacteria. *Appl. Microbiol. Biotechnol.* 57, 467–473.

Dittmann, E., Neilan, B. A., Erhard, M., von Doehren, H., and Boerner, T. (1997). Insertional mutagenesis of a peptide synthetase gene that is responsible for hepatotoxin production in the cyanobacterium *Microcystis aeruginosa* PCC 7806. *Mol. Microbiol.* 26, 779–787.

Dittmann, E., and Wiegand, C. (2006). Cyanobacterial toxins – occurrence, biosynthesis and impact on human affairs. *Mol. Nutr. Food Res.* 50, 7–17.

Dyble, J., Tester, P. A., and Litaker, R. W. (2006). Effects of light intensity on cylindrospermopsin production in the cyanobacterial HAB species *Cylindrospermopsis raciborskii*. *Afr. J. Mar. Sci.* 28, 309–312.

Dziallas, C., and Grossart, H. P. (2011). Temperature and biotic factors influence bacterial communities associated with the cyanobacterium *Microcystis* sp. *Environ. Microbiol.* 13, 1632–1641.

Engene, N., Choi, H., Esquenazi, E., Rottacker, E. C., Ellisman, M. H., Dorrestein, P. C., and Gerwick, W. H. (2011). Underestimated biodiversity as a major explanation for the perceived rich secondary metabolite capacity of the cyanobacterial genus *Lyngbya*. *Environ. Microbiol.* 13, 1601–1610.

Fastner, J., Erhard, M., and von Dohren, H. (2001). Determination of oligopeptide diversity within a natural population of *Microcystis* spp. (cyanobacteria) by typing single colonies by matrix-assisted laser desorption ionization-time of flight mass spectrometry. *Appl. Environ. Microbiol.* 67, 5069–5076.

Froscio, S. M., Humpage, A. R., Burcham, P. C., and Falconer, I. R. (2001). Cell-free protein synthesis inhibition assay for the cyanobacterial toxin cylindrospermopsin. *Environ. Toxicol.* 16, 408–412.

Gerbersdorf, S. U. (2006). An advanced technique for immuno-labelling of microcystins in cryosectioned cells of *Microcystis aeruginosa* PCC 7806 (cyanobacteria), implementations of an experiment with varying light scenarios and culture densities. *Toxicon* 47, 218–228.

Ginn, H. P., Pearson, L. A., and Neilan, B. A. (2010). NtcA from *Microcystis aeruginosa* PCC 7806 is autoregulatory and binds to the microcystin promoter. *Appl. Environ. Microbiol.* 76, 4362–4368.

Griffiths, D. J., and Saker, M. L. (2003). The palm island mystery disease 20 years on: a review of research on the cyanotoxin cylindrospermopsin. *Environ. Toxicol.* 18, 78–93.

Hadas, O., Pinkas, R., Delphine, E., Vardi, A., Kaplan, A., and Sukenik, A. (1999). Limnological and ecophysiological aspects of *Aphanizomenon ovalisporum* bloom in Lake Kinneret. *J. Plankton Res.* 21, 1439–1453.

Hadas, O., Pinkas, R., Malinsky-Roshansky, N., Shalev-Alon, G., Delphine, E., Berner, T., Sukenik, A., and Kaplan, A. (2002). Physiological variables determined under laboratory conditions may explain the bloom of *Aphanizomenon ovalisporum* in Lake Kinneret. *Eur. J. Phycol.* 37, 259–267.

Hawkins, P. R., Putt, E., Falconer, I., and Humpage, A. (2001). Phenotypical variation in a toxic strain of the phytoplankter, *Cylindrospermopsis raciborskii* (Nostocales, Cyanophyceae) during batch culture. *Environ. Toxicol.* 16, 460–467.

Hesse, K., Dittmann, E., and Boerner, T. (2001). Consequence of impaired microcystin production for light-dependent growth and pigmentation of *Microcystis aeruginosa* PCC 7806. *FEMS Microbiol. Ecol.* 37, 39–43.

Humpage, A. R., Fenech, M., Thomas, P., and Falconer, I. R. (2000). Micronucleus induction and chromosome loss in transformed human white cells indicate clastogenic and aneugenic action of the cyanobacterial toxin, cylindrospermopsin. *Mutat. Res.* 472, 155–161.

Humpage, A. R., Fontaine, F., Froscio, S., Burcham, P., and Falconer, I. R. (2005). Cylindrospermopsin genotoxicity and cytotoxicity: role of cytochrome P-450 and oxidative stress. *J. Toxicol. Environ. Health A* 68, 739–753.

Jahnichen, S., Ihle, T., Petzoldt, T., and Benndorf, J. (2007). Impact of inorganic carbon availability on microcystin production by *Microcystis aeruginosa* PCC 7806. *Appl. Environ. Microbiol.* 73, 6994–7002.

Jochimsen, E. M., Carmichael, W. W., An, J. S., Cardo, D. M., Cookson, S. T., Holmes, C. E., Antunes, M. B., de Melo Filho, D. A., Lyra, T. M., and Barreto, V. S. (1998). Liver failure and death after exposure to microcystins at a hemodialysis center in Brazil. *N. Engl. J. Med.* 338, 873–878.

Jones, A. C., Monroe, E. A., Podell, S., Hess, W. R., Klages, S., Esquenazi, E., Niessen, S., Hoover, H., Rothmann, M., Lasken, R. S., Yates, J. R., Reinhardt, R., Kube, M., Burkart, M., Allen, E. E., Dorrestein, P. C., Gerwick, W. H., and Gerwick, L. (2011). Genomic insights into the physiology and ecology of the marine filamentous cyanobacterium *Lyngbya majuscula*. *Proc. Natl. Acad. Sci. U.S.A.* 108, 8815–8820.

Kaebernick, M., Dittmann, E., Boerner, T., and Neilan, B. A. (2002). Multiple alternate transcripts direct the biosynthesis of microcystin, a cyanobacterial nonribosomal peptide. *Appl. Environ. Microbiol.* 68, 449–455.

Kaebernick, M., Neilan, B. A., Boerner, T., and Dittmann, E. (2000). Light and the transcriptional response of the microcystin biosynthetic gene cluster. *Appl. Environ. Microbiol.* 66, 3387–3392.

Kaebernick, M., and Neilan, B. A. (2001). Ecological and molecular investigations of cyanotoxin production. *FEMS Microbiol. Ecol.* 35, 1–9.

Kehr, J. C., Zilliges, Y., Springer, A., Disney, M. D., Ratner, D. D., Bouchier, C., Seeberger, P. H., de Marsac, N. T., and Dittmann, E. (2006). A mannan binding lectin is involved in cell-cell attachment in a toxic strain of *Microcystis aeruginosa*. *Mol. Microbiol.* 59, 893–906.

Kinnear, S. (2010). Cylindrospermopsin: a decade of progress on bioaccumulation research. *Mar. Drugs* 8, 542–564.

Li, R., Carmichael, W. W., Brittain, S., Eaglesham, G. K., Shaw, G. R., Mahakhant, A., Noparatnaraporn, N., Yongmanitchai, W., Kaya, K., and Watanabe, M. M. (2001). Isolation and identification of the cyanotoxin cylindrospermopsin and deoxy-cylindrospermopsin from a Thailand strain of *Cylindrospermopsis raciborskii* (cyanobacteria). *Toxicon* 39, 973–980.

Lieman-Hurwitz, J., Haimovich, M., Shalev-Malul, G., Ishii, A., Hihara, Y., Gaathon, A., Lebendiker, M., and Kaplan, A. (2009). A cyanobacterial AbrB-like protein affects the apparent photosynthetic affinity for CO_2 by modulating low-CO_2-induced gene expression. *Environ. Microbiol.* 11, 927–936.

Liu, L., and Rein, K. S. (2010). New peptides isolated from *lyngbya* species: a review. *Mar. Drugs* 8, 1817–1837.

Long, B. M., Jones, G. J., and Orr, P. T. (2001). Cellular microcystin content in N-limited *Microcystis aeruginosa* can be predicted from growth rate. *Appl. Environ. Microbiol.* 67, 278–283.

Lopez-Gomollon, S., Hernandez, J. A., Pellicer, S., Angarica, V. E., Peleato, M. L., and Fillat, M. F. (2007). Cross-talk between iron and nitrogen regulatory networks in *Anabaena* (*Nostoc*) sp. PCC 7120, identification of overlapping genes in FurA and NtcA regulons. *J. Mol. Biol.* 374, 267–281.

Lukac, M., and Aegerter, R. (1993). Influence of trace-metals on growth and toxin production of *Microcystis aeruginosa*. *Toxicon* 31, 293–305.

Martin-Luna, B., Sevilla, E., Hernandez, J. A., Bes, M. T., Fillat, M. F., and Peleato, M. L. (2006). Fur from *Microcystis aeruginosa* binds in vitro promoter regions of the microcystin biosynthesis gene cluster. *Phytochemistry* 67, 876–881.

Mazmouz, R., Chapuis-Hugon, F., Mann, S., Pichon, V., Mejean, A., and Ploux, O. (2010). Biosynthesis of cylindrospermopsin and 7-epicylindrospermopsin in *Oscillatoria* sp. strain PCC 6506, Identification of the cyr gene cluster and toxin analysis. *Appl. Environ. Microbiol.* 76, 4943–4949.

Mazmouz, R., Chapuis-Hugon, F., Pichon, V., Mejean, A., and Ploux, O. (2011). The last step of the biosynthesis of the cyanotoxins cylindrospermopsin and 7-epicylindrospermopsin is catalysed by CyrI, a 2-oxoglutarate-dependent iron oxygenase. *Chembiochem* 12, 858–862.

Mejean, A., Mazmouz, R., Mann, S., Calteau, A., Medigue, C., and Ploux, O. (2010). The genome sequence of the cyanobacterium *Oscillatoria* sp. PCC 6506 reveals several gene clusters responsible for the biosynthesis of toxins and secondary metabolites. *J. Bacteriol.* 192, 5264–5265.

Metcalf, J. S., Barakate, A., and Codd, G. A. (2004). Inhibition of plant protein synthesis by the cyanobacterial hepatotoxin, cylindrospermopsin. *FEMS Microbiol. Lett.* 235, 125–129.

Mihali, T. K., Kellmann, R., Muenchhoff, J., Barrow, K. D., and Neilan, B. A. (2008). Characterization of the

gene cluster responsible for cylindrospermopsin biosynthesis. *Appl. Environ. Microbiol.* 74, 716–722.

Moffitt, M. C., and Neilan, B. A. (2004). Characterization of the nodularin synthetase gene cluster and proposed theory of the evolution of cyanobacterial hepatotoxins. *Appl. Environ. Microbiol.* 70, 6353–6362.

Murphy, P. J., and Thomas, C. W. (2001). The synthesis and biological activity of the marine metabolite cylindrospermopsin. *Chem. Soc. Rev.* 30, 303–312.

Murray, S. A., Mihali, T. K., and Neilan, B. A. (2011). Extraordinary conservation, gene loss, and positive selection in the evolution of an ancient neurotoxin. *Mol. Biol. Evol.* 28, 1173–1182.

Neilan, B. A., Pearson, L. A., Moffitt, M. C., Mihali, K. T., Kaebemick, M., Kellmann, R., and Pomati, F. (2008). "The genetics and genomics of cyanobacterial toxicity," in *Cyanobacterial Harmful Algal Blooms, State of the Science and Research Needs*, Vol. 619, ed. H. K Hudnell (New York: Springer), 417–452.

Nishizawa, T., Asayama, M., Fujii, K., Harada, K., and Shirai, M. (1999). Genetic analysis of the peptide synthetase genes for a cyclic heptapeptide microcystin in *Microcystis* spp. *J. Biochem.* 126, 520–529.

Nishizawa, T., Ueda, A., Asayama, M., Fujii, K., Harada, K., Ochi, K., and Shirai, M. (2000). Polyketide synthase gene coupled to the peptide synthetase module involved in the biosynthesis of the cyclic heptapeptide microcystin. *J. Biochem.* 127, 779–789.

Ogawa, Y. (1988). Net increase rates and dynamics of phytoplankton populations under hypereutrophic and eutrophic conditions. *Jpn. J. Limnol.* 49, 261–268.

Oliveira, P., and Lindblad, P. (2008). An AbrB-like protein regulates the expression of the bidirectional hydrogenase in *Synechocystis* sp. strain PCC 6803. *J. Bacteriol.* 190, 1011–1019.

Orchard, E. D., Webb, E. A., and Dyhrman, S. T. (2009). Molecular analysis of the phosphorus starvation response in *Trichodesmium* spp. *Environ. Microbiol.* 11, 2400–2411.

Orr, P. T., and Jones, G. J. (1998). Relationship between microcystin production and cell division rates in nitrogen-limited *Microcystis aeruginosa* cultures. *Limnol. Oceanogr.* 43, 1604–1614.

Paerl, H. W., and Huisman, J. (2009). Climate change, a catalyst for global expansion of harmful cyanobacterial blooms. *Environ. Microbiol. Rep.* 1, 27–37.

Pearson, L., Hisbergues, M., Dittmann, E., Boerner, T., and Neilan, B. A. (2004). Inactivation of an ABC transporter, McyH, results in loss of microcystin production in the cyanobacterium *Microcystis aeruginosa* PCC 7806. *Appl. Environ. Microbiol.* 70, 6370–6378.

Pearson, L., Mihali, T., Moffitt, M., Kellmann, R., and Neilan, B. (2010). On the chemistry, toxicology and genetics of the cyanobacterial toxins, microcystin, nodularin, saxitoxin and cylindrospermopsin. *Mar. Drugs* 8, 1650–1680.

Pflugmacher, S. (2002). Possible allelopathic effects of cyanotoxins, with reference to microcystin-LR, in aquatic ecosystems. *Environ. Toxicol.* 17, 407–413.

Preussel, K., Stuken, A., Wiedner, C., Chorus, I., and Fastner, J. (2006). First report on cylindrospermopsin producing *Aphanizomenon flos-aquae* (Cyanobacteria) isolated from two German lakes. *Toxicon* 47, 156–162.

Rantala, A., Fewer, D. P., Hisbergues, M., Rouhiainen, L., Vaitomaa, J., Borner, T., and Sivonen, K. (2004). Phylogenetic evidence for the early evolution of microcystin synthesis. *Proc. Natl. Acad. Sci. U.S.A.* 101, 568–573.

Rapala, J., Sivonen, K., Lyra, C., and Niemela, S.-I. (1997). Variation of microcystins, cyanobacterial hepatotoxins, in *Anabaena* spp. as a function of growth stimuli. *Appl. Environ. Microbiol.* 63, 2206–2212.

Reisner, M., Carmeli, S., Werman, M., and Sukenik, A. (2004). The cyanobacterial toxin cylindrospermopsin inhibits pyrimidine nucleotide synthesis and alters cholesterol distribution in mice. *Toxicol. Sci.* 82, 620–627.

Rengefors, K., Ruttenberg, K. C., Haupert, C. L., Taylor, C., Howes, B. L., and Anderson, D. M. (2003). Experimental investigation of taxon-specific response of alkaline phosphatase activity in natural freshwater phytoplankton. *Limnol. Oceanogr.* 48, 1167–1175.

Rodelas, B., Lithgow, J. K., Wisniewski-Dye, F., Hardman, A., Wilkinson, A., Economou, A., Williams, P., and Downie, J. A. (1999). Analysis of quorum-sensing-dependent control of rhizosphere-expressed (*rhi*) genes in *Rhizobium leguminosarum* bv. viciae. *J. Bacteriol.* 181, 3816–3823.

Rohrlack, T., Dittmann, E., Boerner, T., and Christoffersen, K. (2001). Effects of cell-bound microcystins on survival and feeding of *Daphnia* spp. *Appl. Environ. Microbiol.* 67, 3523–3529.

Rohrlack, T., Dittmann, E., Henning, M., Borner, T., and Kohl, J. G. (1999). Role of microcystins in poisoning and food ingestion inhibition of *Daphnia galeata* caused by the cyanobacterium *Microcystis aeruginosa*. *Appl. Environ. Microbiol.* 65, 737–739.

Rouhiainen, L., Vakkilainen, T., Siemer, B. L., Buikema, W., Haselkorn, R., and Sivonen, K. (2004). Genes coding for hepatotoxic heptapeptides (microcystins) in the cyanobacterium *Anabaena* strain 90. *Appl. Environ. Microbiol.* 70, 686–692.

Runnegar, M., and Lu, S. (1994). The role of glutathione (Gsh) in the hepatotoxicity caused by the cyanobacterial alkaloid cylindrospermopsin (Cy). *FASEB J.* 8, A419.

Runnegar, M. T., Kong, S. M., Zhong, Y. Z., and Lu, S. C. (1995). Inhibition of reduced glutathione synthesis by cyanobacterial alkaloid cylindrospermopsin in cultured rat hepatocytes. *Biochem. Pharmacol.* 49, 219–225.

Runnegar, M. T., Xie, C. Y., Snider, B. B., Wallace, G. A., Weinreb, S. M., and Kuhlenkamp, J. (2002). In vitro hepatotoxicity of the cyanobacterial alkaloid cylindrospermopsin and related synthetic analogues. *Toxicol. Sci.* 67, 81–87.

Saker, M. L., and Griffiths, D. J. (2000). The effect of temperature on growth and cylindrospermopsin content of seven isolates of *Cylindrospermopsis raciborskii* (Nostocales, Cyanophyceae) from water bodies in northern Australia. *Phycologia* 39, 349–354.

Schatz, D., Keren, Y., Hadas, O., Carmeli, S., Sukenik, A., and Kaplan, A. (2005). Ecological implications of the emergence of non-toxic subcultures from toxic *Microcystis* strains. *Environ. Microbiol.* 7, 798–805.

Schatz, D., Keren, Y., Vardi, A., Sukenik, A., Carmeli, S., Boerner, T., Dittmann, E., and Kaplan, A. (2007). Towards clarification of the biological role of microcystins, a family of cyanobacterial toxins. *Environ. Microbiol.* 9, 965–970.

Schembri, M. A., Neilan, B. A., and Saint, C. P. (2001). Identification of genes implicated in toxin production in the cyanobacterium *Cylindrospermopsis raciborskii*. *Environ. Toxicol.* 16, 413–421.

Seifert, M., McGregor, G., Eaglesham, G., Wickramasinghe, W., and Shaw, G. (2007). First evidence for the production of cylindrospermopsin and deoxy-cylindrospermopsin by the freshwater benthic cyanobacterium, *Lyngbya wollei* (Farlow ex Gomont) Speziale and Dyck. *Harmful Algae* 6, 73–80.

Sevilla, E., Martin-Luna, B., Vela, L., Bes, M. T., Fillat, M. F., and Peleato, M. L. (2008). Iron availability affects *mcyD* expression and microcystin-LR synthesis in *Microcystis aeruginosa* PCC7806. *Environ. Microbiol.* 10, 2476–2483.

Sevilla, E., Martin-Luna, B., Vela, L., Bes, M. T., Peleato, M. L., and Fillat, M. F. (2010). Microcystin-LR synthesis as response to nitrogen, transcriptional analysis of the *mcyD* gene in *Microcystis aeruginosa* PCC780. *Ecotoxicology* 19, 1167–1173.

Shalev-Alon, G., Sukenik, A., Livnah, O., Schwarz, R., and Kaplan, A. (2002). A novel gene encoding amidinotransferase in the cylindrospermopsin producing cyanobacterium *Aphanizomenon ovalisporum*. *FEMS Microbiol. Lett.* 209, 87–91.

Shen, X. Y., Lam, P. K. S., Shaw, G. R., and Wickramasinghe, W. (2002). Genotoxicity investigation of a cyanobacterial toxin, cylindrospermopsin. *Toxicon* 40, 1499–1501.

Sivonen, K. (2008). "Emerging high throughput analyses of cyanobacterial toxins and toxic cyanobacteria," in *Cyanobacterial Harmful Algal Blooms, State of the Science and Research Needs*, Vol. 619, ed. H. K. Hudnell (New York: Springer), 539–557.

Sivonen, K., Carmichael, W. W., Namikoshi, M., Rinehart, K. L., Dahlem, A. M., and Niemela, S. I. (1990). Isolation and characterization of hepatotoxic microcystin homologs from the filamentous fresh-water cyanobacterium *Nostoc* sp. strain-152. *Appl. Environ. Microbiol.* 56, 2650–2657.

Sivonen, K., and Jones, G. (1999). "Cyanobacterial toxins," in *Toxic Cyanobacteria in Water*, eds I. Chorus and J. Bartram (London: E & FN Spon), 41–111.

Straser, A., Filipic, M., and Zegura, B. (2011). Genotoxic effects of the cyanobacterial hepatotoxin cylindrospermopsin in the HepG2 cell line. *Arch. Toxicol.* 85, 1617–1626.

Straub, C., Quillardet, P., Vergalli, J., Tandeau de Marsac, N., and Humbert, J.-F. (2011). A day in the life of *Microcystis aeruginosa* strain PCC 7806 as revealed by a transcriptomic

analysis. *PLoS ONE* 6, e16208. doi:10.1371/journal.pone.0016208

Stuken, A., and Jakobsen, K. S. (2010). The cylindrospermopsin gene cluster of *Aphanizomenon* sp strain 10E6, organization and recombination. *Microbiology* 156, 2438–2451.

Sukenik, A., Beardall, J., and Hadas, O. (2007). Photosynthetic characterization of developing and mature akinetes of *Aphanizomenon ovalisporum* (Cyanoprokaryota). *J. Phycol.* 43, 780–788.

Tillett, D., Dittmann, E., Erhard, M., von Dohren, H., Borner, T., and Neilan, B. A. (2000). Structural organization of microcystin biosynthesis in *Microcystis aeruginosa* PCC7806, an integrated peptide- polyketide synthetase system. *Chem. Biol.* 7, 753–764.

Tonk, L., Visser, P. M., Christiansen, G., Dittmann, E., Snelder, E. O., Wiedner, C., Mur, L. R., and Huisman, J. (2005). The microcystin composition of the cyanobacterium *Planktothrix agardhii* changes toward a more toxic variant with increasing light intensity. *Appl. Environ. Microbiol.* 71, 5177–5181.

Utkilen, H., and Gjolme, N. (1992). Toxin production by *Microcystis aeruginosa* as a function of light in continuous cultures and its ecological significance. *Appl. Environ. Microbiol.* 58, 1321–1325.

Van de Waal, D. B., Verspagen, J. M., Finke, J. F., Vournazou, V., Immers, A. K., Kardinaal, W. E., Tonk, L., Becker, S., Van Donk, E., Visser, P. M., and Huisman, J. (2011). Reversal in competitive dominance of a toxic versus non-toxic cyanobacterium in response to rising CO_2. *ISME J.* 5, 1438–1450.

Vanderwesthuizen, A. J., and Eloff, J. N. (1985). Effect of temperature and light on the toxicity and growth of the blue-green-alga *Microcystis aeruginosa* (UV-006). *Planta* 163, 55–59.

Vezie, C., Rapala, J., Vaitomaa, J., Seitsonen, J., and Sivonen, K. (2002). Effect of nitrogen and phosphorus on growth of toxic and nontoxic *Microcystis* strains and on intracellular microcystin concentrations. *Microb. Ecol.* 43, 443–454.

Via-Ordorika, L., Fastner, J., Kurmayer, R., Hisbergues, M., Dittmann, E., Komarek, J., Erhard, M., and Chorus, I. (2004). Distribution of microcystin-producing and non-microcystin-producing *Microcystis* sp in European freshwater bodies: detection of microcystins and microcystin genes in individual colonies. *Syst. Appl. Microbiol.* 27, 592–602.

Walsby, A. E. (1997). Numerical integration of phytoplankton photosynthesis through time and depth in a water column. *New Phytol.* 136, 189–209.

Welker, M., and von Dohren, H. (2006). Cyanobacterial peptides – nature's own combinatorial biosynthesis. *FEMS Microbiol. Rev.* 30, 530–563.

Wiedner, C., Visser, P. M., Fastner, J., Metcalf, J. S., Codd, G. A., and Mur, L. R. (2003). Effects of light on the microcystin content of *Microcystis* strain PCC 7806. *Appl. Environ. Microbiol.* 69, 1475–1481.

Yamauchi, Y., Kaniya, Y., Kaneko, Y., and Hihara, Y. (2011). Physiological roles of the cyAbrB transcriptional regulator pair Sll0822 and Sll0359 in *Synechocystis* sp. strain PCC 6803. *J. Bacteriol.* 193, 3702–3709.

Zegura, B., Straser, A., and Filipic, M. (2011). Genotoxicity and potential carcinogenicity of cyanobacterial toxins – a review. *Mutat. Res.* 727, 16–41.

Zilliges, Y., Kehr, J. C., Meissner, S., Ishida, K., Mikkat, S., Hagemann, M., Kaplan, A., Borner, T., and Dittmann, E. (2011). The cyanobacterial hepatotoxin microcystin binds to proteins andi increases the fitness of *Microcystis* under oxidative stress conditions. *PLoS ONE* 6, e17615. doi:10.1371/journal.pone.0017615

Zilliges, Y., Kehr, J. C., Mikkat, S., Bouchier, C., de Marsac, N. T., Borner, T., and Dittmann, E. (2008). An extracellular glycoprotein is implicated in cell-cell contacts in the toxic cyanobacterium *Microcystis aeruginosa* PCC 7806. *J. Bacteriol.* 190, 2871–2879.

Conflict of Interest Statement: The authors declare that the research was conducted in the absence of any commercial or financial relationships that could be construed as a potential conflict of interest.

Received: 21 January 2012; accepted: 23 March 2012; published online: 18 April 2012.

*Citation: Kaplan A, Harel M, Kaplan-Levy RN, Hadas O, Sukenik A and Dittmann E (2012) The languages spoken in the water body (or the biological role of cyanobacterial toxins). Front. Microbio. **3**:138. doi: 10.3389/fmicb.2012.00138*

This article was submitted to Frontiers in Aquatic Microbiology, a specialty of Frontiers in Microbiology.

frontiers in
MICROBIOLOGY

REVIEW ARTICLE
published: 09 March 2012
doi: 10.3389/fmicb.2012.00086

Invasion of Nostocales (cyanobacteria) to subtropical and temperate freshwater lakes – physiological, regional, and global driving forces

Assaf Sukenik[1]*, Ora Hadas[1], Aaron Kaplan[2] and Antonio Quesada[3]

[1] *The Yigal Allon Kinneret Limnological Laboratory, Israel Oceanographic and Limnological Research, Migdal, Israel*
[2] *Department of Plant and Environmental Sciences, The Hebrew University, Jerusalem, Israel*
[3] *Departamento de Biología, Universidad Autónoma de Madrid, Madrid, Spain*

Edited by:
Anton F. Post, H. Steinitz Marine Biology Laboratory, USA

Reviewed by:
Robert M. McKay, Bowling Green State University, USA
Rachael Marie Morgan-Kiss, Miami University, USA

***Correspondence:**
Assaf Sukenik, The Yigal Allon Kinneret Limnological Laboratory, Israel Oceanographic and Limnological Research, P.O. Box 447, Migdal 14950, Israel.
e-mail: assaf@ocean.org.il

Similar to the increased number of studies on invasive plants and animals in terrestrial and aquatic ecosystems, many reports were recently published on the invasion of Nostocales (cyanobacteria) to freshwater environments worldwide. Invasion and proliferation of Nostocales in new habitats have the potential to significantly alter the structure of the native community and to modify ecosystem functioning. But most importantly, they influence the water quality due to a variety of toxic compounds that some species produce. Therefore a special attention was given to the invasion and persistence of toxic cyanobacteria in many aquatic ecosystems. Here we summarize the currently published records on the invasion of two Nostocales genera, *Cylindrospermopsis* and *Aphanizomenon*, to lakes and water reservoirs in subtropical and temperate zones. These invading species possess traits thought to be common to many invasive organisms: high growth rate, high resource utilization efficiency and overall superior competitive abilities over native species when local conditions vary. Assuming that dispersion routes of cyanobacteria have not been changed much in recent decades, their recent establishment and proliferation in new habitats indicate changes in the environment under which they can exploit their physiological advantage over the native phytoplankton population. In many cases, global warming was identified as the major driving force for the invasion of Nostocales. Due to this uncontrollable trend, invasive Nostocales species are expected to maintain their presence in new habitats and further expand to new environments. In other cases, regional changes in nutrient loads and in biotic conditions were attributed to the invasion events.

Keywords: cyanobacteria, Nostocales, *Cylindrospermopsis*, *Aphanizomenon*, invasive species, climate change, eutrophication

INTRODUCTION

The entry, establishment, and spread of non – native species to a new ecosystem, is frequently described as biological invasion (Vitousek et al., 1997; Ricciardi and Cohen, 2007). In many cases, biological invasions are caused by human – induced environmental interference and have substantial economic impact, serious ecological consequences, and human health hazards (Pimentel et al., 2001). They also may threaten global biodiversity by altering the structure and function of ecosystems and disrupting key biological interactions (Levine et al., 2003; Traveset and Richardson, 2006). The invasion of freshwater and marine ecosystems by non-native species of various taxonomic groups, mostly crustaceans, mussels, fish, and aquatic macrophytes is well documented (Meinesz et al., 2001; Richardson, 2011). The invasion of free-living microorganisms to new aquatic habitats is rather cryptic and difficult to detect therefore invasions of these "invisible invaders" have been rarely reported (Litchman, 2010). Furthermore, information on prior and current composition of the microbial communities, which is required to determine if a given microorganism is an invader, is often missing. Algae and cyanobacteria are exceptions in that sense as they have visible characteristic of spectral signature and microscopic morphological features. This property partly contributed to the increased number of reports on cyanobacteria invasion to lakes and water reservoirs across Europe, North, and South America and the Middle East that were recently published (Dyble et al., 2002; Wiedner et al., 2007; Hadas et al., submitted).

Here we summarize recently published records on the invasion of cyanobacteria to subtropical and temperate lakes and water reservoirs and try to forecast different scenarios of ecological and management consequences. The invasion of two Nostocales genera, *Cylindrospermopsis* and *Aphanizomenon* is presented and analyzed based on the main concepts of invasion ecology. The following issues are critically addressed: recent variations in geographic distribution of invasive Nostocales; How does a Nostocales species become an invader? What are the special traits of the invading Nostocales? What are the level and the role of genetic variability in the invasion of Nostocales? Is invasion of Nostocales to new location further expected and under what conditions? What are the expected ecological effects of the invasion?

THE CONCEPT OF INVADING CYANOBACTERIA

Biological invasion is considered as an extension of normal colonization processes such as succession (Elton, 1958) therefore it was proposed that the term "invasive species" will be restricted to describe non-native species that expanded their geographic range, became abundant and have environmental and economic impact (Colautti and Macisaac, 2004). Because the terminology associated with biological invasion is rather confusing and sometimes misleading (Colautti and Macisaac, 2004), here we define an invading or a non-native species as a species that spreads beyond its native range or a species that enters a habitat where it had not resided before. However, it should be kept in mind that many cyanobacteria species (as well as other microorganisms) can inhabit an aquatic ecosystem unnoticed, since it may remain at a rather low biomass concentration and it does not form a conspicuous fraction of the community. Furthermore, the lack of detailed water quality monitoring program or an insufficiently comprehensive surveillance do not pick up the presence of these species (Kling et al., 2011). Typically it is only when a non-native population is widespread and abundant, and causes ecological or economic harms, that it is named "invasive." It is possible for a species to be invasive in one ecosystem, but non-invasive in another. This can be due to a variety of factors, such as the presence of less-than-ideal habitat conditions (Lockwood et al., 2007). We further suggest evaluating the invasion of free-living microorganisms within an appropriate timeframe, since an invader may become a common resident of a dynamically changing environment. Therefore native and non-native species may be viewed as part of a continuum with respect to their time of residency and the extent of evolutionary and ecological interactions they have within a given environment.

THE GLOBAL EXPANSION OF NOSTOCALES

During the last decades, the number of reports on cyanobacterial domination and persistence in freshwater and marine ecosystems significantly increased covering spatial and temporal distribution of persistent perennial blooms. Many of these bloom events are of toxic *Microcystis* species and strains that proliferate under current environmental alterations, including nutrient enrichment, global warming, and regional hydrologic changes (Paerl and Paul, 2011). However, not all blooms are associated with an invasion process as many species are of broad geographic distribution and rapidly respond to current environmental changes.

The most important freshwater invasive Nostocales are the tropical species *C. raciborskii* and to a lesser extent also *Aph. ovalisporum*. The map in **Figure 1** shows the current global distribution of *C. raciborskii* and *Aph. ovalisporum* in their native tropical region and in subtropical and temperate areas to which they expanded in the last two decades. *C. raciborskii* is a tropical species which was first described from Indonesia (Java) and was subsequently discovered in India and Thailand, Japan, the Philippines, Egypt, Senegal, Brazil, Cuba, Chile, Uruguay, Australia, New Zealand, and Florida (Bouvy et al., 2000; Molica et al., 2002; Dobberfuhl, 2003; Komárek and Komárkova, 2003; Wood and Stirling, 2003; Briand et al., 2004; Chonudomkul et al., 2004; Vidal and Kruk, 2008). Recently Kaštovský et al. (2011) summarized the invasion of freshwater cyanobacteria and algae to aquatic ecosystems in the Czech Republic and portrayed the invasion of *C. raciborskii* from its native tropical area to subtropical and temperate zones. The expansion of *C. raciborskii* and *Aph. ovalisporum* to new geographic regions is described below.

CENTRAL EUROPE (GERMANY, FRANCE) AND THE IBERIAN PENINSULA

The invasion of cyanobacteria strains in Central Europe as high biomass of the typically tropical species *C. raciborskii* was first reported in the 1970s (Romo and Miracle, 1994; Padisák, 1997). Long term phytoplankton records in some European lakes demonstrate a clear increase of some cyanobacterial species that had been absent or overlooked before (Padisák, 1997). Although *C.*

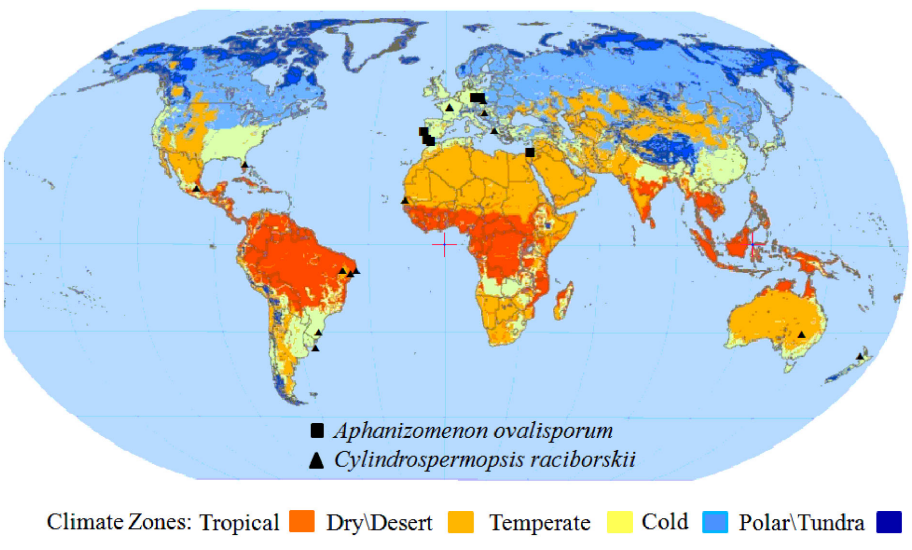

FIGURE 1 | The expansion of the Nostocales *Cylindrospermopsis raciborskii* (triangles) and *Aphanizomenon ovalisporum* (squares) to temperate and subtropical regions shown in a world climate zones map. (Map source: http://sedac.ciesin.columbia.edu/place/mapCollection/Climate_Zone).

raciborskii was known in Europe since the 1930s, it was marginal to the southern European countries (e.g., Greece; see references in Mehnert et al., 2010). However, in the last two decades, this species has appeared in northern European regions and is currently widespread at central latitudes (Kokociński et al., 2009). Other Nostocales such as *Aph. aphanizomenoides* (currently designated as *Sphaerospermum*) and *Aph. ovalisporum*, are also considered invasive species in Europe and have been reported at some locations as newcomers. *Aph. ovalisporum* is especially relevant because it is known to produce cylindrospermopsin, although several non-toxic strains were reported (Ballot et al., 2011). *Aph. ovalisporum* was described in different ecosystems of southern Europe (Bazzichelli and Abdelahad, 1994) and in the Iberian Peninsula where it produced massive blooms for the first time in 2005 (Quesada et al., 2006). Later, it has been found at least in seven water bodies in central Spain (Cirés, 2012) and in several water bodies in the southern areas of the country (C. de Hoyos, Personal Communication). *Aph. ovalisporum* has been found in the Iberian Peninsula, both in deep stratified reservoirs and in very shallow (less than 1 m) ponds of urban gardens. The spread of *Aph. ovalisporum* throughout the peninsula is considered invasion since a solid reference for its presence and bloom prior to the current reports is missing.

While field studies on the adaptation of the European species and their invasive potential are very scarce, laboratory studies with isolated strains have demonstrated that some invasive species have strong competitive abilities under changing scenarios. Mehnert et al. (2010) compared several "native" strains with "invasive" species and found that under low temperature, native species showed a higher growth rate than the invasive ones. However, under higher temperatures, the trend was the opposite and invasive strains performed better. Using these data, the authors, in a modeling effort, demonstrated that under a scenario of climate change with an increase of 4°C in the water temperature, the invasive species *C. raciborskii* would outcompete the native species (*Aph. gracile*) and that the potentially invasive *Aph. ovalisporum* would be an important component in the community (Mehnert et al., 2010). Although akinete production and overwintering/seeding play an important role in the life cycle of Nostocales, it is not necessarily the only mechanism for seeding; for example *Aphanizomenon* can seed from vegetative cells and filaments overwintering under ice (Grossart HP, personal communication). Temperature-dependent release of cylindrospermopsin was reported for *Aph. ovalisporum*, implicating management complications associated with global change scenarios (Cirés et al., 2011).

MIDDLE EAST

An exceptional bloom of *Aph. ovalisporum* first appeared in Lake Kinneret (Sea of Galilee), Israel in July 1994 and dominated the summer phytoplankton population for a few weeks (Pollingher et al., 1998). This toxic species (a producer of cylindrospermopsin) remained a regular member of the summer phytoplankton community since then and variably contributes between 10 and 40% to the summer phytoplankton biomass (Zohary, 2004). The reason for *Aph. ovalisporum's* first appearance and its later establishment in Lake Kinneret was a subject for debate (Berman, 1997, 2001; Berman and Shteinman, 1998; Gophen et al., 1999) but it is clear now that this species took advantage of a new set of conditions that were imposed by global and regional changes (Hadas et al., submitted). The origin of the *Aph. ovalisporum* strain that established in Lake Kinneret remained unclear. A long and detailed record of the phytoplankton population in Lake Kinneret (since 1964) clearly shows its absence, although its presence at a level which is below the detection limit cannot be excluded. Interestingly, the *Aph. ovalisporum* strain isolated from Lake Kinneret was genotypically related to strains of *Anabaena bergii* isolated from constructed man-made lakes in Queensland, Australia (Shaw et al., 1999). Nevertheless, *Anabaena bergii* was not reported to bloom in the lake. The invasion process was repeated once again in Lake Kinneret as *C. rasiborskii* was first reported in 2000 as a minor component of the summer phytoplankton community but dominated the community in summer 2005 with biomass as high as 68 g (ww) m^{-2} (Hadas et al., submitted). Again, it is rather difficult to trace the origin of Lake Kinneret *C. raciborskii* but the fact that it is a non-cylindrospermopsin producing strain suggests that it may be related to European strains. These isolates do not produce cylindrospermopsin as opposed to Australian strains known to produce cylindrospermopsin and to Brazilian strains that have been reported to produce paralytic shellfish poisoning toxins (Neilan et al., 2003).

Other reports on Nostocales species in the Middle East include the Caspian Sea and Egypt. *C. raciborskii* was reported as a dominant phytoplankton species in the open and freshwater basin in the west part of the Anzali Lagoon (Caspian Sea, Iran). It was also dominant for short periods after flooding events in rivers flowing into the lagoon (Ramezanpoor, 2004). Toxic *C. raciborskii* and *Raphidiopsis mediterranea* were reported in an Egyptian shallow (4 m depth) freshwater El-Dowyrat fish pond for the first time in 2002. Human activities at the end of 2001, including removal of trees and elimination of macrophytes around the fish pond have led to an increase in temperature at the surface waters of the pond (25–30°C). Both species showed seasonal variations with highest densities recorded in August each year (Mohamed, 2007). The loss of macrophytes was reported as one of the variables promoting the proliferation of *C. raciborskii* also in New Zealand lakes (Ryan et al., 2003). Thus local maintenance activities may be involved in an increase in temperature of the water column of temperate lakes and expand the distribution of *C. raciborskii* (Briand et al., 2004).

NORTH AND SOUTH AMERICA

The record of *C. raciboskii*-like Nostocales in North America goes back to 1955 when *Anabaenopsis seriata* Prescott, was reported from Kansas. Other reports of morphologically similar species originated from Minneapolis and Lake Erie (Kling, 2009). It was only in the 1990s when *C. raciborskii* was identified in many Florida lakes and rivers (Chapman and Schelske, 1997). Since then, *C. raciborskii* has been found in many water bodies of the central and eastern United States (Kling, 2009) including in many lakes and reservoirs in Indiana (Jones and Sauter, 2005). These sites tended to be shallow and turbid with high epilimnetic phosphorus and high chlorophyll *a* values (Jones and Sauter, 2005). In 2004, *C. raciborskii* was identified in water samples from the Assiniboine River, Manitoba Canada. Variable morphological features

were reported in accordance with earlier reports from Europe, and predictions based on the adaptability of that species to eutrophic conditions, elevated temperatures and turbid waters suggested its expansion in Lake Winnipeg and replacing the original phytoplankton assemblage (Leavitt et al., 2006; Patoine et al., 2006). Indeed summer blooms development and phytoplankton succession was recently reported. Lake Winnipeg shows reduced taxonomic diversity and an increased predominance of nitrogen-fixing cyanobacteria (Kling et al., 2011).

In South America *C. raciborskii* is well known in tropical waters of Brazil (Huszar et al., 2000), although the information about its distribution in southern latitudes is disperse and incomplete (Komárek, 2002). Vidal and Kruk (2008) analyzed spatial distribution and relative frequency of *C. raciborskii* in southern Uruguay, probably its southernmost distribution. *C. raciborskii* was found in several polymictic shallow eutrophic lakes as a dominant summer population and variable morphology. It was suggested higher occurrence of *C. raciborskii* in that climatic zone was associated with shallow, well-mixed eutrophic systems. Furthermore, morphological variations in *C. raciborskii* were not associated with latitudinal, continental, or even country distribution and independent of climatic origin.

THE INVASION PROCESS

Successful biological invasions involve complex interactions between the invading species and the physical and biological characteristics of the recipient environment. Often, invasive cyanobacteria species owe their success in colonizing new ecosystems to unique physiological characteristics (**Figure 2**). The invasion may be initiated with dispersion to new zones and is facilitated by human activities by migrating animals or birds or by winds. Obviously, aeolian transport is an efficient means to transfer free-living microorganisms, prokaryotes, and protists (Smith et al., 2011). But reaching a new environment is not sufficient and the invader needs a variety of traits that support its establishment and proliferation. Two distinctive traits of Nostocalesa are: (1) The ability to form dormant cells (akinetes) that may survive long and extreme dispersion routes, on one hand and serve as overwintering form that survive unfavorable conditions and assure perennial germination and proliferation, on the other hand. (2) The ability to fix atmospheric nitrogen in the absence of combined inorganic sources. This last trait opens invasion opportunities for Nostocales in oligotrophic aquatic ecosystems, besides ecosystems temporarily limited in combined nitrogen and extends the spectrum of ecosystems to which they can invade.

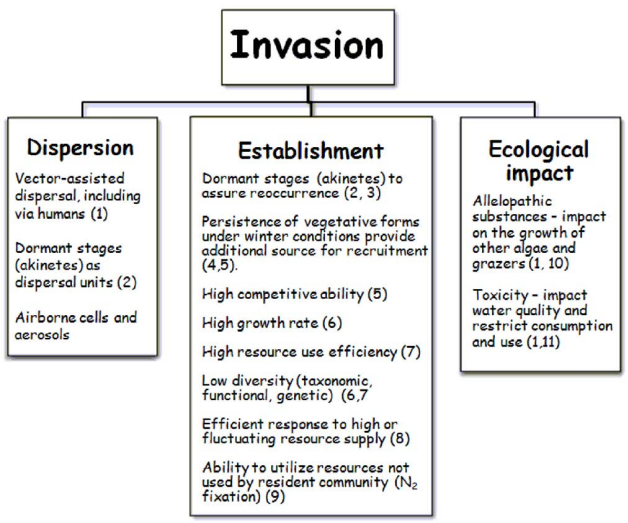

FIGURE 2 | Traits and process that support the invasiveness of cyanobacteria according to its three major components: dispersion, establishment, and ecological impact. References (1) Neilan et al., 2003; (2) Kaplan-Levy et al., 2010; (3) Wiedner et al., 2007; (4) Suikkanen et al., 2010; (5) Rücker et al., 2009;(6) Padisák, 1997; (7) Isvánovics et al., 2000; (8) Posselt et al., 2009; (9) Hadas et al., submitted; (10) Bar-Yosef et al., 2010; (11) Briand et al., 2004.

Invasive cyanobacteria have growth rates that are relatively high compared with those of native species (Isvánovics et al., 2000). They may have high resource use efficiency or possess traits allowing them to gain access to resources unavailable to other species, such as the capacity to fix molecular nitrogen. *C. raciborskii* has high competitiveness under fluctuating nitrogen availability due to efficient uptake capacity for ammonium (Figueredo et al., 2007) and it also can fix atmospheric nitrogen, which allows it to escape N limitation (Briand et al., 2004; Moisander et al., 2011). This species may also utilize other limiting resources, such as phosphorus, more efficiently than other cyanobacteria due to high affinity and P storage capacity (Isvánovics et al., 2000; Wu et al., 2011) and, thus, be a superior nutrient competitor. Padisák (1997) suggested that *C. raciborskii*, tends to invade lakes with very high nutrient concentrations and low phytoplankton diversity, in addition to its ability to form akinetes allowing easy dispersal and environmental resistance. An important feature of *Cylindrospermopsis* is its wide thermal tolerance (Briand et al., 2004), which is essential to maintain the populations during cold winters. Detailed information on the effect of temperature on Nostocales life cycle processes such as akinete formation, their survival and germination, and the recruitment of vegetative filaments is currently scarce, but Cirés (2012) indicated that akinetes production of *Aph. ovalisporum* is rather restricted to a relative narrow temperature range. Padisák (1997) reported that akinetes of *C. raciborskii* germinate at temperatures $<24^{\circ}C$. Further elucidation of life cycle processes responding to temperature is required in order to determine the invasiveness capabilities and limitations of various Nostocales species.

In many cases, floating Nostocales populations create a thick scum that blocks light penetration through the water column and inhibits the growth of other species, thus under high cyanobacterial growth, the populations remain established for longer periods minimizing competition by other algal groups. A scum formation is a dynamic process that depends on a delicate balance between flotation, cellular ballast and water turbulence (Calandrino and Paerl, 2011). Filaments floating at the water surface gain advantage over sub-surface phytoplankton populations. They directly intercept CO_2 diffusing into the water from the atmosphere, thus minimizing inorganic carbon limitation of photosynthetic growth. Buoyant species contain UV-absorbing compounds such as mycosporine-like amino acids (MAAs) and scytonemin that ensure survival under extremely high irradiance conditions (Paerl

and Paul, 2011). However, in some occasions scum formation represents a trap for the organisms that lose their dynamic buoyancy behavior and they are exposed to full sunshine (including high UV radiation in summer), as well as to nutrient deprivation. Frequently they die and remain on the water body shores with extremely low metabolic activities (i.e., C and N uptake, Oliver and Ganf, 2000 and references therein).

Another trait commonly found among Nostocales but also in other cyanobacteria (i.e., *Microcystis*) is the ability to synthesize a suite of secondary metabolites some of which were identified toxic to humans and animals (Stewart et al., 2011) and others may affect community structure functioning as allelo-chemicals that inhibit other phytoplankton species or deter and reduce grazing (Fastner et al., 2007; Paerl et al., 2011). Allelopathy was suggested as a beneficial trait of *C. raciborskii* that contributes to its stable dominance and geographic expansion (Figueredo et al., 2007) but also for other cyanobacteria species (Kaplan et al., in review). A unique feature of *Aph. ovalisporum* to acquire phosphate under oligotrophic conditions was recently reported by Bar-Yosef et al. (2010). Excreted chemicals including the toxin cylindrospermopsin cause cells of some other phytoplankton species to make extracellular alkaline phosphatase whose inorganic phosphate product can be used by *Aph. ovalisporum* due to its high affinity to phosphate, thus contributing to its proliferation and domination. *Aph. ovalisporum* has been also found to outcompete other cyanobacteria at high temperatures due to higher growth rates than other Nostocales under these circumstances (Mehnert et al., 2010; Cirés et al., 2011).

In an attempt to follow the invasion route of *C. raciborskii* to new ecosystems Neilan et al. (2003) studied genetic variations between strains isolated from freshwater rivers and reservoirs in Australia, Brazil, Germany, Hungary, Portugal, and the USA by characterizing their 16S rRNA gene nucleotide sequences and by analyzing cyanobacterium-specific short tandem repeat sequence (HIP1). Three distinct groups of *C. raciborskii* strains were clustered: (1) a group consisting of strains from the USA and Brazil; (2) a group comprised of European strains (Germany, Hungary, and Portugal); (3) a group of strains from Australia. A subsequent study that examined other isolates of *C. raciborskii* revealed the same continental cluster distribution based on the 16S–23S internally transcribed spacer (ITS1) sequences (Gugger et al., 2005). This study suggests that the current expansion of *C. raciborskii* in Europe and in Central – and North America did not result from recent invasion and colonization by African or Australian strains (Padisák, 1997) but rather represent local strains that maintained "cryptic" populations over time and only recently proliferated due to climate change and variations in other environmental conditions. In a recent study, Piccini et al. (2011) proposed that phenotypic and genetic variability of *C. raciborskii* populations is linked to the existence of different ecotypes whose success is subject to the local environmental conditions.

Nevertheless, analysis of the 16S rRNA gene nucleotide sequences revealed 99.1% similarity between the strains of *C. raciborskii* collected from a range of global locations and continental clustering was not supported by statistically significant bootstrap values (Neilan et al., 2003). Therefore it cannot be excluded that *C. raciborskii* was transferred from the Australasian region to Europe unintentionally by humans or by migrating birds, thus providing the source of this cyanobacterium which is now reported in many previously unaffected temperate and subtropical water bodies. It is further speculated that some physiological characteristics unique to *C. raciborskii* support its proliferation in newly invaded ecosystems as they are currently exposed to higher temperature and environmental perturbations.

GLOBAL VERSUS REGIONAL DRIVING FORCES

In order to exploit its wide spectrum of physiological traits and to successfully outcompete native species, the conditions in a new habitat have to fit the invader's needs. Increased water temperatures, mostly during the summer, in subtropical, and temperate zones, is considered one of the major factors supported the invasion of *C. raciborskii* and other Nostocales (**Figure 2**). (Padisák, 1997; Briand et al., 2004; Rücker et al., 2009). Both *C. raciborskii* and *Aph. ovalisporum* are known to proliferate at temperatures higher than 20°C (Hadas et al., 1999, 2002; Mehnert et al., 2010), thus moderate elevation in water temperatures may open new ecological habitats for them. The persistence of Nostocales in their new locations is further maintained by their ability to form dormant cells, akinetes, which stay dormant but viable in the sediment for extended periods of time (Hense and Beckmann, 2006; Kaplan-Levy et al., 2010). This seed bank may reside in the sediment and wait for a warm summer to germinate. Consequently, bloom events may follow local climatic patterns. It is important to note that freshly settled akinetes are more likely to germinate during the next summer relative to those settled in earlier blooms as the latter are already covered deeper in the sediments and probably have lower germination potency.

Nostocales species are recently reported to reside in, and dominate eutrophic as well as oligotrophic aquatic systems (**Figure 3**). Eutrophic conditions provide ample nutrients that can be easily and competitively utilized by opportunistic invaders (Piehler et al., 2009). Such eutrophic systems maintain high internal nutrient recycling processes that fortify primary production and biomass accumulation. Although N_2 fixation is commonly recorded during Nostocales blooms in eutrophic aquatic systems (mainly indicated by the presence of heterocysts, specialized cells formed under N limiting conditions), this process is responsible for up to 2% of N acquisition by the phytoplankton community (Ferber et al., 2004; Ariosa et al., 2006). The ability of many Nostocales to efficiently use low light, allows their growth in turbid waters as well as at high biomass concentrations.

Regional inappropriate management of watersheds and high pollution impact induce eutrophication, and are certainly involved in the Nostocales geographic expansion. But these invading species can survive and propagate also under oligotrophic conditions (**Figure 3**). This is achieved due to their various efficient phosphate acquisition capabilities (Isvánovics et al., 2000; Sprőber et al., 2003; Posselt et al., 2009; Bar-Yosef et al., 2010) and nitrogen fixation which seems to be more relevant under oligotrophic than under eutrophic conditions. Thus, in oligotrophic systems, nitrogen cannot be considered as a limiting factor. Phosphate availability controls the development of the N_2 fixing population and its growth. Consequently, management efforts to control

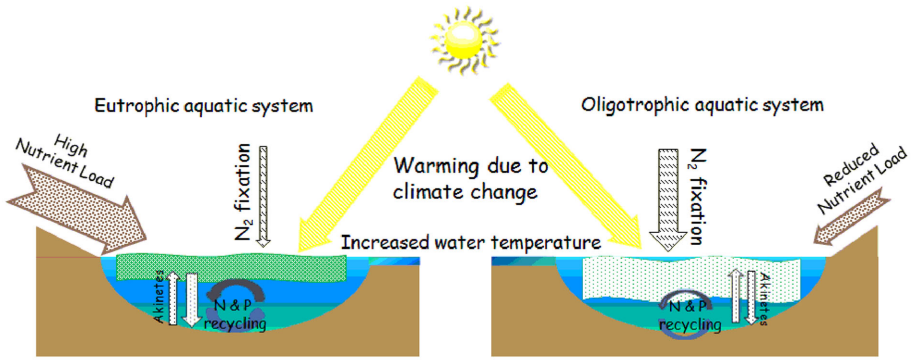

FIGURE 3 | Schematic presentation illustrating the proliferation and bloom potential of invasive Nostocales in eutrophic and oligotrophic lakes. Higher water temperatures open new habitats in which many Nostocales species can proliferate, taking advantage of their efficient physiological process. In eutrophic waters, a massive bloom and scum production is expected (depicted by a dense green patch) due to high external nutrient load and intense internal nutrient recycling (wide arrows). In oligotrophic waters a moderate bloom is likely to occur based on heterocysts formation and N_2 fixation and is controlled by restricted external and internal P load (narrow arrows). Dormant cells, akinetes, are formed in both cases (more akinetes are expected in eutrophic systems due to high biomass content) and provide the basis for perennial blooms. Note that nutrient recycling from bottom sediments occur in both systems but is more essential source for N and P in oligotrophic system. Nitrogen fixation is also evident in eutrophic systems only when the ample inorganic N provided by external and internal sources is exhausted.

eutrophication by reducing N loads, apparently effective in reducing blooms of *Microcystis* and other Chroococcales species, may actually support the growth of Nostocales which easily outcompete native species in such N limited ecosystems (Schindler et al., 2008).

CONSEQUENCES OF NOSTOCALES INVASIONS

The immediate consequence of Nostocales invasion, besides the ecological impairment, is the expansion of toxic blooms as various strains produce harmful substances. Many *Aph. ovalisporum* and *C. raciborskii* strains produce the cytotoxic compound cylindrospermopsin whereas several Brazilian *C. raciborskii* strains have been reported to produce paralytic shellfish poisoning toxins: neosaxitoxin, saxitoxin, and gonyautoxins (Lagos et al., 1999). Interestingly, many strains isolated from temperate lakes in Europe and Northern America did not produce any known toxin, although they were found toxic in various bioassay experiments (Saker et al., 2004). Recent studies indicated that a given population may be composed of toxic and non-toxic strains (Ballot et al., 2011). The bloom of toxic Nostocales presents an immediate threat to human and animals that use the water for drinking, bathing and recreational activities (Carmichael, 2001). Local and governmental authorities are requested to provide solutions to minimize and control the bloom events by taking scientifically based management measures that should include consideration of the invasiveness of this cyanobacterial group under a scenario of global change (Jones and Sauter, 2005; Schindler et al., 2008).

The domination of recently invaded Nostocales affects the entire ecosystem as native phytoplankton species become rare and displaced and higher trophic levels may be affected via their toxins or due to loss of essential components of their food chain. *C. raciborskii* is known to affect the growth, reproduction and feeding of zooplankton (Leonard and Paerl, 2005) and cylindrospermopsin was shown to be accumulated in fish and in freshwater mussels (Saker and Eaglesham, 1999; Saker et al., 2004).

PROSPECTIVE AND PREDICTIONS

The current trend of increasing bloom events of cyanobacteria, including Nostocales, will probably be further enhanced as global warming continues. Any further temperature increase would promote the growth and development of Nostocales species in general, and that of the invasive species in particular, and would enable further expansion in the temperate zone (Mehnert et al., 2010). This trend was further confirmed by a coupled biological–physical model that predicted that high temperatures favor cyanobacteria over other phytoplankton taxa through increased growth rates that boost the development of blooms (Juehnk et al., 2011). A similar conclusion was reached by Wiedner et al. (2007) who evaluated a case of an earlier rise in water temperature associated with climate change. They suggested that such a scenario will prompt further spread of *C. raciborskii* to the temperate zone as earlier warming permits earlier germination, thereby shifting the pelagic populations to conditions which advance population establishment and growth. However, these models do not consider the ecological variations expected after this earlier germination, as different grazing pressure due to different grazer population (e.g., Winder and Schindler, 2004) or nutrient depletion that may follow an early bloom. These ecological variations are hard to predict and should be further investigated to improve models prediction.

While the possibilities to control and reduce the current trend of global climate change are rather limited, the management of eutrophication processes is feasible. Since a synergistic effect of nutrients and climate was frequently indicated in many sites invaded by Nostocales, it is important that nutrient concentrations in many temperate and subtropical lakes be reduced substantially from present values if cyanobacterial dominance is to be controlled (Kosten et al., 2012). Based on long term experimental manipulation, Schindler et al. (2008) concluded that N-fixing cyanobacteria

cannot be limited by a shortage of dissolved N and instead are competitively favored. Thus reducing N inputs could actually intensify the dominance of N-fixing cyanobacteria thus enhancing the expansion of invasive Nostocales. The alternative approach to control and reduce blooms of invasive Nostocales species and their further expansion is to control and reduce external and internal sources of phosphorus, a complex task by itself.

ACKNOWLEDGMENTS

This work was partly supported by the German Ministry of Research and Technology (BMBF) and Israel Ministry of Science and Technology (MOST) under contracts FKZ 02WT0985 and WR803. Assaf Sukenik and Ora Hadas acknowledge the continuous support of the Israel Water Authority provided to the Kinneret Limnological Laboratory, IOLR.

REFERENCES

Ariosa, Y., Carrasco, D., Quesada, A., and Eduardo, F.-V. (2006). Incorporation of different N sources and light response curves of nitrogenase and photosynthesis by cyanobacterial blooms from rice fields. *Microb. Ecol.* 51, 394–403.

Ballot, A., Ramm, J., Rundberget, T., Kaplan-Levy, R. N., Hadas, O., Sukenik, A., and Wiedner, C. (2011). Occurrence of non-cylindrospermopsin-producing *Aphanizomenon ovalisporum* and *Anabaena bergii* in Lake Kinneret (Israel). *J. Plankton Res.* 33, 1736–1746.

Bar-Yosef, Y., Sukenik, A., Hadas, O., Viner-Mozzini, Y., and Kaplan, A. (2010). Enslavement in the water body by toxic *Aphanizomenon ovalisporum*, inducing alkaline phosphatase in phytoplanktons. *Curr. Biol.* 20, 1557–1561.

Bazzichelli, G., and Abdelahad, N. (1994). Caractérisation morphométrique et statistique de deux populations d'Aphanizomenon du groupe *Aphanizomenon ovalisporum* Forti des lacs de Nemi et Albano (Italie). *Algological Studies/Archiv für Hydrobiologie* 73(Suppl.), 1–21.

Berman, T. (1997). Dissolved organic nitrogen utilization by an *Aphanizomenon* bloom in Lake Kinneret. *J. Plankton Res.* 19, 577–586.

Berman, T. (2001). The role of DON and the effect of N:P ratios on occurrence of cyanobacterial blooms: implications from the outgrowth of *Aphanizomenon* in Lake Kinneret. *Limnol. Oceanogr.* 46, 443–447.

Berman, T., and Shteinman, B. (1998). Phytoplankton development and turbulent mixing in Lake Kinneret (1992–1996). *J. Plankton Res.* 20, 709–726.

Bouvy, M., Falcão, D., Marinho, M., Pagano, M., and Moura, A. (2000). Occurrence of *Cylindrospermopsis* (Cyanobacteria) in 39 Brazilian tropical reservoirs during the 1998 drought. *Aquat. Microb. Ecol.* 23, 13–27.

Briand, J.-F., Leboulanger, C., Humbert, J.-F., Bernard, C., and Dufour, P. (2004). *Cylindrospermopsis raciborskii* (cyanobacteria) invasion at mid-latitudes: selection, wide physiological tolerance, or global warming? *J. Phycol.* 40, 231–238.

Calandrino, E. S., and Paerl, H. W. (2011). Determining the potential for the proliferation of the harmful cyanobacterium *Cylindrospermopsis raciborskii* in Currituck Sound, North Carolina. *Harmful Algae* 11, 1–9.

Carmichael, W. W. (2001). Health effects of toxin-producing cyanobacteria: "the CyanoHABs." *Hum. Ecol. Risk Assess.* 7, 1393–1407.

Chapman, A. D., and Schelske, C. L. (1997). Recent appearance of *Cylindrospermopsis* (Cyanobacteria) in five hypertrophic Florida Lakes. *J. Phycol.* 33, 191–195.

Chonudomkul, D., Yongmanitchai, W., Theeragool, G., Kawachi, M., Kasai, F., Kaya, K., and Watanabe, M. M. (2004). Morphology, genetic diversity, temperature tolerance and toxicity of *Cylindrospermopsis raciborskii* (Nostocales, Cyanobacteria) strains from Thailand and Japan. *FEMS Microbiol. Ecol.* 48, 345–355.

Cirés, S. (2012). *Ecophysiology, Annual Life-Cycles and Cyanotoxin Production of Planktonic Cyanobacteria Anabaena, Aphanizomenon and Microcystis in Spanish Freshwater Reservoirs.* Ph.D. thesis, Universidad Autónoma de Madrid, Madrid.

Cirés, S., Wörmer, L., Timón, J., Wiedner, C., and Quesada, A. (2011). Cylindrospermopsin production and release by the potentially invasive cyanobacterium *Aphanizomenon ovalisporum* under temperature and light gradients. *Harmful Algae* 10, 668–675.

Colautti, R. I., and Macisaac, H. J. (2004). A neutral terminology to define "invasive" species. *Divers. Distrib.* 10, 135–141.

Dobberfuhl, D. R. (2003). *Cylindrospermopsis raciborskii* in three central Florida lakes: population dynamics, controls, and management implications. *Lake Reserv. Manag.* 19, 341–348.

Dyble, J., Paerl, H. W., and Neilan, B. A. (2002). Genetic characterization of *Cylindrospermopsis raciborskii* (Cyanobacteria) isolates from diverse geographic origins based on nifH and cpcBA-IGS nucleotide sequence analysis. *Appl. Environ. Microbiol.* 68, 2567–2571.

Elton, C. S. (1958). *The Ecology of Invasions by Animals and Plants.* London: Methuen.

Fastner, J., Rücker, J., Stüken, A., Preußel, K., Nixdorf, B., Chorus, I., Köhler, A., and Wiedner, C. (2007). Occurrence of the cyanobacterial toxin cylindrospermopsin in northeast Germany. *Environ. Toxicol.* 22, 26–32.

Ferber, L. R., Levine, S. N., Lini, A., and Livingston, G. P. (2004). Do cyanobacteria dominate in eutrophic lakes because they fix atmospheric nitrogen? *Freshw. Biol.* 49, 690–708.

Figueredo, C. C., Giani, A., and Bird, D. F. (2007). Does allelopathy contribute to *Cylindrospermopsis raciborskii* (cyanobacteria) bloom occurrence and geographic expansion? *J. Phycol.* 43, 256–265.

Gophen, M., Smith, V. H., Nishri, A., and Threlkeld, S. T. (1999). Nitrogen deficiency, phosphorus sufficiency, and the invasion of Lake Kinneret, Israel, by the N2-fixing cyanobacterium *Aphanizomenon ovalisporum. Aquat. Sci.* 61, 293–306.

Gugger, M., Molica, R., Le Berre, B., Dufour, P., Bernard, C., and Humbert, J.-F. (2005). Genetic diversity of *Cylindrospermopsis* strains (Cyanobacteria) isolated from four continents. *Appl. Environ. Microbiol.* 71, 1097–1100.

Hadas, O., Pinkas, R., Delphine, E., Vardi, A., Kaplan, A., and Sukenik, A. (1999). Limnological and ecophysiological aspects of *Aphanizomenon ovalisporum* bloom in Lake Kinneret, Israel. *J. Plankton Res.* 21, 1439–1453.

Hadas, O., Pinkas, R., Malinsky-Rushansky, N., Shalev-Alon, G., Delphine, E., Berner, T., Sukenik, A., and Kaplan, A. (2002). Physiological variables determined under laboratory conditions may explain the bloom of *Aphanizomenon ovalisporum* in Lake Kinneret. *Eur. J. Phycol.* 37, 259–267.

Hense, I., and Beckmann, A. (2006). Towards a model of cyanobacteria life cycle – effects of growing and resting stages on bloom formation of N2-fixing species. *Ecol. Modell.* 195, 205–218.

Huszar, V. L. M., Silva, L. H. S., Marinho, M., Domingos, P., and Sant'anna, C. L. (2000). Cyanoprokaryote assemblages in eight productive tropical Brazilian waters. *Hydrobiologia* 424, 67–77.

Isvánovics, V., Shafik, H. M., Présing, M., and Juhos, S. (2000). Growth and phosphate uptake kinetics of the cyanobacterium, *Cylindrospermopsis raciborskii* (Cyanophyceae) in throughflow cultures. *Freshw. Biol.* 43, 257–275.

Jones, W. W., and Sauter, S. (2005). Distribution and abundance of *Cylindrospermopsis raciborskii* in Indiana lakes and reservoirs. Schoool of Public and Environmental Affairs, Indiana University. Available al: http://www.spea.indiana.edu/clp/finalcylindro%20web.pdf

Juehnk, K. D., Brueggemann, R., Rücker, J., Luther, B., Simon, U., Nixdorf, B., and Wiedner, C. (2011). Modelling life cycle and population dynamics of Nostocales (cyanobacteria). *Environ. Modell. Softw.* 26, 669–677.

Kaplan-Levy, R. N., Hadas, O., Summers, M. L., Rücker, J., and Sukenik, A. (2010). "Akinetes – dormant cells of cyanobacteria," in *Dormancy of Cells and Organisms*, eds J. Cerdà, M. Clark, and E. Lubzens (Berlin: Springer), 269–300.

Kaštovský, J., Hauer, T., Mareš, J., Krautová, M., Bešta, T., Komárek, J., Desortová, B., Heteša, J., Hindáková, A., Houk, V., Janeček, E., Kopp, R., Marvan, P., Pumann, P., Skácelová, O., and Zapomělová, E. (2011). A review of the alien and expansive species of freshwater cyanobacteria and algae in the Czech Republic. *Biol. Invasions* 12, 3599–3625.

Kling, H. (2009). *Cylindrospermopsis raciborskii* (Nostocales, Cyanobacteria): a brief historic overview and recent discovery in the Assiniboine River (Canada). *Fottea* 9, 45–47.

Kling, H. J., Watson, S. B., Mccullough, G. K., and Stainton, M. P.

(2011). Bloom development and phytoplankton succession in Lake Winnipeg: a comparison of historical records with recent data. *Aquat. Ecosystems Health Manag.* 14, 219–224.

Kokociński, M., Dziga, D., Spoof, L., Stefaniak, K., Jurczak, T., Mankiewicz-Boczek, J., and Meriluoto, J. (2009). First report of the cyanobacterial toxin cylindrospermopsin in the shallow, eutrophic lakes of western Poland. *Chemosphere* 74, 669–675.

Komárek, J. (2002). "Problems in cyanobacterial taxonomy: implications for most common toxin producing species," in *Workshop Freshwater Harmful Algal Blooms: Health Risk and Control Management*, eds S. Melchiorre, E. Viaggiu, and M. Bruno (Rapporti ISTISAN: Rome), 6–43.

Komárek, J., and Komárkova, J. (2003). Phenotype diversity of the cyanoprokaryotic genus *Cylindrospermopsis* (Nostocales); review 2002. *Fottea (Praha)* 3, 1–30.

Kosten, S., Huszar, V. L. M., Bécares, E., Costa, L. S., Van Donk, E., Hansson, L.-A., Jeppesen, E., Kruk, C., Lacerot, G., Mazzeo, N., De Meester, L., Moss, B., Lürling, M., Nõges, T., Romo, S., and Scheffer, M. (2012). Warmer climates boost cyanobacterial dominance in shallow lakes. *Glob. Chang. Biol.* 18, 118–126.

Lagos, N., Onodera, H., Zagatto, P. A., Andrinolo, D., Azevedo, S. M. F. Q., and Oshima, Y. (1999). The first evidence of paralytic shellfish toxins in the freshwater cyanobacterium *Cylindrospermopsis raciborskii*, isolated from Brazil. *Toxicon* 37, 1359–1373.

Leavitt, P. R., Brock, C. S., Ebel, C., and Alain, P. (2006). Landscape-scale effects of urban nitrogen on a chain of freshwater lakes in Central North America. *Limnol. Oceanogr.* 51, 2262–2277.

Leonard, J., and Paerl, H. (2005). Zooplankton community structure, micro-zooplankton grazing impact, and seston energy content in the St. Johns River system, Florida as influenced by the toxic cyanobacterium *Cylindrospermopsis raciborskii*. *Hydrobiologia* 537, 89–97.

Levine, J. M., Vilà, M., Antonio, C. M. D., Dukes, J. S., Grigulis, K., and Lavorel, S. (2003). Mechanisms underlying the impacts of exotic plant invasions. *Proc. R. Soc. Lond. B Biol. Sci.* 270, 775–781.

Litchman, E. (2010). Invisible invaders: non-pathogenic invasive microbes in aquatic and terrestrial ecosystems. *Ecol. Lett.* 13, 1560–1572.

Lockwood, J., Hoopes, M., and Marchetti, M. (2007). *Invasion Ecology*. Malden, MA: Blackwell Publishing.

Mehnert, G., Leunert, F., Cires, S., Johnk, K. D., Rucker, J., Nixdorf, B., and Wiedner, C. (2010). Competitiveness of invasive and native cyanobacteria from temperate freshwaters under various light and temperature conditions. *J. Plankton Res.* 32, 1009–1021.

Meinesz, A., Belsher, T., Thibaut, T., Antolic, B., Mustapha, K. B., Boudouresque, C.-F., Chiaverini, D., Cinelli, F., Cottalorda, J.-M., Djellouli, A., El Abed, A., Orestano, C., Grau, A. M., Ivesa, L., Jaklin, A., Langar, H., Massuti-Pascual, E., Peirano, A., Tunesi, L., De Vaugelas, J., Zavodnik, N., and Zuljevic, A. (2001). The introduced green alga Caulerpa taxifolia continues to spread in the Mediterranean. *Biol. Invasions* 3, 201–210.

Mohamed, Z. A. (2007). First report of toxic *Cylindrospermopsis raciborskii* and *Raphidiopsis mediterranea* (Cyanoprokaryota) in Egyptian fresh waters. *FEMS Microbiol. Ecol.* 59, 749–761.

Moisander, P. H., Cheshire, L. A., Braddy, J., Calandrino, E. S., Hoffman, M., Piehler, M. F., and Paerl, H. W. (2011). Facultative diazotrophy increases *Cylindrospermopsis raciborskii* competitiveness under fluctuating nitrogen availability. *FEMS Microb. Ecol.* 79, 800–811.

Molica, R., Onodera, H., García, C., Rivas, M., Andrinolo, D., Nascimento, S., Meguro, H., Oshima, Y., Azevedo, S., and Lagos, N. (2002). Toxins in the freshwater cyanobacterium *Cylindrospermopsis raciborskii* (Cyanophyceae) isolated from Tabocas reservoir in Caruaru, Brazil, including demonstration of a new saxitoxin analogue. *Phycologia* 41, 606–611.

Neilan, B. A., Saker, M. L., Fastner, J., Törökné, A., and Burns, B. P. (2003). Phylogeography of the invasive cyanobacterium *Cylindrospermopsis raciborskii*. *Mol. Ecol.* 12, 133–140.

Oliver, R., and Ganf, G. (2000). "Freshwater blooms," in *The Ecology of Cyanobacteria*, eds B. Whitton and M. Potts (Dordrecht: Kluwer Academic Publishers), 149–194.

Padisák, J. (1997). *Cylindrospermopsis raciborskii* (Woloszynska) Seenayya et Subba Raju, an expanding, highly adaptive cyanobacterium: worldwide distribution and review of its ecology. *Archiv für Hydrobiologie* 107, 563–593.

Paerl, H. W., Hall, N. S., and Calandrino, E. S. (2011). Controlling harmful cyanobacterial blooms in a world experiencing anthropogenic and climatic-induced change. *Sci. Total Environ.* 409, 1739–1745.

Paerl, H. W., and Paul, V. J. (2011). Climate change: links to global expansion of harmful cyanobacteria. *Water Res.* 46, 1349–1363.

Patoine, A., Graham, M. D., and Leavitt, P. R. (2006). Spatial variation of nitrogen fixation in lakes of the northern Great Plains. *Limnol. Oceanogr.* 51, 1665–1677.

Piccini, C., Aubriot, L., Fabre, A., Amaral, V., Gonzalez-Piana, M., Giani, A., Figueredo, C. C., Vidal, L., Kruk, C., and Bonilla, S. (2011). Genetic and eco-physiological differences of South American *Cylindrospermopsis raciborskii* isolates support the hypothesis of multiple ecotypes. *Harmful Algae* 10, 644–653.

Piehler, M. F., Dyble, J., Moisander, P. H., Chapman, A. D., Hendrickson, J., and Paerl, H. W. (2009). Interactions between nitrogen dynamics and the phytoplankton community in Lake George, Florida, USA. *Lake Reserv. Manag.* 25, 1–14.

Pimentel, D., Mcnair, S., Janecka, J., Wightman, J., Simmonds, C., O'connell, C., Wong, E., Russel, L., Zern, J., Aquino, T., and Tsomondo, T. (2001). Economic and environmental threats of alien plant, animal, and microbe invasions. *Agriculture Ecosystems Environ.* 84, 1–20.

Pollingher, U., Hadas, O., Yacobi, Y. Z., Zohary, T., and Berman, T. (1998). *Aphanizomenon ovalisporum* (Forti) in Lake Kinneret, Israel. *J. Plankton Res.* 20, 1321–1339.

Posselt, A. J., Burford, M. A., and Shaw, G. (2009). Pulses of phosphate promote dominance of the toxic cyanophyte *Cylindrospermopsis raciborskii* in a subtropical water reservoir. *J. Phycol.* 45, 540–546.

Quesada, A., Moreno, E., Carrasco, D., Paniagua, T., Wormer, L., Hoyos, C. D., and Sukenik, A. (2006). Toxicity of *Aphanizomenon ovalisporum* (Cyanobacteria) in a Spanish water reservoir. *Eur. J. Phycol.* 41, 39–45.

Ramezanpoor, Z. (2004). Ecological study of phytoplankton of the Anzali lagoon (N Iran) and its outflow into the Caspian Sea. *Czech Phycol. Olomouc* 4, 145–154.

Ricciardi, A., and Cohen, J. (2007). The invasiveness of an introduced species does not predict its impact. *Biol. Invasions* 9, 309–315.

Richardson, D. (ed.). (2011). *Fifty Years of Invasion Ecology – The Legacy of Charles Elton Chichester*. Oxford: Wiley-Blackwell.

Romo, S., and Miracle, M. R. (1994). Population dynamics and ecology of subdominant phytoplankton species in a shallow hypertrophic lake (Albufera of Valencia, Spain). *Hydrobiologia* 273, 37–56.

Rücker, J., Tingwey, E., Wiedner, C., Anu, C., and Nixdorf, B. (2009). Impact of the inoculum size on the population of Nostocales cyanobacteria in temperate lakes. *J. Plankton Res.* 31, 1151–1159.

Ryan, E. F., P, H. D., and Barnes, G. (2003). Recent occurrence of *Cylindrospermopsis raciborskii* in Waikato lakes of New Zealand. *N. Z. J. Mar. Freshwater Res.* 37, 829–836.

Saker, M. L., and Eaglesham, G. K. (1999). The accumulation of cylindrospermopsin from the cyanobacterium *Cylindrospermopsis raciborskii* in tissues of the redclaw crayfish Cherax quadricarinatus. *Toxicon* 37, 1065–1077.

Saker, M. L., Metcalf, J. S., Codd, G. A., and Vasconcelos, V. M. (2004). Accumulation and depuration of the cyanobacterial toxin cylindrospermopsin in the freshwater mussel Anodonta cygnea. *Toxicon* 43, 185–194.

Schindler, D. W., Hecky, R. E., Findlay, D. L., Stainton, M. P., Parker, B. R., Paterson, M. J., Beaty, K. G., Lyng, M., and Kasian, S. E. M. (2008). Eutrophication of lakes cannot be controlled by reducing nitrogen input: results of a 37-year whole-ecosystem experiment. *Proc. Natl. Acad. Sci. U.S.A.* 105, 11254–11258.

Shaw, G. R., Sukenik, A., Livne, A., Chiswell, R. K., Smith, M. J., Seawright, A. A., Norris, R. L., Eaglesham, G. K., and Moore, M. R. (1999). Blooms of the cylindrospermopsin containing cyanobacterium, *Aphanizomenon ovalisporum* (Forti), in newly constructed lakes, Queensland, Australia. *Environ. Toxicol.* 14, 167–177.

Smith, D. J., Griffin, D. W., and Jaffe, D. A. (2011). The high life: transport of microbes in the atmosphere. *Eos Trans.* 92, 249.

Sprőber, P., Shafik, H. M., Présing, M., Kovács, A. W., and Herodek, S. (2003). Nitrogen uptake and fixation in the cyanobacterium *Cylindrospermopsis raciborskii* under different nitrogen

conditions. *Hydrobiologia* 506–509, 169–174.

Stewart, I., Carmichael, W. W., and Backer, L.C. (2011). "Toxic Cyanobacteria," in *Water and Sanitation-Related Diseases and the Environment*, ed. J. M. H. Selendy (John Wiley and Sons, Inc.), 95–110.

Suikkanen, S., Kaartokallio, H., Hällfors, S., Huttunen, M., and Laamanen, M. (2010). Life cycle strategies of bloom-forming, filamentous cyanobacteria in the Baltic Sea. *Deep Sea Res. Part 2 Top. Stud. Oceanogr.* 57, 199–209.

Traveset, A., and Richardson, D. M. (2006). Biological invasions as disruptors of plant reproductive mutualisms. *Trends Ecol. Evol.* 21, 208–216.

Vidal, L., and Kruk, C. (2008). *Cylindrospermopsis raciborskii* (Cyanobacteria) extends its distribution to Latitude 34(53′S: taxonomical and ecological features in Uruguayan eutrophic lakes. *Pan Am. J. Aquat. Sci.* 3, 142–151.

Vitousek, P. M., Mooney, H. A., Lubchenco, J., and Melillo, J. M. (1997). Human domination of earth's ecosystems. *Science* 277, 494–499.

Wiedner, C., Rücker, J., Brüggemann, R., and Nixdorf, B. (2007). Climate change affects timing and size of populations of an invasive cyanobacterium in temperate regions. *Oecologia* 152, 473–484.

Winder, M., and Schindler, D. E. (2004). Climate change uncouples trophic interactions in a lake ecosystem. *Ecology* 85, 2100–2106.

Wood, S. A., and Stirling, D. J. (2003). First identification of the cylindrospermopsin-producing cyanobacterium *Cylindrospermopsis raciborskii* in New Zealand. *N. Z. J. Mar. Freshwater Res.* 37, 821–828.

Wu, Z., Zeng, B., Li, R., and Song, L. (2011). Physiological regulation of *Cylindrospermopsis raciborskii* (Nostocales, Cyanobacteria) in response to inorganic phosphorus limitation. *Harmful Algae* 15, 53–58.

Zohary, T. (2004). Changes to the phytoplankton assemblage of Lake Kinneret after decades of a predictable, repetitive pattern. *Freshw. Biol.* 49, 1355–1371.

Conflict of Interest Statement: The authors declare that the research was conducted in the absence of any commercial or financial relationships that could be construed as a potential conflict of interest.

Received: 11 January 2012; accepted: 20 February 2012; published online: 09 March 2012.

Citation: Sukenik A, Hadas O, Kaplan A and Quesada A (2012) Invasion of Nostocales (cyanobacteria) to subtropical and temperate freshwater lakes – physiological, regional, and global driving forces. Front. Microbio. ***3****:86. doi: 10.3389/fmicb.2012.00086*

This article was submitted to Frontiers in Aquatic Microbiology, a specialty of Frontiers in Microbiology.

frontiers in
MICROBIOLOGY

ORIGINAL RESEARCH ARTICLE
published: 18 January 2012
doi: 10.3389/fmicb.2012.00003

Plasticity of total and intracellular phosphorus quotas in *Microcystis aeruginosa* cultures and Lake Erie algal assemblages

Matthew A. Saxton[1†], Robert J. Arnold[1], Richard A. Bourbonniere[2], Robert Michael L. McKay[3] and Steven W. Wilhelm[1]*

[1] *Department of Microbiology, University of Tennessee, Knoxville, TN, USA*
[2] *National Water Research Institute, Environment Canada, Burlington, ON, USA*
[3] *Department of Biological Sciences, Bowling Green State University, Bowling Green, OH, USA*

Edited by:
George S. Bullerjahn, Bowling Green State University, USA

Reviewed by:
Assaf Sukenik, Israel Oceanographic and Limnological Research, Israel
Ilana R. Berman-Frank, Bar Ilan University, Israel

****Correspondence:***
Steven W. Wilhelm, Department of Microbiology, The University of Tennessee, M409 Walters Life Sciences, Knoxville, TN 37996-0845, USA.
e-mail: wilhelm@utk.edu

*[†]**Present address:***
Matthew A. Saxton, Keck Environmental Laboratory, Environmental Science and Policy Program, College of William and Mary, 200 Wake Drive, Williamsburg, VA 25185, USA.

Blooms of the potentially toxic cyanobacterium *Microcystis* are common events globally, and as a result significant resources continue to be dedicated to monitoring and controlling these events. Recent studies have shown that a significant proportion of total cell-associated phosphorus (P) in marine phytoplankton can be surface adsorbed; as a result studies completed to date do not accurately report the P demands of these organisms. In this study we measure the total cell-associated and intracellular P as well as growth rates of two toxic strains of *Microcystis aeruginosa* Kütz grown under a range of P concentrations. The results show that the intracellular P pool in *Microcystis* represents a percentage of total cell-associated P (50–90%) similar to what has been reported for actively growing algae in marine systems. Intracellular P concentrations (39–147 fg cell^{-1}) generally increased with increasing P concentrations in the growth medium, but growth rate and the ratio of total cell-associated to intracellular P remained generally stable. Intracellular P quotas and growth rates in cells grown under the different P treatments illustrate the ability of this organism to successfully respond to changes in ambient P loads, and thus have implications for ecosystem scale productivity models employing P concentrations to predict algal bloom events.

Keywords: cyanobacteria, phosphorus, *Microcystis*

INTRODUCTION

Widespread nutrient loading has led to the eutrophication of aquatic ecosystems throughout the developed world. A primary concern linked to eutrophication is the appearance of harmful algal blooms (HABs). HAB events are well-documented, ecosystem-wide problems that can impact human health, kill livestock, foul potable water supplies, and compromise the integrity of both recreational and commercial fisheries (Carmichael, 2001). HABs have also been implicated in contributing to the formation of hypoxic zones (Paerl et al., 1998).

Efforts to limit algal bloom formation have historically focused on reducing nutrient loading. Phosphorus (P) has been suggested to be the nutrient that limits phytoplankton growth in most freshwater ecosystems (Schindler, 1977; Schindler et al., 2008). Regulating P-loading has led to successes in controlling algal bloom formation in some eutrophic systems (Makarewicz and Bertram, 1991). This developing understanding of eutrophication has been critical to the continued development of mathematical environmental models which have become substantially more sophisticated with advances such as coupling hydrodynamic, ecological, and watershed models (Jørgensen, 2010).

Microcystis spp. are among the most common bloom-forming cyanobacteria in freshwaters and have a global distribution (Chorus and Bartram, 1999). The effects of P limitation on P-uptake in *Microcystis* have been extensively studied. Like other cyanobacteria, *Microcystis* possesses the ability to store excess P intracellularly, as polyphosphate granules, and P-starved cells have higher rates of P-uptake than P-sufficient cells (Jacobson and Halmann, 1982). *Microcystis* has been shown to respond to P limitation by rapid P-uptake with a notable increase in V_{max} observed under P-limiting conditions (Kromkamp et al., 1989). The recently sequenced *Microcystis* genomes indicate the presence of ATP driven P-uptake systems similar to what has been described in *Synechococcus* (Ritchie et al., 1997, 2001; Kaneko et al., 2007; Frangeul et al., 2008).

Recently, an oxalate rinse developed to remove surface adsorbed iron (Tovar-Sanchez et al., 2003) was shown to also effectively remove surface adsorbed P from marine plankton (Sãnudo-Wilhelmy et al., 2004; Fu et al., 2005). Subsequently, these studies have shown a significant proportion (15–45%) of total cell-associated P to be surface adsorbed in marine cyanobacteria, and that this P is likely associated with surface adsorbed manganese. These studies have also suggested surface adsorption of P may be part of a two-step process in which surface adsorption is followed by internalization. Arguably, this phenomenon, if universal in nature, is predicted to be of even greater relevance to freshwater

ecosystems given their more universal P-limited nature. A consequence of the presence of adsorbed P on the surface of phytoplankton is that previous estimates of cyanobacterial P requirements may overstate the need for this nutrient. Alternatively, the ability of cyanobacteria to store P on their exterior surface may act as a novel strategy to allow persistence during periods of prolonged P deficiency (or to survive "boom-and-bust" cycles of nutrient availability). As such, a necessary first step is to determine the ability of cells to accumulate extracellular P and, further, to determine the contribution of this pool to estimated total P quotas.

In this study we determined the total cell-associated and intracellular P quotas and growth rates of two toxic *Microcystis* strains grown under a series of P concentrations. We similarly examined the ratio of total cell associated to intracellular P of natural communities in the western basin of Lake Erie where *Microcystis* forms an important part of the endemic plankton assemblage. Establishing accurate P quotas (and their plasticity) for this potentially toxic bloom-forming cyanobacterium is a necessary step toward the development of realistic environmental phytoplankton growth models and management strategies for many important freshwater resources.

MATERIALS AND METHODS

CYANOBACTERIAL CULTURE CONDITIONS

Experiments were performed with *M. aeruginosa* PCC 7806 obtained from the Pasteur Culture Collection. While *M. aeruginosa* PCC 7806 is a globally used type strain, it is not representative of much of the observed *Microcystis* diversity in Lake Erie (Ouellette and Wilhelm, 2003; Ouellette et al., 2006; Ye et al., 2009). *M. aeruginosa* LE3, an isolate from Lake Erie (Brittain et al., 2000), was also included as it has been shown to be representative of Lake Erie *Microcystis* (e.g., Rinta-Kanto and Wilhelm, 2006) and has been used as a standard in numerous studies (e.g., Rinta-Kanto et al., 2009b). Cultures were maintained in BG-11 medium (Rippka et al., 1979) at pH 7.5 with P concentrations ranging from 1.75 to 175 μM K_2HPO_4. Cultures were grown in 50 mL glass culture tubes (Kimble, Vineland, NJ, USA) at 24°C under continuous illumination of ∼30 μmol photons m^{-2} s^{-1}. Prior to use, all culture tubes were soaked overnight in 1% HCl and rinsed multiple times with Milli-Q® water (Millipore Corp., Billerica, MA, USA). Samples were grown and transferred at experimental P concentrations two times prior to data collection. Multiple transfers were performed to ensure the stabilization of cellular P stores and the physiological equilibration of cell cultures to experimental P levels *vis a vis* Wilhelm et al. (1996). Cyanobacterial growth was monitored daily using a Turner Designs TD-700 fluorometer (Sunnyvale, CA, USA) equipped with an *in vivo* chl*a* filter set (excitation λ = 340–500 nm; emission λ = >665 nm). Growth rates were determined through the measurement of the slope of the growth curve during the exponential growth phase plotted as the natural log. All experiments were performed in triplicate unless otherwise noted.

FIELD SAMPLE COLLECTION

Field samples were collected at sites across Lake Erie (**Table 1**) between the dates of August 3 and 7, 2010 aboard the *CCGS Limnos*. Surface water was collected at each site using 10 L Niskin sampling bottles and subsequently stored in 3 L opaque amber polycarbonate bottles until filtration (with the time between collection and storage less than 1 h).

PHYTOPLANKTON ENUMERATION

Phytoplankton enumeration was performed using samples preserved in Lugol's Iodine as previously described (Rodhe et al., 1958; Anderson, 2005). Fifty milliliter samples from each incubation were collected and immediately distributed into amber bottles with predispensed Lugol's Iodine resulting in a final concentration of 2% (vol/vol) fixative. Fixed samples were enumerated using a

Table 1 | Hydrological and biological parameters of surface water sampled from Lake Erie August 2010.

Station	478	970 (357)	973	882	1163	341	880 (84)
Location (Lat°N, Long°W)	41°39′26″ (82°49′01″)	41°49′30″ (82°58′30″)	41°47′30″ (83°20′00″)	41°46′00″ (83°18′30″)	41°28′16″ (82°43′05″)	41°48′00″ (82°17′30″)	41°56′08″ (81°39′14″)
Extracellular P (%)	4.9	10.91	0.74	9.99	16.54	0	34.12
Total particulate P (μg L^{-1} ± SD)	8.2 ± 3.65	8.16 ± 3.65	27.05 ± 4.68	13.18 ± 0.91	96.97 ± 18.76	6.28 ± 0.86	6.25 ± 1.44*
Intracellular P (μg L^{-1} ± SD)	7.3 ± 2.78*	7.27 ± 2.78*	26.85 ± 0.80	11.86 ± 1.17	80.93 ± 13.20	6.30 ± 1.74	4.12 ± 0.099*
SRP (μg L^{-1})	0.8	1.1	1.3	1.7	2.1	0.4	0.6
TDP (μg L^{-1})	7.5	6.9	9.4	10.6	14.0	5.0	4.8
TP (μg L^{-1})	21.6	21.8	37.7	34.7	85.5	13.3	12.9
NO_X^- (mgN L^{-1})[a]	0.25	0.145	0.017	0.016	0.010	0.073	0.059
NH_3 (mgNL^{-1})	0.011	0.010	0.009	0.016	BDL[b]	0.012	0.018
TDN (mg L^{-1})	0.526	0.338	0.301	0.410	0.393	0.361	0.291
PON (mg L^{-1})	0.12	0.178	0.215	0.228	0.678	0.101	0.094
SiO_2 (mg L^{-1})	1.46	1.53	1.77	2.00	3.61	1.53	0.28
SO_4^{2-} (mg L^{-1})	21.8	18.9	19.6	19.4	34.0	21.1	21.8
POC (mg L^{-1})	0.73	1.20	1.38	1.46	3.66	0.842	0.658
Total Chl*a* (μg L^{-1} ± SD)	6.1 ± 0.13	15.82 ± 2.21	18.61 ± 0.61	16.09 ± 1.34	16.25 ± 0.52	5.52 ± 0.68	7.54 ± 0.74

**Indicates n = 2. [a]Nitrate + nitrite as N. [b]BDL, below detectable limits (<0.005 mgN L^{-1}).*

Sedgwick-Rafter counting slide (Wildco) on a Micromaster light microscope (ThermoFisher). Samples were allowed to settle in the counting chamber for 3–5 min prior to enumeration. Four horizontal passes were made across each slide encompassing the full height and width of the slide; no fewer than 40 fields of view were randomly selected across each slide. Each field of view was imaged and saved using Micron imaging software (Westover Scientific); the use of this software allowed for the measurement of the field of view.

QUANTIFICATION OF TOTAL CELLULAR AND INTRACELLULAR P

Total cellular and intracellular P concentrations were independently measured. Surface bound P was removed using an oxalate wash reagent initially designed for removal of iron (Tovar-Sanchez et al., 2003) and subsequently demonstrated to be applicable for removal of surface-sorbed P (Sãnudo-Wilhelmy et al., 2004). Aliquots of 5 mL from individual cultures and 50–200 mL from field samples were harvested onto pre-combusted (450°C for 4 h) 25 mm Whatman (Kent, UK) GF/F glass fiber filters for the determination of total P in samples. The range in sample volumes collected at the individual sites was to account for different phytoplankton concentrations at each station. For the determination of intracellular P from *Microcystis* isolates, aliquots were first mixed with an equal volume of oxalate wash and allowed to incubate for 5 min prior to harvest. Field samples were filtered until approximately 5 mL of sample water remained in the filter unit; 5 mL of oxalate rinse was then applied and incubated for 5 min. A top-up solution containing equal parts oxalate rinse and filtered lakewater was applied as needed to counter losses due to residual vacuum. Following this incubation, the filter was rinsed three times with 5 mL of P-free growth media or filtered lake water. To control for the removal of surface associated P during the washing process, control samples were rinsed with P-free medium or filtered lake water four times in the same manner as experimental samples. Unused growth medium of each of the experimental P concentrations was passed through filters and rinsed with P-free media and oxalate rinse solution as blanks to control for media associated P binding to the filter. Filtered station water was used as blanks for field samples. All treatments were performed in triplicate and blanks were performed in duplicate. Following the oxalate rinse procedure, filters were stored at −20°C until analysis.

P MEASUREMENT

Particulate organic P was collected on filters and converted to inorganic P *via* persulfate oxidation (Menzel and Corwin, 1965; Wetzel and Likens, 2000). Freshly made 5% potassium persulfate solution was added to samples that were then placed in a boiling water bath for 1 h. Total P concentrations were measured spectrophotometrically (885 nm) using the ammonium molybdate method (Wetzel and Likens, 2000). All measurements for field samples were performed on a Thermo Spectronic Genesys 20 spectrophotometer (ThermoFisher Waltham, MA, USA), whereas cultured samples were processed using a Biomate 5 spectrophotometer (ThermoFisher Waltham, MA, USA).

Field samples were prepared by first digesting with 5% potassium persulfate, followed by autoclaving for 30 min. Total P was spectrophotometrically analyzed (880 nm) with the molybdate ascorbic acid method (Strickland and Parsons, 1972) using a 10-cm quartz cell and a Cary 50 UV–vis spectrophotometer (Varian Palo Alto, CA, USA). A calibration was conducted using phosphate reference standards of known concentration processed in the same manner as sample material. Individual replicates were omitted from field sample analysis if one sample was more than 100% different than the average of the two other samples. Variability among replicates was likely the result of the incomplete rinsing of cell aggregates.

Subsamples of cultured samples (1.5 mL) were also collected from each tube for direct counts of cell concentration. *Microcystis* cell densities were determined by epifluorescence microscopy with a Leica (Wetzlar, Germany) DMXRA epifluorescence microscope using the Texas Red filter set targeting accessory pigment (phycobillin) autofluorescence as previously described (Wilhelm et al., 2006). This was performed to normalize P measurements to *Microcystis* cell abundance.

WATER CHEMISTRY

Samples for nutrients, including total dissolved phosphorus (TDP), soluble reactive phosphorus (SRP), total dissolved nitrogen (TDN), NH_4^+ - N, NO_3^- - N + NO_2^- − *N*, silicate (SiO_2), sulfate (SO_4^{2-}), particulate organic nitrogen (PON), and particulate organic carbon (POC), were collected and stored at 4°C until analysis. Analysis was conducted at the National Laboratory for Environmental Testing (Environment Canada) using their standard techniques (NLET, 1994).

EXTRACTED CHLOROPHYLL *a*

Chlorophyll *a* (chl*a*) concentration at field stations was determined as a proxy for total phytoplankton biomass. Seston was filtered through 0.2-μm nominal pore-size polycarbonate membranes. Chl*a* concentrations were determined using the non-acidification method (Welschmeyer, 1994) following extraction in 90% acetone overnight at −20°C using a Turner Designs 10-AU fluorometer.

RESULTS

P-CONSTRAINTS ON MICROCYSTIS GROWTH

Cultured *Microcystis* growth rates across a range of P concentrations are shown in **Table 2**. Growth rates in both strains were only slightly variable across the tested experimental P concentrations. *M. aeruginosa* PCC 7806 growth rates ranged between 0.079 and 0.162 divisions day^{-1} with *M. aeruginosa* LE3 growth rates ranging from 0.058 to 0.142 divisions day^{-1}. Growth rates increased with a slope of 0.0002 in *M. aeruginosa* PCC 7806 while *M. aeruginosa* LE3 rates decreased with a slope of −0.0001. Growth rates were especially steady among those cultures maintained at higher P concentrations. Growth rates were more variable in *M. aeruginosa* LE3 than in *M. aeruginosa* PCC 7806. Although growth rates were stable across concentrations of P, biomass was notably lower in cultures maintained under the lower P concentrations (results not shown). It should also be noted that *Microcystis* PCC 7806 did not grow consistently at the lowest P concentrations in spite of repeated attempts. We recognize that the reported growth rates are lower than published values. These lower growth rates are the result of the cultures being grown in conditions not optimized to

Table 2 | *Microcystis aeruginosa* strains PCC 7806 and LE3 growth rates.

Organism	Growth media P concentration (μM)	Growth rate ($day^{-1} \pm SD$)
M. aeruginosa PCC 7806	1.75	0.079*
	8.75	0.123 ± 0.009
	17.5	0.149 ± 0.005
	87.5	0.162 ± 0.005
	175	0.138 ± 0.023
M. aeruginosa LE3	1.75	0.118 ± 0.008
	8.75	0.142 ± 0.001
	17.5	0.0844*
	87.5	0.058 ± 0.001
	175	0.108 ± 0.001

*Growth rates measured in triplicates except where *n = 1 as replicates would not grow at these concentrations.*

obtain maximum growth rates, but rather they best reflect natural conditions (lower than optimal temperature and light). It is also possible cultures may have became CO_2^- limited as a result of small culture volume.

TOTAL CELL-ASSOCIATED AND INTRACELLULAR P QUOTAS IN CULTURED *MICROCYSTIS*

To obtain accurate intracellular P quotas for *Microcystis aeruginosa*, we utilized the oxalate rinse technique to differentiate between the total cell-associated and intracellular P pools (**Figure 1**). The range of total cell-associated P concentrations reported here (39–173 fg $cell^{-1}$) are within the range of previously reported values (29–433 fg $cell^{-1}$; Rhee and Gotham, 1980; Sbiyyaa et al., 1998; Tsukada et al., 2006; Shen and Song, 2007). As was anticipated, intracellular P quotas (34–146 fg $cell^{-1}$) were significantly smaller (ANOVA $p = 0.001$) than the cell-associated values (39–173 fg $cell^{-1}$). As had been previously reported for marine cyanobacteria (Fu et al., 2005), our results show that surface adsorbed P represents a significant portion (between 10 and 50%) of total cell-associated P in *Microcystis*. We also found that this percentage is stable across growth conditions in each of the strains tested (**Figure 1C**).

TOTAL CELL-ASSOCIATED AND INTRACELLULAR P IN NATURAL SAMPLES

The ratio of total cell-associated P to intracellular P was also investigated in natural phytoplankton communities. Samples were collected across Lake Erie with specific emphasis on the Western Basin. This sampling focus reflects the recurrence of *Microcystis* blooms in this region (Rinta-Kanto et al., 2005, 2009a; Moorhead et al., 2008). *Microcystis* spp. was present at all tested stations, though a diverse assemblage of cyanobacteria and eukaryotic algae were observed (**Table A1** in Appendix). Hydrological and biological parameters measured as part of this study were similar to those previously reported across Lake Erie (**Table 2**; DeBruyn et al., 2004). Intracellular P made up an average of 89% (±11%) with a range of 0–65% of total particulate P in these samples (**Table 1**).

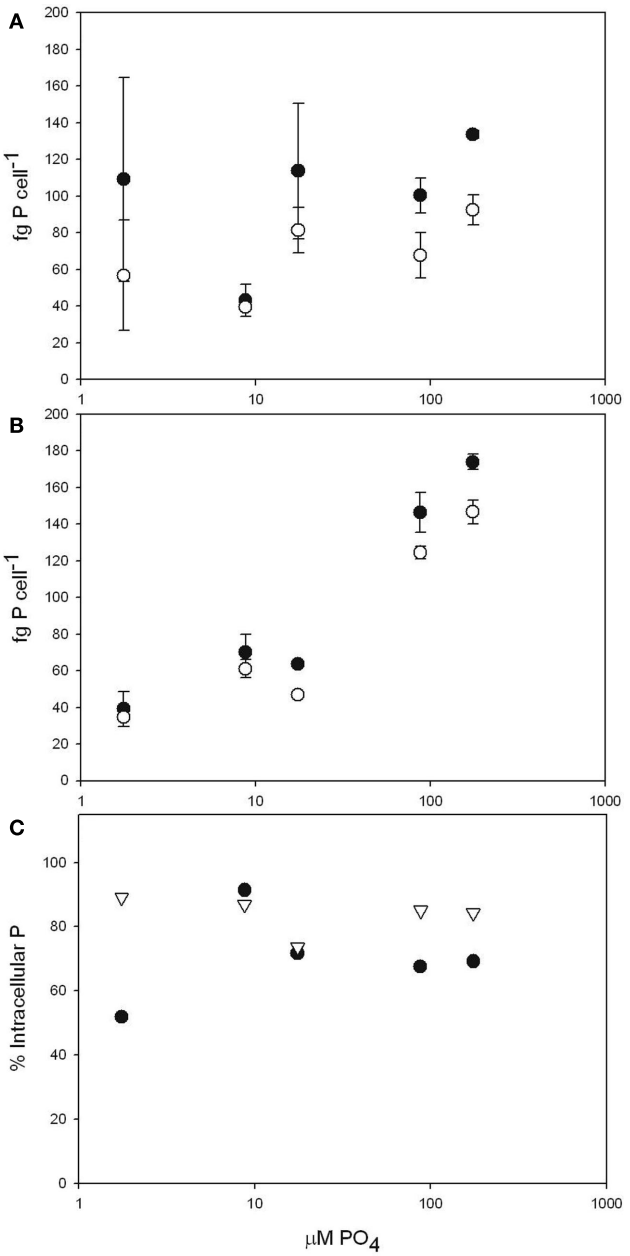

FIGURE 1 | Total cell-associated P (closed circles) and intracellular P (open circles) in femtogram per cell over growth media P concentration. Culture used in the individual figures: **(A)** *M. aeruginosa* PCC 7806 **(B)** *M. aeruginosa* LE3. **(C)** Percent intracellular P of total P pool in *M. aeruginosa* PCC 7806 (•) *M. aeruginosa* LE3 (Δ). All values are shown as mean ± SD.

Pearson correlation analysis of Western Basin samples showed weakly significant correlations ($p < 0.1$) between the proportion of surface associated extracellular P and several environmental variables, including SRP, POC, PON, and SiO_2 (**Table 3**). Notably, no significant correlation was observed between the proportion of extracellular P and either TP or TDP (**Table 3**; **Figure 2**).

Table 3 | Pearson correlation analysis results comparing the extracellular percentage of total particulate P to hydrological and biological parameters.

	r	*p*
Total particulate P	0.648	0.164
Intracellular P	0.619	0.189
SRP	0.784	0.065
TDP	0.714	0.111
TP	0.706	0.117
$NO_X^- N$[a]	−0.169	0.748
NH_3^-N	−0.508	0.304
TDN	0.144	0.785
PON	0.764	0.077
SiO_2	0.733	0.09
POC	0.757	0.081
Chl*a*	0.451	0.369

[a]*Nitrate + nitrite as N.*

DISCUSSION

A general tenet of limnology is that P is the nutrient limiting phytoplankton biomass in many freshwater systems and that, by reducing P loading to eutrophic bodies of water, we can begin to control formation of algal blooms and biomass accumulation (Schindler et al., 2008). While the previous statement is a commonly held assumption (although not always true, e.g., Scott and McCarthy, 2010; Wilhelm et al., 2011), it is important to note that individual HAB organisms have specific nutrient needs and differ in their abilities to assimilate nutrients from different chemical species. For example, it is now well established that some freshwater cyanobacteria possess the capacity to assimilate P from complex organic sources, such as phosphonates (Ilikchyan et al., 2009; Saxton et al., 2011). Moreover, the addition of organic sources of nutrient have been shown to influence phytoplankton community structure in bioassays performed using natural assemblages (Wang et al., 2010). To this end, we examined the P requirements of one of the most prominent bloom-forming cyanobacteria, *M. aeruginosa*, so as to develop a dynamic cellular quota that can be used to inform credible data reporting. To do so, we applied recently developed techniques that allow for the individual analysis of total cell-associated vs. intracellular P pools in phytoplankton.

Our results show plasticity in both cellular and surface absorbed P quotas. The ability to adjust intracellular P levels while maintaining a stable growth rate across a range of P concentrations is important for bloom-forming cyanobacteria as it allows for persistence in conditions that do not allow for the accumulation of significant biomass. This nutritional flexibility is important for microbes in environments that experience large nutrient variability, such as large lakes and estuarine systems. The plasticity of cellular P quotas is in contrast to the stability of the total cell-associated P to intracellular P ratio. Our data show this ratio to be stable, demonstrating an ability of *Microcystis* to adjust its P needs. These observations imply that surface associated P is a function of the external concentration in the environment. One potential route for P adjustment has been described in marine cyanobacteria that substitute phospholipids for nitrogen and sulfur containing lipids in response to P limitation (Van Mooy et al., 2009), though this ability has not yet been described in *Microcystis*. Observed variability in P quota values in the tested strains is likely attributable to variance between strains. This variance is also observed in genetic differences between the sequenced *Microcystis* strains (Kaneko et al., 2007; Frangeul et al., 2008).

In contrast to our observations in cultured *Microcystis*, the ratio of intracellular to extracellular P was not constant between Lake Erie stations.

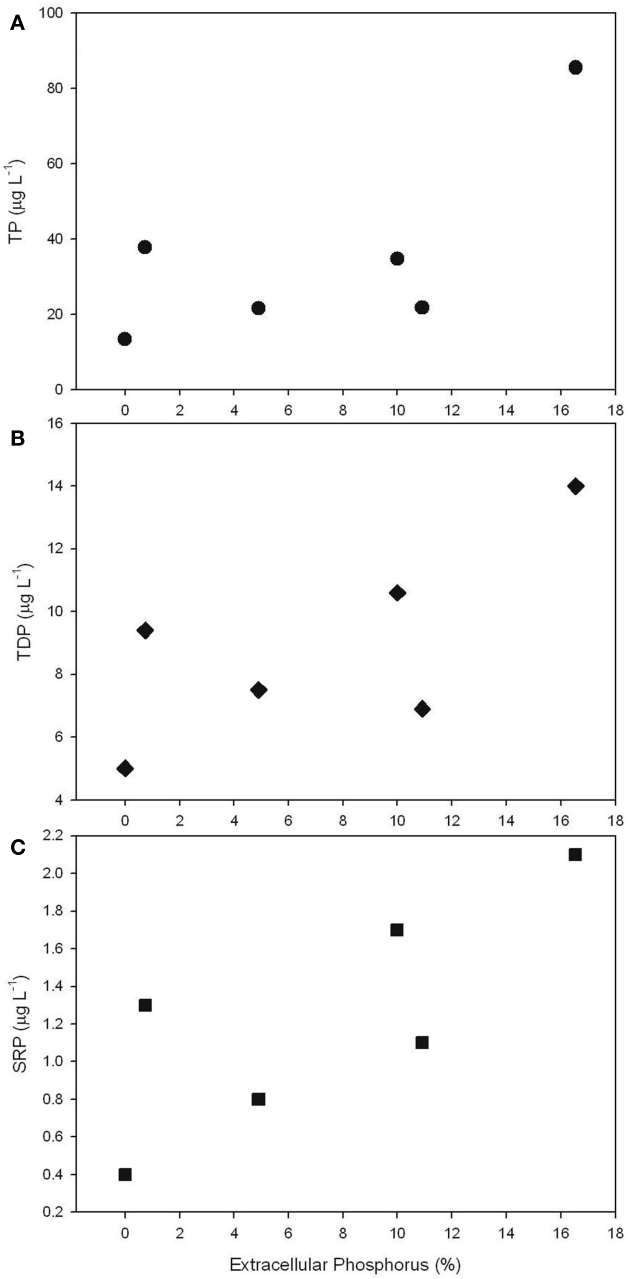

FIGURE 2 | Scatter plots depicting the relationship between the percentage of total particulate P that is localized to the cell surface relative to TP (A), TDP (B), and SRP (C).

Whereas this variability is correlated to differences in ambient SRP concentrations, dissimilarity in plankton communities between these sites may also contribute. The high proportion of intracellular P as compared to the total P pool in Lake Erie is indicative of an actively growing phytoplankton community (Sānudo-Wilhelmy et al., 2004). Another factor influencing the intracellular-total P ratio in natural *Microcystis* populations may be colony morphology. If exposure to dissolved phosphate is a driver of the presence of extracellular P, as is suggested by the positive correlation between SRP and the percentage of extracellular P, then the cellular surfaces not exposed to the environment will not have externally bound P.

Unfortunately the fate of stored P on the cell surface remains elusive; it is possible that when cells are shifted from P-replete to P-limiting conditions, this surface associated material can be assimilated by cells as opposed to the alternative of this P being lost back to the environment as has been previously hypothesized (Sānudo-Wilhelmy et al., 2004). While the hypothesis that surface adsorbed P is available to phytoplankton is intriguing, we observed no evidence to suggest that it is the case in *Microcystis*. Were this true we would expect the ratio of surface-intracellular P to shift toward the intracellular fraction under conditions of P stress as the cells scavenged P from the surface. However, we observed this ratio to remain constant across the growth conditions tested in this study. This observation paired with the positive correlation between SRP and surface adsorbed P in our Lake Erie samples suggests that the presence of P on the surface of these cells is a by-product of living in an environment where dissolved P is present.

Models of eutrophication and phytoplankton growth remain a critical tool for systems managers attempting to control frequent bloom formation and have been applied to Lake Erie since the middle of the twentieth century (Di Toro et al., 1975; Léon et al., 2005; Zhang et al., 2008; Schwab et al., 2009). *Microcystis* growth has been specifically targeted in many models because it is a problematic, bloom-forming cyanobacterium. Physiological parameters, such as cellular nutrient quotas, nutrient uptake rates and cellular growth rates, are integral to generating accurate predictions of cellular growth and toxin production under specific environmental conditions. Cellular P quota is a variable used (or is integral to variables used) in environmental models that have been applied to both *Microcystis* and Lake Erie (Robson and Hamilton, 2004; Léon et al., 2011; Burger et al., 2008; Trolle et al., 2008). This use of P quota as a modeling variable coupled with the fact that literature P quotas in *Microcystis* do not take into account the presence of externally bound P hinders the ability of these models to accurately project the occurrence of blooms and underestimates the algal biomass that can be supported by current P inputs. For example, the minimum internal *p* value applied to the CAEDYM model by Robson and Hamilton (2004) of 0.4 mg P (mg chl*a*)$^{-1}$ represents approximately a 40× overestimation of the P needs of this organism compared to the values reported here. The accurate prediction of natural conditions by environmental models is dependent on the use of precisely measured variables, so it is critical that the modeling community use the most appropriate values. Moreover, the significant metabolic plasticity with respect to P quotas demonstrated by *Microcystis* in the present study is also not taken into account in current models. The current mathematical models use one or two values, often the minimum and maximum, to describe biological parameters such as growth rate or internal P quota (to limit the complexity of already complex models). *Microcystis*, however, has the ability to adapt to environmental challenge. As such, the ability of new hydrodynamic models, such as ELCOM, to more effectively describe changing physical conditions and nutrient concentrations in the water column suggest biological models would benefit from incorporating a more complex view of cyanobacterial growth over nutrient and temperature gradients.

The importance of controlling the growth of HAB cyanobacteria cannot be understated because of the water quality effects in both undeveloped and industrial countries. Previous studies examining P quotas in *Microcystis* measured only the total cell-associated P pool. In this study we differentiate between the total cell-associated P pools, including surface bound P, and the intracellular P pool; thus the P quotas reported here are a more representative examination of the P needs of *Microcystis* than has been previously reported. These results will be useful to resource managers attempting to model and control this nuisance alga.

ACKNOWLEDGMENTS

We thank Michael Schultz for processing particulate organic phosphorus samples and Jennifer DeBruyn for aid with statistical analyses. We would also like to thank the captain and crew of the *CCGS Limnos*. This research was supported by NOAA Oceans and Human Health external grant NA05NO54781251, Ohio Sea Grant College Program award R/ER-73, and NSF-IOS #0841918 and NSF–CBET#0826838).

REFERENCES

Anderson, R. A. (ed.). (2005). *Algal Culturing Techniques*. Boston: Academic Press.

Brittain, S. M., Wang, J., Babcock-Jackson, L., Carmichael, W. W., Rinehart, K. L., and Culver, D. A. (2000). Isolation and characterization of microcystins, cyclic heptapeptide hepatotoxins from a Lake Erie strain of *Microcystis aeruginosa*. *J. Great Lakes Res.* 26, 241–249.

Burger, D. F., Hamilton, D. P., and Pilditch, C. A. (2008). Modelling the relative importance of internal and external nutrient loads on water column nutrient concentrations and phytoplankton biomass in a shallow polymictic lake. *Ecol. Modell.* 211, 411–423.

Carmichael, W. W. (2001). Health effects of toxin-producing cyanobacteria: "The CyanoHABs". *Hum. Ecol. Risk Assess.* 7, 1393–1407.

Chorus, I., and Bartram, J. E. (1999). *Toxic Cyanobacteria in Water: A Guide to Public Health Significance, Monitoring and Management*. London: EF&N Spon.

DeBruyn, J. M., Leigh-Bell, J. A., Mckay, R. M. L., Bourbonniere, R. A., and Wilhelm, S. W. (2004). Microbial distributions and the impact of phosphorus on bacterial activity in Lake Erie. *J. Great Lakes Res.* 30, 166–183.

Di Toro, D. M., O'Connor, D. J., Thomann, R. V., and Mancini, J. L. (1975). "A preliminary phytoplankton-zooplankton-nutrient model of western Lake Erie," in *Systems Analysis and Simulation in Ecology*, ed. B. C. Patten (New York, NY: Academic Press), 423–474.

Frangeul, L., Quillardet, P., Castets, A.-M., Humbert, J.-F., Matthijs, H., Cortez, D., Tolonen, A., Zhang, C.-C., Gribaldo, S., Kehr, J.-C., Zilliges, Y., Ziemert, N., Becker, S., Talla, E., Latifi, A., Billault, A., Lepelletier, A., Dittmann, E., Bouchier, C., and Tandeau De Marsac, N. (2008). Highly plastic genome of *Microcystis aeruginosa* PCC 7806, a ubiquitous toxic freshwater cyanobacterium. *BMC Genomics* 9, 274. doi:10.1186/1471-2164-9-274

Fu, F. X., Zhang, Y. H., Leblanc, K., Sanudo-Wilhelmy, S. A., and

Hutchins, D. A. (2005). The biological and biogeochemical consequences of phosphate scavenging onto phytoplankton cell surfaces. *Limnol. Oceanogr.* 50, 1459–1472.

Ilikchyan, I. N., Mckay, R. M. L., Zehr, J. P., Dyhrman, S. T., and Bullerjahn, G. S. (2009). Detection and expression of the phosphonate transporter gene phnD in marine and freshwater picocyanobacteria. *Environ. Microbiol.* 11, 1314–1324.

Jacobson, L., and Halmann, M. (1982). Polyphosphate metabolism in the blue-green alga *Microcystis aeruginosa. J. Plankton Res.* 4, 481–488.

Jørgensen, S. E. (2010). A review of recent developments in lake modelling. *Ecol. Modell.* 221, 689–692.

Kaneko, T., Narajima, N., Okamoto, S., Suzuki, I., Tanabe, Y., Tamaoki, M., Nakamura, Y., Kasai, F., Watanabe, A., and Kawashima, K. (2007). Complete genomic structure of the bloom-forming toxic cyanobacterium *Microcystis aeruginosa* NIES-843. *DNA Res.* 14, 247–256.

Kromkamp, J., Vandenheuvel, A., and Mur, L. R. (1989). Phosphorus uptake and photosynthesis by phosphate-limited cultures of the cyanobacterium *Microcystis aeruginosa. Br. Phycol. J.* 24, 347–355.

Léon, L. K., Imberger, J., Smith, R. E. H., Hecky, R. E., Lam, D. C. L., and Schertzer, W. M. (2005). Modeling as a tool for nutrient management in Lake Erie: a hydrodynamics study. *J. Great Lakes Res.* 31, 309–318.

Léon, L. F., Smith, R. E. H., Hipsey, M. R., Bocaniov, S. A., Higgins, S. N., Hecky, R. E., Antenucci, J. P., Imberger, J. A. and Guildford, S. J. (2011). Application of a 3D hydrodynamic-biological model for seasonal and spatial dynamics of water quality and phytoplankton in Lake Erie. *J. Great Lakes Res.* 37, 41–53.

Makarewicz, J. C., and Bertram, P. (1991). Evidence for the restoration of the Lake Erie ecosystem. *Bioscience* 41, 216–223.

Menzel, D. W., and Corwin, N. (1965). The measurement of total phosphorus in seawater based on the liberation of organically pound fractions by persulfate oxidation. *Limnol. Oceanogr.* 10, 280–282.

Moorhead, D., Bridgeman, T., and Morris, J. (2008). "Changes in water quality of Maumee Bay 1928-2003," in *Checking the Pulse of Lake Erie*, eds M. Munawar and R. Heath (New Delhi: Backhuys Publishers), 123–158.

NLET. (1994). *Manual of Analytical Methods, Vol. 1, Major Ion and Nutrients.* Burlington, ON: Environment Canada.

Ouellette, A. J. A., Handy, S. M., and Wilhelm, S. W. (2006). Toxic *Microcystis* is widespread in Lake Erie: PCR detection of toxin genes and molecular characterization of associated cyanobacterial communities. *Microb. Ecol.* 51, 154–165.

Ouellette, A. J. A., and Wilhelm, S. W. (2003). Toxic cyanobacteria: the evolving molecular toolbox. *Front. Ecol. Environ.* 7, 359–366.

Paerl, H. W., Pinckney, J. L., Fear, J. M., and Peierls, B. L. (1998). Ecosystem responses to internal and watershed organic matter loading: consequences for hypoxia in the eutrophying Neuse river estuary, North Carolina, USA. *Mar. Ecol. Prog. Ser.* 166, 17–25.

Rhee, G. Y., and Gotham, I. J. (1980). Optimum N-P ratios and coexistence of planktonic algae. *J. Phycol.* 16, 486–489.

Rinta-Kanto, J. M., Konopko, E. A., Debruyn, J. M., Bourbonniere, R. A., Boyer, G. L., and Wilhelm, S. W. (2009a). Lake Erie *Microcystis*: relationship between microcystin production, dynamics of genotypes and environmental parameters in a large lake. *Harmful Algae* 8, 665–673.

Rinta-Kanto, J. M., Saxton, M. A., Debruyn, J. M., Smith, J. L., Marvin, C. H., Krieger, K. A., Sayler, G. S., Boyer, G. L., and Wilhelm, S. W. (2009b). The diversity and distribution of toxigenic *Microcystis* spp. in present day and archived pelagic and sediment samples from Lake Erie. *Harmful Algae* 8, 385–394.

Rinta-Kanto, J. M., Ouellette, A. J. A., Boyer, G. L., Twiss, M. R., Bridgeman, T. B., and Wilhelm, S. W. (2005). Quantification of toxic *Microcystis* spp. during the 2003 and 2004 blooms in western Lake Erie using quantitative real-time PCR. *Environ. Sci. Technol.* 39, 4198–4205.

Rinta-Kanto, J. M., and Wilhelm, S. W. (2006). Diversity of microcystin-producing cyanobacteria in spatially isolated regions of Lake Erie. *Appl. Environ. Microbiol.* 72, 5083–5085.

Rippka, R., Derulles, J., Waterbury, J. B., Herdman, M., and Stanier, R. Y. (1979). Generic assignments, strain histories and properties of pure cultures of cyanobacteria. *J. Gen. Microbiol.* 111, 1–61.

Ritchie, R. J., Trautman, D. A., and Larkum, A. W. D. (1997). Phosphate uptake in the cyanobacterium *Synechococcus* R-2 PCC 7942. *Plant Cell Physiol.* 38, 1232–1241.

Ritchie, R. J., Trautman, D. A., and Larkum, A. W. D. (2001). Phosphate limited cultures of the cyanobacterium *Synechococcus* are capable of very rapid, opportunistic uptake of phosphate. *New Phytol.* 152, 189–201.

Robson, B. J., and Hamilton, D. P. (2004). Three-dimensional modelling of a Microcystis bloom event in the Swan River estuary, Western Australia. *Ecol. Modell.* 174, 203–222.

Rodhe, W., Vollenweider, R. A., and Nauwerck, A. (1958). "The primary production and standing crop of phytoplankton," in *Perspectives in Marine Biology*, ed. A. A. Buzzati-Traverso (San Francisco: University of California Press), 299–322.

Sānudo-Wilhelmy, S. A., Tovar-Sanchez, A., Fe, F. X., Capone, D. G., Carpenter, E. J., and Hutchins, D. A. (2004). The impact of surface-absorbed phosphorus on phytoplankton Redfield stoichiometry. *Nature* 432, 897–901.

Saxton, M. A., Morrow, E. A., Bourbonniere, R. A., and Wilhelm, S. W. (2011). Glyphosate influence on phytoplankton community structure in Lake Erie. *J. Great Lakes Res.* 37, 683–690.

Sbiyyaa, B., Loudiki, M., and Oudra, B. (1998). Nitrogen and phosphorus intracellular capacity in storage by *Microcystis aeruginosa* Kutz and *Synechocystis* sp.: toxic cyanobacteria occasionally forming blooms in Marrakesch area (Morocco). *Ann. Limnol. Int. J. Limnol.* 34, 247–257.

Schindler, D. W. (1977). Evolution of phosphorus limitation in lakes. *Science* 195, 260–262.

Schindler, D. W., Hecky, R. E., Findlay, D. L., Stainton, M. P., Parker, B. R., Paterson, M. J., Beaty, K. G., Lyng, M., and Kasian, S. E. M. (2008). Eutrophication of lakes cannot be controlled by reducing nitrogen input: results of a 37-year whole-ecosystem experiment. *Proc. Natl. Acad. Sci. U.S.A.* 105, 11254–11258.

Schwab, D. J., Beletsky, D., Depinto, J., and Dolan, D. M. (2009). A hydrodynamic approach to modeling phosphorus distribution in Lake Erie. *J. Great Lakes Res.* 35, 50–60.

Scott, J. T., and McCarthy, M. J. (2010). Nitrogen fixation may not balance the nitrogen pool in lakes over timescales relevant to eutrophication management. *Limnol. Oceanogr.* 53, 1265–1270.

Shen, H., and Song, L. R. (2007). Comparative studies on physiological responses to phosphorus in two phenotypes of bloom-forming *Microcystis. Hydrobiologia* 592, 475–486.

Strickland, J. D. H., and Parsons, T. R. (1972). *A Practical Handbook of Seawater Analysis.* Ottawa: Fisheries Research Board of Canada.

Tovar-Sanchez, A., Sānudo-Wilhelmy, S., Garcia-Vargas, M., Weaver, R. S., Popels, L. C., and Hutchins, D. A. (2003). A trace metal clean reagent to remove surface-bound iron from marine phytoplankton. *Mar. Chem.* 82, 91–99.

Trolle, D., Skovgaard, H., and Jeppesen, E. (2008). The Water Framework Directive: setting the phosphorus loading target for a deep lake in Denmark using the 1D lake ecosystem model DYRESM-CAEDYM. *Ecol. Modell.* 219, 138–152.

Tsukada, H., Tsujimura, S., and Nakahara, H. (2006). Effect of nutrient availability on the C, N, and P elemental ratios in the cyanobacterium *Microcystis aeruginosa. Limnology* 7, 185–192.

Van Mooy, B. A. S., Fredricks, H. F., Pedler, B. E., Dyhrman, S. T., Karl, D. M., Koblizek, M., Lomas, M. W., Mincer, T. J., Moore, L. R., Moutin, T., Rappe, M. S., and Webb, E. A. (2009). Phytoplankton in the ocean use non-phosphorus lipids in response to phosphorus scarcity. *Nature* 458, 69–72.

Wang, X., Qin, B., Gao, G., Wang, Y., Tang, X., and Otten, T. (2010). Phytoplankton community from Lake Taihu, China, has dissimilar responses to inorganic and organic nutrients. *J. Environ. Sci.* 22, 1491–1499.

Welschmeyer, N. A. (1994). Fluorometric analysis of chlorophyll-a in the presence of chlorophyll-b and pheopigments. *Limnol. Oceanogr.* 39, 1985–1992.

Wetzel, R. G., and Likens, G. E. (2000). *Limnological Analyses.* New York: Springer.

Wilhelm, S. W., Bullerjahn, G. S., Eldridge, M. L., Rinta-Kanto, J. M., Poorvin, L., and Bourbonniere, R. A. (2006). Seasonal hypoxia and the genetic diversity of prokaryote populations in the central basin hypolimnion of Lake Erie: evidence for abundant cyanobacteria and photosynthesis. *J. Great Lakes Res.* 32, 657–671.

Wilhelm, S. W., Farnsley, S. E., Lecleir, G. R., Layton, A. C., Satchwell, M. F., Debruyn, J. M., Boyer, G. L., Zhu, G., and Paerl, H. W. (2011).

The relationship between nutrients, cyanobacterial toxin and the microbial community in Lake Tai (Taihu), China. *Harmful Algae* 10, 207–215.

Wilhelm, S. W., Maxwell, D. P., and Trick, C. G. (1996). Growth, iron requirements, and siderophore production in iron-limited *Synechococcus* PCC 7002. *Limnol. Oceanogr.* 41, 89–97.

Ye, W., Liu, X., Tan, J., Li, D., and Yang, H. (2009). Diversity and dynamics of microcystin – Producing cyanobacteria in Chinas third largest lake, Lake Taihu. *Harmful Algae* 8, 637–644.

Zhang, H., Culver, D. A., and Boegman, L. (2008). A two-dimensional ecological model of Lake Erie: Application to estimate dreissenid impacts on large lake plankton populations. *Ecol. Modell.* 214, 219–241.

Conflict of Interest Statement: The authors declare that the research was conducted in the absence of any commercial or financial relationships that could be construed as a potential conflict of interest.

Received: 18 October 2011; paper pending published: 23 November 2011; accepted: 03 January 2012; published online: 18 January 2012.

*Citation: Saxton MA, Arnold RJ, Bourbonniere RA, McKay RML and Wilhelm SW (2012) Plasticity of total and intracellular phosphorus quotas in Microcystis aeruginosa cultures and Lake Erie algal assemblages. Front. Microbio. **3**:3. doi: 10.3389/fmicb.2012.00003*

This article was submitted to Frontiers in Aquatic Microbiology, a specialty of Frontiers in Microbiology.

APPENDIX

Table A1 | Abundance of selected phytoplankton genus determine *via* microscopic examination of samples collected from Lake Erie in August 2010.

	478	970 (357)	973	882	1163	341	880 (84)
Microcystis spp. (colonies mL^{-1})	74.98	374.91	299.93	224.95	299.93	149.96	224.95
Planktothrix spp. (filaments mL^{-1})	149.96	449.89	1274.69	599.85	12222.04	1049.75	1049.75
Leptolyngbya spp. (filaments mL^{-1})	ND	74.98	374.91	74.98	749.81	824.8	374.9
Anabaena spp. (filaments mL^{-1})	ND	ND	ND	ND	524.87	ND	74.98
Aulacosiera spp. (filaments mL^{-1})	ND	149.96	74.98	ND	149.96	ND	ND
Fragilaria spp. (colonies mL^{-1})	ND	74.98	ND	74.98	ND	ND	74.98
Cryptomonas spp. (cells mL^{-1})	74.98	224.95	749.82	374.91	ND	ND	ND
Chlamydomonas spp. (cells mL^{-1})	224.95	74.98	149.96	74.98	74.98	ND	ND
Gloeocapsa spp. (colonies mL^{-1})	ND	ND	74.98	ND	ND	ND	224.95
Closteriopsis spp. (cells mL^{-1})	ND	74.98	149.96	149.96	149.96	ND	ND
Ceratium spp. (cells mL^{-1})	ND	ND	ND	ND	ND	ND	74.98

frontiers in
MICROBIOLOGY

ORIGINAL RESEARCH ARTICLE
published: 12 June 2012
doi: 10.3389/fmicb.2012.00211

Effect of nitrogen on cellular production and release of the neurotoxin anatoxin-a in a nitrogen-fixing cyanobacterium

Alexis Gagnon* and Frances R. Pick

Center for Advanced Research in Environmental Genomics, University of Ottawa, Ottawa, ON, Canada

Edited by:
George S. Bullerjahn, Bowling Green State University, USA

Reviewed by:
Xosé Anxelu G. Morán, Instituto Español de Oceanografía, Spain
Shawn R. Campagna, University of Tennessee Knoxville, USA

****Correspondence:***
Alexis Gagnon, Center for Advanced Research in Environmental Genomics, University of Ottawa, Ottawa, ON, Canada K1N 6N5.
e-mail: agagn042@gmail.com

Anatoxin-a (ANTX) is a neurotoxin produced by several freshwater cyanobacteria and implicated in lethal poisonings of domesticated animals and wildlife. The factors leading to its production in nature and in culture are not well understood. Resource availability may influence its cellular production as suggested by the carbon-nutrient hypothesis, which links the amount of secondary metabolites produced by plants or microbes to the relative abundance of nutrients. We tested the effects of nitrogen supply (as 1, 5, and 100% N of standard cyanobacterial medium corresponding to 15, 75, and 1500 mg L^{-1} of $NaNO_3$ respectively) on ANTX production and release in a toxic strain of the planktonic cyanobacterium *Aphanizomenon issatschenkoi* (Nostocales). We hypothesized that nitrogen deficiency might constrain the production of ANTX. However, the total concentration and more significantly the cellular content of anatoxin-a peaked (max. 146 μg/L and 1683 μg g^{-1} dry weight) at intermediate levels of nitrogen supply when N-deficiency was evident based on phycocyanin to chlorophyll *a* and carbon to nitrogen ratios. The results suggest that the cellular production of anatoxin-a may be stimulated by moderate nitrogen stress. Maximal cellular contents of other cyanotoxins have recently been reported under severe stress conditions in another Nostocales species.

Keywords: cyanobacteria, anatoxin-a, nitrogen deficiency, carbon-nutrient hypothesis

INTRODUCTION

Many cyanobacteria are capable of producing compounds that are toxic to other organisms. The cyanotoxins have been classified into four main groups according to their mode of action. In addition to the hepatoxins, cytotoxins, and gastrointestinal toxins, there are several types of neurotoxins (Codd et al., 2005). A potent neurotoxin synthesized by freshwater cyanobacteria is anatoxin-a (ANTX), likely one of the smallest toxic alkaloids described to date (LD50 of 0.2 mg/kg IP in mice, Carmichael et al., 1979). Prior to its chemical identification, ANTX was labeled the Very Fast Death Factor due to its ability to induce death within 4 min following intraperitonial injection in mice. ANTX has now been detected in lakes and rivers throughout the world (e.g., Codd et al., 2005; Cadel-Six et al., 2007; Wood et al., 2007; Aráoz et al., 2008), and, in some cases, at concentrations leading to lethal poisonings of livestock, domestic animals, and wildlife.

The factors regulating ANTX production, whether in the field or in the laboratory, are not well understood (Osswald et al., 2007). The toxin has been studied less that the more commonly encountered microcystins associated with freshwater cyanobacterial blooms (a Web of Science search since 1995 yields about a quarter of the number of papers on ANTX relative to the number of papers on microcystins). ANTX production is strain specific with cellular contents ranging up to 13,000 μg/g dry weight in *Anabaena* (reviewed by Osswald et al., 2007). The optimal temperature for production appears to lie between 19.8 and 22.0°C and is maximal during the exponential phase of growth in batch cultures.

Several hypotheses have been proposed to explain why toxins more generally are produced by cyanobacteria. They may be produced as a defense mechanism against grazers or other organisms in order to gain ecological advantage. Or they may be involved in cell signaling processes (Wiegand and Pflugmacher, 2005). Cyanotoxins including ANTX have been labeled as secondary metabolites as they do not appear to be involved in primary metabolism (Carmichael, 1992). In this regard, an increase in demand for resources at the cellular level would in theory lead to a decrease in ANTX production.

The availability of nutrients may play a role in the production of secondary metabolites, including nitrogen containing alkaloids such as ANTX, as suggested by the carbon-nutrient balance hypothesis (Hamilton et al., 2001). This hypothesis links the amount of secondary metabolites produced by plants to the relative abundance of nutrients. Recently, the production and composition of microcystins (MC) was investigated in relation to nitrogen to carbon supply ratios (N:C) in the freshwater cyanobacterium *Microcystis aeruginosa* (van de Waal et al., 2009). Consistent with the carbon-nutrient balance hypothesis, a high N:C ratio in the external media and within the cells led to higher concentrations of microcystins (and of the nitrogen-rich MC variant MC-RR) in comparison to lower N:C ratios. Despite the fact that less than 1% of the total cellular nitrogen was invested in microcystins, the availability of inorganic nitrogen appeared to influence secondary metabolite concentrations and composition. Nitrogen availability may also play an analogous role in the production of other nitrogen containing secondary metabolites such as ANTX.

In the following study, the relationship between nitrogen availability and ANTX production was investigated in *Aphanizomenon issatschenkoi* (Ussaczew) Proschkina-Lavrenko using an ANTX producing strain isolated from a hypereutrophic New Zealand lake (CAWBG02, Wood et al., 2007). *A. issatschenkoi* is a colonial planktonic species, which can produce heterocysts (Ballot et al., 2010), the primary site for atmospheric nitrogen (N_2) fixation in the Nostocales in the absence of available inorganic nitrogen. The process of nitrogen fixation being energy demanding, this study hypothesized that nitrogen fixation might lead to further reductions in the production of secondary metabolites containing nitrogen when the supply of inorganic N was low. Both intracellular and extracellular production was estimated: given its small molecular weight ANTX can be found in significant but variable amounts in solution (Rapala et al., 1993).

MATERIALS AND METHODS

CULTURE CONDITIONS AND SAMPLING

A culture of *A. issatschenkoi* was obtained from the Cawthron Institute, New Zealand (strain CAWBG02). Batch cultures were grown at a light intensity of 85 $\mu E\, m^{-2}\, s^{-1}$ on a 12:12 light: dark cycle at $20 \pm 1^{\circ}C$ in a Conviron growth chamber (E-15) in 500 mL Erlenmeyer flasks. Three different growth media were used with sodium nitrate ($NaNO_3$) at 100, 5, and 1% of full strength BG11 (Andersen, 2005) corresponding to 1500, 75, and 15 $mg\, L^{-1}$ of $NaNO_3$ respectively. Total culture volumes were 250 mL and inocula for all the experimental cultures came from the same parent culture in exponential phase acclimated to the same temperature and light regime. Under these conditions, *A. issatschenkoi* grew as single trichomes and minimal clumping occurred which facilitated subsampling. Two milliliters from each flask were sub-sampled every 3–4 days to measure optical density using a Pye-Unicam SP-100 UV-spectrophotometer at 750 nm. The optical density at 750 nm provides a measure of turbidity of the culture and is a function of both cell density and cell size. Growth rates were obtained by plotting the natural logarithm of absorbance readings at 750 nm during the exponential growth and using linear analysis (Guillard, 1973). Optical densities at 627 and 438 nm were also measured as an estimate of phycocyanin to chlorophyll *a* changes (van de Waal et al., 2009). Phycocyanin is a protein and accessory pigment found in all cyanobacteria and involved in light harvesting (Whitton and Potts, 2000).

For toxin extraction from cells, 10 mL from each flask was filtered on days 10, 20, 30, and 40 of growth using pre-ashed and pre-weighed Whatman GF/C filters. The first three time points corresponded to early, mid, and late exponential phases whereas the last corresponded to stationary phase at least in the 1 and 5% N cultures. A subsequent 10 mL was filtered from each flask using the same filter type for the analysis of particulate organic carbon (C) and nitrogen (N). Filters were oven dried overnight at 60°C, re-weighed to obtain the dry weight ($mg\, mL^{-1}$) and stored frozen at −20°C. During filtrations, one 20 mL of filtrate was collected from each culture in solvent rinsed (acetone and hexane) scintillation vials wrapped in foil. Filtrates were spiked with 50 μL formic acid to stabilize ANTX and frozen immediately at −20°C. For chlorophyll *a* analysis, 5 mL were sub-sampled and filtered using 934-AH glass microfiber filters with approximately the same pore size as GF/C. Filters were inserted in clean 15 mL plastic test tubes and stored at −20°C for subsequent analysis. The experiment was terminated when the 1 and 5% N cultures had clearly reached stationary phase.

EXTRACTION AND ANALYSIS OF ANATOXIN-A, PARTICULATE ORGANIC CARBON AND NITROGEN, AND CHLOROPHYLL *a*

The extraction of ANTX from cyanobacterial cells was performed using an ASE 200 device Dionex Corporation (Bannockburn, IL, USA). Frozen GF-C filters with cyanobacterial biomass were thawed and inserted in stainless-steel ASE cells (11 mL) packed with pre-washed Hydromatrix. The ASE parameters were optimized for anatoxin-a specifically (**Table 1**) based on a previous ASE protocol optimized for microcystins (Aranda-Rodriguez et al., 2005). Extracts were collected in solvent (acetone and hexane) rinsed amber vials and then spiked with 50 μL formic acid (pH ∼3). Extracts were then evaporated down to dryness at 59°C under a gentle nitrogen flow using a Zymark Turbovap II and then resuspended in 1 mL of 50% methanol in water. Filtrates were freeze-dried and then resuspended in 1 mL of 50% methanol in water. All extracts, both particulate and liquid phase, were filtered with pre-conditioned 0.2 μm Acrodisc filters and stored at −20°C until analysis.

Toxin analyses were performed on a Sciex QTRAP 3200 LC-MS/MS (ABSciex, Toronto, Canada). The system consisted of a 1200 series Agilent liquid chromatograph with a high performance autosampler (model G1376B), a binary pump (model G1312A), a column thermostat (model G1316A), and a triple quadrupole linear ion trap mass spectrometer equipped with a turbospray ion source, specifically electrospray ionization (ESI) in positive mode with a voltage of 4500 eV and setpoint temperature of 350°C. The acquisition of data was performed with Analyst software (version 1.4.1). Chromatographic separations were achieved with a Zobrax SB-C18 Rapid Resolution column (50 × 2.1 mm I.D., 1.8 μm particle size column) and a guard column (12.5 × 2.1 mm I.D, 5 μm; Agilent Technologies, Canada) at 40°C. The optimal mobile phase conditions were: water and MeOH with 0.1% formic acid and ammonium formate 20 mM with a constant flow rate of 0.3 mL/min. Injection volume for samples was set to 1 μL. The needle was washed with 50% methanol, 50% acetonitrile, and 0.01% formic acid at the flush port (3×) after each injection to minimize carry over. The method successfully separated anatoxin-a from phenylalanine which often interferes with anatoxin analyses

Table 1 | ASE parameters for ANTX pressurized liquid extraction.

Parameters	Experimental conditions
Pressure (psi)	2000
Temperature (°C)	80
Preheat (min)	1
Heat(min)	5
Static (min)	5
Flush (%)	100
Purge (s)	120
Number of cycles	2

as the compounds are isobaric (Furey et al., 2005). ANTX and PHE standards were individually infused in the MS with a 4.6 mm I.D Harvard syringe at a flow rate of 10 μL/min. Multiple reaction monitoring (MRM) scans were performed for each standard by selecting the protonated molecular ion $[M+H]^{+1}$ (parent ion) with the first mass filter quadrupole (Q1). The product ions, yielded by collision-induced dissociation, were scanned by the third quadrupole (Q3). Unambiguous Q1/Q3 pair transitions were obtained by manually optimizing the declustering potential to get characteristic product ions of ANTX and PHE (**Table 2**). Standard curves were produced with anatoxin-a fumarate obtained from Tocris Bioscience (USA) and analyzed in line with unknowns. All samples were analyzed on the same run to minimize any day to day instrument variability. The instrument limit of detection was 1 pg of ANTX and the limit of quantification 3.5 pg on column.

Particulate organic C and N were measured using a Costech elemental analyzer (ECS 4010; Costech, Valencia, CA, USA) following Frost et al. (2009). Chlorophyll *a* was extracted by incubating the frozen 934-AH filters with culture material in 13 mL of 95% ethanol at 4°C for about 24 h (Jespersen and Christoffersen, 1987). Following centrifugation of the extracts, chlorophyll *a* concentrations were then estimated based on optical densities at 750, 665, and 649 nm (Bergmann and Peters, 1980).

STATISTICAL ANALYSES

In order to compare the effects of N treatments, one-way analyses of variance (ANOVA) were performed on the following end-points: total and cellular toxin concentrations, growth rates, chlorophyll *a*, phycocyanin to chlorophyll *a* ratios, and particulate organic carbon to nitrogen (C:N) ratios at time intervals corresponding to the early to late exponential phase as well as the early stationary phase. A one-way ANOVA was chosen over a repeated measures ANOVA in order to focus analyses on specific and predictable growth phases. In the case of significant treatment effects ($p < 0.05$), Tukey's pairwise comparison test was subsequently used to determine differences between treatments. All statistical analyses were carried out using SigmaStat (version 3.1) software.

RESULTS

GROWTH AND NITROGEN STRESS

All cultures entered the exponential phase of growth after about 18 days and reached the stationary phase after approximately 34 days for the 1% N treatment and 40 days for both 5 and 100% N treatments (**Figure 1**). The growth curves based on optical density were clearly different between the three nitrogen treatments (**Figure 1**). By day 30, the mean optical density of the 100% N treatment was significantly higher ($p < 0.001$) than that at the lower N concentrations. On days 34 and 40, the treatments were all significantly different from one another, with the lowest optical densities corresponding to the 1% N treatment. The average biomass as dry weight (**Table 3**) of both the 1 and 5% N treatments was also significantly lower than that of 100% N treatment on all four sampling dates (10, 20, 30, and 40). Population growth rates ranged from 0.03 to 0.07 day^{-1} and were significantly higher in the 100% N cultures in comparison to the 1% N (**Table 3**).

Chlorophyll *a* concentrations of the cultures showed an analogous pattern to absorbance (data not presented). By day 20 and on three subsequent sampling dates all three treatments were significantly different from one another ($p < 0.001$). The highest chlorophyll *a* concentrations were measured in the 100% N treatment, followed by the 5 and 1% N treatments: maximum values were attained on day 30 (584 ± 26, 382 ± 8, and 192 ± 16 $\mu g\,L^{-1}$ respectively). In contrast to the optical density data (**Figure 1**), by day 40 chlorophyll *a* concentrations began to decline across all treatments.

With respect to the ratio of phycocyanin to chlorophyll *a*, the 100% N batch cultures had clearly the highest mean ratio and the 1% N the lowest (**Figure 2**). Significant differences between either all treatments or the 1 and 100% N treatments were observed from day 7 to day 34. On day 40, the mean ratio for the 1% N was significantly different ($p < 0.001$) from both higher N treatments. With respect to cellular nutrient composition, the particulate organic carbon to nitrogen ratios (**Table 3**) began to differ from day 20 onward. Batch cultures grown in 100% N medium were significantly different ($p < 0.001$) from the other two treatments with a lower mean ratio on both day 20 and 30. At day 40 however, no difference between the C:N mean ratios of batch cultures grown in 100 and 1% N was detected using Tukey's all pair wise test. This was due to the high standard error between triplicates of the

Table 2 | MRM transitions of each analyte obtained after infusion into turboV electrospray source of 3200 QTRAP and their respective voltages.

MS parameters	Analytes	
	Anatoxin-a	**Phenylalanine**
Q1 transition (*m/z*)	166.1	166.1
Q3 transition (*m/z*)	149.2	120.0
Declustering potential (eV)	21	36
Entrance potential (eV)	6.5	4.5

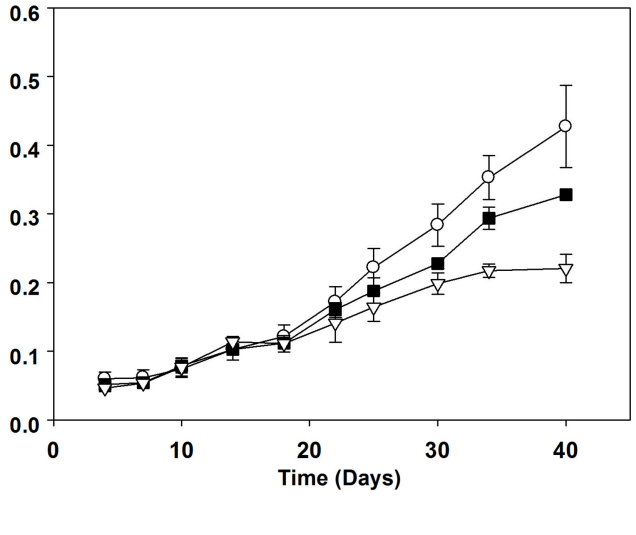

FIGURE 1 | Batch culture growth of *Aphanizomenon issatschenkoi* in 100% (open circles), 5% (filled squares), and 1% (open triangles) nitrogen-rich media. The error bars are standard errors of mean ($n = 3$).

Table 3 | Average growth rate based on optical density changes (± standard error), carbon to nitrogen (C:N) molar ratios and yield as dry weight biomass (mg/mL) for *Aphanizomenon issatschenkoi* grown in different nitrogen concentrations (shown as % of full strength BG11 media).

Treatment	Growth rate (day^{-1})	Time (days)							
		10		20		30		40	
		C:N	Biomass	C:N	Biomass	C:N	Biomass	C:N	Biomass
100% N	0.07 (0.009)a	0.96 (0.22)a	0.098 (0.002)a	1.56 (0.07)a	0.134 (0.005)a	2.59 (0.08)a	0.157 (0.005)a	2.92 (0.3)a	0.220 (0.015)a
5% N	0.05 (0.002)a,b	4.04 (1.49)a	0.041 (0.005)b	4.63 (0.1)b	0.060 (0.005)b	5.16 (0.1)b	0.080 (0.004)b	5.17 (0.05)b	0.135 (0.003)b
1% N	0.03 (0.042)b	2.79 (0.75)a	0.049 (0.008)b	5.00 (0.36)b	0.061 (0.002)b	6.01 (0.49)b	0.092 (0.001)b	5.49 (1.00)b	0.093 (0.007)b

Within the same column (parameter) values with different letters are significantly different from each other as determined by a one-way ANOVA and Tukey's post hoc pairwise comparisons ($n = 3$, $p < 0.05$). The different letters signify significant differences between the means in each column at $p<0.05$.

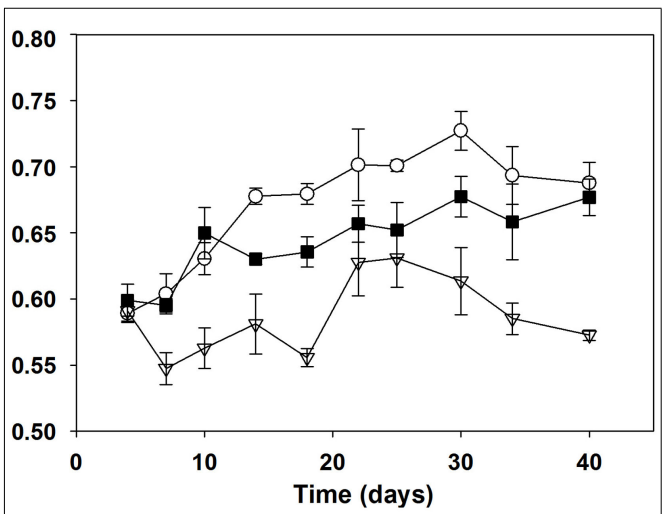

FIGURE 2 | Phycocyanin to chl-*a* ratios (627 nm: 438 nm) of *Aphanizomenon issatschenkoi* grown in 100% (open circles), 5% (filled squares), and 1% (open triangles) nitrogen-rich media. The error bars are standard errors of mean ($n = 3$).

1% N treatment. However, a Duncan all pair wise test showed a significant difference ($p = 0.045$) between the 100% N treatment and the other two treatments.

ANATOXIN-a

The total ANTX concentrations ranged from 4 to 146 $\mu g\,L^{-1}$ across time and treatments with the highest concentrations observed during the exponential phase (day 30) for all three nitrogen concentrations (**Figure 3**). On day 10, the highest total ANTX mean concentration corresponded to the 5% N treatment and the lowest to the 1% N. By day 30, the 5% N cultures had the highest total ANTX concentrations with a mean concentration of $111 \pm 18\,\mu g\,L^{-1}$; the 100% N cultures had the lowest concentrations ranging from 51 to 74 $\mu g\,L^{-1}$. However, with the exception of day 10, the total ANTX culture concentrations were not statistically different between the three treatments on a given day, with the exception of day 10, despite highly significant differences in culture biomass.

The ANTX cellular content ranged from 6 to 1683 $\mu g\,g^{-1}$ dry weight with the highest values in each treatment corresponding to 30 days of growth or the late exponential phase (**Figure 4**). ANTX content was significantly different among treatments on all dates, with higher content for the 5% N treatment compared to the other two treatments on day 20 ($p = 0.018$) and 30 ($p = 0.003$). The highest ANTX cellular content was measured in the 5% N treatment on day 30 with a mean of $1408 \pm 181\,\mu g\,g^{-1}$. The 5 and 1% N treatment had higher ANTX cell content than the batch cultures grown in 100% N with the 5% N treatment resulting in the highest amounts except on day 40, which corresponded to the onset of the stationary phase.

The extracellular ANTX concentrations ranged from below detection ($<0.1\,\mu g\,L^{-1}$) to 13 $\mu g\,L^{-1}$ and were considerably lower than particulate concentrations (**Figure 3**) while representing between 3 and 47% of the total production. Cultures grown in 100% N medium had significantly ($p < 0.001$) lower ANTX extracellular concentrations and lower percent extracellular release than the other two treatments on days 20 and 30. The highest mean extracellular concentrations were found in the 1% N treatments on days 30 and 40, reaching $9 \pm 0.12\,\mu g\,L^{-1}$. Two of the 1% cultures also had higher concentrations of ANTX in the extracellular phase compared to the intracellular phase one on day 10 and one on day 20.

DISCUSSION

The total amount of ANTX produced by *A. issatchenkoi* CAWBG02 was lower in this study than that reported for this strain when first isolated. For a 23 day culture Selwood et al. (2007) reported a maximum concentration of 1105 $\mu g\,L^{-1}$, whereas a maximum of 146 $\mu g\,L^{-1}$was estimated here. This could stem in part from differences in growing conditions related to differences in the composition of media, temperature, and light as well as aeration since the present cultures were not bubble aerated which Selwood et al. (2007) mentioned could double the toxin production. Furthermore differences in both extraction and analytical procedures for ANTX could also lead to differences: there are

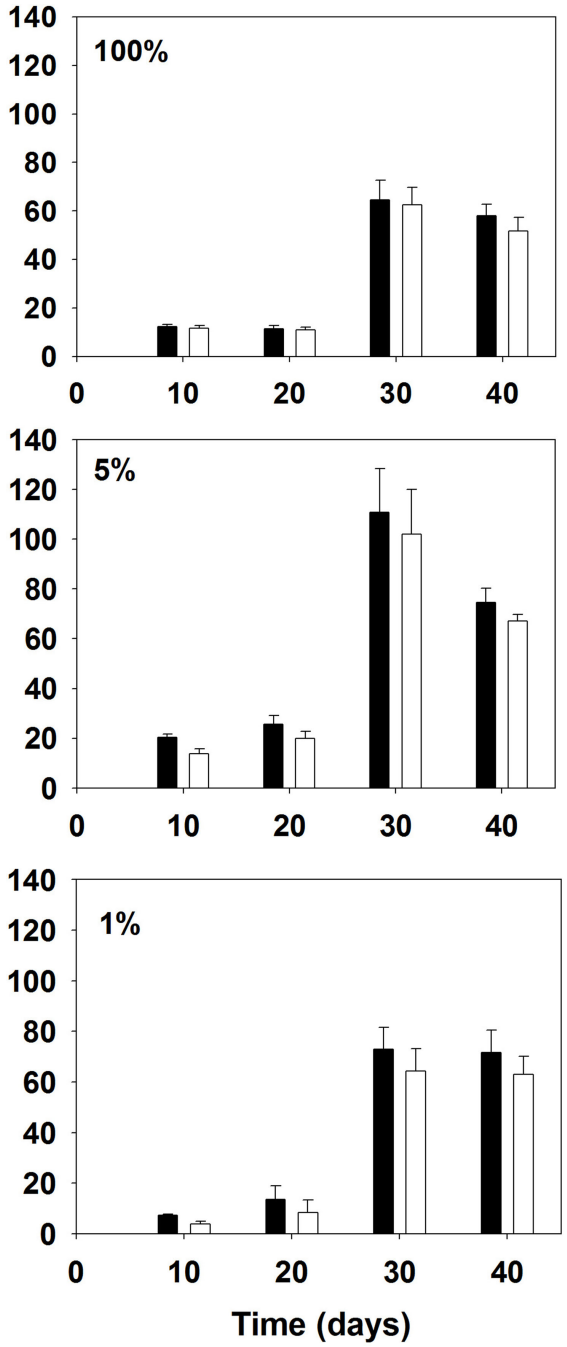

FIGURE 3 | ANTX culture concentrations (μg/L) of total toxin (filled bars) and intracellular toxin (open bars) of *Aphanizomenon issatschenkoi* grown in 100% (top panel), 5% (middle panel), and 1% (bottom panel) nitrogen-rich media. The error bars are standard errors of mean ($n = 3$).

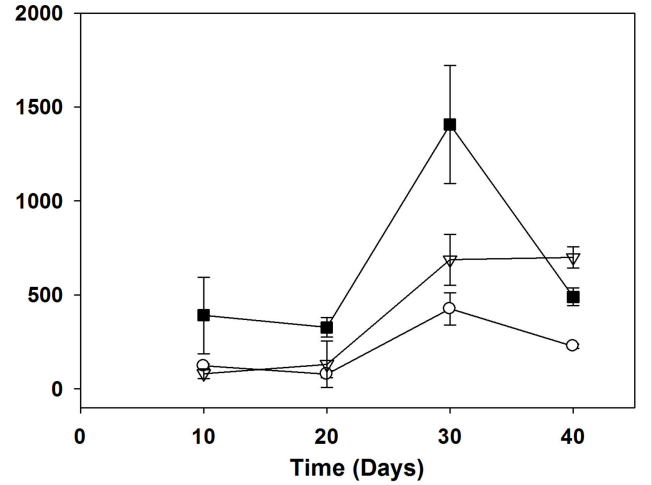

FIGURE 4 | Anatoxin-a cellular content (μg/g dry weight) of *Aphanizomenon issatschenkoi* grown in 100% (open circles), 5% (filled squares), and 1% (open triangles) nitrogen-rich media. The error bars are standard errors of mean ($n = 3$).

at present no common standard methods for most algal toxins or certified reference materials in use. The cellular content reported is within the range of that reported for a recently isolated strain of *A. issatschenkoi* from northeastern Germany (Ballot et al., 2010). Collectively the species appears less toxic than the benthic cyanobacterium *Phormidium favosum* which produces 8000 $\mu g\,g^{-1}$ per dry weight (Gugger et al., 2005) or previous reports for *Anabaena* strains (summarized in Osswald et al., 2007), although the problem of analytical interference from phenylalanine may have inflated these earlier estimates of ANTX which did not clearly separate these isobaric compounds.

In this study, nitrogen limited the biomass yield of *A. issatschenkoi* in the low N cultures as evidenced by lower dry weights and overall final yields under the 1 and 5% relative to 100% N (**Table 3**). The growth rate was also reduced in the 1% cultures and, to a lesser extent, in 5% cultures. Nitrogen deficiency was also reflected in cellular constituents: in particular lower chlorophyll *a* concentrations and overall lower ratios of phycocyanin to chlorophyll *a* (**Figure 2**). The phycobiliproteins, being nitrogen-rich accessory pigments, are typically reduced relative to chlorophyll *a* under nitrogen stress in cyanobacteria (Turpin, 1991).

When soluble inorganic nitrogen becomes limiting in the environment, many cyanobacteria belonging to the *Nostocales*, such as *Aphanizomenon*, are capable of fixing atmospheric nitrogen to compensate for their needs for that specific nutrient. Hence, the particulate organic nitrogen content should have been more or less constant throughout the 40 days in all three treatments if N_2 fixation had occurred to compensate for nitrogen limitation. On days 20 and 30, the C:N ratios were significantly higher for cultures grown in 1 and 5% N compared to 100% N treatment. This further confirms that nitrogen was limiting and that N_2 fixation did not compensate for the N-deficiency, particularly in the 1% N treatment. In fact, heterocysts were not evident in the cultures and were either non-existent or too small to differentiate from vegetative cells. This may be consistent for CAWBG02 as it did not produce heterocysts in culture with or without nitrogen supplementation in the original report (Wood et al., 2007). With respect to another non-fixing cyanobacterium, van de Waal et al. (2009)

reported molar C:N ratios ranging from 6.25 to 7.14 for *M. aeruginosa* when neither N nor C was limiting. *A. issatschenkoi* in the present study had lower C:N ratios overall. Nevertheless, significantly higher ratios of C:N were reached in the cultures grown under low nitrogen concentrations (**Table 3**).

According to the carbon-nutrient balance hypothesis, nutrients should be allocated to the production of secondary metabolites once growth is assured (Hamilton et al., 2001). Because cyanotoxins are generally considered secondary metabolites (Carmichael, 1992), their production should increase whenever the availability of essential nutrients increases. A higher production of anatoxin-a, an alkaloid that contains a nitrogen atom, was expected under higher nitrogen availability. In this study, the highest nitrogen supply corresponded to the highest growth rate and yield (**Table 3**) of CAWBG02 but not necessarily to higher total ANTX concentrations (**Figure 3**). In fact, the highest concentrations of total ANTX were produced by cultures grown in 5% N while the lowest mean concentrations of total ANTX were found in the 100% N treatment although the differences were not highly significant. Highly significant differences were observed in ANTX cellular contents (**Figure 4**): the 5% N cultures produced the highest cellular content and the 100% N treatment the lowest. The 100% N cultures had the highest growth rate, the highest biomass yield, the highest levels of particulate organic nitrogen and the highest phycocyanin to chlorophyll *a* ratios (**Table 3**; **Figure 2**), yet they produced the lowest ANTX cellular content. Additional concentrations of nitrogen should be tested to confirm these results based on only three contrasting treatments. If ANTX is indeed a type of defense compound then, its production might be a mechanism that confers ecological advantage particularly under low nutrient conditions that are common in aquatic systems during summer stratification when cyanobacteria tend to thrive and zooplankton grazing is typically high (Sommer et al., 1986).

The mean extracellular to total toxin concentration ratios were higher in 1% N treatment than in the other two treatments, the extracellular fraction almost exceeding the particulate fraction in stationary phase (**Figure 3**). Stress conditions in cyanobacteria can lead to permeability changes of the cell membrane that result in leakage (Whitton and Potts, 2000). However, it should be noted that the extracellular ANTX concentrations presented in this study were likely underestimated, as is likely the case for previous studies (Rapala et al., 1993). ANTX is quite labile under light and may degrade once released into the medium (Stevens and Krieger, 1988). Short-term radio-labeling experiments would be required to estimate more accurately the extracellular release. Furthermore, although the cultures were initially bacteria free, prepared and sub-sampled under sterile conditions, it is possible that some biodegradation arose.

This study suggests that toxin production may be higher when cyanobacterial cells are under moderate nutrient stress. Recently, Kurmayer (2011) reported that another nitrogen-fixing cyanobacterium *Nostoc* produced higher levels of microcystin cell content under stress conditions, particularly under low phosphorous ($P\text{-}PO_4$) and low light irradiance, even though growth rates were reduced up to 100-fold compared to controls. As a result, microcystin content per cell was negatively correlated to $P\text{-}PO_4$ and irradiance. Interestingly nitrogen reduction did not have the same effect, but, in this case, the number of heterocysts increased suggesting some alleviation of N-deficiency. Even if *Nostoc* produced higher levels of microcystin per cell when grown under stress conditions, the total toxin production was still lower than when grown under optimal conditions. In contrast, in the present study, both cellular and total ANTX concentrations in *A. issatschenkoi* were higher in cultures grown at intermediate N concentrations (**Figures 3** and **4**). Similarly, Rapala et al. (1993) observed that ANTX cellular contents were higher in both *A. flos-aquae* and *Anabaena flos-aquae* when grown in nitrogen-free media as opposed to nitrogen-rich control media. In this study, mean ANTX cell contents of CAWBG02 were both significantly lower in 100 and 1% N media than in 5% N. Stress conditions may increase ANTX cellular production to a certain point where cyanobacterial cells are still capable of producing the toxin without compromising primary metabolism. Mean cellular ANTX concentrations for the 1% N were slightly higher than those of the 100% N, but the difference was not significant. Based on cellular composition, the 1% N cultures were more severely stressed and the N concentration may have been too low to sustain much toxin production.

The results presented in this study suggest that ANTX production may increase in *A. issatschenkoi* under moderate nitrogen limitation. According to the carbon-nutrient balance hypothesis and our current understanding of secondary metabolism, the opposite was expected. One possible ecological advantage of such a strategy could be that when nitrogen is limiting and population density declines, additional population losses through grazing would be minimized via higher cell specific toxin concentrations. In the present experiments batch cultures were used as they best represent algal bloom dynamics typical of nuisance cyanobacterial growth in nature. However, it is possible that factors that are not well controlled in batch cultures may have influenced the results. Growth rates were slightly different among the treatments and might have had an effect on ANTX concentrations. Although it has not been specifically demonstrated for anatoxin-a, in the case of microcystins the cellular growth rate is the primary factor regulating production (Orr and Jones, 1998). However, in this case the higher growth rate observed in the 100% N culture did not lead to the higher anatoxin concentration or cellular content. Further studies encompassing a wider range of nutrient concentrations and using other toxin producing cyanobacterial taxa are necessary to confirm these results and to determine if physiological stress maximizes toxin production more generally.

ACKNOWLEDGMENTS

We thank A. Saleem (University of Ottawa), R. Aranda-Rodriguez, and Z. Jin (Health Canada, Ottawa), along with M. Quilliam (National Research Council of Canada, Halifax) for advice with LS/MS/MS instrumentation and analyses. We thank L. Kimpe for her assistance with the Accelerated Solvent Extraction (ASE) and S. Bhatti with algal culturing. This work was supported by an Ontario Ministry of Environment Best in Science to Frances R. Pick and M. Quilliam.

REFERENCES

Anderson, R. A. (ed.). (2005). *Algal Culturing Techniques*. Burlington: Elsevier Academic Press, 578.

Aranda-Rodriguez, R., Tillmanns, A., Benoit, F. M., Pick, F. R., Harvie, J., and Solenaia, L. (2005). Pressurized liquid extraction of toxins from cyanobacterial cells. *Environ. Toxicol.* 20, 390–396.

Aráoz, R., Herman, M., Rippka, R., Ledreux, A., Molgo, J., Changeux, J, Tandeau de Massac, N., and Nghiêm, H. O. (2008). A non-radioactive ligand-binding assay for detection of cyanobacterial anatoxins using Torpedo electrocyte membranes. *Toxicon* 52, 163–174.

Ballot, A., Fastner, J., Lentz, M., and Wiedner, C. (2010). First report of anatoxin-a producing cyanobacterium *Aphanizomenon issatschenkoi* in northeastern Germany. *Toxicon* 56, 964–971.

Bergmann, M., and Peters, R. H. (1980). A simple reflectance method for the measurement of particulate pigment in lake water and its application to phosphorus-chlorophyll-seston relationships. *Can. J. Fish. Aquat. Sci.* 37, 111–114.

Cadel-Six, S., Peyraud-Thomas, C., Brient, L., Marsac, N. T., Rippka, R., and Méjean, A. (2007). Different genotypes of anatoxin-producing cyanobacteria coexist in the Tarn River, France. *Appl. Environ. Microbiol.* 73, 7605–7614.

Carmichael, W. W. (1992). Cyanobacteria secondary metabolites – the cyanotoxins. *J. Appl. Bacteriol.* 72, 445–459.

Carmichael, W. W., Biggs, D. F., and Peterson, M. A. (1979). Pharmacology of anatoxin-a, produced by the freshwater cyanophyte *Anabaena flos-aquae* NRC-44-1. *Toxicon* 17, 229–236.,

Codd, G. A., Morrison, L. F., and Metcalf, S. J. (2005). Cyanobacterial toxins: risk, management for health protection. *Toxicol. Appl. Pharmacol.* 203, 264–272.

Frost, P. C., Kinsman, L. E., Johnston, C. A., and Larson, J. H. (2009). Watershed discharge modulates relationships between landscape components and nutrient ratios in stream seston. *Ecology* 90, 1631–1640.

Furey, A., Crowley, J., Hamilton, B., Lehane, M., and James, K. J. (2005). Strategies to avoid the misidentification of anatoxin-a using mass spectrometry in the forensic investigation of acute neurotoxic poisoning. *J. Chromatogr. A* 1082, 91–97.

Gugger, M., Lenoir, S., Berger, C., Ledreux, A., Druart, J., and Humbert, J.-F. (2005). First report in a river in France of the benthic cyanobacterium *Phormidium favosum* producing anatoxin-a associated with dog neurotoxicosis. *Toxicon* 45, 919–928.

Guillard, R. R. L. (1973). "Division rates," in *Handbook of Phycological Methods*, ed. J. R. Stein (Cambridge: Cambridge University Press), 289–312.

Hamilton, J. G., Zangerl, A. R., De Lucia, E. H., and Berenbaum, M. R. (2001). The carbon-nutrient balance hypothesis: its rise and fall. *Ecol. Lett.* 4, 86–95.

Jespersen, A., and Christoffersen, K. (1987). Measurements of chlorophyll-a from phytoplankton using ethanol as extraction solvent. *Arch. Fur. Hydrobiol. Stuttg.* 109, 445–454.

Kurmayer, R. (2011). The toxic cyanobacterium *Nostoc* sp. strain 152 produces highest amounts of microcystin and nostophycin under stress conditions. *J. Phycol.* 47, 200–207.

Orr, P. T., and Jones, G. J. (1998). Relationships between microcystin production and cell division rates in nitrogen-limited *Microcystis aeruginosa* cultures. *Limnol. Oceanogr.* 43, 1604–1614.

Osswald, J., Rellan, S., Gago, A., and Vasconcelos, V. (2007). Toxicology and detection methods of the alkaloid neurotoxin produced by cyanobacteria, anatoxin-a. *Environ. Int.* 33, 1070–1089.

Rapala, J., Sivonen, K., Luukainen, R., and Niemalä, S. I. (1993). Anatoxin-a concentration in *Anabaena* and *Aphanizomenon* under different environmental conditions and comparison of growth by toxic and non-toxic *Anabaena* strains – a laboratory study. *J. Appl. Phycol.* 5, 581–591.

Selwood, A. I., Holland, P. T., Wood, S. A., Smith, K. F., and Mcnabb, P. S. (2007). Production of anatoxin-a and a novel biosynthetic precursor by the cyanobacterium *Aphanizomenon issatschenkoi*. *Environ. Sci. Technol.* 41, 506–510.

Sommer, U., and Gliwicz, Z. M., Lambert, W., and Duncan, A. (1986). The PEG-model of seasonal succession of planktonic events in fresh waters. *Arch. Hydrobiol.* 106, 433–471.

Stevens, D. K., and Krieger, R. I. (1988). Analysis of anatoxin-a by GC/ECD. *J. Anal. Toxicol.* 12, 126–131.

Turpin, D. H. (1991). Effect of inorganic N availability on algal photosynthesis and carbon metabolism. *J. Phycol.* 27, 14–20.

van de Waal, D. B., Verspagen, M. H., Lürling, M., van Donk, E., Visser, P. M., and Huisman, J. (2009). The ecological stoichiometry of toxins produced by harmful cyanobacteria: an experimental test of the carbon-nutrient balance hypothesis. *Ecol. Lett.* 12, 1326–1335.

Whitton, B. A., and Potts, M. (2000). *Introduction to the Cyanobacteria, the Ecology of Cyanobacteria: Their Diversity in Time and Space*. Dordrecht: Kluwer Academic Publishers, 1–11.

Wiegand, C., and Pflugmacher, S. (2005). Ecotoxicological effects of selected cyanobacterial secondary metabolites a short review. *Toxicol. Appl. Pharmacol.* 203, 201–218.

Wood, S. A., Rasmussen, J. P., Holland, P. T., Campbell, R., and Crowe, A. L. M. (2007). First report of the anatoxin-a from *Aphanizomenon issatschenkoi* (cyanobacteria). *J. Phycol.* 43, 356–365.

Conflict of Interest Statement: The authors declare that the research was conducted in the absence of any commercial or financial relationships that could be construed as a potential conflict of interest.

Received: 06 February 2012; accepted: 24 May 2012; published online: 12 June 2012.

Citation: Gagnon A and Pick FR (2012) Effect of nitrogen on cellular production and release of the neurotoxin anatoxin-a in a nitrogen-fixing cyanobacterium. Front. Microbio. ***3****:211. doi: 10.3389/fmicb.2012.00211*

This article was submitted to Frontiers in Aquatic Microbiology, a specialty of Frontiers in Microbiology.